frontiers
RESEARCH TOPICS

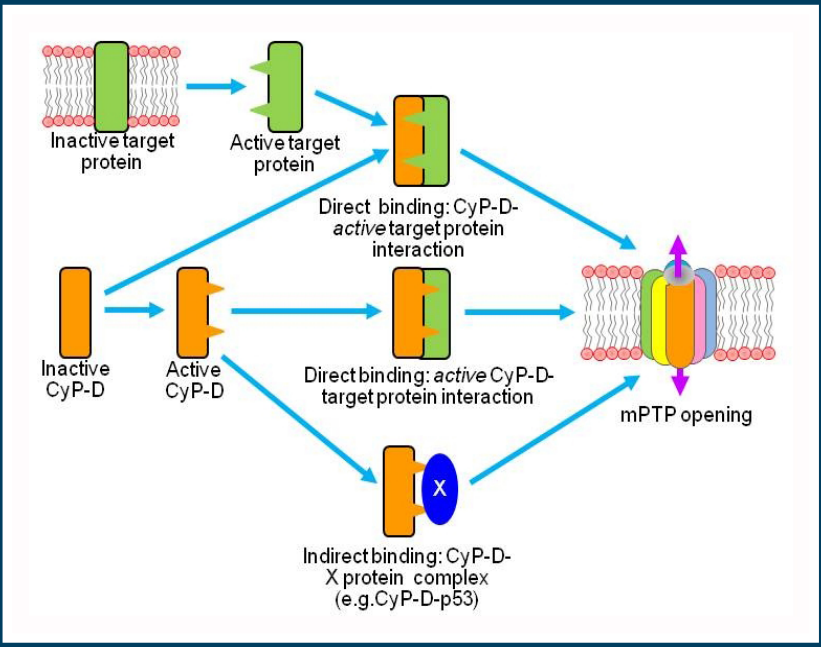

MITOCHONDRIA: THE CELL POWERHOUSE AND NEXUS OF STRESS

Topic Editors
Sabzali Javadov and Andrey V. Kuznetsov

frontiers in PHYSIOLOGY

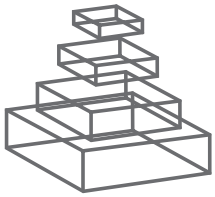

frontiers

ISSN 1664-8714
ISBN 978-2-88919-283-0
DOI 10.3389/978-2-88919-283-0

ABOUT FRONTIERS

Frontiers is more than just an open-access publisher of scholarly articles: it is a pioneering approach to the world of academia, radically improving the way scholarly research is managed. The grand vision of Frontiers is a world where all people have an equal opportunity to seek, share and generate knowledge. Frontiers provides immediate and permanent online open access to all its publications, but this alone is not enough to realize our grand goals.

FRONTIERS JOURNAL SERIES

The Frontiers Journal Series is a multi-tier and interdisciplinary set of open-access, online journals, promising a paradigm shift from the current review, selection and dissemination processes in academic publishing.
All Frontiers journals are driven by researchers for researchers; therefore, they constitute a service to the scholarly community. At the same time, the Frontiers Journal Series operates on a revolutionary invention, the tiered publishing system, initially addressing specific communities of scholars, and gradually climbing up to broader public understanding, thus serving the interests of the lay society, too.

DEDICATION TO QUALITY

Each Frontiers article is a landmark of the highest quality, thanks to genuinely collaborative interactions between authors and review editors, who include some of the world's best academicians. Research must be certified by peers before entering a stream of knowledge that may eventually reach the public - and shape society; therefore, Frontiers only applies the most rigorous and unbiased reviews.
Frontiers revolutionizes research publishing by freely delivering the most outstanding research, evaluated with no bias from both the academic and social point of view.
By applying the most advanced information technologies, Frontiers is catapulting scholarly publishing into a new generation.

WHAT ARE FRONTIERS RESEARCH TOPICS?

Frontiers Research Topics are very popular trademarks of the Frontiers Journals Series: they are collections of at least ten articles, all centered on a particular subject. With their unique mix of varied contributions from Original Research to Review Articles, Frontiers Research Topics unify the most influential researchers, the latest key findings and historical advances in a hot research area!
Find out more on how to host your own Frontiers Research Topic or contribute to one as an author by contacting the Frontiers Editorial Office: researchtopics@frontiersin.org

MITOCHONDRIA: THE CELL POWERHOUSE AND NEXUS OF STRESS

Topic Editors:
Sabzali Javadov, University of Puerto Rico School of Medicine, Puerto Rico
Andrey V. Kuznetsov, Innsbruck Medical University, Austria

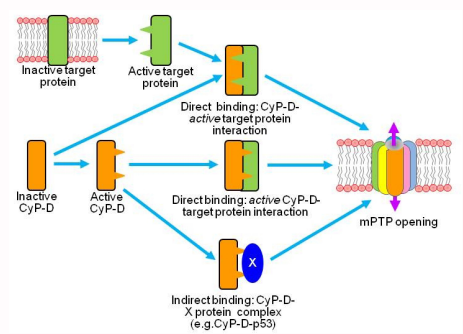

Image taken from: Javadov S and Kuznetsov A (2013) Mitochondrial permeability transition and cell death: the role of cyclophilin D. Front. *Physiol.* 4:76. doi: 10.3389/fphys.2013.00076

Mitochondrion, a sub-cellular organelle originated from primary endosymbiosis, plays a vital role in energy metabolism of eukaryotic cells. The transfer of electrons through the electron transport chain (ETC) to molecular oxygen accompanied by the extrusion of protons from the matrix generate an electrochemical gradient across the inner mitochondrial membrane (IMM) that is used for ATP synthesis by oxidative phosphorylation. Despite many aspects of ATP synthesis have been delineated, regulatory mechanisms responsible for energy synthesis and transfer still remain to be uncovered. In addition to energy function, mitochondria play a crucial role in cell metabolism under both physiological and pathological conditions through their participation in many intracellular signaling pathways. Studies over the last 30 years provide strong evidence that mitochondria are the nexus of various stresses which initiate cell death through apoptosis, oncosis, necrosis and autophagy depending on the severity of the stress and cellular energy status. The release of several pro-apoptotic proteins such as cytochrome c, Smac/DIABLO, AIF, endonuclease G from intermembrane space initiates both caspase-dependent and caspase-independent apoptosis. The formation of the mitochondrial permeability transition pore in the IMM promotes cell death mostly through necrosis whereas a mild stress activates autophagy. Due to their critical roles in both cell death and survival mitochondria have been widely considered as an important target for various pharmacological and conditional therapeutic approaches. Currently, a large number of mitochondria-targeted agents are suggested to prevent (in ischemia reperfusion injury, cardiovascular, neurodegenerative and other diseases) or stimulate (in various cancers) cell death.

This Research Topic focuses on the role of mitochondria in the regulation of cell metabolism and signaling under physiological and pathological conditions. Studies performed on cultured cells and isolated organs/tissues using different animal and cellular models of various diseases are also included and discussed.

Table of Contents

frontiers in
PHYSIOLOGY

EDITORIAL
published: 07 August 2013
doi: 10.3389/fphys.2013.00207

Mitochondria: the cell powerhouse and nexus of stress

***Sabzali Javadov*[1]* *and Andrey V. Kuznetsov*[2]**

[1] *Department of Physiology, School of Medicine, University of Puerto Rico, San Juan, Puerto Rico*
[2] *Cardiac Surgery Research Laboratory, Department of Cardiac Surgery, Innsbruck Medical University, Innsbruck, Austria*
**Correspondence: sabzali.javadov@upr.edu*

Edited by:
Paolo Bernardi, University of Padova, Italy

Mitochondria, sub-cellular organelles originated from primary endosymbiosis, play a vital role in the energy metabolism of eukaryotic cells. Despite many aspects of ATP synthesis have been delineated, regulatory mechanisms responsible for energy synthesis and transfer still remain to be uncovered. In addition to production of energy, mitochondria play a crucial role in entire cell metabolism under both physiological and pathological conditions through their participation in cell death, ion homeostasis, reactive oxygen species (ROS) generation, redox signaling as well as various intracellular signaling pathways. Studies over the last 30 years provide strong evidence that mitochondria are the nexus of various stresses which initiate cell death. The Research Topic "Mitochondria: the cell powerhouse and nexus of stress" presents state-of-the-art studies in mitochondrial research performed by prominent experts from different laboratories around the world. All 13 original research and review articles presented in the topic are dedicated to several aspects of mitochondriology including morphology, dynamics, metabolism, function, and regulation of these organelles under normal and pathophysiological conditions.

It should be noted that despite many studies, numerous aspects of mitochondrial functioning including the precise mechanisms of protein synthesis in mitochondria remain unclear. In the study presented by Koc et al. (2013) two novel small subunit proteins, CHCHD1 and AURKAIP1, and the large subunit protein, CRIF1 were characterized as new members of the mammalian mitochondrial ribosome. Using siRNA knock-down studies the authors demonstrated crucial roles of these proteins in mitochondrial protein synthesis, and revealed their significant effects on the expression of mitochondrially encoded proteins. Also, interaction of mitochondria with cytoplasmic proteins plays a causative role in the regulation of energy metabolism and cell death. Recent studies revealed interaction between elements of cytoskeleton and mitochondria which may modulate energy synthesis and transfer (Rostovtseva and Bezrukov, 2008; Guzun et al., 2011). The review by Kuznetsov et al. (2013) summarizes studies on the possible role of the cytoskeletal protein β-tubulin II in the regulation of mitochondrial metabolism, respiratory function, and energy transfer. The authors suggest that interaction of β-tubulin II with mitochondria can participate in the coupling of ATP-ADP translocase (ANT), mitochondrial creatine kinase (MtCK), and voltage-dependent anion channel (VDAC), and the ANT-MtCK-VDAC complex is responsible for the efficient intracellular energy transfer via the phosphocreatine pathway. Kaambre et al. (2013) demonstrated the applicability of the metabolic control analysis as a promising method for quantification of the flux control exerted by different enzymatic steps in total metabolic network that can be applied to study mechanisms of energy metabolism in human breast and colorectal cancer cells. In addition to interaction with other proteins/organelles, mitochondria *per se* can undergo structural modifications known as mitochondrial dynamics which is associated with changes in their number, size, shape, and intracellular localization. Mitochondrial dynamics is regulated by the balanced action of various proteins responsible for fission and fusion. These processes play also a key role in Ca^{2+} regulations, as well as in biogenesis and the quality-control of mitochondria under normal physiological conditions. Enhanced fission of mitochondria is associated with mitochondrial fragmentation, which is early sign of apoptosis in various cell stresses, including cardiac diseases or ischemia-reperfusion injury although molecular mechanisms of cell death induced by alterations in mitochondrial dynamics remain poorly understood. In this respect, the study presented by Piquereau et al. (2013) discusses the possible role of mitochondrial dynamics in mitochondria-mediated cardiac dysfunction in ischemia/reperfusion and heart failure. The authors highlight an importance of mitochondrial dynamics in mitochondrial and cellular physiology.

It is known that a number of signaling molecules including cytoplasmic and/or mitochondrial nitric oxide (NO) and ROS participate in the regulation of mitochondrial metabolism. Synthesis of NO from its precursor, nitrite increases during hypoxia and enhanced NO through cGMP and can protect the heart from ischemia/reperfusion injury. However, the mechanisms of the synthesis of NO from nitrite in cardiomyocytes are still not fully understood. Dungel et al. (2013) demonstrated that mitochondria play a predominant role in nitrite reduction to NO, leading to enhanced cGMP synthesis in cardiomyocytes. Notably, mitochondrial ROS levels can be strongly regulated by several distinct ROS-detoxification mechanisms. Expression of the major ROS scavenger enzymes superoxide dismutase 2 (SOD2), catalase, or sestrins is shown to be regulated by Forkhead box O (FOXO) transcription factors. Hagenbuchner and Ausserlechner (2013) discuss balanced action between Bim, mitochondrial architecture, and ROS-detoxifying proteins that are regulated by FOXO. Importantly, ROS-mediated modulation of various intracellular signaling pathways can also be involved in the regulation of heart contractility by the cardiac renin-angiotensin II-aldosterone system (RAAS). Activation of RAAS enhances both cytoplasmic and mitochondrial ROS generation although the cause-effect relationship between these two sources for ROS remains to be elucidated. De Giusti et al. (2013) presented a comprehensive review on the relationship between chronic RAAS stimulation and mitochondrial ROS, and the possible role of sodium exchangers in RAAS-mediated cardiac hypertrophy. Consequently,

pharmacological inhibition of mitochondrial ROS generation exerts a beneficial effect. Investigating ROS in skeletal muscles, La Guardia et al. (2013) demonstrated that oxidative damage induced by simvastatin in fibers from rat skeletal muscle is associated with the enhanced mitochondrial superoxide generation, whereas pretreatment with L-carnitine prevented the toxic effects of simvastatin. Interestingly, the study presented by Canzoniero et al. (2013) shows that neurons expressing large amounts of nNOS produce significantly less mitochondrial ROS in response to an excitotoxic challenge, thereby providing a potential mechanism for reduced cells vulnerability to the excitotoxicity in patients with Huntington's disease. It is well-known that a number of various mitochondrial diseases are associated with mutations, deletions, or deficiency of genes encoding mitochondrial proteins. Deficiency of mitochondrial phospholipid cardiolipin in humans known as Barth syndrome is caused due to absence of mitochondrial acyl-transferase, tafazzin that is essential for remodeling acyl chains of cardiolipin. Powers et al. (2013) demonstrated that diminished exercise capacity in tafazzin-knockdown mice can be explained by the respiratory dysfunction of mitochondria. A causative link between mitochondrial dysfunction and pathological disorders has been shown using different other models of diseases. For example, it has been shown that mitochondria dysfunction plays also an important role in developing of inflammation. Experiments using rat liver slices and isolated mitochondria demonstrated that inflammation induced by inflammatory mediators resulted in mitochondrial dysfunction due to secondary hypoxia (Weidinger et al., 2013). This study revealed hypoxia-induced attenuation of complexes I and II function in response to inflammation.

Accumulation of ROS along with Ca^{2+} overload can be considered as the major factors causing mitochondrial permeability transition (mPT) associated with depolarization of mitochondrial membrane, ATP depletion and opening of non-specific pathological mPT pores (mPTP). Irreversible high-conductance mPTP opening plays a critical role in mitochondria-mediated cell death. Although opening of mPTP is well-known phenomenon, the molecular identity of the pores is still elusive. Previous findings that the mPTP consists of VDAC and ANT were not proven by genetic studies when VDAC- or ANT-null mitochondria still exhibited a CsA-sensitive pore opening [reviewed in Bernardi (2013)]. Cyclophilin D (CyP-D) is the only defined component which plays an important regulatory role in pore opening. Interestingly, recent studies demonstrated that CyP-D binds the lateral stalk of the F_0F_1 ATP synthase and modulates its activity (Giorgio et al., 2009). Furthermore, the authors provided strong evidence that dimers of the F_0F_1 ATP synthase incorporated into lipid bilayers form $Ca^{2\pm}$-activated channels with the key features of the mPTP (Bernardi, 2013; Giorgio et al., 2013). The review by Javadov and Kuznetsov (2013) summarizes and discusses the possible mechanisms of the activation of CyP-D to interact with a target protein in the inner mitochondrial membrane and initiate opening of the mPTP. Notably, physiological (low-conductance) mPTP opening can regulate mitochondrial Ca^{2+} homeostasis through modulation of Ca^{2+} efflux, and generate and convey calcium signals from one mitochondrion to another (reviewed in Brenner and Moulin, 2012). Indeed, the low-conductance mPTP is one of dozens of channels/exchangers which regulate ion homeostasis in mitochondria. In this aspect, Na^+/H^+ exchanger 1 (NHE1) is one of most interesting ion transporters recently found in the mitochondrial inner membrane (Javadov et al., 2011; Villa-Abrille et al., 2011). Although NHE1 is the main transporter of the plasma membrane regulating H^+ concentration in cytoplasm, its role in mitochondrial physiology is still unknown. In this Topic, the potential role of mitochondrial NHE1 as a target to prevent cardiac diseases such as ischemia/reperfusion and heart failure was described by Alvarez and Villa-Abrille (2013).

In conclusion, this Frontiers Review Topic highlights several important aspects of mitochondrial research under normal and pathological/stressful conditions. This will hopefully be useful for further understanding of mitochondrial biology as well as molecular mechanisms of mitochondria-mediated cell dysfunction aiming to develop a number of new therapeutic approaches for the treatment of various human diseases by targeting mitochondria.

ACKNOWLEDGMENTS

This study was supported by the National Heart, Lung, And Blood Institute of the National Institutes of Health through Research Grant SC1HL118669 (Sabzali Javadov) and by a research grant from the Austrian Science Fund (FWF): [P 22080-B20] (Andrey V. Kuznetsov).

REFERENCES

Alvarez, B. V., and Villa-Abrille, M. C. (2013). Mitochondrial NHE1: a newly identified target to prevent heart disease. *Front. Physiol.* 4:152. doi: 10.3389/fphys.2013.00152

Bernardi, P. (2013). The mitochondrial permeability transition pore: a mystery solved. *Front. Physiol.* 4:95. doi: 10.3389/fphys.2013.00095

Brenner, C., and Moulin, M. (2012). Physiological roles of the permeability transition pore. *Circ. Res.* 111, 1237–1247.

Canzoniero, L. M., Granzotto, A., Turetsky, D. M., Choi, D. W., Dugan, L. L., and Sensi, S. L. (2013). nNOS(+) striatal neurons, a subpopulation spared in Huntington's Disease, possess functional NMDA receptors but fail to generate mitochondrial ROS in response to an excitotoxic challenge. *Front. Physiol.* 4:112. doi: 10.3389/fphys.2013.00112

De Giusti, V. C., Caldiz, C. I., Ennis, I. E., Perez, N. G., Cingolani, H. E., and Aiello, E. A. (2013). Mitochondrial reactive oxygen species (ROS) as signaling molecules of intracellular pathways triggered by the cardiac renin-angiotensin II-aldosterone system (RAAS). *Front. Physiol.* 4:126. doi: 10.3389/fphys.2013.00126

Dungel, P., Teuschl, A. H., Banerjee, A., Paier-Pourani, J., Redl, H., and Kozlov, A. V. (2013). Impact of mitochondria on nitrite metabolism in HL-1 cardiomyocytes. *Front. Physiol.* 4:101. doi: 10.3389/fphys.2013.00101

Giorgio, V., Bisetto, E., Soriano, M. E., Dabbeni-Sala, F., Basso, E., Petronilli, V., et al. (2009). Cyclophilin D modulates mitochondrial F0F1-ATP synthase by interacting with the lateral stalk of the complex. *J. Biol. Chem.* 284, 33982–33988.

Giorgio, V., von Stockum, S., Antoniel, M., Fabbro, A., Fogolari, F., Forte, M., et al. (2013). Dimers of mitochondrial ATP synthase form the permeability transition pore. *Proc. Natl. Acad. Sci. U.S.A.* 110, 5887–5892.

Guzun, R., Karu-Varikmaa, M., Gonzalez-Granillo, M., Kuznetsov, A. V., Michel, L., Cottet-Rousselle, C., et al. (2011). Mitochondria-cytoskeleton interaction: distribution of beta-tubulins

in cardiomyocytes and HL-1 cells. *Biochim. Biophys. Acta.* 1807, 458–469.

Hagenbuchner, J., and Ausserlechner, M. J. (2013). Mitochondria and FOXO3: breath or die. *Front. Physiol.* 4:147. doi: 10.3389/fphys.2013.00147

Javadov, S., and Kuznetsov, A. (2013). Mitochondrial permeability transition and cell death: the role of cyclophilin D. *Front. Physiol.* 4:76. doi: 10.3389/fphys.2013.00076

Javadov, S., Rajapurohitam, V., Kilic, A., Hunter, J. C., Zeidan, A., Said Faruq, N., et al. (2011). Expression of mitochondrial fusion-fission proteins during post-infarction remodeling: the effect of NHE-1 inhibition. *Basic Res. Cardiol.* 106, 99–109.

Kaambre, T., Chekulayev, V., Shevchuk, I., Tepp, K., Timohhina, N., Varikmaa, M., et al. (2013). Metabolic control analysis of respiration in human cancer tissue. *Front. Physiol.* 4:151. doi: 10.3389/fphys.2013.00151.

Koc, E. C., Cimen, H., Kumcuoglu, B., Abu, N., Akpinar, G., Haque, M. E., et al. (2013). Identification and characterization of CHCHD1, AURKAIP1, and CRIF1 as new members of the mammalian mitochondrial ribosome. *Front. Physiol.* 4:183. doi: 10.3389/fphys.2013.00183

Kuznetsov, A. V., Javadov, S., Guzun, R., Grimm, M., and Saks, V. (2013). Cytoskeleton and regulation of mitochondrial function: the role of beta-tubulin II. *Front. Physiol.* 4:82. doi: 10.3389/fphys.2013.00082

La Guardia, P. G., Alberici, L. C., Ravagnani, F. G., Catharino, R. R., and Vercesi, A. E. (2013). Protection of rat skeletal muscle fibers by either L-carnitine or coenzyme Q10 against statins toxicity mediated by mitochondrial reactive oxygen generation. *Front. Physiol.* 4:103. doi: 10.3389/fphys.2013.00103

Piquereau, J., Caffin, F., Novotova, M., Lemaire, C., Veksler, V., Garnier, A., et al. (2013). Mitochondrial dynamics in the adult cardiomyocytes: which roles for a highly specialized cell. *Front. Physiol.* 4:102. doi: 10.3389/fphys.2013.00102

Powers, C., Huang, Y., Strauss, A., and Khuchua, Z. (2013). Diminished exercise capacity and mitochondrial bc1 complex deficiency in tafazzin-knockdown mice. *Front. Physiol.* 4:74. doi: 10.3389/fphys.2013.00074

Rostovtseva, T. K., and Bezrukov, S. M. (2008). VDAC regulation: role of cytosolic proteins and mitochondrial lipids. *J. Bioenerg. Biomembr.* 40, 163–170.

Villa-Abrille, M. C., Cingolani, E., Cingolani, H. E., and Alvarez, B. V. (2011). Silencing of cardiac mitochondrial NHE1 prevents mitochondrial permeability transition pore opening. *Am. J. Physiol. Heart Circ. Physiol.* 300, H1237–1251.

Weidinger, A., Dungel, P., Perlinger, M., Singer, K., Ghebes, C., Duvigneau, J. C., et al. (2013). Experimental data suggesting that inflammation mediated rat liver mitochondrial dysfunction results from secondary hypoxia rather than from direct effects of inflammatory mediators. *Front. Physiol.* 4:138. doi: 10.3389/fphys.2013.00138

Received: 03 July 2013; accepted: 21 July 2013; published online: 07 August 2013.
*Citation: Javadov S and Kuznetsov AV (2013) Mitochondria: the cell powerhouse and nexus of stress. Front. Physiol. **4**:207. doi: 10.3389/fphys.2013.00207*
This article was submitted to Frontiers in Mitochondrial Research, a specialty of Frontiers in Physiology.

frontiers in
PHYSIOLOGY

REVIEW ARTICLE
published: 10 May 2013
doi: 10.3389/fphys.2013.00102

Mitochondrial dynamics in the adult cardiomyocytes: which roles for a highly specialized cell?

Jerome Piquereau[1,2], Fanny Caffin[1,2], Marta Novotova[3], Christophe Lemaire[1,2], Vladimir Veksler[1,2], Anne Garnier[1,2], Renee Ventura-Clapier[1,2] and Frederic Joubert[1,2]*

[1] *Department of Signaling and Cardiac Pathophysiology, U-769, INSERM, Châtenay-Malabry, France*
[2] *IFR141, Université Paris-Sud, Châtenay-Malabry, France*
[3] *Department of Cellular Morphology, Institute of Molecular Physiology and Genetics, Slovak Academy of Sciences, Bratislava, Slovak Republic*

Edited by:
Andrey V. Kuznetsov, Innsbruck Medical University, Austria

Reviewed by:
Alberto A. Iglesias, Instituto de Agrobiotecnología del Litoral (UNL-CONICET), Argentina
Ove Eriksson, University of Helsinki, Finland

***Correspondence:**
Frederic Joubert, Faculté de Pharmacie, U-769 INSERM, Université Paris-Sud, 5 rue J-B Clément, 92296 Châtenay-Malabry, France.
e-mail: frederic.joubert@u-psud.fr

Mitochondrial dynamics is a recent topic of research in the field of cardiac physiology. The study of mechanisms involved in the morphological changes and in the mobility of mitochondria is legitimate since the adult cardiomyocytes possess numerous mitochondria which occupy at least 30% of cell volume. However, architectural constraints exist in the cardiomyocyte that limit mitochondrial movements and communication between adjacent mitochondria. Still, the proteins involved in mitochondrial fusion and fission are highly expressed in these cells and could be involved in different processes important for the cardiac function. For example, they are required for mitochondrial biogenesis to synthesize new mitochondria and for the quality-control of the organelles. They are also involved in inner membrane organization and may play a role in apoptosis. More generally, change in mitochondrial morphology can have consequences in the functioning of the respiratory chain, in the regulation of the mitochondrial permeability transition pore (MPTP), and in the interactions with other organelles. Furthermore, the proteins involved in fusion and fission of mitochondria are altered in cardiac pathologies such as ischemia/reperfusion or heart failure (HF), and appear to be valuable targets for pharmacological therapies. Thus, mitochondrial dynamics deserves particular attention in cardiac research. The present review draws up a report of our knowledge on these phenomena.

Keywords: mitochondrial dynamics, cardiomyocytes, adult, energetic metabolism, cytoarchitecture

INTRODUCTION

Mitochondria, which have long been regarded only as energy producers, are actually recognized at the crossroads of many cellular functions. Obviously, they play a crucial role in energy production in cells, but they are involved in other phenomena such as ion homeostasis, free radical production, and ultimately cell death. Many of their characteristics, as morphology, location in the cell, proximity to other organelles are important parameters that have to be considered to understand the mitochondrial functions. This is particularly true in the adult cardiac cells where mitochondria, which produce 90% of ATP, occupy 30% of cardiac cell volume and are embedded in a dense and complex organization. This interlinking reflects the challenging function of the heart which requires rhythmic contractions of the pump throughout the life, and consequently needs a fast and effective intracellular energy delivery to the ATP consumers of the cardiomyocyte (for review, see Ventura-Clapier et al., 2011). Moreover, the main phosphorylated metabolites do not vary with the increase in work (Balaban, 2012). This metabolic homeostasis and the tight coupling between mitochondria and ATP consumer sites are two of the peculiarities of the cardiac cell and require an optimized cellular organization to ensure efficient energy fluxes. Any modification of the cellular architecture, but also of the internal organization of mitochondria could thus impair cell energetic and as a consequence cell function.

In the majority of cells, mitochondria are able to adjust their morphology and their location depending on energy needs and metabolic conditions (Hackenbrock, 1966; Bereiter-Hahn, 1990; Karbowski and Youle, 2003; Rossignol et al., 2004; Mannella, 2006; Benard et al., 2007; Soubannier and McBride, 2009). This "mitochondrial dynamics" seems to be particularly important during cell division and for mitochondrial quality control; it may also play a role under pathological conditions. At some point, mitochondrial network morphology actually is the result of several processes, including fusion and fragmentation of the organelles which are usually controlled by a complex protein machinery (for review, see Liesa et al., 2009). It is generally admitted that a connected mitochondrial network is observed in active metabolic cells (Skulachev, 2001) while the mitochondria are rather fragmented in quiescent cells (Collins et al., 2002). However, it should be kept in mind that mitochondria exhibit a high structural and functional tissue specificity in connection with cell functions. Thus, any finding on mitochondrial organization and functioning cannot be directly extrapolated before being considered in the framework of the considered cell or tissue. For example in adult cardiac cells, the relationship between mitochondrial morphology and function does not seem to be rigorous,

since cardiomyocytes are metabolically active but exhibit an apparently fragmented network (Kuznetsov et al., 2009).

Mitochondrial dynamics, however, depends on the cellular environment and architecture constraints. In adult cardiomyocytes, the large amount of myofilaments, the presence of a rigid cytoskeleton and the densely packed mitochondrial network clearly impedes mitochondrial movements (Vendelin et al., 2005). Moreover, the arrangement of the different organelles between them is so crucial for cardiac cell function that mitochondrial morphology has to be efficiently controlled (Wilding et al., 2006; Piquereau et al., 2010). Although abundance of proteins of the mitochondrial dynamics can appear paradoxical in cardiac cells, where the mitochondrial network appears to be frozen, it may be less rigid than believed. Proteins of the mitochondrial dynamics are involved in multiple processes and can thus be important for cardiac physiology out of their role in mitochondrial network organization. In this review, we present some evidences for the importance of these proteins in physiological and pathological situations.

MITOCHONDRIAL FUNCTIONS IN THE ADULT CARDIAC CELL: TANGLED IN A COMPLEX ARCHITECTURE

ROLE OF THE INTERNAL ORGANIZATION OF MITOCHONDRIA

Since the discovery of the chemiosmotic mechanism of ATP synthesis by PD Mitchell in the 1960s, the importance of mitochondrial internal organization and of a local regulation of energy production has been pointed out by many authors. Indeed, organization of internal membranes of mitochondria is critical for an optimal function of respiratory complexes and ATP formation (Davies et al., 2011). The existence of a large inner membrane folded in cristae, where oxidative-phosphorylation coupling occurs, is a prerequisite for local proton gradient generation and maximal ATP synthase functioning (Strauss et al., 2008). Phospholipids, and in particular cardiolipins, are involved in the formation of these cristae (Khalifat et al., 2008). However, the all set of elements inducing cristae generation is far from being elucidated. For example, the presence of oligomers of ATP synthase (Davies et al., 2012) and of dynamin proteins (Hinshaw, 2000) could also play a role in the cristae organization. Different dynamin proteins, such as the optic atrophy protein 1 (Opa1) or Mitofilin, have been recognized as important actors regulating cristae formation (Frezza et al., 2006; Hoppins et al., 2011a). Those cristae are dynamic structures which can rapidly and reversibly fuse and divide, depending on energetic state (Mannella, 2006), from orthodox to condensed conformations upon activation of ATP synthesis (Hackenbrock, 1966; Mannella, 2008). Thus, optimal mitochondrial function seems to require the morphological control of inner membrane organization. This is particularly evident for mitochondria of the adult cardiomyocyte that exhibit the highest density of cristae (Vafai and Mootha, 2012). Finally, it is also well-known that changes in mitochondrial morphology can play a role in different events, in particular in mitochondrial permeability transition pore (MPTP) function, and in apoptosis (Nogueira et al., 2005; Wasilewski and Scorrano, 2009; Campello and Scorrano, 2010). So it is now evident that all the phenomena that modify mitochondrial morphology can modify mitochondrial functions, and possibly cell functions.

Another important feature of mitochondria, especially in cardiac cells, is the existence of local control of energy production in the intermembrane space by different phosphotransfer enzyme systems. For example, we and others have shown that the mitochondrial creatine kinase isoform (miCK), which is located in the vicinity of the adenine nucleotide translocase (ANT), allows a local supply of ADP, a local control of proton concentration, and an efficient transfer of energy via phosphocreatine (PCr) diffusion (Joubert et al., 2000, 2001a, 2002a; Saks et al., 2000; Guzun et al., 2012). Such enzymes also play a role in the structural organization of the intermembrane space by bridging inner and outer membranes (Wallimann et al., 1992; Speer et al., 2005). Any modification of this energetic microdomain organization by alteration of mitochondrial morphology could affect local regulation of energy production.

IMPORTANCE OF CELL ARCHITECTURE FOR ENERGY TRANSFER AND COMMUNICATION BETWEEN ORGANELLES

Adult cardiomyocytes are characterized by a complex cytoarchitecture which allows an efficient and synchronized contraction of the entire cell. The maintenance of this cytoarchitecture is ensured by the cytoskeleton which holds sarcomeres in lateral register, mechanically couples myofibrils of adjacent myocytes, and transduces mechanical stress signals. Mitochondria are an integral part of this cytoarchitecture; different populations of those organelles are usually defined according to their location: intermyofibrillar mitochondria, subsarcolemmal mitochondria and perinuclear mitochondria. Those mitochondria are easily identifiable by electron microscopy (**Figure 1**). Intermyofibrillar mitochondria are strictly ordered between rows of contractile proteins, apparently isolated from each other by repeated arrays of T-tubules, and in close contact with myofibrils and sarcoplasmic reticulum (SR) (Vendelin et al., 2005; Kuznetsov et al., 2009; Guzun et al., 2012); they are mainly devoted to the energy supply of myosin and

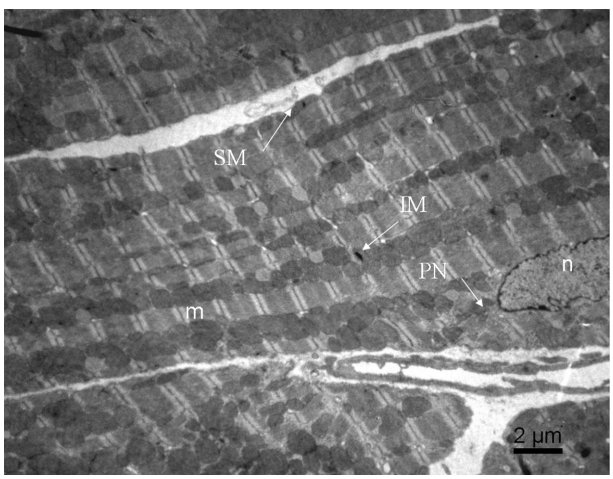

FIGURE 1 | Image of adult mouse cardiomyocyte obtained by electron microscopy. Three subpopulations of mitochondria are observed: intermyofibrillar mitochondria (IM) along the contractile proteins, the subsarcolemmal mitochondria (SM) just beneath the sarcolemmal and perinuclear mitochondria (PN) around the nucleus. m, myofibrils; n, nucleus.

SR-ATPases. The subsarcolemmal mitochondria present a lower degree of organization and are probably mainly involved in other roles such as ion homeostasis or signaling pathways. Finally, perinuclear mitochondria are organized in clusters and are most probably involved in transcription and translation processes. Concurrently to these functional differences, those mitochondria do not exhibit exactly the same morphology; for example, some authors have shown that intermyofibrillar mitochondria can be larger in certain situations (Ong et al., 2010).

Thus, the mitochondria in muscle cells seem separated from each other and exhibit a unique feature of a highly ordered crystal-like structure which appears optimized for maximal efficacy of energy supply and sustained contraction (Vendelin et al., 2005). Due to spatial constraints and isolation of mitochondria from each other, the energetic regulation of contraction would be confined in the small regions surrounding each sarcomere where the intracellular components interact with each other and compose the ≪Intracellular Energetic Units≫ (ICEU) (Saks et al., 2001; Guzun et al., 2012). The family of creatine kinases (CK), specifically located on the inner-membrane of the mitochondrion, but also at the M-line of myofibrils and on the outer surface of the SR, is an important component of these ICEUs and allows efficient local control over adenine nucleotides and fast energy transfer (Joubert et al., 2001b, 2002b; Tepp et al., 2011), thus emphasizing the importance of subcellular organization and compartmentalization of energy transfer (Joubert et al., 2002c; Piquereau et al., 2010).

Another evidence of the importance of cardiac cell architecture is the existence of microdomains of Ca^{2+} at the interface of the organelles. Different authors have shown that the close association between mitochondria and SR provides "hot spots" of very high calcium concentration in the vicinity of mitochondria (Dorn and Maack, 2013). At energetic level, the existence of direct adenine nucleotide canalization (DANC) (Kaasik et al., 2001) has also been shown to represent a pathway complementary to phosphotransfer enzymes to directly transfer and regulate ATP and ADP levels in microdomains at the interface of the organelles. Interestingly, this cytoarchitecture develops at the time of early cardiac ontogenic development (Piquereau et al., 2010), and when disturbed, the efficiency of this direct canalization is decreased (Wilding et al., 2006). Moreover, a change in osmotic pressure which can induce swelling or shrinkage of mitochondria can modulate the function of other compartments (Kaasik et al., 2004, 2010). Any change of cell architecture, and particularly of mitochondrial morphology, can therefore impact mitochondrial function and energy transfer (Joubert et al., 2008; Piquereau et al., 2012). This is why many authors address the question of how mitochondrial dynamics play a regulatory role in energy production and cell signaling in the heart.

MITOCHONDRIAL DYNAMICS PROTEINS IN THE HEART

Mitochondria are dynamic organelles able to change their morphology in response to different signals. Phenomena that govern mitochondrial morphology aroused real interest since the 1970s when the first fusion events have been described (Kimberg and Loeb, 1972; Wakabayashi et al., 1975; Wakabayashi and Green, 1977). For the last four decades, the mechanistic knowledge of mitochondrial dynamics has been well-developed and, even if some phenomena involved in mitochondrial fusion and fission remain shrouded in mystery, the major proteins governing these processes have been identified. The complete protein machinery of mitochondrial fusion and fission exists in cardiac cells and specifically regulates mitochondrial morphology and size. The currently identified of such proteins and their possible roles in the adult heart are summarized next.

PROTEINS INVOLVED IN FUSION AND FISSION OF MITOCHONDRIA

All studies agree so far that fusion of the outer and inner mitochondrial membranes occurs separately and involves distinct molecules. The outer membrane fusion is governed by mitofusins (Mfn1 and Mfn2) (Santel and Fuller, 2001; Legros et al., 2002) while the inner membrane fusion involves Opa1 (Alexander et al., 2000). Interestingly, these two kinds of proteins (Mfns and Opa1) exhibit strong similarities in their structure and their mode of action. Indeed, these proteins contain a GTPase domain, a transmembrane domain allowing the anchorage of the proteins to the outer (Mfns) or inner (Opa1) membranes, and a coiled-coil domain. Whereas their GTPase domain implies a GTP-dependence of the phenomena involved in the mitochondrial fusion (Chen et al., 2003; Ishihara et al., 2004; Olichon et al., 2007), the coiled-coil domain also plays a major role since it allows homotypic (Mfn1-Mfn1, Mfn2-Mfn2 et Opa1-Opa1) or heterotypic (Mfn1-Mfn2) interaction of these proteins (Chen et al., 2003). The non-transmembrane part of Mfns, which is located in the cytosol, allows, through the interaction of the coiled-coil domains of two distinct Mfn proteins, the formation of a physical link between the outer membranes of two neighboring mitochondria (Koshiba et al., 2004; Chan, 2006). Thus, these two outer membranes become closer and the fusion of the involved mitochondria is initiated. In a similar way, the formation of Opa1-Opa1 homotypic complexes leads to the fusion of the inner membranes of the mitochondria engaged in the fusion process (for review see Liesa et al., 2009).

The specificity of action of these proteins is partly due to their anchorage to the membranes of which they control the fusion. However, the specific localization of each protein does not seem to be exclusive since Opa1 exists in a soluble form, which has been detected in an isolated outer mitochondrial membrane fraction, indicating that this Opa1 isoform is able to interact with the outer membrane (Satoh et al., 2003). Besides, this observation combined to the description of a direct interaction between Mfns and Opa1 (Guillery et al., 2008) could in part explain the synchronization of Mfns and Opa1 action. Indeed, the coordination of these proteins is still mysterious because no clear mechanism has been claimed and no equivalent to Ugo1, the yeast protein known to be involved in the coordination of Mfns and Opa1 yeast orthologs (Fzo et Mgm1, Hales and Fuller, 1997; Alexander et al., 2000), has been described in mammals.

Whereas the mechanisms involved in mitochondrial fusion seem to be relatively well-understood, the processes regulating mitochondrial fission still raise some questions. During the end of the 1990s and the beginning of the 2000s, many studies were interested in the dynamin-related protein 1 (Drp1), also called Dynamin-like protein 1 (Dlp1), and the mitochondrial fission

protein 1 (Fis1), which were considered as the major actors of mitochondrial fission. Drp1 is a cytosolic protein which comprises a GTPase domain and migrates to mitochondria using dynein and the microtubule (Varadi et al., 2004) or the actine network (De Vos et al., 2005), depending on the fission initiating factor. After this migration, Drp1 is specifically found at the level of the future fission site where it oligomerizes to form a ring, the GTP-dependence constriction of this ring leading to mitochondrial division (Yoon et al., 2001; Ingerman et al., 2005). Interestingly, while phosphorylated Drp1 stays inactive in the cytosol, Drp1 activity can be modulated by calcium through the activation of calcineurin which participates in Drp1 mitochondrial recruitment by dephosphorylating it. This mechanism could be of high significance in muscle cells where calcium is cyclically released from the SR (Cribbs and Strack, 2007; Cereghetti et al., 2008). Knowing that this protein does not exhibit any transmembrane domain necessary for its anchorage to the mitochondrial membranes, its mitochondrial localization requires a docking receptor on the outer mitochondrial membrane. Fis1 was the first protein described as the mitochondrial receptor (Yoon et al., 2003). Fis1 which is anchored in the outer mitochondrial membrane has an intracellular facing domain containing five α-helices which allow oligomerization (for the first α-helix) and direct or indirect interaction with Drp1 (for the all set of α-helices) (Jofuku et al., 2005).

Although many experimental studies have established an undeniable role of Fis1 in mitochondrial fission, the recruitment of Drp1 to mitochondria is not affected by Fis1 deficiency (Lee et al., 2004; Wasiak et al., 2007). Thus, Fis1 does not appear to be the only factor involved in Drp1 mitochondrial recruitment. Three other proteins have been described like the mitochondria fission factor (Mff) (Otera et al., 2010), the mitochondrial dynamics protein of 49 kDa (MiD49) or 51 kDa (MiD51) (Palmer et al., 2011). As Fis1, these three proteins are anchored to the outer mitochondrial membrane (Gandre-Babbe and van der Bliek, 2008; Palmer et al., 2011). The involvement of each protein in mitochondrial fission is, however, not yet clearly defined, and the interaction of these proteins with Drp1 could require other intermediary proteins. This is the case in the yeast in which the interaction of Drp1 and Fis1 orthologs needs several other proteins like Mdv1 and Caf4 (Tieu et al., 2002; Griffin et al., 2005); however, no such proteins have been described in mammals so far.

If a specific machinery of the inner mitochondrial membrane fission exists, it remains unknown. Although, it is suggested that the MDM33 protein is involved in the fission of the inner membrane of *Saccharomyces cerevisae* mitochondria (Messerschmitt et al., 2003), no MDM33 ortholog has been found in mammals. Even if a study proposes that a protein called Mtp18 (Mitochondrial protein 18) could be an actor of this unknown inner mitochondrial membrane fission machinery (Tondera et al., 2005), this clearly requires further investigations.

Finally, mechanisms governing mitochondrial fragmentation seem to be less specific than those involved in mitochondrial fusion. Indeed, Drp1, Fis1, and Mff which are responsible for mitochondrial fission are also implicated in peroxisome fission (Koch et al., 2003, 2005; Gandre-Babbe and van der Bliek, 2008); however, the synchronization or the joint regulation of these two phenomena has never been explored. The fact that the fission of these two organelles involves the same proteins should not be coincidental. It can be noticed that mutations in genes encoding these proteins have been involved in serious diseases, and in particular in neurological diseases such as Charcot-Marie-Tooth type 2A or autosomal dominant optic atrophy (ADOA) (Alexander et al., 2000; Delettre et al., 2001; Zuchner et al., 2004). In heart failure (HF), recent data also suggest their possible implication in the progression of the pathology (Chen et al., 2009), suggesting a role of these proteins in cardiac tissue.

WHAT ABOUT MITOCHONDRIAL DYNAMICS IN THE HEART?

Whereas it has long been suggested that adult cardiomyocytes would show a limited mitochondrial dynamics because of the complex cytoarchitecture of this cell, the high expression level of dynamin proteins in the heart (Alexander et al., 2000; Delettre et al., 2001; Santel et al., 2003; Gandre-Babbe and van der Bliek, 2008) implies that these actors could play roles which would not be anecdotal. Thus, many research groups have tried to explain mitochondrial dynamics in the heart for a few years. However, knowing that the initial experiments were done with immortalized cardiac cell lines (H9c2, HL-1) or with neonatal cardiomyocytes (Shen et al., 2007; Parra et al., 2008; Twig et al., 2008a) in which mitochondria face an environment very different from the adult one (Leu et al., 2001; Piquereau et al., 2010), the first data about mitochondrial fusion and fission obtained in the mature heart are relatively new and consequently these phenomena are not clearly understood yet.

Existence of mitochondrial dynamics in the adult heart

Mitochondrial dynamics comprises two main notions, one is the capacity of mitochondrial to move within the cell and the second relates to the capacity to undergo fusion and fission, these two notions not being mutually exclusive. As presented above, the adult cardiac muscle cell is an extremely organized cell in which the mitochondrial movements are greatly restricted (Beraud et al., 2009; Hom and Sheu, 2009). Moreover, the fusion/fission events appear to be greatly slowed compared to neonatal cardiomyocytes, and mitochondria are poorly connected. It has been recently suggested that the fusion/fission cycle would last 14–16 days in adult cardiomyocytes (Chen et al., 2011). Thus, mitochondrial dynamics could seem irrelevant, although mitochondria have a limited life span, being subjected to biogenesis and autophagy/mitophagy, which are strictly dependent on fusion and fission phenomena (Diaz and Moraes, 2008; Twig et al., 2008b). Consequently, even if fusion or fission events have never been observed in real time, this mitochondrial turnover imposes mitochondrial dynamics as an essential cog of cardiac physiology.

Phenotypic examination of genetically modified mice has recently substantiated our knowledge. Major changes in mitochondrial morphology have been described in mice with inducible cardiac Mfn2 ablation (Papanicolaou et al., 2011), or decrease in Opa1 protein content (Piquereau et al., 2012). However, the observation of larger mitochondria in Mfn2 and Opa1 deficient mice made by Walsh's group (Papanicolaou et al., 2011) and our team (Piquereau et al., 2012) is surprising because

it contradicts the previously published data. Indeed, while several studies on non-cardiac cells (Chen et al., 2003; Olichon et al., 2003; Yoon et al., 2003; Cipolat et al., 2004; Stojanovski et al., 2004; Griparic et al., 2007) evidenced that a decrease in expression of a fusion protein would lead, respectively, to mitochondrial network fragmentation, in these animal studies, deficiency in the fusion proteins Mfn2 or Opa1 led to paradoxically larger cardiac mitochondria. Thus, it appears that the specific architectural organization of this cell impact on the phenomena and presumably affects the mode of action of these proteins. On the other hand, the cardiac-specific Mfn1-null mice showed a fragmentation of the mitochondrial network (Papanicolaou et al., 2012); this observation reinforces the idea that Mfn1 and Mfn2 play different roles. Finally, the conditional combined Mfn1/Mfn2 ablation in adult hearts induces mitochondrial network fragmentation (Chen et al., 2011). Thus, mitochondrial dynamics exists in the heart tissue, but is a complex process that depends on the specific cell architecture.

Beyond the fact that these genetically-manipulated mice show obvious changes in cardiac mitochondrial morphology, significant deleterious consequences on their cardiac function were observed under stress (Papanicolaou et al., 2011; Piquereau et al., 2012), suggesting a direct involvement of the mitochondrial morphology in the heart function. At present, it is complicated to determine how and to which extent the morphology of mitochondria affects cardiac efficiency. For example, our group has already evidenced that changes in the mitochondrial volume may directly impact the force developed by myofibrils (Kaasik et al., 2004) as well as the direct energetic transfers between mitochondria and myofilaments (Piquereau et al., 2012). Even if these studies are insufficient to conclude that these mechanisms are responsible for the cardiac alterations observed in the previously described models, they suggest a direct link between mitochondrial morphology and cardiac contractile function. However, it is not easy to get an overall understanding of the mechanisms governing mitochondrial fusion and fission in the heart, even if it obviously seems that mitochondrial dynamics exists in this organ on a very slow time-course in the normal heart.

Impact of mitochondrial dynamics alterations on respiratory capacities

It is generally accepted that fusion-fission processes impact on the mitochondrial energetics in cultured cells (Chen et al., 2003). Disruption of mitochondrial dynamics by overexpression or suppression of fusion (Mfn2, Opa1) (Olichon et al., 2003; Chen et al., 2005) or mitochondrial fission (Benard et al., 2007), can cause alterations in mitochondrial metabolism (Chen and Chan, 2005), according to the degree of differentiation of the considered cell type. These changes may be accompanied by the modulation of the mitochondrial membrane potential, and of the expression of complex I, IV, and V subunits (Pich et al., 2005; Chan, 2006; Liesa et al., 2009). However, in patients and in mouse models, direct effect of dynamin mutations on mitochondrial function gave conflicting results, probably because of the diversity of the cell types and the mutations studied (Olichon et al., 2006). In general, it is considered that fragmentation induced by an increase in Drp1 or a decrease in Mfn2 or Opa1 is harmful and leads to metabolic disorders (Parra et al., 2011). In contrast, fusion is generally considered rather beneficial. But a careful look at the literature shows that there is no clear link between mitochondria morphology and respiratory capacities, especially in mature cardiac cell. Indeed, in three different studies, no obvious alterations of respiratory chain function were observed when Opa1, Mfn1 or Mfn2 were separately genetically downregulated (Papanicolaou et al., 2011, 2012; Piquereau et al., 2012), except for free fatty-acid utilization in Opa1$^{+/-}$ mice (Piquereau et al., 2012). In another study where a different Opa1 mutation was studied, mitochondrial function alterations were only observed in old mice (Chen et al., 2012). Finally, when complete/double KO (Mfn1/Mfn2) was used to suppress fusion proteins, decreased oxygen consumption or increased oxidative stress was observed (Chen et al., 2011; Dorn et al., 2011). Thus, compensatory mechanisms with other dynamin proteins may exist and attenuate the consequences of one dynamin protein deficiency, but complete loss or aging will be detrimental for mitochondrial function. In addition to an effect on respiratory chain function, other mitochondrial functions can also be affected by mitochondrial dynamics protein alterations.

Implication in mitochondrial biogenesis

As mentioned above, the mechanisms involved in mitochondrial dynamics in the cardiomyocyte seem not to be exactly similar to those observed in proliferative cells. However, this complexity is easily understood when the cardiomyocyte is regarded as a cell presenting a strictly organized intracellular architecture which is not in favor of mitochondrial plasticity as in dividing cells. It is thus important to keep in mind this notion when extrapolating results obtained during the early development to adulthood. Obviously, the role of mitochondrial dynamics is different in prenatal and neonatal cardiomyocytes which proliferate and consequently need the synthesis of new mitochondria to assure a suitable repartition of these organelles between daughter cells obtained after mitosis, and in non-dividing adult cardiomyocytes. Not surprisingly, we already described a remarkably high level of expression of mitochondrial biogenesis and dynamics genes during the early stages of postnatal development in the heart (Piquereau et al., 2013). Thus, this important stimulation of mitochondrial biogenesis and therefore of mitochondrial dynamics during development could explain why the cardiac-specific ablation of dynamins during prenatal or early postnatal development quickly leads to HF and death while several months are needed when the ablation occurs at the beginning of adulthood (Chen et al., 2011; Papanicolaou et al., 2012; Dorn, 2013). More generally, this could explain the lethality of the total dynamin knock-out models which die *in utero* (Alavi et al., 2007; Chen et al., 2011), a period during which the mitotic activity is undeniably substantial.

Globally, it would seem that mitochondrial dynamics is particularly important when the heart is under conditions which require the synthesis of new mitochondria. This is the case during development, but also in stress conditions like ischemia (Ong et al., 2010) or pressure overload (Piquereau et al., 2012) or ageing (Chen et al., 2012) which induce increased energetic demand and mitochondrial damages and consequently requires an adequate mitochondrial turnover. That is certainly the reason

why the mice genetically manipulated to abolish Mfn2 expression or to decrease Opa1 expression exhibit a high sensitivity to stress. This highlights the fact that the reduced mitochondrial dynamics can be partly compensated under baseline conditions while under stress the mitochondrial turnover cannot be ensured and precipitates cardiac dysfunction. Finally, inducible cardiac-specific double ablation of Mfn1 and Mfn2 genes quickly led to dilated cardiomyopathy before inducing death within 9 weeks after gene ablation. Interestingly, the heterozygous mutation of the Drp1 gene also induced a dilated cardiomyopathy in mice (Ashrafian et al., 2010). The cardiac dysfunction observed in these genetically-manipulated mice clearly shows that these proteins play a fully-fledged role in cardiac muscular cell physiology.

Other roles of mitochondrial dynamics proteins

All dynamins described above are of course widely known for the role they play in mitochondrial dynamics; however, these proteins could have a broader field of action than it seems (**Figure 2**). Several studies assigned them an effect on the property of the MPTP, a non-selective pore which induces, in particular situations, a high permeability of the mitochondrial membranes and can lead to cell death (Di Lisa and Bernardi, 2009). Indeed, we and others showed that the adult cardiomyocytes partially deficient in Opa1 (Piquereau et al., 2012) or totally deficient in Mfn1 or Mfn2 (Papanicolaou et al., 2011, 2012) exhibit a delayed Ca^{2+}-induced MPTP opening. Knowing that these observations have been obtained in isolated cardiomyocytes with enlarged or fragmented mitochondria, they suggest that the individual volume of the mitochondria are not directly involved and that Opa1 and mitofusins could facilitate MPTP opening under normal conditions. The mechanisms leading to this protection are far from being elucidated. Moreover, the data obtained from adult heart deficient in the two mitofusins, which did not show any change in MPTP sensitivity in comparison with wild type (Chen et al., 2011), complicate the understanding even if the experimental conditions differ (isolated mitochondria vs. cardiomyocytes).

Whereas their involvement in the prevention of MPTP opening could indirectly confer to Opa1 and mitofusins an indirect role in cardiomyocyte death, it seems, however, that the role of the mitochondrial dynamics proteins in cell death is not really clear. It is well-known that mitochondria are central elements in cell death, and a link between mitochondrial network fragmentation and apoptosis has been already described in cell lines (Frank et al., 2001; Breckenridge et al., 2003) and in neonatal cardiomyocytes, suggesting an important role of fission protein, especially Drp1 (Parra et al., 2008; Wakabayashi et al., 2009), in this form of cell death. The fusion proteins could also be directly involved in cell death by acting in an original way. Even if the data obtained from studies realized with cell lines assert that fusion is prosurvival while fission is proaptotic, Mfn2 could participate in apoptosis. The participation of Mfn2 to this particular death has been demonstrated in cardiomyocytes and smooth muscle cells (Guo et al., 2007; Shen et al., 2007). The details of this mechanism are still unclear, although an interaction between Mfn2 and the pro-apoptotic protein Bax has been described (Hoppins et al., 2011b). On the other hand, Opa1 would have an opposite role and could be an antiapoptotic factor. Indeed, this protein would regulate cell death by forming oligomers of two Opa1 proteins creating a "bottle neck"-like structure which allows cytochrome c sequestration in the cristae (Frezza et al., 2006). By this oligomerization, Opa1

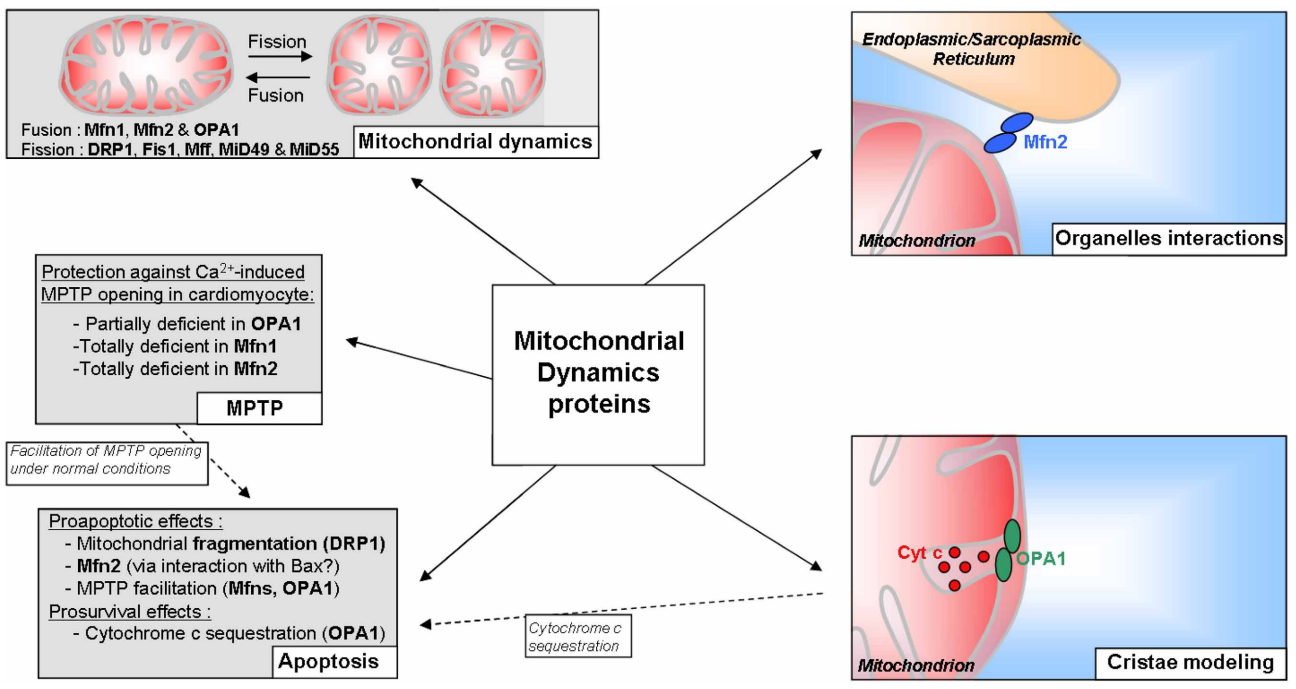

FIGURE 2 | Scheme summarizing the potential roles of mitochondrial dynamics proteins in the adult cardiomyocyte.

is in fact a crucial protein in the mitochondrial internal organization which is, as stated above, essential for the functions of these organelles.

Thus, mitochondrial dynamics proteins are clearly essential for the adaptation of those organelles to cell status. Moreover, some of them could be at the heart of the interaction between mitochondria and other components of the cell. Indeed, Mfn2, but not Mfn1, is also found at the endoplasmic reticulum (ER) membrane and thus can create physical links between ER and mitochondria (de Brito and Scorrano, 2008). This link has been recently shown between mitochondria and SR in muscle cells (Dorn and Maack, 2013); considering the calcium and energetic microdomains at the interface of mitochondria and SR described in the cardiomyocytes, Mfn2 could be a major actor of the contractile function of the heart.

Moreover, the physical links between ER and mitochondria were demonstrated to increase following ER stress (Csordas et al., 2006), a specific response triggered when ER homeostasis is disrupted and ER function is compromised. In the heart, ER stress has recently been recognized as an important contributor to the development of cardiac dysfunction (Groenendyk et al., 2013), and the link between ER stress and Mfns has started to be investigated. By using knock-out mice, Ngoh and colleagues demonstrated that cardiomyocyte-specific deletion of Mfn2, but not Mfn1, induces ER stress *in vivo*, leading to the conclusion that Mfn2 is a negative regulator of ER stress required for the homeostasis of the ER (Ngoh et al., 2012).

Even if the mechanism is not fully understood, Mfn2 is also involved in cardiac autophagic processes (Zhao et al., 2012). These authors showed that Mfn2 could participate in autophagosome-lysosome fusion. Due to the presence of Mfn2 in the ER and thus autophagosome membrane, it might act as an adaptor protein mediating autophagosome maturation. This link between Mfn2 and autophagy is reminiscent of the fact that mitochondrial dynamics proteins are also major actors of selective mitochondrial autophagy, i.e., mitophagy. Indeed, it is largely admitted that selective clearance of mitochondria are preceded by fission phenomena (Twig et al., 2008b). In fact, in the early event of mitophagy, Drp1 is recruited to mitochondria (Lee et al., 2011) and Mfns, present at the membrane of damaged mitochondria, are rapidly ubiquitined (Ziviani et al., 2010). This Mfns ubiquitination could thus address these proteins to the proteasome or could interfere with mitochondrial tethering and prevent altered mitochondria to join the mitochondria network (Ziviani and Whitworth, 2010). Besides, in addition to the low mitochondrial potential allowing identification of mitochondria destined to mitophagy, these mitochondria would exhibit a low Opa1 amount at the inner membrane (Twig et al., 2008a). This creates non-fusing mitochondria which thus have only one destiny: degradation.

Finally, changes in the components of mitochondrial dynamics can also alter mtDNA. Observations in S. cerevisiae and MEF cells indicate that the normal activity of Opa1 (Jones and Fangman, 1992; Guan et al., 1993; Chen et al., 2007) or Mfns (Hermann et al., 1998; Rappaport et al., 1998; Chen et al., 2003, 2007) are crucial for maintaining the integrity of mtDNA nucleoids (Liesa et al., 2009). Part of Opa1 could be involved in the attachment of mtDNA to the inner mitochondrial membrane and to promote mtDNA replication and distribution (Elachouri et al., 2011). In the mature heart, one study reported that heterozygous Opa1$^{+/-}$ mice exhibit reduced mtDNA copy number (Chen et al., 2012), which could be involved in the development of cardiac mitochondrial dysfunction.

Finally, even if the number of studies devoted to the role of mitochondrial dynamics proteins in the heart is limited (**Table 1**), it can be asserted that these proteins are clearly integral part of cardiomyocyte life by ensuring fusion/fission processes and by participating in the several mechanisms described above. Interestingly, it seems that these proteins would be particularly important under stress conditions which are known to mobilize or affect mitochondrial functions. These kinds of situations exacerbate mitochondrial biogenesis and turnover which are relatively low under basal conditions, showing the major significance of the processes governed by these proteins in cardiac adaptations.

ALTERATIONS OF MITOCHONDRIAL DYNAMICS IN CARDIAC PATHOLOGIES AND POSSIBLE THERAPEUTIC APPROACHES

Chronic HF is associated with morphologic abnormalities of cardiac mitochondria including increased number, reduced organelles size, and compromised structural integrity (Schaper et al., 1991; Sabbah et al., 1992; Beutner et al., 2001), suggesting fragmentation of the mitochondrial network (Joubert et al., 2008). Mitochondrial damages as the depletion of the mitochondrial matrix and disruption of membranes positively correlate with the HF severity index (Sabbah et al., 1992) and it is recognized that mitochondria can determine the cellular fate (Di Lisa and Bernardi, 1998). In other pathologies, mega-mitochondria can appear (for review, see Wakabayashi, 2002 and Hoppel et al., 2009). Most of the time, heterogeneity of the size and distribution of cardiac mitochondria increases in HF, evidencing unbalanced fusion/fission cycles. Thus, an emerging hypothesis is that the mechanisms that control the shape of mitochondria may play a role in cardiac pathologies. In particular, a recent study suggested that Opa1 could be downregulated in HF (Chen et al., 2009; Chen and Knowlton, 2010). Another study observed a decrease in Mfn2, an increase in Fis1, and no change in Opa1 expression in rat hearts 12–18 weeks after myocardial infarction (Javadov et al., 2011). However, alteration of dynamin proteins could merely be the consequence of the alteration of mitochondrial biogenesis as it has been suggested (Garnier et al., 2005; Ventura-Clapier et al., 2011). Indeed, a strict relation exists between the PPAR gamma coactivator-1 (PGC-1α), a master regulator of mitochondrial biogenesis, and the expression of these proteins (Garnier et al., 2005). Moreover, in most cardiac pathologies where defect in dynamin proteins are observed, a decrease in mitochondrial mass is also present (Ventura-Clapier et al., 2011; Parra et al., 2011). So it is not clear so far which protein alteration is responsible for a possible unbalance in fusion/fission, and the post-translational modifications of, for example, Drp1 (see above) could also be involved. Similarly, nothing is known about a possible implication of GTP/GDP supply in mitochondrial dynamics regulation.

Cell death is also an important pathophysiological process in both HF and in cardiac ischemia. However, the underlying mechanisms by which the heart looses myocytes in HF are not

Table 1 | Mitochondrial dynamic studies on the mature heart.

Authors	Tissue	Model	Mitochondrial morphology	Alterations	Observations
Shahrestani et al., 2009	Drosophila	OPA1$^{+/-}$		Decreased heart rate and increased heart arrhythmia	Poor tolerance to stress induced by electrical pacing
Dorn et al., 2011	Drosophila	OPA1 RNAi	Decrease of mean mitochondrial size	Contractile abnormality and remodeling	Stimulation of mitochondrial biogenesis
Piquereau et al., 2012	Mouse (3–6 months)	OPA1$^{+/-}$	Enlarged mitochondria, cristae disorganization	No alteration of cardiac function nor change in QO_2, but delay of MPTP opening and energy transfer alteration	More sensitive to transaortic constriction (TAC)
Chen et al., 2012	Mouse (12 months)	OPA1$^{+/-}$	Disorganization of mitochondrial network	Reduced mtDNA level, mitochondria and cell dysfunction	Increased of oxidative stress and late-onset cardiomyopathy
Dorn et al., 2011	Drosophila	Marf RNAi	Decrease of mean mitochondrial size	Contractile abnormality and remodeling	Stimulation of mitochondrial biogenesis
Papanicolaou et al., 2011	Mouse	Mfn2 KO	Enlarged mitochondria	No major cardiac and mitochondrial dysfunction, delay of MPTP opening	Protection against cell death induced injury and better recovery after I/R
Papanicolaou et al., 2012	Mouse	Mfn1 KO	Fragmented mitochondria	Normal cardiac and mitochondrial function, decreased of ROS induced MPTP opening	protection against ROS induced mitochondrial dysfunction
Chen et al., 2012	Mouse	Mfn1/Mfn2 DKO	Fragmented mitochondria	Cardiomyocyte and mitochondrial respiratory dysfunction	Progressive and lethal dilated cardiomyopathy
Ngoh et al., 2012	mice	Inducible Mfn2 KO	Fragmentation	Increased markers of the ER stress	Mfn2 is necessary for ER homeostasis
Ashrafian et al., 2010	Mouse	Drp1 mutation$^{+/-}$		Reduced mitochondrial complexes levels and cardiac ATP depletion	Energy deficiency may contribute to cardiomyopathy
Chen et al., 2009	Rat	Heart failure	Decrease of mean individual mitochondrial size	decrease of OPA1 protein level	
Ong et al., 2010	Rat	Ischemia/ reperfusion and drp1 inhibition by mdivi-1	Presence of elongated mitochondria in control heart	Mitochondrial fragmentation prevented by mdivi-1 after I/R	Decrease of infarct size in I/R after treatment with an inhibitor of Drp1

completely understood. Mitochondria have a critical role in regulating cardiac cell death. If fission is interrupted, large networks of fused mitochondria occur. If fusion fails, mitochondria become smaller and fragmented. Abnormalities in fission and fusion can lead to apoptosis (Lee et al., 2004; Cassidy-Stone et al., 2008) which is an important mechanism of cardiac myocyte loss in HF (Olivetti et al., 1997; Narula et al., 1999). So both HF and ischemia could be associated with abnormalities of fission and fusion that would contribute to cardiac cell death and change of MPTP sensitivity. In particular, after ischemia-reperfusion, mitochondria of cardiomyocytes show heterogeneous damages in their morphology, in redox status and in calcium homeostasis, which could be related to an overproduction of local ROS (Ong et al., 2012).

Modulation of mitochondrial dynamics appears as a novel pharmacological strategy for cardioprotection, in particular to protect the heart after a heart attack, and in ischemia-reperfusion [see reviews by Ong et al. (2012) and Dorn (2013)]. Several studies have shown that changes in mitochondrial morphology, including targeting proteins of the mitochondrial dynamics could allow the heart to better recover from an ischemic insult (Ong et al., 2010; Papanicolaou et al., 2011). In the first study, the authors used a specific inhibitor of Drp1, Mdiv-1, to prevent mitochondrial fission, and observed a significant reduction in myocardial infarct size in the *in vivo* murine heart. In the second one, using a genetic model of Mfn2 KO mice, they observed an improvement of cardiac performance following *ex vivo* ischemia/reperfusion. In both cases, even if the strategy was different (decrease the fission in one case, decrease the fusion in the second case), they linked the protection to the inhibition of MPTP opening, which is a classical target of cardioprotection. However, it should be kept in mind that although inhibition of MPTP can be beneficial in short term, it could be detrimental on the long term (Elrod et al., 2010; Piquereau et al., 2012).

CONCLUSION

Generally, studies described above prove that mitochondrial dynamics proteins are necessary for normal mitochondrial functions in the cardiomyocyte. In this cell where the internal organization is an obstacle to organelles mobility, these proteins govern slow fusion/fission processes which ensure mitochondrial turnover required to maintain mitochondrial function and consequently organ function. It also seems that mitochondrial dynamics would be a key element of cardiomyocyte adaptation under stress which induce alteration of mitochondria and thus lead to generation of new mitochondria and degradation of damaged mitochondria. Under such conditions, mitochondrial dynamics processes would be exacerbated and would assume greater significance, explaining why the genetically-manipulated mice for mitochondrial dynamics genes are particularly sensitive to stress. Therefore, the high expression level of dynamins under basal conditions, despite the slow fusion/fission cycle, could be a major element of cardiac adaptation. In addition, those proteins could be activated by post-translational modifications involved in signaling pathways activated in response to stress. It can be anticipated that those potential post-translational modifications would be the more efficient way to ensure an optimal reactivity of mitochondrial dynamics machinery under stress.

Finally, mitochondrial dynamics proteins are involved in several phenomena irrespectively of their role in mitochondrial dynamics. This aspect of these dynamins has to be kept in mind because they are essential for the adequate function of mitochondria and cell life. By their extended field of action, these proteins are clearly established as major components of cardiac physiology.

ACKNOWLEDGMENTS

We thank Dominique Fortin for skillful technical assistance and R. Fischmeister for continuous support. We are grateful to Marcel Alavi (Johannes-Gutenberg Universität Mainz, Germany) for sharing the *Opa1*$^{+/-}$ mouse line. This work was supported by grants from Région Ile de France CORDDIM, VEGA project to Marta Novotova VEGA 2/0116/12, APVV projects APVV-SK-FR-0021-11 and APVV-0721-10, Labex Lermit and a French/Slovak grant PHC STEFANIK 2013 N° 26340QF. Renee Ventura-Clapier and Frederic Joubert are scientists at the Centre National de la Recherche Scientifique.

REFERENCES

Alavi, M. V., Bette, S., Schimpf, S., Schuettauf, F., Schraermeyer, U., Wehrl, H. F., et al. (2007). A splice site mutation in the murine Opa1 gene features pathology of autosomal dominant optic atrophy. *Brain* 130, 1029–1042.

Alexander, C., Votruba, M., Pesch, U. E., Thiselton, D. L., Mayer, S., Moore, A., et al. (2000). OPA1, encoding a dynamin-related GTPase, is mutated in autosomal dominant optic atrophy linked to chromosome 3q28. *Nat. Genet.* 26, 211–215.

Ashrafian, H., Docherty, L., Leo, V., Towlson, C., Neilan, M., Steeples, V., et al. (2010). A mutation in the mitochondrial fission gene Dnm1l leads to cardiomyopathy. *PLoS Genet.* 6:e1001000. doi: 10.1371/journal.pgen.1001000

Balaban, R. S. (2012). Perspectives on: SGP symposium on mitochondrial physiology and medicine: metabolic homeostasis of the heart. *J. Gen. Physiol.* 139, 407–414.

Benard, G., Bellance, N., James, D., Parrone, P., Fernandez, H., Letellier, T., et al. (2007). Mitochondrial bioenergetics and structural network organization. *J. Cell Sci.* 120, 838–848.

Beraud, N., Pelloux, S., Usson, Y., Kuznetsov, A. V., Ronot, X., Tourneur, Y., et al. (2009). Mitochondrial dynamics in heart cells: very low amplitude high frequency fluctuations in adult cardiomyocytes and flow motion in non beating Hl-1 cells. *J. Bioenerg. Biomembr.* 41, 195–214.

Bereiter-Hahn, J. (1990). Behavior of mitochondria in the living cell. *Int. Rev. Cytol.* 122, 1–63.

Beutner, G., Sharma, V. K., Giovannucci, D. R., Yule, D. I., and Sheu, S. S. (2001). Identification of a ryanodine receptor in rat heart mitochondria. *J. Biol. Chem.* 276, 21482–21488.

Breckenridge, D. G., Stojanovic, M., Marcellus, R. C., and Shore, G. C. (2003). Caspase cleavage product of BAP31 induces mitochondrial fission through endoplasmic reticulum calcium signals, enhancing cytochrome c release to the cytosol. *J. Cell Biol.* 160, 1115–1127.

Campello, S., and Scorrano, L. (2010). Mitochondrial shape changes: orchestrating cell pathophysiology. *EMBO Rep.* 11, 678–684.

Cassidy-Stone, A., Chipuk, J. E., Ingerman, E., Song, C., Yoo, C., Kuwana, T., et al. (2008). Chemical inhibition of the mitochondrial division dynamin reveals its role in Bax/Bak-dependent mitochondrial outer membrane permeabilization. *Dev. Cell* 14, 193–204.

Cereghetti, G. M., Stangherlin, A., Martins de Brito, O., Chang, C. R., Blackstone, C., Bernardi, P., et al. (2008). Dephosphorylation by calcineurin regulates translocation of Drp1 to mitochondria. *Proc. Natl. Acad. Sci. U.S.A.* 105, 15803–15808.

Chan, D. C. (2006). Mitochondrial fusion and fission in mammals. *Annu. Rev. Cell Dev. Biol.* 22, 79–99.

Chen, H., and Chan, D. C. (2005). Emerging functions of mammalian mitochondrial fusion and fission. *Hum. Mol. Genet.*14, R283–R289.

Chen, H., Chomyn, A., and Chan, D. C. (2005). Disruption of fusion results in mitochondrial heterogeneity and dysfunction. *J. Biol. Chem.* 280, 26185–26192.

Chen, H., Detmer, S. A., Ewald, A. J., Griffin, E. E., Fraser, S. E., and Chan, D. C. (2003). Mitofusins Mfn1 and Mfn2 coordinately regulate mitochondrial fusion and are essential for embryonic development. *J. Cell Biol.* 160, 189–200.

Chen, H., McCaffery, J. M., and Chan, D. C. (2007). Mitochondrial fusion protects against neurodegeneration in the cerebellum. *Cell* 130, 548–562.

Chen, L., Gong, Q., Stice, J. P., and Knowlton, A. A. (2009). Mitochondrial OPA1, apoptosis, and heart failure. *Cardiovasc. Res.* 84, 91–99.

Chen, L., and Knowlton, A. A. (2010). Mitochondria and heart failure: new insights into an energetic problem. *Minerva Cardioangiol.* 58, 213–229.

Chen, L., Liu, T., Tran, A., Lu, X., Tomilov, A. A., Davies, V., et al. (2012). OPA1 mutation

and late-onset cardiomyopathy: mitochondrial dysfunction and mtDNA instability. *J. Am. Heart Assoc.* 1:e003012. doi: 10.1161/JAHA.112.003012

Chen, Y., Liu, Y., and Dorn, G. W. 2nd. (2011). Mitochondrial fusion is essential for organelle function and cardiac homeostasis. *Circ. Res.* 109, 1327–1331.

Cipolat, S., Martins de Brito, O., Dal Zilio, B., and Scorrano, L. (2004). OPA1 requires mitofusin 1 to promote mitochondrial fusion. *Proc. Natl. Acad. Sci. U.S.A.* 101, 15927–15932.

Collins, T. J., Berridge, M. J., Lipp, P., and Bootman, M. D. (2002). Mitochondria are morphologically and functionally heterogeneous within cells. *EMBO J.* 21, 1616–1627.

Cribbs, J. T., and Strack, S. (2007). Reversible phosphorylation of Drp1 by cyclic AMP-dependent protein kinase and calcineurin regulates mitochondrial fission and cell death. *EMBO Rep.* 8, 939–944.

Csordas, G., Renken, C., Varnai, P., Walter, L., Weaver, D., Buttle, K. F., et al. (2006). Structural and functional features and significance of the physical linkage between ER and mitochondria. *J. Cell Biol.* 174, 915–921.

Davies, K. M., Daum, B., Kuhlbrandt, W., Anselmi, C., and Faraldo-Gomez, J. (2012). Structure of the mitochondrial ATP synthase and its role in shaping mitochondria cristae. *Microsc. Microanal.* 18(Suppl. 2), 56–57.

Davies, K. M., Strauss, M., Daum, B., Kief, J. H., Osiewacz, H. D., Rycovska, A., et al. (2011). Macromolecular organization of ATP synthase and complex I in whole mitochondria. *Proc. Natl. Acad. Sci. U.S.A.* 108, 14121–14126.

de Brito, O. M., and Scorrano, L. (2008). Mitofusin 2 tethers endoplasmic reticulum to mitochondria. *Nature* 456, 605–610.

Delettre, C., Griffoin, J. M., Kaplan, J., Dollfus, H., Lorenz, B., Faivre, L., et al. (2001). Mutation spectrum and splicing variants in the OPA1 gene. *Hum. Genet.* 109, 584–591.

De Vos, K. J., Allan, V. J., Grierson, A. J., and Sheetz, M. P. (2005). Mitochondrial function and actin regulate dynamin-related protein 1-dependent mitochondrial fission. *Curr. Biol.* 15, 678–683.

Diaz, F., and Moraes, C. T. (2008). Mitochondrial biogenesis and turnover. *Cell Calcium* 44, 24–35.

Di Lisa, F., and Bernardi, P. (1998). Mitochondrial function as a determinant of recovery or death in cell response to injury. *Mol. Cell Biochem.* 184, 379–391.

Di Lisa, F., and Bernardi, P. (2009). A CaPful of mechanisms regulating the mitochondrial permeability transition. *J. Mol. Cell Cardiol.* 46, 775–780.

Dorn, G. W. 2nd. (2013). Mitochondrial dynamics in heart disease. *Biochim. Biophys. Acta* 1833, 233–241.

Dorn, G. W. 2nd., Clark, C. F., Eschenbacher, W. H., Kang, M. Y., Engelhard, J. T., Warner, S. J., et al. (2011). MARF and Opa1 control mitochondrial and cardiac function in Drosophila. *Circ. Res.* 108, 12–17.

Dorn, G. W. 2nd., and Maack, C. (2013). SR and mitochondria: calcium cross-talk between kissing cousins. *J. Mol. Cell Cardiol.* 55, 42–49.

Elachouri, G., Vidoni, S., Zanna, C., Pattyn, A., Boukhaddaoui, H., Gaget, K., et al. (2011). OPA1 links human mitochondrial genome maintenance to mtDNA replication and distribution. *Genome Res.* 21, 12–20.

Elrod, J. W., Wong, R., Mishra, S., Vagnozzi, R. J., Sakthievel, B., Goonasekera, S. A., et al. (2010). Cyclophilin D controls mitochondrial pore-dependent Ca(2+) exchange, metabolic flexibility, and propensity for heart failure in mice. *J. Clin. Invest.* 120, 3680–3687.

Frank, S., Gaume, B., Bergmann-Leitner, E. S., Leitner, W. W., Robert, E. G., Catez, F., et al. (2001). The role of dynamin-related protein 1, a mediator of mitochondrial fission, in apoptosis. *Dev. Cell* 1, 515–525.

Frezza, C., Cipolat, S., Martins de Brito, O., Micaroni, M., Beznoussenko, G. V., Rudka, T., et al. (2006). OPA1 controls apoptotic cristae remodeling independently from mitochondrial fusion. *Cell* 126, 177–189.

Gandre-Babbe, S., and van der Bliek, A. M. (2008). The novel tail-anchored membrane protein Mff controls mitochondrial and peroxisomal fission in mammalian cells. *Mol. Biol. Cell* 19, 2402–2412.

Garnier, A., Fortin, D., Zoll, J., N'Guessan, B., Mettauer, B., Lampert, E., et al. (2005). Coordinated changes in mitochondrial function and biogenesis in healthy and diseased human skeletal muscle. *FASEB J.* 19, 43–52.

Griffin, E. E., Graumann, J., and Chan, D. C. (2005). The WD40 protein Caf4p is a component of the mitochondrial fission machinery and recruits Dnm1p to mitochondria. *J. Cell Biol.* 170, 237–248.

Griparic, L., Kanazawa, T., and van der Bliek, A. M. (2007). Regulation of the mitochondrial dynamin-like protein Opa1 by proteolytic cleavage. *J. Cell Biol.* 178, 757–764.

Groenendyk, J., Agellon, L. B., and Michalak, M. (2013). Coping with endoplasmic reticulum stress in the cardiovascular system. *Annu. Rev. Physiol.* 75, 49–67.

Guan, K., Farh, L., Marshall, T. K., and Deschenes, R. J. (1993). Normal mitochondrial structure and genome maintenance in yeast requires the dynamin-like product of the MGM1 gene. *Curr. Genet.* 24, 141–148.

Guillery, O., Malka, F., Landes, T., Guillou, E., Blackstone, C., Lombes, A., et al. (2008). Metalloprotease-mediated OPA1 processing is modulated by the mitochondrial membrane potential. *Biol. Cell* 100, 315–325.

Guo, X., Chen, K. H., Guo, Y., Liao, H., Tang, J., and Xiao, R. P. (2007). Mitofusin 2 triggers vascular smooth muscle cell apoptosis via mitochondrial death pathway. *Circ. Res.* 101, 1113–1122.

Guzun, R., Gonzalez-Granillo, M., Karu-Varikmaa, M., Grichine, A., Usson, Y., Kaambre, T., et al. (2012). Regulation of respiration in muscle cells *in vivo* by VDAC through interaction with the cytoskeleton and MtCK within mitochondrial interactosome. *Biochim. Biophys. Acta* 1818, 1545–1554.

Hackenbrock, C. R. (1966). Ultrastructural bases for metabolically linked mechanical activity in mitochondria. I. Reversible ultrastructural changes with change in metabolic steady state in isolated liver mitochondria. *J. Cell Biol.* 30, 269–297.

Hales, K. G., and Fuller, M. T. (1997). Developmentally regulated mitochondrial fusion mediated by a conserved, novel, predicted GTPase. *Cell* 90, 121–129.

Hermann, G. J., Thatcher, J. W., Mills, J. P., Hales, K. G., Fuller, M. T., Nunnari, J., et al. (1998). Mitochondrial fusion in yeast requires the transmembrane GTPase Fzo1p. *J. Cell Biol.* 143, 359–373.

Hinshaw, J. E. (2000). Dynamin and its role in membrane fission. *Annu. Rev. Cell Dev. Biol.* 16, 483–519.

Hom, J., and Sheu, S. S. (2009). Morphological dynamics of mitochondria–a special emphasis on cardiac muscle cells. *J. Mol. Cell Cardiol.* 46, 811–820.

Hoppel, C. L., Tandler, B., Fujioka, H., and Riva, A. (2009). Dynamic organization of mitochondria in human heart and in myocardial disease. *Int. J. Biochem. Cell Biol.* 41, 1949–1956.

Hoppins, S., Collins, S. R., Cassidy-Stone, A., Hummel, E., Devay, R. M., Lackner, L. L., et al. (2011a). A mitochondrial-focused genetic interaction map reveals a scaffold-like complex required for inner membrane organization in mitochondria. *J. Cell Biol.* 195, 323–340.

Hoppins, S., Edlich, F., Cleland, M. M., Banerjee, S., McCaffery, J. M., Youle, R. J., et al. (2011b). The soluble form of Bax regulates mitochondrial fusion via MFN2 homotypic complexes. *Mol. Cell* 41, 150–160.

Ingerman, E., Perkins, E. M., Marino, M., Mears, J. A., McCaffery, J. M., Hinshaw, J. E., et al. (2005). Dnm1 forms spirals that are structurally tailored to fit mitochondria. *J. Cell Biol.* 170, 1021–1027.

Ishihara, N., Eura, Y., and Mihara, K. (2004). Mitofusin 1 and 2 play distinct roles in mitochondrial fusion reactions via GTPase activity. *J. Cell Sci.* 117, 6535–6546.

Javadov, S., Rajapurohitam, V., Kilic, A., Hunter, J. C., Zeidan, A., Said Faruq, N., et al. (2011). Expression of mitochondrial fusion-fission proteins during post-infarction remodeling: the effect of NHE-1 inhibition. *Basic Res. Cardiol.* 106, 99–109.

Jofuku, A., Ishihara, N., and Mihara, K. (2005). Analysis of functional domains of rat mitochondrial Fis1, the mitochondrial fission-stimulating protein. *Biochem. Biophys. Res. Commun.* 333, 650–659.

Jones, B. A., and Fangman, W. L. (1992). Mitochondrial DNA maintenance in yeast requires a protein containing a region related to the GTP-binding domain of dynamin. *Genes Dev.* 6, 380–389.

Joubert, F., Gillet, B., Mazet, J. L., Mateo, P., Beloeil, J., and Hoerter, J. A. (2000). Evidence for myocardial ATP compartmentation from NMR inversion transfer analysis of creatine kinase fluxes. *Biophys. J.* 79, 1–13.

Joubert, F., Hoerter, J. A., and Mazet, J. L. (2001a). Discrimination of cardiac subcellular creatine kinase fluxes by NMR spectroscopy: a new method of analysis. *Biophys. J.* 81, 2995–3004.

Joubert, F., Vrezas, I., Mateo, P., Gillet, B., Beloeil, J. C., Soboll, S., et al. (2001b). Cardiac creatine kinase metabolite compartments revealed by NMR magnetization transfer

spectroscopy and subcellular fractionation. *Biochemistry* 40, 2129–2137.

Joubert, F., Mazet, J. L., Mateo, P., and Hoerter, J. A. (2002a). 31P NMR detection of subcellular creatine kinase fluxes in the perfused rat heart: contractility modifies energy transfer pathways. *J. Biol. Chem.* 277, 18469–18476.

Joubert, F., Hoerter, J. A., and Mazet, J. L. (2002b). Modeling the energy transfer pathways. creatine kinase activities and heterogeneous distribution of ADP in the perfused heart. *Mol. Biol. Rep.* 29, 177–182.

Joubert, F., Mazet, J. L., Mateo, P., and Hoerter, J. A. (2002c). Identification of subcellular energy fluxes by P NMR spectroscopy in the perfused heart: contractility induced modifications of energy transfer pathways. *Mol. Biol. Rep.* 29, 171–176.

Joubert, F., Wilding, J. R., Fortin, D., Domergue-Dupont, V., Novotova, M., Ventura-Clapier, R., et al. (2008). Local energetic regulation of sarcoplasmic and myosin ATPase is differently impaired in rats with heart failure. *J. Physiol.* 586, 5181–5192.

Kaasik, A., Joubert, F., Ventura Clapier, R., and Veksler, V. (2004). A novel mechanism of regulation of cardiac contractility by mitochondrial functional state. *FASEB J.* 18, 1219–1227.

Kaasik, A., Kuum, M., Joubert, F., Wilding, J., Ventura-Clapier, R., and Veksler, V. (2010). Mitochondria as a source of mechanical signals in cardiomyocytes. *Cardiovasc. Res.* 87, 83–91.

Kaasik, A., Veksler, V., Boehm, E., Novotova, M., Minajeva, A., and Ventura-Clapier, R. (2001). Energetic crosstalk between organelles: architectural integration of energy production and utilization. *Circ. Res.* 89, 153–159.

Karbowski, M., and Youle, R. J. (2003). Dynamics of mitochondrial morphology in healthy cells and during apoptosis. *Cell Death Differ.* 10, 870–880.

Khalifat, N., Puff, N., Bonneau, S., Fournier, J. B., and Angelova, M. I. (2008). Membrane deformation under local pH gradient: mimicking mitochondrial cristae dynamics. *Biophys. J.* 95, 4924–4933.

Kimberg, D. V., and Loeb, J. N. (1972). Effects of cortisone administration on rat liver mitochondria. Support for the concept of mitochondrial fusion. *J. Cell Biol.* 55, 635–643.

Koch, A., Thiemann, M., Grabenbauer, M., Yoon, Y., McNiven, M. A., and Schrader, M. (2003). Dynamin-like protein 1 is involved in peroxisomal fission. *J. Biol. Chem.* 278, 8597–8605.

Koch, A., Yoon, Y., Bonekamp, N. A., McNiven, M. A., and Schrader, M. (2005). A role for Fis1 in both mitochondrial and peroxisomal fission in mammalian cells. *Mol. Biol. Cell* 16, 5077–5086.

Koshiba, T., Detmer, S. A., Kaiser, J. T., Chen, H., McCaffery, J. M., and Chan, D. C. (2004). Structural basis of mitochondrial tethering by mitofusin complexes. *Science* 305, 858–862.

Kuznetsov, A. V., Hermann, M., Saks, V., Hengster, P., and Margreiter, R. (2009). The cell-type specificity of mitochondrial dynamics. *Int. J. Biochem. Cell Biol.* 41, 1928–1939.

Lee, Y., Lee, H. Y., Hanna, R. A., and Gustafsson, A. B. (2011). Mitochondrial autophagy by Bnip3 involves Drp1-mediated mitochondrial fission and recruitment of Parkin in cardiac myocytes. *Am. J. Physiol. Heart Circ. Physiol.* 301, H1924–H1931.

Lee, Y. J., Jeong, S. Y., Karbowski, M., Smith, C. L., and Youle, R. J. (2004). Roles of the mammalian mitochondrial fission and fusion mediators Fis1, Drp1, and Opa1 in apoptosis. *Mol. Biol. Cell* 15, 5001–5011.

Legros, F., Lombes, A., Frachon, P., and Rojo, M. (2002). Mitochondrial fusion in human cells is efficient, requires the inner membrane potential, and is mediated by mitofusins. *Mol. Biol. Cell* 13, 4343–4354.

Leu, M., Ehler, E., and Perriard, J. C. (2001). Characterisation of postnatal growth of the murine heart. *Anat. Embryol. (Berl.)* 204, 217–224.

Liesa, M., Palacin, M., and Zorzano, A. (2009). Mitochondrial dynamics in mammalian health and disease. *Physiol. Rev.* 89, 799–845.

Mannella, C. A. (2006). Structure and dynamics of the mitochondrial inner membrane cristae. *Biochim. Biophys. Acta* 1763, 542–548.

Mannella, C. A. (2008). Structural diversity of mitochondria: functional implications. *Ann. N.Y. Acad. Sci.* 1147, 171–179.

Messerschmitt, M., Jakobs, S., Vogel, F., Fritz, S., Dimmer, K. S., Neupert, W., et al. (2003). The inner membrane protein Mdm33 controls mitochondrial morphology in yeast. *J. Cell Biol.* 160, 553–564.

Narula, J., Pandey, P., Arbustini, E., Haider, N., Narula, N., Kolodgie, F. D., et al. (1999). Apoptosis in heart failure: release of cytochrome c from mitochondria and activation of caspase-3 in human cardiomyopathy. *Proc. Natl. Acad. Sci. U.S.A.* 96, 8144–8149.

Ngoh, G. A., Papanicolaou, K. N., and Walsh, K. (2012). Loss of mitofusin 2 promotes endoplasmic reticulum stress. *J. Biol. Chem.* 287, 20321–20332.

Nogueira, V., Devin, A., Walter, L., Rigoulet, M., Leverve, X., and Fontaine, E. (2005). Effects of decreasing mitochondrial volume on the regulation of the permeability transition pore. *J. Bioenerg. Biomembr.* 37, 25–33.

Olichon, A., Baricault, L., Gas, N., Guillou, E., Valette, A., Belenguer, P., et al. (2003). Loss of OPA1 perturbates the mitochondrial inner membrane structure and integrity, leading to cytochrome c release and apoptosis. *J. Biol. Chem.* 278, 7743–7746.

Olichon, A., Guillou, E., Delettre, C., Landes, T., Arnaune-Pelloquin, L., Emorine, L. J., et al. (2006). Mitochondrial dynamics and disease, OPA1. *Biochim. Biophys. Acta.* 1763, 500–509.

Olichon, A., Landes, T., Arnaune-Pelloquin, L., Emorine, L. J., Mils, V., Guichet, A., et al. (2007). Effects of OPA1 mutations on mitochondrial morphology and apoptosis: relevance to ADOA pathogenesis. *J. Cell Physiol.* 211, 423–430.

Olivetti, G., Abbi, R., Quaini, F., Kajstura, J., Cheng, W., Nitahara, J. A., et al. (1997). Apoptosis in the failing human heart. *N. Engl. J. Med.* 336, 1131–1141.

Ong, S. B., Hall, A. R., and Hausenloy, D. J. (2012). Mitochondrial dynamics in cardiovascular health and disease. *Antioxid. Redox. Signal.* doi: 10.1089/ars.2012.4777. [Epub ahead of print].

Ong, S. B., Subrayan, S., Lim, S. Y., Yellon, D. M., Davidson, S. M., and Hausenloy, D. J. (2010). Inhibiting mitochondrial fission protects the heart against ischemia/reperfusion injury. *Circulation* 121, 2012–2022.

Otera, H., Wang, C., Cleland, M. M., Setoguchi, K., Yokota, S., Youle, R. J., et al. (2010). Mff is an essential factor for mitochondrial recruitment of Drp1 during mitochondrial fission in mammalian cells. *J. Cell Biol.* 191, 1141–1158.

Palmer, C. S., Osellame, L. D., Laine, D., Koutsopoulos, O. S., Frazier, A. E., and Ryan, M. T. (2011). MiD49 and MiD51, new components of the mitochondrial fission machinery. *EMBO Rep.* 12, 565–573.

Papanicolaou, K. N., Khairallah, R. J., Ngoh, G. A., Chikando, A., Luptak, I., O'Shea, K. M., et al. (2011). Mitofusin-2 maintains mitochondrial structure and contributes to stress-induced permeability transition in cardiac myocytes. *Mol. Cell Biol.* 31, 1309–1328.

Papanicolaou, K. N., Ngoh, G. A., Dabkowski, E. R., O'Connell, K. A., Ribeiro, R. F. Jr., Stanley, W. C., et al. (2012). Cardiomyocyte deletion of mitofusin-1 leads to mitochondrial fragmentation and improves tolerance to ROS-induced mitochondrial dysfunction and cell death. *Am. J. Physiol. Heart Circ. Physiol.* 302, H167–H179.

Parra, V., Eisner, V., Chiong, M., Criollo, A., Moraga, F., Garcia, A., et al. (2008). Changes in mitochondrial dynamics during ceramide-induced cardiomyocyte early apoptosis. *Cardiovasc. Res.* 77, 387–397.

Parra, V., Verdejo, H., del Campo, A., Pennanen, C., Kuzmicic, J., Iglewski, M., et al. (2011). The complex interplay between mitochondrial dynamics and cardiac metabolism. *J. Bioenerg. Biomembr.* 43, 47–51.

Pich, S., Bach, D., Briones, P., Liesa, M., Camps, M., Testar, X., et al. (2005). The Charcot-Marie-Tooth type 2A gene product, Mfn2, up-regulates fuel oxidation through expression of OXPHOS system. *Hum. Mol. Genet.* 14, 1405–1415.

Piquereau, J., Caffin, F., Novotova, M., Prola, A., Garnier, A., Mateo, P., et al. (2012). Down-regulation of OPA1 alters mouse mitochondrial morphology, PTP function, and cardiac adaptation to pressure overload. *Cardiovasc. Res.* 94, 408–417.

Piquereau, J., Novotova, M., Fortin, D., Garnier, A., Ventura-Clapier, R., Veksler, V., et al. (2010). Postnatal development of mouse heart: formation of energetic microdomains. *J. Physiol.* 588, 2443–2454.

Piquereau, J., Novotova, M., Garnier, A., Joubert, F., Veksler, V., and Ventura-Clapier, R. (2013). "Cardiac metabolic adaptation during postnatal development," in *Cardiac Adaptations, Advances in Biochemistry in Health and Disease*, Vol. 4, eds B. Ostadal and N. S. Dhalla (New York, NY: Springer), 79–98.

Rappaport, L., Oliviero, P., and Samuel, J. L. (1998). Cytoskeleton and mitochondrial morphology and function. *Mol. Cell Biochem.* 184, 101–105.

Rossignol, R., Gilkerson, R., Aggeler, R., Yamagata, K., Remington, S. J., and Capaldi, R. A. (2004). Energy substrate modulates mitochondrial structure and oxidative capacity in cancer cells. *Cancer Res.* 64, 985–993.

Sabbah, H. N., Sharov, V., Riddle, J. M., Kono, T., Lesch, M., and Goldstein,

S. (1992). Mitochondrial abnormalities in myocardium of dogs with chronic heart failure. *J. Mol. Cell Cardiol.* 24, 1333–1347.

Saks, V. A., Kaambre, T., Sikk, P., Eimre, M., Orlova, E., Paju, K., et al. (2001). Intracellular energetic units in red muscle cells. *Biochem. J.* 356, 643–657.

Saks, V. A., Kongas, O., Vendelin, M., and Kay, L. (2000). Role of the creatine/phosphocreatine system in the regulation of mitochondrial respiration. *Acta Physiol. Scand.* 168, 635–641.

Santel, A., Frank, S., Gaume, B., Herrler, M., Youle, R. J., and Fuller, M. T. (2003). Mitofusin-1 protein is a generally expressed mediator of mitochondrial fusion in mammalian cells. *J. Cell Sci.* 116, 2763–2774.

Santel, A., and Fuller, M. T. (2001). Control of mitochondrial morphology by a human mitofusin. *J. Cell Sci.* 114, 867–874.

Satoh, M., Hamamoto, T., Seo, N., Kagawa, Y., and Endo, H. (2003). Differential sublocalization of the dynamin-related protein OPA1 isoforms in mitochondria. *Biochem. Biophys. Res. Commun.* 300, 482–493.

Schaper, J., Froede, R., Hein, S., Buck, A., Hashizume, H., Speiser, B., et al. (1991). Impairment of the myocardial ultrastructure and changes of the cytoskeleton in dilated cardiomyopathy. *Circulation* 83, 504–514.

Shahrestani, P., Leung, H. T., Le, P. K., Pak, W. L., Tse, S., Ocorr, K., et al. (2009). Heterozygous mutation of Drosophila Opa1 causes the development of multiple organ abnormalities in an age-dependent and organ-specific manner. *PLos One* 4:e6867. doi: 10.1371/journal.pone.0006867.

Shen, T., Zheng, M., Cao, C., Chen, C., Tang, J., Zhang, W., et al. (2007). Mitofusin-2 is a major determinant of oxidative stress-mediated heart muscle cell apoptosis. *J. Biol. Chem.* 282, 23354–23361.

Skulachev, V. P. (2001). Mitochondrial filaments and clusters as intracellular power-transmitting cables. *Trends Biochem. Sci.* 26, 23–29.

Soubannier, V., and McBride, H. M. (2009). Positioning mitochondrial plasticity within cellular signaling cascades. *Biochim. Biophys. Acta* 1793, 154–170.

Speer, O., Back, N., Buerklen, T., Brdiczka, D., Koretsky, A., Wallimann, T., et al. (2005). Octameric mitochondrial creatine kinase induces and stabilizes contact sites between the inner and outer membrane. *Biochem. J.* 385, 445–450.

Stojanovski, D., Koutsopoulos, O. S., Okamoto, K., and Ryan, M. T. (2004). Levels of human Fis1 at the mitochondrial outer membrane regulate mitochondrial morphology. *J. Cell Sci.* 117, 1201–1210.

Strauss, M., Hofhaus, G., Schroder, R. R., and Kuhlbrandt, W. (2008). Dimer ribbons of ATP synthase shape the inner mitochondrial membrane. *EMBO J.* 27, 1154–1160.

Tepp, K., Shevchuk, I., Chekulayev, V., Timohhina, N., Kuznetsov, A. V., Guzun, R., et al. (2011). High efficiency of energy flux controls within mitochondrial interactosome in cardiac intracellular energetic units. *Biochim. Biophys. Acta* 1807, 1549–1561.

Tieu, Q., Okreglak, V., Naylor, K., and Nunnari, J. (2002). The WD repeat protein, Mdv1p, functions as a molecular adaptor by interacting with Dnm1p and Fis1p during mitochondrial fission. *J. Cell Biol.* 158, 445–452.

Tondera, D., Czauderna, F., Paulick, K., Schwarzer, R., Kaufmann, J., and Santel, A. (2005). The mitochondrial protein MTP18 contributes to mitochondrial fission in mammalian cells. *J. Cell Sci.* 118, 3049–3059.

Twig, G., Elorza, A., Molina, A. J., Mohamed, H., Wikstrom, J. D., Walzer, G., et al. (2008a). Fission and selective fusion govern mitochondrial segregation and elimination by autophagy. *EMBO J.* 27, 433–446.

Twig, G., Hyde, B., and Shirihai, O. S. (2008b). Mitochondrial fusion, fission and autophagy as a quality control axis: the bioenergetic view. *Biochim. Biophys. Acta* 1777, 1092–1097.

Vafai, S. B., and Mootha, V. K. (2012). Mitochondrial disorders as windows into an ancient organelle. *Nature* 491, 374–383.

Varadi, A., Johnson-Cadwell, L. I., Cirulli, V., Yoon, Y., Allan, V. J., and Rutter, G. A. (2004). Cytoplasmic dynein regulates the subcellular distribution of mitochondria by controlling the recruitment of the fission factor dynamin-related protein-1. *J. Cell Sci.* 117, 4389–4400.

Vendelin, M., Beraud, N., Guerrero, K., Andrienko, T., Kuznetsov, A. V., Olivares, J., et al. (2005). Mitochondrial regular arrangement in muscle cells: a "crystal-like" pattern. *Am. J. Physiol. Cell Physiol.* 288, C757–C767.

Ventura-Clapier, R., Garnier, A., Veksler, V., and Joubert, F. (2011). Bioenergetics of the failing heart. *Biochim. Biophys. Acta* 1813, 1360–1372.

Wakabayashi, T. (2002). Megamitochondria formation – physiology and pathology. *J. Cell Mol. Med.* 6, 497–538.

Wakabayashi, J., Zhang, Z., Wakabayashi, N., Tamura, Y., Fukaya, M., Kensler, T. W., et al. (2009). The dynamin-related GTPase Drp1 is required for embryonic and brain development in mice. *J. Cell Biol.* 186, 805–816.

Wakabayashi, T., Asano, M., and Kurono, C. (1975). Mechanism of the formation of megamitochondria induced by copper-chelating agents. I. On the formation process of megamitochondria in cuprizone-treated mouse liver. *Acta Pathol. Jpn.* 25, 15–37.

Wakabayashi, T., and Green, D. E. (1977). Membrane fusion in mitochondria. I. Ultrastructural basis for fusion. *J. Electron Microsc. (Tokyo)* 26, 305–320.

Wallimann, T., Wyss, M., Brdiczka, D., Nicolay, K., and Eppenberger, H. M. (1992). Intracellular compartmentation, structure and function of creatine kinase isoenzymes in tissues with high and fluctuating energy demands: the 'phosphocreatine circuit' for cellular energy homeostasis. *Biochem. J.* 281(Pt 1), 21–40.

Wasiak, S., Zunino, R., and McBride, H. M. (2007). Bax/Bak promote sumoylation of DRP1 and its stable association with mitochondria during apoptotic cell death. *J. Cell Biol.* 177, 439–450.

Wasilewski, M., and Scorrano, L. (2009). The changing shape of mitochondrial apoptosis. *Trends Endocrinol. Metab.* 20, 287–294.

Wilding, J. R., Joubert, F., de Araujo, C., Fortin, D., Novotova, M., Veksler, V., et al. (2006). Altered energy transfer from mitochondria to sarcoplasmic reticulum after cytoarchitectural perturbations in mice hearts. *J. Physiol.* 575, 191–200.

Yoon, Y., Krueger, E. W., Oswald, B. J., and McNiven, M. A. (2003). The mitochondrial protein hFis1 regulates mitochondrial fission in mammalian cells through an interaction with the dynamin-like protein DLP1. *Mol. Cell Biol.* 23, 5409–5420.

Yoon, Y., Pitts, K. R., and McNiven, M. A. (2001). Mammalian dynamin-like protein DLP1 tubulates membranes. *Mol. Biol. Cell* 12, 2894–2905.

Zhao, T., Huang, X., Han, L., Wang, X., Cheng, H., Zhao, Y., et al. (2012). Central role of mitofusin 2 in autophagosome-lysosome fusion in cardiomyocytes. *J. Biol. Chem.* 287, 23615–23625.

Ziviani, E., Tao, R. N., and Whitworth, A. J. (2010). Drosophila parkin requires PINK1 for mitochondrial translocation and ubiquitinates mitofusin. *Proc. Natl. Acad. Sci. U.S.A.* 107, 5018–5023.

Ziviani, E., and Whitworth, A. J. (2010). How could Parkin-mediated ubiquitination of mitofusin promote mitophagy? *Autophagy* 6, 660–662.

Zuchner, S., Mersiyanova, I. V., Muglia, M., Bissar-Tadmouri, N., Rochelle, J., Dadali, E. L., et al. (2004). Mutations in the mitochondrial GTPase mitofusin 2 cause Charcot-Marie-Tooth neuropathy type 2A. *Nat. Genet.* 36, 449–451.

Conflict of Interest Statement: The authors declare that the research was conducted in the absence of any commercial or financial relationships that could be construed as a potential conflict of interest.

Received: 28 February 2013; accepted: 23 April 2013; published online: 10 May 2013.

*Citation: Piquereau J, Caffin F, Novotova M, Lemaire C, Veksler V, Garnier A, Ventura-Clapier R and Joubert F (2013) Mitochondrial dynamics in the adult cardiomyocytes: which roles for a highly specialized cell? Front. Physiol. **4**:102. doi: 10.3389/fphys.2013.00102*

This article was submitted to Frontiers in Mitochondrial Research, a specialty of Frontiers in Physiology.

frontiers in
PHYSIOLOGY

MINI REVIEW ARTICLE
published: 22 April 2013
doi: 10.3389/fphys.2013.00082

Cytoskeleton and regulation of mitochondrial function: the role of beta-tubulin II

Andrey V. Kuznetsov[1]*, Sabzali Javadov[2], Rita Guzun[3,4], Michael Grimm[1] and Valdur Saks[4]

[1] Cardiac Surgery Research Laboratory, Department of Cardiac Surgery, Innsbruck Medical University, Innsbruck, Tirol, Austria
[2] Department of Physiology, School of Medicine, University of Puerto Rico, San Juan, PR, USA
[3] EFCR and Sleep Laboratory, INSERM U1042, University Hospital of Grenoble, France
[4] Laboratory of Fundamental and Applied Bioenergetics, INSERM U1055, Joseph Fourier University, Grenoble, France

Edited by:
Paolo Bernardi, University of Padova, Italy

Reviewed by:
Shey-Shing Sheu, University of Rochester, USA
Tatiana Rostovtseva, National Institutes of Health, USA
Nina Kaludercic, National Research Council, Italy

***Correspondence:**
Andrey V. Kuznetsov, Cardiac Surgery Research Laboratory, Department of Cardiac Surgery, Innsbruck Medical University, Innrain 66, A-6020 Innsbruck, Tirol, Austria.
e-mail: andrey.kuznetsov@uki.at

The control of mitochondrial function is a cardinal issue in the field of cardiac bioenergetics, and the analysis of mitochondrial regulations is central to basic research and in the diagnosis of many diseases. Interaction between cytoskeletal proteins and mitochondria can actively participate in mitochondrial regulation. Potential candidates for the key roles in this regulation are the cytoskeletal proteins plectin and tubulin. Analysis of cardiac cells has revealed regular arrangement of β-tubulin II, fully co-localized with mitochondria. β-Tubulin IV demonstrated a characteristic staining of branched network, β-tubulin III was matched with Z-lines, and β-tubulin I was diffusely spotted and fragmentary polymerized. In contrast, HL-1 cells were characterized by the complete absence of β-tubulin II. Comparative analysis of cardiomyocytes and HL-1 cells revealed a dramatic difference in the mechanisms of mitochondrial regulation. In the heart, colocalization of β-tubulin isotype II with mitochondria suggests that it can participate in the coupling of ATP-ADP translocase (ANT), mitochondrial creatine kinase (MtCK), and VDAC (ANT-MtCK-VDAC). This mitochondrial supercomplex is responsible for the efficient intracellular energy transfer via the phosphocreatine pathway. Existing data suggest that cytoskeletal proteins may control the VDAC, contributing to maintenance of mitochondrial and cellular physiology.

Keywords: beta tubulin isotypes, cardiomyocytes, confocal microscopy, creatine kinase, HL-1 cells, mitochondrial regulation, mitochondria-cytoskeleton interactions, VDAC

THE ROLE OF CYTOSKELETON IN THE REGULATION OF MITOCHONDRIAL RESPIRATORY FUNCTION

High requirements for energy supply in oxidative muscles are met by aerobic oxidation of fatty acids and glucose coupled to ATP production in mitochondria. In spite of the fundamental progress in our knowledge of mitochondrial bioenergetics, the nature of respiratory control and the mechanisms of regulation of energy fluxes *in vivo* are still highly debated. In the heart and other tissues with high oxidative phosphorylation capacity, the respiration rate is linearly dependent on the workload, and elevation of the workload results in a proportional elevation of the respiration rates without changing in the cytosolic concentration of ADP, ATP, and Pi (Williamson, 1979; Balaban, 1990). This makes it impossible to interpret these data on the basis of a simple "feedback model" and ADP kinetics characteristic for isolated (*in vitro*) mitochondria in which the rate of oxidative phosphorylation is controlled by the concentration of ADP. Important role of the cytosolic and mitochondrial calcium as regulator of both the energy utilization by ATPases and, in parallel, the mitochondrial oxidative phosphorylation was emphasized in several studies and reviews (Balaban, 2002; Balaban et al., 2003; Glancy and Balaban, 2012). Also, it has been shown that in the heart the mitochondrial creatine kinase (MtCK) system plays a key role in intracellular channeling and metabolic micro-compartmentalization with a functional and structural coupling between MtCK and oxidative phosphorylation via ATP-ADP translocase (ANT) (Saks et al., 1985). This phenomenon was then largely documented. The central role of the creatine kinase/phosphocreatine (CK-PCr) system in muscle, brain and other cells for intracellular energy transport and regulation is now generally accepted. Furthermore, significant changes in the CK-PCr system and mitochondrial remodeling have been demonstrated in various pathologies, such as cardiomyopathies, cold and warm ischemia and subsequent reperfusion, different models of hypertrophy injuries, etc. (Khuchua et al., 1989; Saks et al., 1991b; Kay et al., 1997b; Laclau et al., 2001). One important result obtained from studies in animal models and from the analysis of human cardiac biopsies was the observation that the MtCK-coupled system (functional and structural coupling) is extremely sensitive to pathological processes and can be used for precise diagnosis (Saks et al., 1991b).

Mitochondrial oxidative capacity and affinity to the main regulator ADP are key components of mitochondrial physiology. Studies of permeabilized cells and muscle fibers have shown very different kinetics of ATP synthesis (remarkably increased apparent *Km* for ADP in the regulation of mitochondrial respiration) in comparison to isolated mitochondria (Belikova et al., 1990; Saks et al., 1991a, 1993). Plausibly, the cytoskeleton plays a role here. It has been suggested that increased *Km* for ADP is related

to the local restriction on ADP diffusion in the cells due to the interaction between cytoskeletal proteins and VDAC (**Figure 1**) of the mitochondrial outer membrane (MOM) (Belikova et al., 1990; Saks et al., 1991a, 1993, 2003). Recent data have shown the importance of the cell's structural organization for energy metabolism and regulation of mitochondrial function *in vivo*. In cardiac and skeletal muscles mitochondria form a regular arrangement between myofibrils (Vendelin et al., 2005), actively interacting with other intracellular systems like the cytoskeleton and sarcoplasmic reticulum. This type of organization provides a bioenergetic basis for contraction, recruiting cytoskeletal proteins, controlling both mitochondrial shape and arrangement in the cell. Importantly, the mitochondrial interactions with various cytoskeletal proteins (tubulin, desmin, vimentin, plectin) are suggested to be involved in the regulation of mitochondrial respiratory function (**Figure 1A**) (Kay et al., 1997a; Milner et al., 2000; Capetanaki, 2002; Andrienko et al., 2003; Appaix et al., 2003; Tang et al., 2008; Winter et al., 2008).

STUDIES OF *in situ* MITOCHONDRIA: PROPERTIES OF MITOCHONDRIA DIFFER *in vitro* AND *in vivo*

Oxidative phosphorylation has been extensively studied in intact mitochondria, which can be achieved by measuring the oxygen consumption of mitochondria isolated from a tissue. However, studies of isolated (*in vitro*) mitochondria are certainly insufficient to understand the molecular mechanisms of their regulation in living cells. There is a growing body of evidence to demonstrate that important properties of mitochondria differ *in vivo* and *in vitro*. The *in situ* analysis is based on selective permeabilization of the plasma membrane (Saks et al., 1991a, 1993, 2003; Kuznetsov et al., 1998a, 2008; Villani et al., 1998). Compared with isolated mitochondria, this approach has a number of important advantages: (1) artifacts of mitochondrial isolation are avoided; (2) very small tissue samples are required; (3) all cellular population of mitochondria can be investigated; and (4) most importantly, the *in situ* approach resembles more closely to the situation in the living cell than does the analysis of isolated mitochondria.

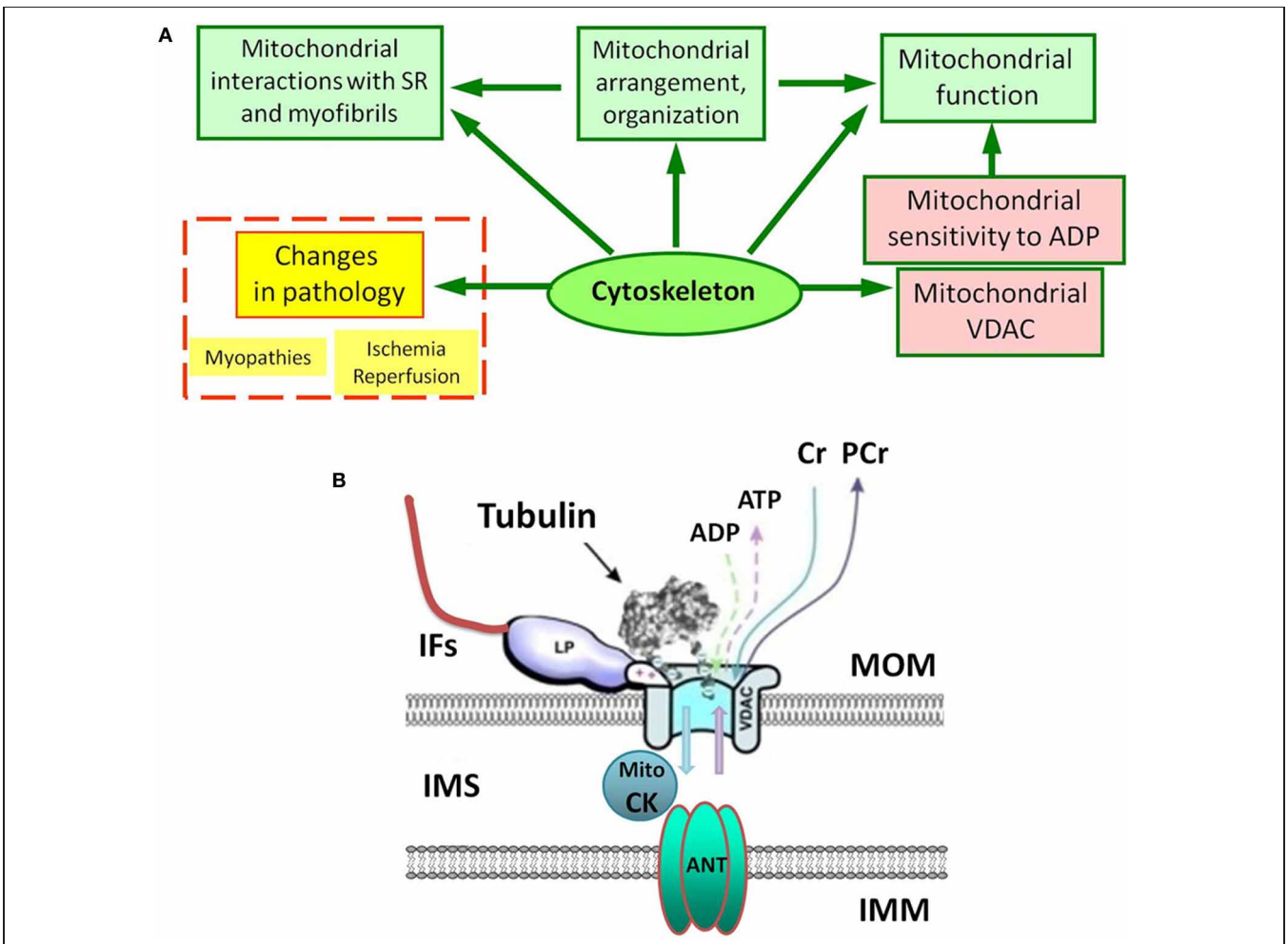

FIGURE 1 | (A) Complex and multiple role of the cytoskeleton in mitochondrial regulations under normal and pathological conditions. SR, sarcoplasmic reticulum. **(B)** Possible interactions of porin (VDAC) of the mitochondrial outer membrane (MOM). IFs, intermediate filaments; IMM, the inner mitochondrial membrane; IMS, inter-membrane space; Mito CK, mitochondrial creatine kinase. Tubulin controls VDAC permeability for ADP and ATP. LP is a still unknown cytoskeletal linker protein, which may also interact with VDAC and tubulin to regulate permeability of the MOM.

This allows mitochondria to be analyzed within an integrated cellular system, in their normal intracellular position and assembly, preserving essential interactions with the cytoskeleton, nucleus, and endoplasmic reticulum. In addition, permeabilized preparations of muscle fibers display functional mitochondria stability, probably due to the immobilization of mitochondria in these preparations. Importantly, *in situ* analysis is suitable for studies of mitochondrial physiology in small quantities of tissue, which is crucial in cases involving limited amounts of material, like the analysis of expensive knock-out mouse models. Previous studies have shown that permeabilized cells and muscle fibers are suitable for *in situ* affinity analysis of the main substrate of phosphorylation, ADP. This is done by measuring its apparent *Km* value as a sensitive parameter of the organization and functional state of mitochondria and mitochondrial membranes (Veksler et al., 1995; Zoll et al., 2001, 2002; Burelle and Hochachka, 2002). Classical studies of ADP kinetics have shown that preparations of isolated mitochondria exhibit a very high affinity for ADP (low apparent *Km* value for ADP in the range 10–25 μM). However, in permeabilized muscle fibers isolated from oxidative muscles (e.g., heart, or M. soleus) in which mitochondrial function is analyzed *in situ*, the apparent *Km* value for ADP was found to be astonishingly high (250–300 μM), exceeding that for mitochondria *in vitro* by more than one order of magnitude (Kuznetsov et al., 1996). Similar results were also obtained for various permeabilized cells, such as adult cardiomyocytes (Saks et al., 1991a, 1993) and hepatocytes (Fontaine et al., 1995). It has been shown that the decrease in mitochondrial affinity for exogenous ADP in permeabilized cardiac cells is related to the local restrictions on ADP diffusion in cardiac cells, including limitation of the permeability of the voltage-dependent anion channel (VDAC) also known as porin in the MOM (**Figure 1B**) (Saks et al., 1993, 1995; Kuznetsov et al., 1996; Milner et al., 2000; Appaix et al., 2003; Rostovtseva and Bezrukov, 2008; Rostovtseva et al., 2008). Importantly, this functional parameter has been shown to be strongly tissue/muscle type-specific (Kuznetsov et al., 1996), and to change significantly during development, after intense physical exercise or in pathology (Veksler et al., 1995; Tiivel et al., 2000; Burelle and Hochachka, 2002; Tonkonogi and Sahlin, 2002; Zoll et al., 2002; Eimre et al., 2006). Also, the sensitivity of mitochondria to ADP is dramatically changed by proteases (Appaix et al., 2003), which indicates the involvement of certain proteins.

High apparent *Km* for exogenous ADP found in oxidative muscles *in situ* can be significantly decreased (from 300 to about 80 μM) when MtCK is activated by creatine. This decrease is due to the functional coupling of MtCK to mitochondrial oxidative phosphorylation, a finding that supports the hypothesis that *in vivo*, the stimulation of oxidative phosphorylation depends on the activity of peripheral kinases, such as creatine kinase, adenylate kinase and hexokinase. Creatine-stimulated respiration at submaximal concentrations of ADP (50–100 μM) and significant *Km* (ADP) decrease occur when MtCK is functionally coupled to oxidative phosphorylation. It has been shown that the octameric form of MtCK located in the intermembrane space connects the MOM via VDAC to ANT (**Figure 1B**), providing a basis for direct metabolite channeling (Kay et al., 2000; Saks et al., 2006a, 2010). It has been theorized that creatine diffuses through VDAC and is converted by MtCK in the presence of ATP to phosphocreatine and ADP. Phosphocreatine then leaves the mitochondria and is used at ATP-consuming sites, whereas ADP returns to the mitochondrial matrix via ANT to generate ATP, thus creating a local and efficient ADP-regenerating system in the vicinity of ANT, under conditions of low permeability of the MOM to ADP.

There is an evident tissue specificity of mitochondria with respect to morphology, structural organization, oxidative capacity, and dynamics. Kinetic studies of the *in situ* regulation of mitochondrial respiration by ADP in the cells showed that the sensitivity of mitochondria to ADP and kinetics of ATP synthesis are also tissue specific (Veksler et al., 1995; Kuznetsov et al., 1996). In permeabilized cardiac cells, the affinity of mitochondria for ADP is decreased by an order of magnitude as compared to isolated mitochondria. A similar situation is observed in the oxidative slow-twitch skeletal muscle such as M. soleus, but is absent in the fast glycolytic skeletal muscle (Kuznetsov et al., 1996) and in some cultured cells like HL-1 cells with cardiac phenotype (Anmann et al., 2006). It has been found that while in cardiac and soleus muscle fibers the apparent *Km* for ADP in respiration regulation was about 300 μM, in permeabilized fibers from the glycolytic M. gastrocnemius and M. plantaris its value was very low (10–20 μM), not different from that for isolated muscle mitochondria. This tissue-specific control of ADP sensitivity has been proposed to be related to specific proteins, most probably associated with the cytoskeleton (**Figure 1A**).

THE ROLE OF CYTOSKELETAL PROTEINS IN THE CONTROLLING MITOCHONDRIAL SENSITIVITY TO ADP IN OXIDATIVE TISSUES

A growing body of evidence suggests that the cytoskeletal network may interact with mitochondria to control mitochondrial respiration (Kuznetsov et al., 1996; Appaix et al., 2003; Rostovtseva et al., 2008). These interactions may involve the association of various cytoskeletal proteins with VDAC in the MOM directly or via intermediate filament (IF)-associated proteins. The cytoskeleton is very important for cellular architecture and signaling (Mose-Larsen et al., 1982; Rappaport et al., 1998; Anesti and Scorrano, 2006). It is well known that the cytoskeletal proteins are crucial for mitochondrial motility (Hollenbeck and Saxton, 2005). Moreover, mitochondrial interactions with the cytoskeleton are shown to be critical for control of mitochondrial morphology and organization, which, in turn, suggested that they are also important for their functioning, including control of the VDAC and mitochondrial affinity to ADP (**Figure 1**). For example, the striking difference between both morphology, arrangement, and ADP kinetics in adult cardiomyocytes (apparent *Km* for ADP 250–300 μM) and HL-1 cells (apparent Km for ADP 25–60 μM) suggests the importance of specific mitochondrial organization controlled by cytoskeletal proteins (Anmann et al., 2006). It has been demonstrated that in striated muscles, desmin regulates proper mitochondrial positioning and shape and might also regulate the formation and stabilization of mitochondrial contact sites. This cytoskeletal IF protein was also suggested to participate in mitochondrial regulation since respiratory function

of mitochondria was significantly changed in a desmin-null model (Milner et al., 2000). Previous findings suggested also that vimentin could be important for the association between the mitochondria and the cytoskeleton (Tang et al., 2008), contributing to the maintenance of mitochondrial morphology and intracellular organization, potentially playing a role in mitochondrial regulation. Also, recent evidence shows that the plectin 1b isoform is associated with mitochondria (Winter et al., 2008), suggesting that plectin can play important role in regulating mitochondrial respiratory function and the permeability of the MOM (through VDAC) to ADP and ATP. Moreover, using a conditional knockout mouse model in combination with isoform-specific knockouts it has been demonstrated that plectin deficiency causes mitochondrial dysfunction with significant changes in mitochondrial activities and affinity to ADP (Konieczny et al., 2008).

The cytoskeletal protein tubulin can also control the permeability of the MOM. Using monoclonal antibodies, immunogold labeling and high resolution electron microscopy, a clear colocalization of β-tubulin with mitochondria and its association with the outer mitochondrial membrane has been demonstrated first by Saetersdal et al. (1990). Unfortunately, in this pioneering work the isotype of β-tubulin was not identified. Also, the presence of tubulin in mitochondria has been shown by Carré et al. for different cell types, where both alpha and beta tubulin were localized at the outer mitochondrial membrane (Carre et al., 2002). Authors suggested that this "mitochondrial" tubulin can be organized in alpha/beta dimers and using immunoprecipitation they found that this tubulin is associated with mitochondrial VDAC. Notably, the addition of dimeric tubulin induces reversible closure of the reconstituted VDAC. For instance, in the model of isolated (*in vitro*) mitochondria, tubulin can restore the low permeability of the outer membrane, increasing apparent *Km* for ADP to the value of *in situ* mitochondria (Rostovtseva et al., 2008).

Using confocal microscopy in combination with immunoblotting, the intracellular distribution of β-tubulin isotypes I, II, III, and IV and expression of MtCK were investigated (Guzun et al., 2011) and their roles in energy metabolism in cardiomyocytes and cancerous HL-1 cells of cardiac phenotype were compared (Guzun et al., 2011). Antibodies against total β-tubulin and β-tubulin IV revealed characteristic staining of branched microtubular network in cardiac cells (**Figures 2A,B**). Polymerized transversal lines of β-tubulin III were well detected and matched with Z-lines (alpha-actinin antibodies, not shown), whereas β-tubulin I distribution was diffusely spotted and fragmentary polymerized. Most importantly, immunofluorescent analysis of adult rat cardiac cells revealed regular arrangement of β-tubulin II (**Figure 2C**), fully colocalized with mitochondria visualized by TMRM (**Figure 2D**), MitoTracker or other mitochondria-specific fluorescent probes (Guzun et al., 2011; Gonzalez-Granillo et al., 2012; Saks et al., 2012). Therefore, in adult rat cardiomyocytes, β-tubulin-II was identified as a specific mitochondrial isotype (**Figure 1B**). These results show that different isotypes of β-tubulin have different intracellular distribution and organization and may thus play different roles in the control of energy fluxes and mitochondrial respiration in cardiac muscle cells. In contrast, cancerous HL-1 cells were characterized by the complete absence of β-tubulin II (confirmed also by Western blot), by the presence of bundles of filamentous β-tubulin IV and by diffusely distributed β-tubulin I and III. Other important characteristic of these cells was also full absence of MtCK. Notably, comparative functional analysis of permeabilized cardiomyocytes and HL-1 cells, such as ADP-kinetics, stimulatory effects of creatine and glucose revealed dramatic difference in the mechanisms of regulation of respiration in cardiac and cancerous HL-1 cells. This demonstrates that two events—high apparent Km for exogenous ADP and expression of MtCK both correlate with the expression of mitochondrial β-tubulin II. The supercomplex ANT-MtCK-VDAC,

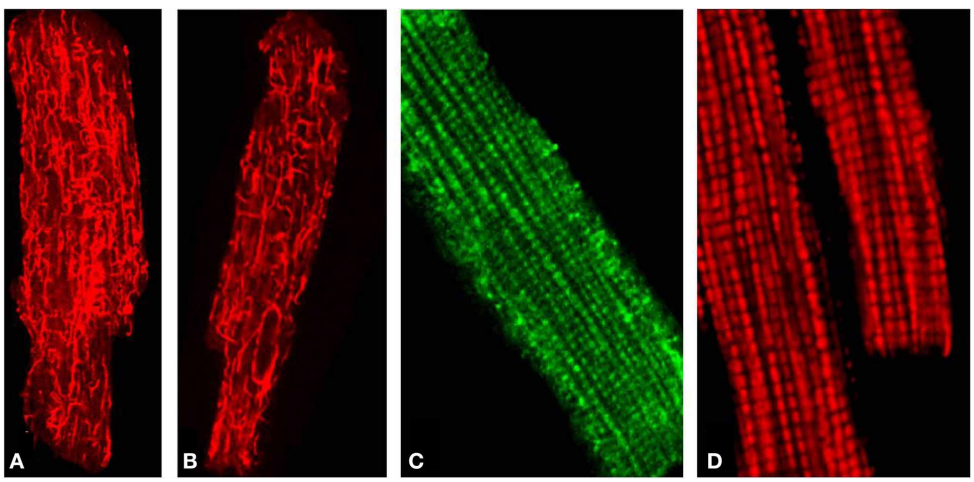

FIGURE 2 | (A) Distribution of total β-tubulins (microtubular network), **(B)** β-Tubulin IV. **(C)** The mitochondria-specific isoform β-tubulin II stained with anti-β-tubulin II antibody followed by FITC secondary antibodies and demonstrating a typical mitochondria-like staining/arrangement in isolated adult rat heart cardiomyocytes (comparable to **D**). **(D)** Imaging of mitochondria in the same cells stained with fluorescent mitochondria-specific probe TMRM.

localized at contact sites of two mitochondrial membranes, represents a key system for efficient energy transport from mitochondria to places of intracellular energy utilization such as myofibrils, sarcoplasmic reticulum, plasmalemma ion pumps, etc., by phosphotransfer pathway ("phosphocreatine shuttle") (Kaasik et al., 2001; Saks et al., 2001, 2006a,b, 2010). This complex might be regulated by the VDAC-β-tubulin II interaction, although an involvement of some other cytoskeletal proteins (e.g., plectin) cannot be excluded (**Figure 1B**). In contrast, in HL-1 cells with cardiac phenotype, lack of β-tubulin II and MtCK induce significant changes of main regulatory mechanisms of mitochondrial function and appear to be directly involved in the formation of their more glycolytic phenotype of energy metabolism.

Importantly, the structural changes occurring in the cytoskeletal network in pathology (dystrophies, myopathies) can result in mitochondrial impairment (**Figure 1A**). For example, in an animal model for Duchenne muscular dystrophy (mdx mice) dystrophin-deficient muscles suffer from a change in energy metabolism and mitochondrial dysfunction (Kuznetsov et al., 1998b). In skeletal muscles from mdx mice, mitochondrial respiration is about twice lower and similar findings were observed in a skeletal muscle biopsy from Duchenne muscular dystrophy patients. Also, the absence of dystrophin was associated with the disturbance of intracellular energy transfer between mitochondria and ATP-consuming systems. In mdx cardiac fibers, the accessibility of the ADP-trap system for endogenously produced ADP was reduced (Braun et al., 2001). Mitochondrial impairment was found also in plectin- and desmin-related muscular dystrophies. Similarly to the altered mitochondrial properties and network organization demonstrated in desmin-deficient mice (Milner et al., 2000), plectin deficiency leads to disruption of the mitochondrial network combined with dysfunction and loss of mitochondria (Konieczny et al., 2008).

LIMITATIONS

However, many aspects related to mitochondria-cytoskeleton interplay have yet to be elucidated. In particular, revealing precise nature of the VDAC-cytoskeleton interactions needs further studies using most modern methodological approaches (e.g., FRET) which will provide direct evidence, as well as a visualization of these interactions. Another important question to address is the possible different localization, function, and roles of various α-tubulin isoforms. Moreover, in future, reconstruction/reconstitution studies using β-tubulin II transfection and plectin fragments will certainly be required for further validation of the functional roles of these cytoskeletal elements in mitochondrial and entire cell physiology.

CONCLUSION

Thus, several lines of evidence suggest that certain cytoskeletal proteins may be involved in the control of the VDAC permeability for adenine nucleotides. In particular, specific mitochondrial localization of plectin 1b and β-tubulin II makes them best candidates for key roles to control the VDAC and thus, for the regulation of mitochondrial function. On the other hand, over-expression of β-tubulin II and enhanced VDAC-β-tubulin II interaction can explain ineffective energy transfer in aging and aging-related diseases. Indeed, our most recent studies demonstrate upregulation of β-tubulin II expression in the skeletal muscle of aged rats accompanied by energy metabolism impairments (Javadov, unpublished data).

ACKNOWLEDGMENTS

This work was supported by a research grant from the Austrian Science Fund (FWF): [P 22080-B20] (Andrey V. Kuznetsov) and by the National Heart, Lung, and Blood Institute of the National Institutes of Health through Research Grant SC1HL118669 (Sabzali Javadov).

REFERENCES

Andrienko, T., Kuznetsov, A. V., Kaambre, T., Usson, Y., Orosco, A., Appaix, F., et al. (2003). Metabolic consequences of functional complexes of mitochondria, myofibrils and sarcoplasmic reticulum in muscle cells. *J. Exp. Biol.* 206, 2059–2072.

Anesti, V., and Scorrano, L. (2006). The relationship between mitochondrial shape and function and the cytoskeleton. *Biochim. Biophys. Acta* 1757, 692–699.

Anmann, T., Guzun, R., Beraud, N., Pelloux, S., Kuznetsov, A. V., Kogerman, L., et al. (2006). Different kinetics of the regulation of respiration in permeabilized cardiomyocytes and in HL-1 cardiac cells. Importance of cell structure/organization for respiration regulation. *Biochim. Biophys. Acta* 1757, 1597–1606.

Appaix, F., Kuznetsov, A. V., Usson, Y., Kay, L., Andrienko, T., Olivares, J., et al. (2003). Possible role of cytoskeleton in intracellular arrangement and regulation of mitochondria. *Exp. Physiol.* 88, 175–190.

Balaban, R. S. (1990). Regulation of oxidative phosphorylation in the mammalian cell. *Am. J. Physiol.* 258, C377–C389.

Balaban, R. S. (2002). Cardiac energy metabolism homeostasis: role of cytosolic calcium. *J. Mol. Cell Cardiol.* 34, 1259–1271.

Balaban, R. S., Bose, S., French, S. A., and Territo, P. R. (2003). Role of calcium in metabolic signaling between cardiac sarcoplasmic reticulum and mitochondria *in vitro*. *Am. J. Physiol. Cell Physiol.* 284, C285–C293.

Belikova, Y. O., Kuznetsov, A. V., and Saks, V. A. (1990). Specific limitations for intracellular diffusion of ADP in cardiomyocytes. *Biochemistry* 55, 1450–1460.

Braun, U., Paju, K., Eimre, M., Seppet, E., Orlova, E., Kadaja, L., et al. (2001). Lack of dystrophin is associated with altered integration of the mitochondria and ATPases in slow-twitch muscle cells of MDX mice. *Biochim. Biophys. Acta* 1505, 258–270.

Burelle, Y., and Hochachka, P. W. (2002). Endurance training induces muscle-specific changes in mitochondrial function in skinned muscle fibers. *J. Appl. Physiol.* 92, 2429–2438.

Capetanaki, Y. (2002). Desmin cytoskeleton: a potential regulator of muscle mitochondrial behavior and function. *Trends Cardiovasc. Med.* 12, 339–348.

Carre, M., Andre, N., Carles, G., Borghi, H., Brichese, L., Briand, C., et al. (2002). Tubulin is an inherent component of mitochondrial membranes that interacts with the voltage-dependent anion channel. *J. Biol. Chem.* 277, 33664–33669.

Eimre, M., Puhke, R., Alev, K., Seppet, E., Sikkut, A., Peet, N., et al. (2006). Altered mitochondrial apparent affinity for ADP and impaired function of mitochondrial creatine kinase in gluteus medius of patients with hip osteoarthritis. *Am. J. Physiol. Regul. Integr. Comp. Physiol.* 290, R1271–R1275.

Fontaine, E. M., Keriel, C., Lantuejoul, S., Rigoulet, M., Leverve, X. M., and Saks, V. A. (1995). Cytoplasmic cellular structures control permeability of outer mitochondrial membrane for ADP and oxidative phosphorylation in rat liver cells. *Biochem. Biophys. Res. Commun.* 213, 138–146.

Glancy, B., and Balaban, R. S. (2012). Role of mitochondrial Ca2+ in the regulation of cellular energetics. *Biochemistry* 51, 2959–2973.

Gonzalez-Granillo, M., Grichine, A., Guzun, R., Usson, Y., Tepp, K., Chekulayev, V., et al. (2012). Studies of the role of tubulin beta II isotype in regulation of mitochondrial respiration in intracellular energetic units in cardiac cells. *J. Mol. Cell Cardiol.* 52, 437–447.

Guzun, R., Karu-Varikmaa, M., Gonzalez-Granillo, M., Kuznetsov, A. V., Michel, L., Cottet-Rousselle, C., et al. (2011). Mitochondria-cytoskeleton interaction: distribution of beta-tubulins in cardiomyocytes and HL-1 cells. *Biochim. Biophys. Acta* 1807, 458–469.

Hollenbeck, P. J., and Saxton, W. M. (2005). The axonal transport of mitochondria. *J. Cell Sci.* 118, 5411–5419.

Kaasik, A., Veksler, V., Boehm, E., Novotova, M., Minajeva, A., and Ventura-Clapier, R. (2001). Energetic crosstalk between organelles: architectural integration of energy production and utilization. *Circ. Res.* 89, 153–159.

Kay, L., Li, Z., Mericskay, M., Olivares, J., Tranqui, L., Fontaine, E., et al. (1997a). Study of regulation of mitochondrial respiration *in vivo*. An analysis of influence of ADP diffusion and possible role of cytoskeleton. *Biochim. Biophys. Acta* 1322, 41–59.

Kay, L., Rossi, A., and Saks, V. (1997b). Detection of early ischemic damage by analysis of mitochondrial function in skinned fibers. *Mol. Cell Biochem.* 174, 79–85.

Kay, L., Nicolay, K., Wieringa, B., Saks, V., and Wallimann, T. (2000). Direct evidence for the control of mitochondrial respiration by mitochondrial creatine kinase in oxidative muscle cells *in situ*. *J. Biol. Chem.* 275, 6937–6944.

Khuchua, Z. A., Ventura-Clapier, R., Kuznetsov, A. V., Grishin, M. N., and Saks, V. A. (1989). Alterations in the creatine kinase system in the myocardium of cardiomyopathic hamsters. *Biochem. Biophys. Res. Commun.* 165, 748–757.

Konieczny, P., Fuchs, P., Reipert, S., Kunz, W. S., Zeold, A., Fischer, I., et al. (2008). Myofiber integrity depends on desmin network targeting to Z-disks and costameres via distinct plectin isoforms. *J. Cell Biol.* 181, 667–681.

Kuznetsov, A. V., Mayboroda, O., Kunz, D., Winkler, K., Schubert, W., and Kunz, W. S. (1998a). Functional imaging of mitochondria in saponin-permeabilized mice muscle fibers. *J. Cell Biol.* 140, 1091–1099.

Kuznetsov, A. V., Winkler, K., Wiedemann, F. R., von Bossanyi, P., Dietzmann, K., and Kunz, W. S. (1998b). Impaired mitochondrial oxidative phosphorylation in skeletal muscle of the dystrophin-deficient mdx mouse. *Mol. Cell. Biochem.* 183, 87–96.

Kuznetsov, A. V., Tiivel, T., Sikk, P., Kaambre, T., Kay, L., Daneshrad, Z., et al. (1996). Striking differences between the kinetics of regulation of respiration by ADP in slow-twitch and fast-twitch muscles *in vivo*. *Eur. J. Biochem.* 241, 909–915.

Kuznetsov, A. V., Veksler, V., Gellerich, F. N., Saks, V., Margreiter, R., and Kunz, W. S. (2008). Analysis of mitochondrial function *in situ* in permeabilized muscle fibers, tissues and cells. *Nat. Protoc.* 3, 965–976.

Laclau, M. N., Boudina, S., Thambo, J. B., Tariosse, L., Gouverneur, G., Bonoron-Adele, S., et al. (2001). Cardioprotection by ischemic preconditioning preserves mitochondrial function and functional coupling between adenine nucleotide translocase and creatine kinase. *J. Mol. Cell Cardiol.* 33, 947–956.

Milner, D. J., Mavroidis, M., Weisleder, N., and Capetanaki, Y. (2000). Desmin cytoskeleton linked to muscle mitochondrial distribution and respiratory function. *J. Cell Biol.* 150, 1283–1298.

Mose-Larsen, P., Bravo, R., Fey, S. J., Small, J. V., and Celis, J. E. (1982). Putative association of mitochondria with a subpopulation of intermediate-sized filaments in cultured human skin fibroblasts. *Cell* 31, 681–692.

Rappaport, L., Oliviero, P., and Samuel, J. L. (1998). Cytoskeleton and mitochondrial morphology and function. *Mol. Cell Biochem.* 184, 101–105.

Rostovtseva, T. K., and Bezrukov, S. M. (2008). VDAC regulation: role of cytosolic proteins and mitochondrial lipids. *J. Bioenerg. Biomembr.* 40, 163–170.

Rostovtseva, T. K., Sheldon, K. L., Hassanzadeh, E., Monge, C., Saks, V., Bezrukov, S. M., et al. (2008). Tubulin binding blocks mitochondrial voltage-dependent anion channel and regulates respiration. *Proc. Natl. Acad. Sci. U.S.A.* 105, 18746–18751.

Saetersdal, T., Greve, G., and Dalen, H. (1990). Associations between beta-tubulin and mitochondria in adult isolated heart myocytes as shown by immunofluorescence and immunoelectron microscopy. *Histochemistry* 95, 1–10.

Saks, V., Belikova, Y., Vasilyeva, E., Kuznetsov, A., Fontaine, E., Keriel, C., et al. (1995). Correlation between degree of rupture of outer mitochondrial membrane and changes of kinetics of regulation of respiration by ADP in permeabilized heart and liver cells. *Biochem. Biophys. Res. Commun.* 208, 919–926.

Saks, V., Dzeja, P., Schlattner, U., Vendelin, M., Terzic, A., and Wallimann, T. (2006a). Cardiac system bioenergetics: metabolic basis of the Frank-Starling law. *J. Physiol.* 571, 253–273.

Saks, V., Favier, R., Guzun, R., Schlattner, U., and Wallimann, T. (2006b). Molecular system bioenergetics: regulation of substrate supply in response to heart energy demands. *J. Physiol.* 577, 769–777.

Saks, V., Guzun, R., Timohhina, N., Tepp, K., Varikmaa, M., Monge, C., et al. (2010). Structure-function relationships in feedback regulation of energy fluxes *in vivo* in health and disease: mitochondrial interactosome. *Biochim. Biophys. Acta* 1797, 678–697.

Saks, V., Kuznetsov, A., Andrienko, T., Usson, Y., Appaix, F., Guerrero, K., et al. (2003). Heterogeneity of ADP diffusion and regulation of respiration in cardiac cells. *Biophys. J.* 84, 3436–3456.

Saks, V., Kuznetsov, A. V., Gonzalez-Granillo, M., Tepp, K., Timohhina, N., Karu-Varikmaa, M., et al. (2012). Intracellular energetic units regulate metabolism in cardiac cells. *J. Mol. Cell Cardiol.* 52, 419–436.

Saks, V. A., Belikova, Y. O., and Kuznetsov, A. V. (1991a). *In vivo* regulation of mitochondrial respiration in cardiomyocytes: specific restrictions for intracellular diffusion of ADP. *Biochim. Biophys. Acta* 1074, 302–311.

Saks, V. A., Belikova, Y. O., Kuznetsov, A. V., Khuchua, Z. A., Branishte, T. H., Semenovsky, M. L., et al. (1991b). Phosphocreatine pathway for energy transport: ADP diffusion and cardiomyopathy. *Am. J. Physiol.* 261, 30–38.

Saks, V. A., Kaambre, T., Sikk, P., Eimre, M., Orlova, E., Paju, K., et al. (2001). Intracellular energetic units in red muscle cells. *Biochem. J.* 356, 643–657.

Saks, V. A., Kuznetsov, A. V., Kupriyanov, V. V., Miceli, M. V., and Jacobus, W. E. (1985). Creatine kinase of rat heart mitochondria. The demonstration of functional coupling to oxidative phosphorylation in an inner membrane-matrix preparation. *J. Biol. Chem.* 260, 7757–7764.

Saks, V. A., Vasil'eva, E., Belikova, Y., Kuznetsov, A. V., Lyapina, S., Petrova, L., et al. (1993). Retarded diffusion of ADP in cardiomyocytes: possible role of mitochondrial outer membrane and creatine kinase in cellular regulation of oxidative phosphorylation. *Biochim. Biophys. Acta* 1144, 134–148.

Tang, H. L., Lung, H. L., Wu, K. C., Le, A. H. P., Tang, H. M., and Fung, M. C. (2008). Vimentin supports mitochondrial morphology and organization. *Biochem. J.* 410, 141–146.

Tiivel, T., Kadaya, L., Kuznetsov, A., Kaambre, T., Peet, N., Sikk, P., et al. (2000). Developmental changes in regulation of mitochondrial respiration by ADP and creatine in rat heart *in vivo*. *Mol. Cell Biochem.* 208, 119–128.

Tonkonogi, M., and Sahlin, K. (2002). Physical exercise and mitochondrial function in human skeletal muscle. *Exerc. Sport Sci. Rev.* 30, 129–137.

Veksler, V. I., Kuznetsov, A. V., Anflous, K., Mateo, P., van Deursen, J., Wieringa, B., et al. (1995). Muscle creatine kinase-deficient mice. II. Cardiac and skeletal muscles exhibit tissue-specific adaptation of the mitochondrial function. *J. Biol. Chem.* 270, 19921–19929.

Vendelin, M., Beraud, N., Guerrero, K., Andrienko, T., Kuznetsov, A. V., Olivares, J., et al. (2005). Mitochondrial regular arrangement in muscle cells: a "crystal-like" pattern. *Am. J. Physiol. Cell Physiol.* 288, C757–C767.

Villani, G., Greco, M., Papa, S., and Attardi, G. (1998). Low reserve of cytochrome c oxidase capacity *in vivo* in the respiratory chain of a variety of human cell types. *J. Biol. Chem.* 273, 31829–31836.

Williamson, J. R. (1979). Mitochondrial function in the heart. *Annu. Rev. Physiol.* 41, 485–506.

Winter, L., Abrahamsberg, C., and Wiche, G. (2008). Plectin isoform 1b mediates mitochondrion-intermediate lament network linkage and controls organelle shape. *J. Cell Biol.* 181, 903–911.

Zoll, J., Sanchez, H., N'Guessan, B., Ribera, F., Lampert, E., Bigard, X., et al. (2002). Physical activity changes the regulation of mitochondrial respiration in human skeletal muscle. *J. Physiol.* 543, 191–200.

Zoll, J., Ventura-Clapier, R., Serrurier, B., and Bigard, A. X. (2001). Response of mitochondrial function to hypothyroidism in normal and regenerated rat skeletal muscle. *J. Muscle Res. Cell Motil.* 22, 141–147.

Conflict of Interest Statement: The authors declare that the research was conducted in the absence of any commercial or financial relationships that could be construed as a potential conflict of interest.

Received: 29 January 2013; accepted: 26 March 2013; published online: 22 April 2013.

Citation: Kuznetsov AV, Javadov S, Guzun R, Grimm M and Saks V (2013) Cytoskeleton and regulation of mitochondrial function: the role of beta-tubulin II. Front. Physiol. ***4****:82. doi: 10.3389/fphys.2013.00082*

This article was submitted to Frontiers in Mitochondrial Research, a specialty of Frontiers in Physiology.

frontiers in
PHYSIOLOGY

REVIEW ARTICLE
published: 30 May 2013
doi: 10.3389/fphys.2013.00126

Mitochondrial reactive oxygen species (ROS) as signaling molecules of intracellular pathways triggered by the cardiac renin-angiotensin II-aldosterone system (RAAS)

V. C. De Giusti, C. I. Caldiz, I. L. Ennis, N. G. Pérez, H. E. Cingolani and E. A. Aiello*

Facultad de Ciencias Médicas, Centro de Investigaciones Cardiovasculares, UNLP-CONICET, La Plata, Argentina

Edited by:
Sabzali Javadov, University of Puerto Rico School of Medicine, Puerto Rico

Reviewed by:
Amadou K. Camara, Medical College of Wisconsin, USA
Elena N. Dedkova, Rush University Medical Center, USA
John Hollander, West Virginia University School of Medicine, USA

***Correspondence:**
E. A. Aiello, Facultad de Ciencias Médicas, Centro de Investigaciones Cardiovasculares, UNLP-CONICET, Calle 60 y 120, La Plata 1900, Argentina
e-mail: aaiello@med.unlp.edu.ar

Mitochondria represent major sources of basal reactive oxygen species (ROS) production of the cardiomyocyte. The role of ROS as signaling molecules that mediate different intracellular pathways has gained increasing interest among physiologists in the last years. In our lab, we have been studying the participation of mitochondrial ROS in the intracellular pathways triggered by the renin-angiotensin II-aldosterone system (RAAS) in the myocardium during the past few years. We have demonstrated that acute activation of cardiac RAAS induces mitochondrial ATP-dependent potassium channel ($mitoK_{ATP}$) opening with the consequent enhanced production of mitochondrial ROS. These oxidant molecules, in turn, activate membrane transporters, as sodium/hydrogen exchanger (NHE-1) and sodium/bicarbonate cotransporter (NBC) via the stimulation of the ROS-sensitive MAPK cascade. The stimulation of such effectors leads to an increase in cardiac contractility. In addition, it is feasible to suggest that a sustained enhanced production of mitochondrial ROS induced by chronic cardiac RAAS, and hence, chronic NHE-1 and NBC stimulation, would also result in the development of cardiac hypertrophy.

Keywords: cardiac myocyte, second messenger systems, sodium-hydrogen antiporter, sodium-bicarbonate symporters, reactive oxygen species

INTRODUCTION

The renin-angiotensin-aldosterone-system (RAAS) represents one of the main endocrine systems that regulate cardiac physiology. At present, it is well recognized that angiotensin II (Ang II) is produced and secreted locally in several tissues, including the heart (Husain et al., 1994). Sadoshima's group has shown that the hormone is secreted from intracellular vacuoles in response to myocyte stretching for the first time. This Ang II exerts autocrine and paracrine effects, leading to cardiac hypertrophy (Sadoshima et al., 1993; Sadoshima and Izumo, 1996). Cingolani's group conducted an in depth study of this autocrine pathway as a physiological mechanism responsible for the slow force response (SFR) to myocardial stretch (Cingolani et al., 2001, 2003) and showed the similarities of both the physiological and pathological pathways (Cingolani et al., 2008). The critical role played by the cardiac Na^+/H^+ exchanger (NHE-1) activation in both physiological and pathological responses was demonstrated not only pharmacologically with NHE-1 inhibitors (Cingolani et al., 2011) but also by specific NHE-1 silencing following direct intramyocardial injection of small interfering RNA into rat left ventricular wall (Morgan et al., 2011; Cingolani et al., 2013). The precise mechanism to explain pathological responses is unclear and warrants further investigation. However, it is possible that the time of exposure to the stimulus and the amount of ROS produced could be important in determining the physiological or pathological pathways. Increasing time and amount of ROS exposure could exert a differential impact in calcium handling, an initial acute response leading to inotropic effects followed by a sustained response that could involve calcium-activated targets that participate in cardiac hypertrophy or heart failure, like calcineurin, or Ca^{2+}-calmodulin-dependent kinase type II (CaMKII).

Although still somewhat controversial (Silvestre et al., 1998, 1999; Takeda et al., 2000; Gomez-Sanchez et al., 2004; Chai and Danser, 2006), it has been suggested that aldosterone synthase exists in the myocyte (Silvestre et al., 1998, 1999; Takeda et al., 2000), supporting the presence of a local RAAS (Varagic and Frohlich, 2002). Furthermore, the link between Ang II or its AT_1 receptor, and the mineralocorticoid receptor (MR) is an accepted fact (Lemarie et al., 2008; Grossmann and Gekle, 2009). Consistently, it has also been described that some physiological cardiac effects of Ang II, as the SFR, can be prevented in the presence of MR blockers (Caldiz et al., 2011).

Although the idea that mitochondria are the main sources of basal reactive oxygen species (ROS) in other mammalian cells has been recently challenged, (Brown and Borutaite, 2012) their role as a very important source of ROS in the heart has been widely accepted. Mitochondrial superoxide anion (O_2^-) and its product, hydrogen peroxide (H_2O_2), were demonstrated to be important molecules implicated in several cardiac functions usually acting as second signal molecules of RAAS (Kimura et al., 2005a,b; Caldiz et al., 2007, 2011; De Giusti et al., 2008, 2009).

In this review, we will briefly summarize the current knowledge about the involvement of mitochondrial ROS as mediators of the signaling pathways triggered by RAAS in cardiac

myocytes without stressing out if they participate in acute or chronic signals. We will discuss the participation of the different components of RAAS in ROS production and in cardiac signaling leading to physiological and pathological responses. Particularly, we will remark the implication of the ion transporters (NHE-1 and NBC) in sodium and calcium overload and its relation with ROS signaling.

ANGIOTENSIN II, ENDOTHELIN-1, ALDOSTERONE AND EPIDERMAL GROWTH FACTOR: INDEPENDENT SIGNALS OR DIFFERENT COMPONENTS OF THE SAME CARDIAC SYSTEM?

Ang II is involved in the regulation of almost all cardiac functions. At present, it is well known that Ang II stimulates membrane ions transporters as NHE-1 (Fliegel and Karmazyn, 2004; Cingolani et al., 2005) and Na^+/HCO_3^- cotransporter (NBC) (Baetz et al., 2002; De Giusti et al., 2009; Aiello and De Giusti, 2012). These regulations are crucial for the correct electrical and mechanical cardiac functions. On the other hand, it is important to keep in mind that when RAAS is chronically active it is responsible for several cardiac diseases, for example, hypertrophy, heart failure and electrical disturbances (Domenighetti et al., 2007; Fischer et al., 2007; Mehta and Griendling, 2007; Palomeque et al., 2009; Li et al., 2013).

The mechanism of how the activation of NHE-1 or NBC regulates cardiac contractility seems to involve the increase in intracellular Na^+ concentration ($[Na^+]_i$) (Vaughan-Jones et al., 2006) due to the activation of these transporters and the subsequent increase in intracellular calcium concentration ($[Ca^{2+}]_i$) due to the activation of the reverse mode of the Na^+/Ca^{2+} exchanger (NCX) (Perez et al., 2001; Rothstein et al., 2002; Bril, 2003; Morgan et al., 2011). Interestingly, the same pathway is proposed to explain the development of cardiac hypertrophy (Ennis et al., 2007; Cingolani et al., 2008).

In addition, endothelin-1 (ET-1) and aldosterone (Ald) are key modulators of cardiac physiology *per se*. We have shown that ET-1 activates the NHE-1 (Aiello et al., 2005; De Giusti et al., 2008) leading to a positive inotropic effect (Szokodi et al., 2008). Moreover, Ald has been shown to activate NHE-1, (De Giusti et al., 2011) increase NHE-1 expression (Karmazyn et al., 2003) and induce left ventricular hypertrophy independently from its classical effects on regulation of renal Na^+ excretion and blood pressure (Qin et al., 2003; Yoshida et al., 2005; Diez, 2008). Classically, Ald enters the cells and binds to the MR located mainly in the cytosol. This binding translocates the MR to the nucleus, where it acts as a ligand-induced transcription factor. However, evidence has been presented that activated MR can elicit additional non-classical effects, which do not require transcription or translation of genes (Ebata et al., 1999; Mihailidou et al., 2004; Chai et al., 2005; Grossmann and Gekle, 2009). In addition, several of these rapid non-genomic effects of Ald involves the transactivation of the epidermal growth factor receptor (EGFR) (Grossmann and Gekle, 2007; Grossmann et al., 2007), which can, in turn, stimulate the NHE-1 (De Giusti et al., 2011). Moreover, it was reported that at least a small fraction of the classic MR is located in the cell plasma membrane where it is co-localized with the EGFR, inducing the transactivation of the latter (Grossmann et al., 2010).

More recently, it was demonstrated that certain non-genomic effects of Ald in vascular smooth muscle were due to simultaneous activation of MR and a surface membrane G protein–coupled receptor, the GPR30 (Gros et al., 2011, 2013). In agreement, growing evidence is appearing which demonstrate that GPR30 could be another Ald receptor involved in the rapid effects of the hormone in the cardiovascular system (Gros et al., 2011; Meyer et al., 2011).

At present, it is accepted that many effects initially believed to be mediated by Ang II, as the positive inotropic effect (PIE), and the increase in the SFR after myocardial stretching, are in fact attributable to the action of ET-1, which is released by Ang II (Perez et al., 2003; Cingolani et al., 2006, 2008; Villa-Abrille et al., 2006). Moreover, Ald appears to mediate some Ang II effects that participate in the same pathway of Ang II and ET-1 (**Figure 1**) (Xiao et al., 2004; Lemarie et al., 2008; Caldiz et al., 2011). Recently, it has been demonstrated that EGF is also implicated in cardiac physiology (De Giusti et al., 2011), and it has been described that the transactivation of the EGF receptor (EGFR) is involved in some RAAS effects (Shah and Catt, 2003; Zhai et al., 2006; De Giusti et al., 2011). We have suggested that all these extracellular and intracellular stimuli are pieces of the same signaling pathway (**Figure 1**). In this scenario, the activation of the MR takes place downstream from the Ang II/ET-1 receptors and upstream of the EGFR. The activation of EGFR triggers the intracellular ROS production, which leads to the stimulation of different kinases that finally activate the NHE-1 (Caldiz et al., 2011).

Interestingly, almost all the effects of these hormones involve ROS-mediated pathways (Zhang et al., 2001; Caldiz et al., 2007, 2011; Bartosz, 2009). In this regard, it is accepted that Ang II, (Giordano, 2005; Kimura et al., 2005b; De Giusti et al., 2009), ET-1 (De Giusti et al., 2008; Kubin et al., 2011), Ald (Hayashi et al., 2008; Caldiz et al., 2011) and EGF (De Giusti et al., 2011) can activate NADPH oxidase (NOX), which then, as further explained below, can stimulate mitochondrial ROS production and mediate the effects of such hormones (**Figure 1**). Therefore, it seems clear that RAAS effects are in close relationship with ROS generation, and in order to be able to modulate RAAS signaling, we should investigate the regulation of ROS production in detail.

MAJOR SOURCES OF ROS: NOX, MITOCHONDRIA AND THEIR CROSS-TALK

ROS have been considered deleterious agents for a long time. However, in the last years, evidence has emerged supporting their role as second messengers (D'autreaux and Toledano, 2007). Under physiological conditions, the production of ROS is highly restricted to specific subcellular sites. The major sources of ROS in the cardiomyocytes are NOX (Bedard and Krause, 2007) and the I, II and III complexes of the mitochondrial respiratory chain (Camara et al., 2010; Dedkova et al., 2013; Drose, 2013; Li et al., 2013; Wojtovich et al., 2013). In this regard, complex II is emerging as the major modulator of mitochondrial

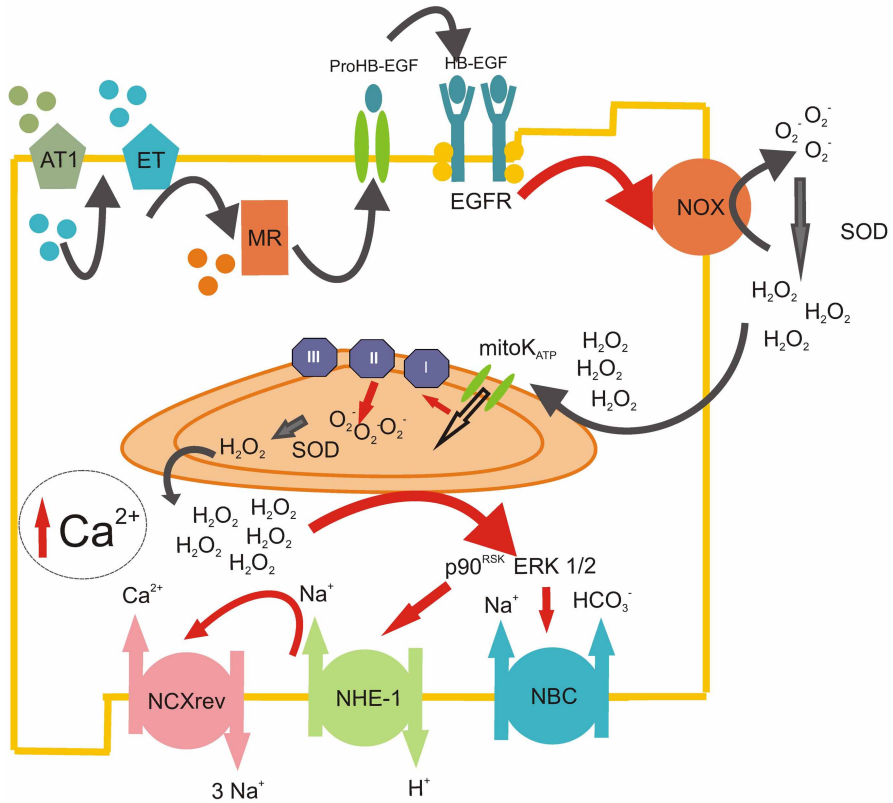

FIGURE 1 | ROS-induced ROS-release mechanism triggered by RAAS. Scheme representing the sequential steps involved in the production of mitochondrial ROS after the initial Ang II stimulation. Ang II acting on AT_1 receptors induces the release of intracellular ET-1, which, in turn, acts in an autocrine manner on ET_A receptors. This autocrine action leads to the activation of the mineralocorticoid receptor (MR), which induces the transactivation of the EGFR, possibly via the release of membrane heparin-bound EGF (HB-EGF). The stimulation of the EGFR leads to the activation of the NADPH oxidase (NOX), which produces superoxide anion (O_2^-) and quickly dismutate by superoxide dismutase (SOD) to hydrogen peroxide (H_2O_2). This permanent and stable oxidant molecule produces the opening of mitochondrial ATP-dependant potassium channels (mitoK$_{ATP}$) with the subsequent enhanced production of mitochondrial O_2^- by the electron transport chain (mainly by complex II). These mitochondrial ROS are released to the cytosol (ROS-induced ROS-release mechanism), where they stimulate redox sensitive MAPkinases ERK 1/2 and p90^{RSK}, which, in turn, activate NHE-1 and NBC, pH regulation transporters that induce the increase in intracellular Na^+. Finally, this cytosolic Na^+ increase favors the operation of the reverse mode of NCX, promoting the influx of Ca^{2+} into the cell. The enhancement of intracellular Ca^{2+} in the cardiomyocyte could lead to a positive inotropic effect in the short term and/or the development of cardiac hypertrophy in a time-prolonged scenario.

ROS production (Drose, 2013). Moreover, it was proposed that complex II can adopt different roles as a producer or modulator of mitochondrial ROS, depending on the substrate supply and the activities of the other respiratory chain complexes (Drose, 2013). The primary function of complex II is to maintain the reduced state of mitochondrial chain complexes (Wojtovich et al., 2013). Importantly, it was demonstrated that complex II, instead of complex I or III, is the major source of ROS during heart failure (Dedkova et al., 2013). On the other hand, it has been proposed that the production of "deleterious ROS" during reperfusion can be related to complex I, while the generation of "signaling ROS" during preconditioning occurs at complex II (Drose, 2013). Although the precise mechanism is not clear yet, the modulation of complex II seems to be cardioprotective during ischemic preconditioning (Wojtovich et al., 2013). These data, however, do not support previous results which suggested that the production of ROS induced after mitoK$_{ATP}$ opening is accounted by complex I (Andrukhiv et al., 2006), and that ischemic preconditioning is mediated by ROS generated after the activation of these channels (Oldenburg et al., 2004).

At present it is accepted that NOX produce extracellular O_2^-, which dismutate to H_2O_2. Although it has been generally assumed that H_2O_2 diffuses back into the cell across the plasma membrane, recent evidence suggests that it might preferentially enter the cell through specific aquaporin channels (Bienert et al., 2007; Miller et al., 2010), providing a potential mechanism through which ROS signaling could be regulated. It is also accepted that matrix H_2O_2 permeates through the mitochondrial inner membrane after being produced by the action of Mn-SOD, which dismutates mitochondrial O_2^-. However, it is important to note that O_2^- also permeates mitochondrial membrane through anion channels (Bedard and Krause, 2007) and hence could potentially act as a signaling molecule. The SFR, which represents an acute and physiological response triggered by RAAS activation, was reported to be due to H_2O_2 signaling

(Caldiz et al., 2007). Moreover, experiments by Sabri et al. (1998) and Rothstein et al. (2002) indicated that H_2O_2 is the intracellular signal leading to the activation of kinases that phosphorylate the NHE-1. On the other hand, O_2^-- not H_2O_2- was reported to be the signaling molecule in the ET-1-induced stimulation of cardiac L-type calcium channels (Zeng et al., 2008). Nevertheless, if mitochondrial H_2O_2 or O_2^- could cause different responses to RAAS activation, i.e., acute versus chronic, it would be an interesting topic that deserves future investigation.

NOX and mitochondria are not totally independent sources of ROS, since recent evidence demonstrate the existence of a substantial interplay between both sources, such as activation of one leading to the activation of the other (Dikalov, 2011). In 2000, Zorov et al. (2000) published the first study describing the phenomenon called "ROS-induced ROS-release" by which a small amount of ROS triggers greater ROS production from the mitochondria. Five years later, Dr. Kimura's group proposed the Ang II-induced NOX stimulation as the generator of the small amount of ROS triggering mitochondrial ROS production (Kimura et al., 2005a) (**Figure 1**). It is important to note that this "ROS-induced ROS-release" mechanism is implicated in Ang II-mediated preconditioning.

The main link between both sources of ROS seems to be the mitochondrial ATP-dependent potassium channel (mitoK_{ATP}). It was demonstrated that the opening of these channels is crucial to stimulate ROS production by the respiratory chain. Three phenomena were proposed to activate the mitochondrial respiratory chain and produce ROS: moderate matrix swelling, matrix alkalinization and inner membrane depolarization (Pain et al., 2000; Andrukhiv et al., 2006). A still unresolved issue is how the mitoK_{ATP} are opened. On the one hand, it has been reported that O_2^- can directly stimulate the mitoK_{ATP}, (Zhang et al., 2001, 2007) on the other hand, there is enough evidence that demonstrate the involvement of PKC as an activator of mitoK_{ATP} (Sato et al., 1998; Costa et al., 2006; Costa and Garlid, 2008). In addition, other studies have proposed that the cardioprotective effect of G_i-coupled receptor agonists are due to EGFR transactivation and subsequent stimulation of the PI3K/Akt pathway, which lead to a PKG-mediated opening of mK_{ATP} channels and increased O_2^- production (Krieg et al., 2002, 2003, 2004). These authors proposed that PI3K/Akt increase nitric oxide levels, which, in turn, stimulates the guanylate cyclase, augmenting cGMP content and activating PKG, inducing the opening of mitoK_{ATP} channels (Krieg et al., 2004; Oldenburg et al., 2004).

Interestingly, it seems that not only NOX-derived ROS trigger mitochondrial ROS production, but also a small amount of mitochondrial ROS released to the cytosol could potentially further activate ROS-induced ROS-release in neighboring mitochondria (Costa and Garlid, 2008). In addition, mitochondrial ROS can stimulate NOX directly or mediated by PKC activation (Doughan et al., 2008; Wenzel et al., 2008; Camara et al., 2010; Dikalov, 2011). These different signaling regulations create a truly cross-talk between the major sources of ROS (Daiber, 2010). This issue is important because it converts the mitochondrion to a ROS-amplifier. Myocytes spend little energy to start the intracellular signaling and then the cycle helps to potentiate ROS-production (**Figure 2**).

THE MITOCHONDRIAL ROS ARE THE MEDIATORS OF RAAS-INDUCED NHE-1 AND NBC REGULATION, OR IS IT THE OPPOSITE?

ROS-mediated activation of NHE-1 (Sabri et al., 1998; Snabaitis et al., 2002; Caldiz et al., 2007, 2011; De Giusti et al., 2008) and NBC (De Giusti et al., 2009; Aiello and De Giusti, 2012) has been reported to be due to redox sensitive kinase-mediated phosphorylation. In this regard, there is enough evidence supporting the notion that ROS favors the activation of ERK 1/2 and $p90^{RSK}$ in neonatal and adult cardiomyocytes (Sabri et al., 1998; Rothstein et al., 2002).

As described above, the components of RAAS are well known activators of ROS production (Hanna et al., 2002; Seshiah et al., 2002; Kimura et al., 2005b; Doughan et al., 2008). Moreover, in our lab, we have investigated the pathway by which myocardial stretch sequentially stimulates ROS production, activates ERK 1/2 and $p90^{RSK}$ and finally leads to the stimulation of NHE-1 (Caldiz et al., 2007, 2011; Villa-Abrille et al., 2010). We demonstrated that NHE-1 stimulation is responsible for the SFR in the acute phase. Thus, we proposed that NHE-1 stimulation is potentially responsible, in a more prolonged term, for chronic and pathological responses, such as the development of cardiac hypertrophy (Cingolani et al., 2008).

As **Figure 1** shows, RAAS signaling leads to an increase in ROS production and subsequent activation of ERK 1/2 and $p90^{RSK}$ kinases, which stimulate both transporters, NHE-1 and NBC. The stimulation of these transporters might lead to an increase in $[Na^+]_i$ (Vaughan-Jones et al., 2006), which is known to induce the operation of the reverse mode of NCX, leading to an increase in $[Ca^{2+}]_i$ and a positive inotropic effect. Mitochondrial Ca^{2+} (mCa^{2+}) uptake through the calcium uniporter (CaU) is in part dependent on the Ca^{2+} gradient between the cytosol and the mitochondrial matrix (Camara et al., 2010). Thus, it seems evident that the cytosolic Ca^{2+} increase, following the activation of NHE-1 and NBC, may lead to an increase in mCa^{2+}. Mitochondrial Ca^{2+} loading regulates cellular respiration and mediates cell death (Camara et al., 2010). Calcium, through the activation of the CaMKII, was described as one of the main activators of NOX (Nishio et al., 2012) and mitochondrial ROS production (Song et al., 2011), creating a positive feed-back (feed-back 3, **Figure 2**) by which the ROS pathways acquire a central role in cell physiology (Trebak et al., 2010; Gul et al., 2012).

It has been described that the NHE-1 blockers attenuate the mCa^{2+} overload, ROS production and mPTP opening induced by ouabain (Toda et al., 2007). These authors proposed two possible mechanisms: (a) the NHE-1 inhibition prevents the increase in $[Na^+]_i$ and subsequent $[Ca^{2+}]_i$, which reduces the driving force for mCa^{2+} uptake, and (b) NHE-1 inhibition might indirectly activate the mitoK_{ATP} channel (the protection induced by NHE-1 blockers is prevented with the mitoK_{ATP} blocker 5-HD). In addition, it has been demonstrated that NHE-1 inhibition prevents mPTP opening during the first minutes after reperfusion, leading to an improvement of mitochondrial function as well as an attenuation of pro-apoptotic factors. In this work, the authors discussed several possibilities for the NHE-1-inhibition-induced protection, being the most important the attenuation of $[Ca^{2+}]_i$ overload and the delay of pH_i recovery

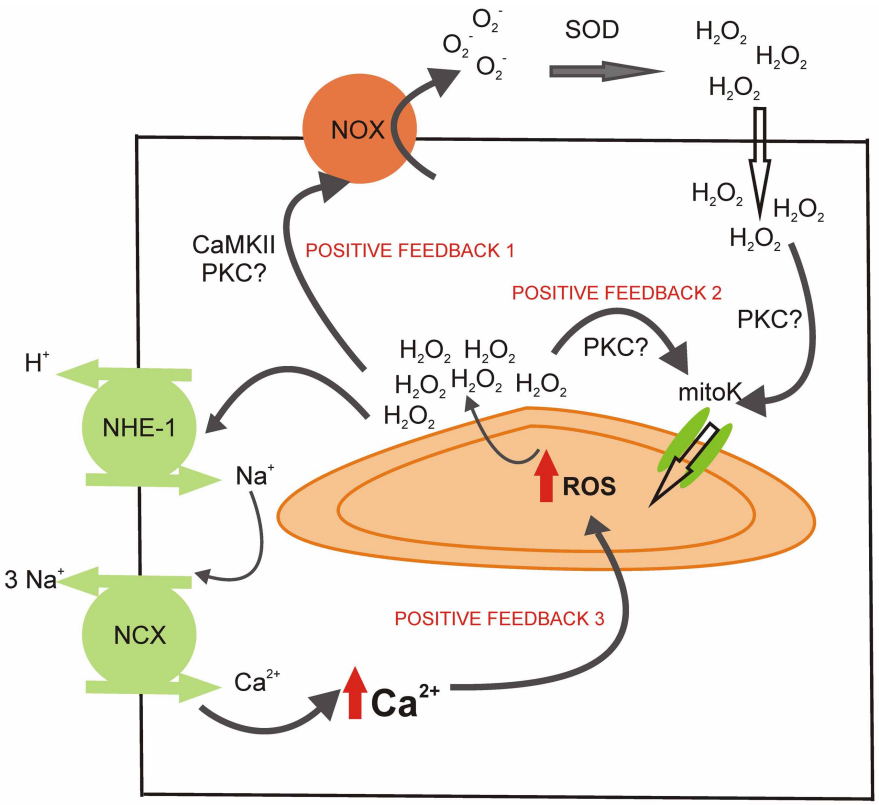

FIGURE 2 | Potential sites of positive feedback mechanisms involved in the mitochondrial ROS production during the activation of RAAS. The H_2O_2 released by the mitochondria during the ROS-induced ROS-release mechanism could activate NOX (possibly via CaMKII or PKC activation), cycling the mitochondrial ROS production (positive feedback 1). The mitochondrial ROS could also help to maintain the opening of $mitoK_{ATP}$ (positive feedback 2), perhaps through the activation of PKC. Finally, the intracellular Ca^{2+} augmentation after NHE-1 and NCX reverse mode stimulation could induce mitochondrial Ca^{2+} load and further ROS production (positive feedback 3).

during reperfusion (Javadov et al., 2008). Moreover, Garciarena et al. (2008) working on isolated mitochondria, showed that the NHE-1 inhibitors modulate mitochondrial ROS production via a direct mitochondrial action. However, the site of action has not been elucidated. Nevertheless, it is important to point out again that the careful regulation of ROS production, which involves the modulation of calcium handling, represents a crucial process in myocardial intracellular signaling (**Figure 2**).

MITOCHONDRIAL ROS AND CARDIAC PATHOLOGY

When the cells are exposed to the same stimuli for long periods of time, they begin to lose their equilibrium, and in this scenario ROS and Ca^{2+} might represent dangerous molecules, leading to arrhythmias and cardiac hypertrophy (Terentyev et al., 2008; Zhao et al., 2011; Maulik and Kumar, 2012). In this regard, high mCa^{2+} impairs ATP synthesis leading to a loss in ion homeostasis, opening of mPTP and matrix swelling. The irreversible mPTP opening is associated with release of cytochrome C and more ROS production, resulting in a harmful vicious cycle of further amplification of ROS production, mCa^{2+} overload and irreversible cell damage, which lead to cell death (Camara et al., 2010). On the other hand, several investigations have demonstrated that a low increase in matrix ROS is sufficient to trigger brief, stochastic openings of mPTP, perhaps through reversible thiol oxidation (Wang et al., 2008). Moreover, these transient brief openings of mPTP have been involved as a "physiological valve", alleviating mCa^{2+} overload and providing protection against cellular injury (Smaili and Russell, 1999; Kindler et al., 2003).

There are several evidences that involve the participation of ROS produced by NOX in different models of heart failure with RAAS activation (Sorescu and Griendling, 2002; Guo et al., 2006). Since NOX-produced ROS can be amplified by ROS generated by mitochondria during the ROS-induced-ROS release mechanism, this process could be also involved in the development of cardiac hypertrophy and the transition to heart failure. Indeed, it was reported that mice that overexpress catalase (antioxidant enzyme that degrades H_2O_2) targeted to mitochondria are resistant to cardiac hypertrophy, fibrosis and mitochondrial damage induced by Ang II as well as heart failure induced by overexpression of Gαq (Dai et al., 2011). In addition, Ang II-induced mitochondrial ROS are implicated in the development of apoptosis (Choudhary et al., 2008). Thus, breaking the ROS vicious cycle within mitochondria by antioxidants specifically targeted to this organelle would be effective to attenuate both cardiac hypertrophy and failure.

It was recently demonstrated that Ang II binds to AT_1 and AT_2 receptors localized in the mitochondrial inner membrane

(mAT_1 and mAT_2) (Abadir et al., 2011). The authors of this study proposed an interesting model, where they associated the subtype of Ang II receptor and the type of ROS generated by mitochondria. In young animals, the activation of mAT_2 induced protective mitochondrial NO generation. However, this protection disappeared with aging, possibly, due to harmful ROS producing an increased expression of mAT_1. A similar speculation of mAT_1 and mAT_2 remodeling with aging could be done for cardiovascular diseases. In contrast, Doughan et al. (2008) demonstrated that Ang II does not exert any effect on isolated mitochondria. Moreover, it will be necessary to elucidate how Ang II gains access to the intracellular space, either by internalization or by local synthesis (Inagami, 2011). The relevance of this intracellular action of Ang II on mitochondrial ROS production remains to be studied.

FINAL NOTES AND PERSPECTIVES

The main objective of this review was to emphasize the participation of mitochondria in the signaling pathways of RAAS. As we have shown, almost all the effects of RAAS involve the production of ROS, and the main source of them appears to be mitochondria. In summary, we attempted to call attention to the central role of cardiomyocyte mitochondria as the sites where the cellular signaling mediated by ROS converge.

Mitochondria have been mainly thought as the organelles that generate energy. However, in the last years, we have learned that mitochondria are much more than only an "ATP-plant production". They are involved in cellular ion homeostasis, oxidative stress and cell survival or death. The main role of mitochondria seems to be the supervisor of cell functions. Mitochondria are the main source of ROS and, more important, they can interact with others sources of ROS in order to amplify the signal. Moreover, ROS regulate calcium signaling, which can also act as second messenger and further stimulate ROS production, creating a cycle, capable of being regulated at many steps (**Figure 2**).

As commented above, in the past ROS were thought exclusively as deleterious molecules. However, recent studies show that they appear to be very important second messengers that mediate different intracellular pathways. What has changed? The molecules, the stimuli and the sources are the same. Perhaps, we should believe that we are just beginning to uncover how the cells can use harmful reactive species for their own benefit.

Finally, we would like to highlight that mitochondrial ROS signaling may be an attractive target for therapeutic drugs in order to suppress RAAS signals. However, due to the complexity of the mechanisms involved, this idea requires careful evaluation, since targeting the wrong site at the wrong moment could not only worsen the disease, but could also suppress important physiological signaling pathways.

REFERENCES

Abadir, P. M., Foster, D. B., Crow, M., Cooke, C. A., Rucker, J. J., Jain, A., et al. (2011). Identification and characterization of a functional mitochondrial angiotensin system. *Proc. Natl. Acad. Sci. U.S.A.* 108, 14849–14854. doi: 10.1073/pnas.1101507108

Aiello, E. A., and De Giusti, V. C. (2012). Regulation of the cardiac sodium/bicarbonate cotransporter by angiotensin II: potential contribution to sodium and calcium overload. *Curr. Cardiol. Rev*. 9, 24–32. doi: 10.2174/1573403X11309010005

Aiello, E. A., Villa-Abrille, M. C., Dulce, R. A., Cingolani, H. E., and Perez, N. G. (2005). Endothelin-1 stimulates the Na^+/Ca^{2+} exchanger reverse mode through intracellular Na^+ ($Na^+{}_i$)-dependent and $Na^+{}_i$-independent pathways. *Hypertension* 45, 288–293. doi: 10.1161/01.HYP.0000152700.58940.b2

Andrukhiv, A., Costa, A. D., West, I. C., and Garlid, K. D. (2006). Opening $_{mito}$KATP increases superoxide generation from complex I of the electron transport chain. *Am. J. Physiol. Heart Circ. Physiol.* 291, H2067–H2074. doi: 10.1152/ajpheart.00272.2006 pp.H2067-74

Baetz, D., Haworth, R. S., Avkiran, M., and Feuvray, D. (2002). The ERK pathway regulates Na^+-HCO_3^- cotransport activity in adult rat cardiomyocytes. *Am. J. Physiol. Heart Circ. Physiol.* 283, H2102–H2109. doi: 10.1152/ajpheart.01071.2001

Bartosz, G. (2009). Reactive oxygen species: destroyers or messengers? *Biochem. Pharmacol.* 77, 1303–1315. doi: 10.1016/j.bcp.2008.11.009

Bedard, K., and Krause, K. H. (2007). The NOX family of ROS-generating NADPH oxidases: physiology and pathophysiology. *Physiol. Rev.* 87, 245–313. doi: 10.1152/physrev.00044.2005

Bienert, G. P., Moller, A. L., Kristiansen, K. A., Schulz, A., Moller, I. M., Schjoerring, J. K., et al. (2007). Specific aquaporins facilitate the diffusion of hydrogen peroxide across membranes. *J. Biol. Chem.* 282, 1183–1192. doi: 10.1074/jbc

Bril, A. (2003). Ion transporters and cardiovascular diseases: pH control or modulation of intracellular calcium concentration. *Ann. Cardiol. Angeiol. (Paris)* 52, 41–51.

Brown, G. C., and Borutaite, V. (2012). There is no evidence that mitochondria are the main source of reactive oxygen species in mammalian cells. *Mitochondrion* 12, 1–4. doi: 10.1016/j.mito.2011.02.001

Caldiz, C. I., Diaz, R. G., Nolly, M. B., Chiappe De Cingolani, G. E., Ennis, I. L., Cingolani, H. E., et al. (2011). Mineralocorticoid receptor activation is crucial in the signaling pathway leading to the Anrep effect. *J. Physiol.* 589, 6051–6061. doi: 10.1113/jphysiol.2011.218750

Caldiz, C. I., Garciarena, C. D., Dulce, R. A., Novaretto, L. P., Yeves, A. M., Ennis, I. L., et al. (2007). Mitochondrial reactive oxygen species activate the slow force response to stretch in feline myocardium. *J. Physiol.* 584, 895–905. doi: 10.1113/jphysiol.2007.141689

Camara, A. K., Lesnefsky, E. J., and Stowe, D. F. (2010). Potential therapeutic benefits of strategies directed to mitochondria. *Antioxid. Redox Signal.* 13, 279–347. doi: 10.1089/ars.2009.2788

Chai, W., and Danser, A. H. (2006). Why are mineralocorticoid receptor antagonists cardioprotective? Naunyn Schmiedebergs. *Arch. Pharmacol.* 374, 153–162. doi: 10.1007/s00210-006-0107-9

Chai, W., Garrelds, I. M., Arulmani, U., Schoemaker, R. G., Lamers, J. M., and Danser, A. H. (2005). Genomic and nongenomic effects of aldosterone in the rat heart: why is spironolactone cardioprotective? *Br. J. Pharmacol.* 145, 664–671. doi: 10.1038/sj.bjp.0706220

Choudhary, R., Baker, K. M., and Pan, J. (2008). All-trans retinoic acid prevents angiotensin II- and mechanical stretch-induced reactive oxygen species generation and cardiomyocyte apoptosis. *J. Cell. Physiol.* 215, 172–181. doi: 10.1002/jcp.21297

Cingolani, H. E., Ennis, I. L., Aiello, E. A., and Perez, N. G. (2011). Role of autocrine/paracrine mechanisms in response to myocardial strain. *Pflugers Arch.* 462, 29–38. doi: 10.1007/s00424-011-0930-9

Cingolani, H. E., Perez, N. G., Aiello, E. A., and De Hurtado, M. C. (2005). Intracellular signaling following myocardial stretch: an autocrine/paracrine loop. *Regul. Pept.* 128, 211–220. doi: 10.1016/j.regpep.2004.12.011

Cingolani, H. E., Perez, N. G., Aiello, E. A., Ennis, I. L., Garciarena, C. D., Villa-Abrille, M. C., et al. (2008). Early signals after stretch leading to cardiac hypertrophy. Key role of NHE-1. *Front. Biosci.* 13, 7096–7114. doi: 10.2741/3213

Cingolani, H. E., Perez, N. G., and Camilion De Hurtado, M. C. (2001). An autocrine/paracrine mechanism triggered by myocardial stretch induces changes in contractility. *News Physiol. Sci.* 16, 88–91.

Cingolani, H. E., Perez, N. G., Cingolani, O. H., and Ennis, I. L. (2013). The Anrep effect: 100 years later. *Am. J. Physiol. Heart Circ. Physiol.* 304, H175–H182. doi: 10.1152/ajpheart.00508.2012

Cingolani, H. E., Perez, N. G., Pieske, B., Von Lewinski, D., and Camilion De Hurtado, M. C. (2003). Stretch-elicited Na^+/H^+ exchanger activation: the autocrine/paracrine loop and its mechanical counterpart. *Cardiovasc. Res.* 57, 953–960. doi: 10.1016/S0008-6363(02)00861-1

Cingolani, H. E., Villa-Abrille, M. C., Cornelli, M., Nolly, A., Ennis, I. L., Garciarena, C., et al. (2006). The positive inotropic effect of angiotensin II: role of endothelin-1 and reactive oxygen species. *Hypertension* 47, 727–734. doi: 10.1161/01.HYP.0000208302.62399.68

Costa, A. D., and Garlid, K. D. (2008). Intramitochondrial signaling: interactions among $_{mito}$KATP, PKCepsilon, ROS, and MPT. *Am. J. Physiol. Heart Circ. Physiol.* 295, H874–H882. doi: 10.1152/ajpheart.01189.2007

Costa, A. D., Jakob, R., Costa, C. L., Andrukhiv, K., West, I. C., and Garlid, K. D. (2006). The mechanism by which the mitochondrial ATP-sensitive K^+ channel opening and H_2O_2 inhibit the mitochondrial permeability transition. *J. Biol. Chem.* 281, 20801–20808. doi: 10.1074/jbc.M600959200

D'autreaux, B., and Toledano, M. B. (2007). ROS as signaling molecules: mechanisms that generate specificity in ROS homeostasis. *Nat. Rev. Mol. Cell. Biol.* 8, 813–824. doi: 10.1038/nrm2256

Dai, D. F., Johnson, S. C., Villarin, J. J., Chin, M. T., Nieves-Cintron, M., Chen, T., et al. (2011). Mitochondrial oxidative stress mediates angiotensin II-induced cardiac hypertrophy and Galphaq overexpression-induced heart failure. *Circ. Res.* 108, 837–846. doi: 10.1161/CIRCRESAHA.110.232306

Daiber, A. (2010). Redox signaling (cross-talk) from and to mitochondria involves mitochondrial pores and reactive oxygen species. *Biochim. Biophys. Acta* 1797, 897–906. doi: 10.1016/j.bbabio.2010.01.032

De Giusti, V. C., Correa, M. V., Villa-Abrille, M. C., Beltrano, C., Yeves, A. M., De Cingolani, G. E., et al. (2008). The positive inotropic effect of endothelin-1 is mediated by mitochondrial reactive oxygen species. *Life Sci.* 83, 264–271. doi: 10.1016/j.lfs.2008.06.008

De Giusti, V. C., Garciarena, C. D., and Aiello, E. A. (2009). Role of reactive oxygen species (ROS) in angiotensin II-induced stimulation of the cardiac Na^+/HCO_3^- cotransport. *J. Mol. Cell. Cardiol.* 47, 716–722. doi: 10.1016/j.yjmcc.2009.07.023

De Giusti, V. C., Nolly, M. B., Yeves, A. M., Caldiz, C. I., Villa-Abrille, M. C., Chiappe De Cingolani, G. E., et al. (2011). Aldosterone stimulates the cardiac Na^+/H^+ exchanger via transactivation of the epidermal growth factor receptor. *Hypertension* 58, 912–919. doi: 10.1161/HYPERTENSIONAHA.111.176024

Dedkova, E. N., Seidlmayer, L. K., and Blatter, L. A. (2013). Mitochondria-mediated cardioprotection by trimetazidine in rabbit heart failure. *J. Mol. Cell. Cardiol.* 59C, 41–54. doi: 10.1016/j.yjmcc.2013.01.016

Diez, J. (2008). Effects of aldosterone on the heart: beyond systemic hemodynamics? *Hypertension* 52, 462–464. doi: 10.1161/HYPERTENSIONAHA.108.117044

Dikalov, S. (2011). Cross talk between mitochondria and NADPH oxidases. *Free Radic. Biol. Med.* 51, 1289–1301. doi: 10.1016/j.freeradbiomed.2011.06.033

Domenighetti, A. A., Boixel, C., Cefai, D., Abriel, H., and Pedrazzini, T. (2007). Chronic angiotensin II stimulation in the heart produces an acquired long QT syndrome associated with IK1 potassium current downregulation. *J. Mol. Cell. Cardiol.* 42, 63–70. doi: 10.1016/j.yjmcc.2006.09.019

Doughan, A. K., Harrison, D. G., and Dikalov, S. I. (2008). Molecular mechanisms of angiotensin II-mediated mitochondrial dysfunction: linking mitochondrial oxidative damage and vascular endothelial dysfunction. *Circ. Res.* 102, 488–496. doi: 10.1161/CIRCRESAHA.107.162800

Drose, S. (2013). Differential effects of complex II on mitochondrial ROS production and their relation to cardioprotective pre- and postconditioning. *Biochim. Biophys. Acta* 1827, 578–587. doi: 10.1016/j.bbabio.2013.01.004

Ebata, S., Muto, S., Okada, K., Nemoto, J., Amemiya, M., Saito, T., et al. (1999). Aldosterone activates Na^+/H^+ exchange in vascular smooth muscle cells by nongenomic and genomic mechanisms. *Kidney Int.* 56, 1400–1412. doi: 10.1046/j.1523-1755.1999.00674.x

Ennis, I. L., Garciarena, C. D., Escudero, E. M., Perez, N. G., Dulce, R. A., Camilion De Hurtado, M. C., et al. (2007). Normalization of the calcineurin pathway underlies the regression of hypertensive hypertrophy induced by Na^+/H^+ exchanger-1 (NHE-1) inhibition. *Can. J. Physiol. Pharmacol.* 85, 301–310. doi: 10.1139/Y06-072

Fischer, R., Dechend, R., Gapelyuk, A., Shagdarsuren, E., Gruner, K., Gruner, A., et al. (2007). Angiotensin II-induced sudden arrhythmic death and electrical remodeling. *Am. J. Physiol. Heart Circ. Physiol.* 293, H1242–H1253. doi: 10.1152/ajpheart.01400.2006

Fliegel, L., and Karmazyn, M. (2004). The cardiac Na-H exchanger: a key downstream mediator for the cellular hypertrophic effects of paracrine, autocrine and hormonal factors. *Biochem. Cell. Biol.* 82, 626–635. doi: 10.1139/o04-129

Garciarena, C. D., Caldiz, C. I., Correa, M. V., Schinella, G. R., Mosca, S. M., Chiappe De Cingolani, G. E., et al. (2008). Na^+/H^+ exchanger-1 inhibitors decrease myocardial superoxide production via direct mitochondrial action. *J. Appl. Physiol.* 105, 1706–1713. doi: 10.1152/japplphysiol.90616.2008

Giordano, F. J. (2005). Oxygen, oxidative stress, hypoxia, and heart failure. *J. Clin. Invest.* 115, 500–508. doi: 10.1172/JCI24408

Gomez-Sanchez, E. P., Ahmad, N., Romero, D. G., and Gomez-Sanchez, C. E. (2004). Origin of aldosterone in the rat heart. *Endocrinology* 145, 4796–4802. doi: 10.1210/en.2004-0295

Gros, R., Ding, Q., Liu, B., Chorazyczewski, J., and Feldman, R. D. (2013). Aldosterone mediates its rapid effects in vascular endothelial cells through Gper/Gpr30 activation. *Am. J. Physiol. Cell Physiol.* 304, C532–C540. doi: 10.1152/ajpcell.00203.2012

Gros, R., Ding, Q., Sklar, L. A., Prossnitz, E. E., Arterburn, J. B., Chorazyczewski, J., et al. (2011). GPR30 expression is required for the mineralocorticoid receptor-independent rapid vascular effects of aldosterone. *Hypertension* 57, 442–451. doi: 10.1161/HYPERTENSIONAHA.110.161653

Grossmann, C., and Gekle, M. (2007). Non-classical actions of the mineralocorticoid receptor: misuse of EGF receptors? *Mol. Cell. Endocrinol.* 277, 6–12. doi: 10.1016/j.mce.2007.07.001

Grossmann, C., and Gekle, M. (2009). New aspects of rapid aldosterone signaling. *Mol. Cell Endocrinol.* 308, 53–62. doi: 10.1016/j.mce.2009.02.005

Grossmann, C., Husse, B., Mildenberger, S., Schreier, B., Schuman, K., and Gekle, M. (2010). Colocalization of mineralocorticoid and EGF receptor at the plasma membrane. *Biochim. Biophys. Acta* 1803, 584–590. doi: 10.1016/j.bbamcr.2010.02.008

Grossmann, C., Krug, A. W., Freudinger, R., Mildenberger, S., Voelker, K., and Gekle, M. (2007). Aldosterone-induced EGFR expression: interaction between the human mineralocorticoid receptor and the human EGFR promoter. *Am. J. Physiol. Endocrinol. Metab.* 292, E1790–E1800. doi: 10.1152/ajpendo.00708.2006

Gul, R., Shawl, A. I., Kim, S. H., and Kim, U. H. (2012). Cooperative interaction between reactive oxygen species and Ca^{2+} signals contributes to angiotensin II-induced hypertrophy in adult rat cardiomyocytes. *Am. J. Physiol. Heart Circ. Physiol.* 302, H901–H909. doi: 10.1152/ajpheart.00250.2011

Guo, P., Nishiyama, A., Rahman, M., Nagai, Y., Noma, T., Namba, T., et al. (2006). Contribution of reactive oxygen species to the pathogenesis of left ventricular failure in Dahl salt-sensitive hypertensive rats: effects of angiotensin II blockade. *J. Hypertens.* 24, 1097–1104. doi: 10.1097/01.hjh.0000226200.73065.5d

Hanna, I. R., Taniyama, Y., Szocs, K., Rocic, P., and Griendling, K. K. (2002). NAD(P)H oxidase-derived reactive oxygen species as mediators of angiotensin II signaling. *Antioxid. Redox. Signal.* 4, 899–914. doi: 10.1089/152308602762197443

Hayashi, H., Kobara, M., Abe, M., Tanaka, N., Gouda, E., Toba, H., et al. (2008). Aldosterone nongenomically produces NADPH oxidase-dependent reactive oxygen species and induces myocyte apoptosis. *Hypertens. Res.* 31, 363–375. doi: 10.1291/hypres.31.363

Husain, A., Kinoshita, A., Sung, S. S., Urata, H., and Bumpus, F. M. (1994). "Human heart chymase," in *The Cardiac Renin-Angiotensin System,* ed G. D. E. Lindpaintner (Armonk, NY: Futura Publishing), 309–332.

Inagami, T. (2011). Mitochondrial angiotensin receptors and aging. *Circ. Res.* 109, 1323–1324. doi: 10.1161/RES.0b013e31823f05e0

Javadov, S., Choi, A., Rajapurohitam, V., Zeidan, A., Basnakian, A. G., and Karmazyn, M. (2008). NHE-1 inhibition-induced cardioprotection against ischaemia/reperfusion is associated with attenuation of the mitochondrial permeability transition. *Cardiovasc. Res.* 77, 416–424. doi: 10.1093/cvr/cvm039

Karmazyn, M., Liu, Q., Gan, X. T., Brix, B. J., and Fliegel, L. (2003). Aldosterone increases NHE-1 expression and induces NHE-1-dependent hypertrophy in neonatal rat ventricular myocytes. *Hypertension* 42, 1171–1176. doi: 10.1161/01.HYP.0000102863.23854.0B

Kimura, S., Zhang, G. X., Nishiyama, A., Shokoji, T., Yao, L., Fan, Y. Y., et al. (2005a). Mitochondria-derived reactive oxygen species and vascular MAP kinases: comparison of angiotensin II and diazoxide. *Hypertension* 45, 438–444. doi: 10.1161/01.HYP.0000157169.27818.ae

Kimura, S., Zhang, G. X., Nishiyama, A., Shokoji, T., Yao, L., Fan, Y. Y., et al. (2005b). Role of NAD(P)H oxidase- and mitochondria-derived reactive oxygen species in cardioprotection of ischemic reperfusion injury by angiotensin II. *Hypertension* 45, 860–866. doi: 10.1161/01.HYP.0000163462.98381.7f

Kindler, D. D., Thiffault, C., Solenski, N. J., Dennis, J., Kostecki, V., Jenkins, R., et al. (2003). Neurotoxic nitric oxide rapidly depolarizes and permeabilizes mitochondria by dynamically opening the mitochondrial transition pore. *Mol. Cell. Neurosci.* 23, 559–573.

Krieg, T., Landsberger, M., Alexeyev, M. F., Felix, S. B., Cohen, M. V., and Downey, J. M. (2003). Activation of Akt is essential for acetylcholine to trigger generation of oxygen free radicals. *Cardiovasc. Res.* 58, 196–202.

Krieg, T., Qin, Q., Mcintosh, E. C., Cohen, M. V., and Downey, J. M. (2002). ACh and adenosine activate PI3-kinase in rabbit hearts through transactivation of receptor tyrosine kinases. *Am. J. Physiol. Heart Circ. Physiol.* 283, H2322–H2330. doi: 10.1152/ajpheart.00474.2002

Krieg, T., Qin, Q., Philipp, S., Alexeyev, M. F., Cohen, M. V., and Downey, J. M. (2004). Acetylcholine and bradykinin trigger preconditioning in the heart through a pathway that includes Akt and NOS. *Am. J. Physiol. Heart Circ. Physiol.* 287, H2606–H2611. doi: 10.1152/ajpheart.00600.2004

Kubin, A. M., Skoumal, R., Tavi, P., Konyi, A., Perjes, A., Leskinen, H., et al. (2011). Role of reactive oxygen species in the regulation of cardiac contractility. *J. Mol. Cell. Cardiol.* 50, 884–893. doi: 10.1016/j.yjmcc.2011.02.005

Lemarie, C. A., Paradis, P., and Schiffrin, E. L. (2008). New insights on signaling cascades induced by cross-talk between angiotensin II and aldosterone. *J. Mol. Med. (Berl.)* 86, 673–678. doi: 10.1007/s00109-008-0323-5

Li, L., Zhang, Z. G., Lei, H., Wang, C., Wu, L. P., Wang, J. Y., et al. (2013). Angiotensin II reduces cardiac AdipoR1 expression through AT1 receptor/ROS/ERK1/2/c-Myc pathway. *PLoS ONE* 8:e49915. doi: 10.1371/journal.pone.0049915

Maulik, S. K., and Kumar, S. (2012). Oxidative stress and cardiac hypertrophy: a review. *Toxicol. Mech. Methods* 22, 359–366. doi: 10.3109/15376516.2012.666650

Mehta, P. K., and Griendling, K. K. (2007). Angiotensin II cell signaling: physiological and pathological effects in the cardiovascular system. *Am. J. Physiol. Cell Physiol.* 292, C82–C97. doi: 10.1152/ajpcell.00287.2006

Meyer, M. R., Prossnitz, E. R., and Barton, M. (2011). The G protein-coupled estrogen receptor GPER/GPR30 as a regulator of cardiovascular function. *Vascul. Pharmacol.* 55, 17–25. doi: 10.1016/j.vph.2011.06.003

Mihailidou, A. S., Mardini, M., and Funder, J. W. (2004). Rapid, nongenomic effects of aldosterone in the heart mediated by epsilon protein kinase C. *Endocrinology* 145, 773–780. doi: 10.1210/en.2003-1137

Miller, E. W., Dickinson, B. C., and Chang, C. J. (2010). Aquaporin-3 mediates hydrogen peroxide uptake to regulate downstream intracellular signaling. *Proc. Natl. Acad. Sci. U.S.A.* 107, 15681–15686. doi: 10.1073/pnas.1005776107

Morgan, P. E., Correa, M. V., Ennis, I. L., Diez, A. A., Perez, N. G., and Cingolani, H. E. (2011). Silencing of sodium/hydrogen exchanger in the heart by direct injection of naked siRNA. *J. Appl. Physiol.* 111, 566–572. doi: 10.1152/japplphysiol.00200.2011

Nishio, S., Teshima, Y., Takahashi, N., Thuc, L. C., Saito, S., Fukui, A., et al. (2012). Activation of CaMKII as a key regulator of reactive oxygen species production in diabetic rat heart. *J. Mol. Cell Cardiol.* 52, 1103–1111. doi: 10.1016/j.yjmcc.2012.02.006

Oldenburg, O., Qin, Q., Krieg, T., Yang, X. M., Philipp, S., Critz, S. D., et al. (2004). Bradykinin induces mitochondrial ROS generation via NO, cGMP, PKG, and $_{mito}$KATP channel opening and leads to cardioprotection. *Am. J. Physiol. Heart Circ. Physiol.* 286, H468–H476. doi: 10.1152/ajpheart.00360.2003

Pain, T., Yang, X. M., Critz, S. D., Yue, Y., Nakano, A., Liu, G. S., et al. (2000). Opening of mitochondrial K_{ATP} channels triggers the preconditioned state by generating free radicals. *Circ. Res.* 87, 460–466. doi: 10.1161/01.RES.87.6.460

Palomeque, J., Delbridge, L., and Petroff, M. V. (2009). Angiotensin II: a regulator of cardiomyocyte function and survival. *Front. Biosci.* 14:5118–5133. doi: 10.2741/3590

Perez, N. G., De Hurtado, M. C., and Cingolani, H. E. (2001). Reverse mode of the Na^+-Ca^{2+} exchange after myocardial stretch: underlying mechanism of the slow force response. *Circ. Res.* 88, 376–382. doi: 10.1161/01.RES.88.4.376

Perez, N. G., Villa-Abrille, M. C., Aiello, E. A., Dulce, R. A., Cingolani, H. E., and Camilion De Hurtado, M. C. (2003). A low dose of angiotensin II increases inotropism through activation of reverse Na^+/Ca^{2+} exchange by endothelin release. *Cardiovasc. Res.* 60, 589–597. doi: 10.1016/j.cardiores.2003.09.004

Qin, W., Rudolph, A. E., Bond, B. R., Rocha, R., Blomme, E. A., Goellner, J. J., et al. (2003). Transgenic model of aldosterone-driven cardiac hypertrophy and heart failure. *Circ. Res.* 93, 69–76. doi: 10.1161/01.RES.0000080521.15238.E5

Rothstein, E. C., Byron, K. L., Reed, R. E., Fliegel, L., and Lucchesi, P. A. (2002). H_2O_2-induced Ca^{2+} overload in NRVM involves ERK1/2 MAP kinases: role for an NHE-1-dependent pathway. *Am. J. Physiol. Heart Circ. Physiol.* 283, H598–H605. doi: 10.1152/ajpheart.00198.2002

Sabri, A., Byron, K. L., Samarel, A. M., Bell, J., and Lucchesi, P. A. (1998). Hydrogen peroxide activates mitogen-activated protein kinases and Na^+-H^+ exchange in neonatal rat cardiac myocytes. *Circ. Res.* 82, 1053–1062. doi: 10.1161/01.RES.82.10.1053

Sadoshima, J., and Izumo, S. (1996). Autocrine secretion of angiotensin II mediates stretch-induced hypertrophy of cardiac myocytes *in vitro*. *Contrib. Nephrol.* 118, 214–221. doi: 10.1016/0092-8674(93)90541-W

Sadoshima, J., Xu, Y., Slayter, H. S., and Izumo, S. (1993). Autocrine release of angiotensin II mediates stretch-induced hypertrophy of cardiac myocytes *in vitro*. *Cell* 75, 977–984.

Sato, T., O'rourke, B., and Marban, E. (1998). Modulation of mitochondrial ATP-dependent K+ channels by protein kinase C. *Circ. Res.* 83, 110–114. doi: 10.1161/01.RES.83.1.110

Seshiah, P. N., Weber, D. S., Rocic, P., Valppu, L., Taniyama, Y., and Griendling, K. K. (2002). Angiotensin II stimulation of NAD(P)H oxidase activity: upstream mediators. *Circ. Res.* 91, 406–413. doi: 10.1161/01.RES.0000033523.08033.16

Shah, B. H., and Catt, K. J. (2003). A central role of EGF receptor transactivation in angiotensin II -induced cardiac hypertrophy. *Trends Pharmacol. Sci.* 24, 239–244. doi: 10.1016/S0165-6147(03)00079-8

Silvestre, J. S., Heymes, C., Oubenaissa, A., Robert, V., Aupetit-Faisant, B., Carayon, A., et al. (1999). Activation of cardiac aldosterone production in rat myocardial infarction: effect of angiotensin II receptor blockade and role in cardiac fibrosis. *Circulation* 99, 2694–2701. doi: 10.1161/01.CIR.99.20.2694

Silvestre, J. S., Robert, V., Heymes, C., Aupetit-Faisant, B., Mouas, C., Moalic, J. M., et al. (1998). Myocardial production of aldosterone and corticosterone in the rat. Physiological regulation. *J. Biol. Chem.* 273, 4883–4891. doi: 10.1074/jbc.273.9.4883

Smaili, S. S., and Russell, J. T. (1999). Permeability transition pore regulates both mitochondrial membrane potential and agonist-evoked Ca^{2+} signals in oligodendrocyte progenitors. *Cell. Calcium* 26, 121–130. doi: 10.1054/ceca.1999.0061

Snabaitis, A. K., Hearse, D. J., and Avkiran, M. (2002). Regulation of sarcolemmal Na^+/H^+ exchange by hydrogen peroxide in adult rat ventricular myocytes. *Cardiovasc. Res.* 53, 470–480.

Song, Y. H., Choi, E., Park, S. H., Lee, S. H., Cho, H., Ho, W. K., et al. (2011). Sustained CaMKII activity mediates transient oxidative stress-induced long-term facilitation of L-type Ca^{2+} current in cardiomyocytes. *Free Radic. Biol. Med.* 51, 1708–1716. doi: 10.1016/j.freeradbiomed.2011.07.022

Sorescu, D., and Griendling, K. K. (2002). Reactive oxygen species, mitochondria, and NAD(P)H oxidases in the development and progression of heart failure. *Congest. Heart Fail.* 8, 132–140. doi: 10.1111/j.1527-5299.2002.00717.x

Szokodi, I., Kerkela, R., Kubin, A. M., Sarman, B., Pikkarainen, S., Konyi, A., et al. (2008). Functionally opposing roles of extracellular signal-regulated kinase 1/2 and

p38 mitogen-activated protein kinase in the regulation of cardiac contractility. *Circulation* 118, 1651–1658. doi: 10.1161/CIRCULATIONAHA.107.758623

Takeda, Y., Yoneda, T., Demura, M., Miyamori, I., and Mabuchi, H. (2000). Cardiac aldosterone production in genetically hypertensive rats. *Hypertension* 36, 495–500. doi: 10.1161/01.HYP.36.4.495

Terentyev, D., Gyorke, I., Belevych, A. E., Terentyeva, R., Sridhar, A., Nishijima, Y., et al. (2008). Redox modification of ryanodine receptors contributes to sarcoplasmic reticulum Ca^{2+} leak in chronic heart failure. *Circ. Res.* 103, 1466–1472. doi: 10.1161/CIRCRESAHA.108.184457

Toda, T., Kadono, T., Hoshiai, M., Eguchi, Y., Nakazawa, S., Nakazawa, H., et al. (2007). Na^+/H^+ exchanger inhibitor cariporide attenuates the mitochondrial Ca^{2+} overload and PTP opening. *Am. J. Physiol. Heart Circ. Physiol.* 293, H3517–H3523. doi: 10.1152/ajpheart.00483.2006

Trebak, M., Ginnan, R., Singer, H. A., and Jourd'heuil, D. (2010). Interplay between calcium and reactive oxygen/nitrogen species: an essential paradigm for vascular smooth muscle signaling. *Antioxid. Redox. Signal* 12, 657–674. doi: 10.1089/ars.2009.2842

Varagic, J., and Frohlich, E. D. (2002). Local cardiac renin-angiotensin system: hypertension and cardiac failure. *J. Mol. Cell Cardiol.* 34, 1435–1442. doi: 10.1006/jmcc.2002.2075

Vaughan-Jones, R. D., Villafuerte, F. C., Swietach, P., Yamamoto, T., Rossini, A., and Spitzer, K. W. (2006). pH-Regulated Na^+ influx into the mammalian ventricular myocyte: the relative role of Na^+-H^+ exchange and Na^+-HCO Co-transport. *J. Cardiovasc. Electrophysiol.* 17(Suppl. 1), S134–S140. doi: 10.1111/j.1540-8167.2006.00394.x

Villa-Abrille, M. C., Caldiz, C. I., Ennis, I. L., Nolly, M. B., Casarini, M. J., Chiappe De Cingolani, G. E., et al. (2010). The Anrep effect requires transactivation of the epidermal growth factor receptor. *J. Physiol.* 588, 1579–1590. doi: 10.1113/jphysiol.2009.186619.

Villa-Abrille, M. C., Cingolani, H. E., Garciarena, C. D., Ennis, I. L., and Aiello, E. A. (2006). [Angiotensin II-induced endothelin-1 release in cardiac myocytes]. *Medicina (B Aires)* 66, 229–236.

Wang, Y. H., Shi, C. X., Dong, F., Sheng, J. W., and Xu, Y. F. (2008). Inhibition of the rapid component of the delayed rectifier potassium current in ventricular myocytes by angiotensin II via the AT1 receptor. *Br. J. Pharmacol.* 154, 429–439. doi: 10.1038/bjp.2008.95

Wenzel, P., Mollnau, H., Oelze, M., Schulz, E., Wickramanayake, J. M., Muller, J., et al. (2008). First evidence for a crosstalk between mitochondrial and NADPH oxidase-derived reactive oxygen species in nitroglycerin-triggered vascular dysfunction. *Antioxid. Redox. Signal.* 10, 1435–1447. doi: 10.1089/ars.2007.1969

Wojtovich, A. P., Smith, C. O., Haynes, C. M., Nehrke, K. W., and Brookes, P. S. (2013). Physiological consequences of complex II inhibition for aging, disease, and the mK_{ATP} channel. *Biochim. Biophys. Acta* 1827 (5), 598–611. doi: 10.1016/j.bbabio.2012.12.007

Xiao, F., Puddefoot, J. R., Barker, S., and Vinson, G. P. (2004). Mechanism for aldosterone potentiation of angiotensin II-stimulated rat arterial smooth muscle cell proliferation. *Hypertension* 44, 340–345. doi: 10.1161/01.HYP.0000140771.21243.ed

Yoshida, K., Kim-Mitsuyama, S., Wake, R., Izumiya, Y., Izumi, Y., Yukimura, T., et al. (2005). Excess aldosterone under normal salt diet induces cardiac hypertrophy and infiltration via oxidative stress. *Hypertens. Res.* 28, 447–455. doi: 10.1291/hypres.28.447

Zeng, Q., Zhou, Q., Yao, F., O'rourke, S. T., and Sun, C. (2008). Endothelin-1 regulates cardiac L-type calcium channels via NAD(P)H oxidase-derived superoxide. *J. Pharmacol. Exp. Ther.* 326, 732–738. doi: 10.1124/jpet.108.140301

Zhai, P., Galeotti, J., Liu, J., Holle, E., Yu, X., Wagner, T., et al. (2006). An angiotensin II type 1 receptor mutant lacking epidermal growth factor receptor transactivation does not induce angiotensin II-mediated cardiac hypertrophy. *Circ. Res.* 99, 528–536. doi: 10.1161/01.RES.0000240147.49390.61

Zhang, D. X., Chen, Y. F., Campbell, W. B., Zou, A. P., Gross, G. J., and Li, P. L. (2001). Characteristics and superoxide-induced activation of reconstituted myocardial mitochondrial ATP-sensitive potassium channels. *Circ. Res.* 89, 1177–1183. doi: 10.1161/hh2401.101752

Zhang, G. X., Lu, X. M., Kimura, S., and Nishiyama, A. (2007). Role of mitochondria in angiotensin II-induced reactive oxygen species and mitogen-activated protein kinase activation. *Cardiovasc. Res.* 76, 204–212. doi: 10.1016/j.cardiores.2007.07.014

Zhao, Z., Fefelova, N., Shanmugam, M., Bishara, P., Babu, G. J., and Xie, L. H. (2011). Angiotensin II induces afterdepolarizations via reactive oxygen species and calmodulin kinase II signaling. *J. Mol. Cell Cardiol.* 50, 128–136. doi: 10.1016/j.yjmcc.2010.11.001

Zorov, D. B., Filburn, C. R., Klotz, L. O., Zweier, J. L., and Sollott, S. J. (2000). Reactive oxygen species (ROS)-induced ROS release: a new phenomenon accompanying induction of the mitochondrial permeability transition in cardiac myocytes. *J. Exp. Med.* 192, 1001–1014. doi: 10.1084/jem.192.7.1001

Conflict of Interest Statement: The authors declare that the research was conducted in the absence of any commercial or financial relationships that could be construed as a potential conflict of interest.

Received: 25 January 2013; accepted: 13 May 2013; published online: 30 May 2013.

Citation: De Giusti VC, Caldiz CI, Ennis IL, Pérez NG, Cingolani HE and Aiello EA (2013) Mitochondrial reactive oxygen species (ROS) as signaling molecules of intracellular pathways triggered by the cardiac renin-angiotensin II-aldosterone system (RAAS). Front. Physiol. ***4****:126. doi: 10.3389/fphys.2013.00126*

This article was submitted to Frontiers in Mitochondrial Research, a specialty of Frontiers in Physiology.

frontiers in
PHYSIOLOGY

ORIGINAL RESEARCH ARTICLE
published: 20 May 2013
doi: 10.3389/fphys.2013.00101

Impact of mitochondria on nitrite metabolism in HL-1 cardiomyocytes

Peter Dungel[1], Andreas H. Teuschl[2], Asmita Banerjee[1], Jamile Paier-Pourani[1], Heinz Redl[1] and Andrey V. Kozlov[1]*

[1] Ludwig Boltzmann Institute for Experimental and Clinical Traumatology in AUVA research centre, Vienna, Austria
[2] Department of Biochemical Engineering, University of Applied Sciences Technikum Wien, Vienna, Austria

Edited by:
Andrey V. Kuznetsov, Innsbruck Medical University, Austria

Reviewed by:
Steven P. Jones, University of Louisville, USA
Sergey Dikalov, Vanderbilt University Medical Center, USA

***Correspondence:**
Andrey V. Kozlov, Ludwig Boltzmann Institute for Experimental and Clinical Traumatology in AUVA research centre, Donaueschingen Str. 13, 1200 Vienna, Austria.
e-mail: andrey.kozlov@trauma.lbg.ac.at

Apart from ATP synthesis mitochondria have many other functions, one being nitrite reductase activity. Nitric oxide (NO) released from nitrite has been shown to protect the heart from ischemia/reperfusion (I/R) injury in a cGMP-dependent manner. However, the exact impact of mitochondria on the release of NO from nitrite in cardiomyocytes is not completely understood. Besides mitochondria, a number of non-mitochondrial metalloproteins have been suggested to facilitate this process. The aim of this study was to investigate the impact of mitochondria on the bioactivation of nitrite in HL-1 cardiomyocytes. The levels of nitrosyl complexes of hemoglobin (NO-Hb) and cGMP levels were measured by electron spin resonance spectroscopy and enzyme immunoassay. In addition the formation of free NO was determined by confocal microscopy as well as intracellular nitrite and S-nitrosothiols by chemoluminescence analysis. NO was released from nitrite in cell culture in an oxygen-dependent manner. Application of specific inhibitors of the respiratory chain, p450, NO synthases (NOS) and xanthine oxidoreductase (XOR) showed that all four enzymatic systems are involved in the release of NO, but more than 50% of NO is released via the mitochondrial pathway. Only NO released by mitochondria activated cGMP synthesis. Cardiomyocytes co-cultured with red blood cells (RBC) competed with RBC for nitrite, but free NO was detected only in HL-1 cells suggesting that RBC are not a source of NO in this model. Apart from activation of cGMP synthesis, NO formed in HL-1 cells diffused out of the cells and formed NO-Hb complexes. In addition nitrite was converted by HL-1 cells to S-nitrosyl complexes. In HL-1 cardiomyocytes, several enzymatic systems are involved in nitrite reduction to NO but only the mitochondrial pathway of NO release activates cGMP synthesis. Our data suggest that this pathway may be a key regulator of myocardial contractility especially under hypoxic conditions.

Keywords: nitrite, HL-1 cardiomyocytes, mitochondria, nitric oxide, hypoxia

INTRODUCTION

For decades nitrite and nitrate were thought to be the stable end products of nitric oxide (NO) produced by various isoforms of NO synthase (NOS). However, this concept became outdated when it was recognized that, under hypoxic conditions, nitrite can be reduced back to NO (Zweier et al., 1995; Lepore et al., 1999; Cosby et al., 2003; Vanin et al., 2007; van Faassen et al., 2009). Nitrite-derived NO creates a number of effects, for example increased levels of nitroso species, alters redox status and induces protein modifications (Dezfulian et al., 2007, 2009; Perlman et al., 2009). These effects may be involved in the cytoprotective effects of nitrite seen in models of local ischemia/reperfusion (I/R) injury in the heart, liver and brain (Lu et al., 2005; Jung et al., 2006; Bryan et al., 2008; Calvert and Lefer, 2009). Cytoprotection is attributed to the reduction of nitrite to NO and consequent activation of cGMP synthesis (Shiva and Gladwin, 2009), which leads to vasodilation and thus, better perfusion and increased oxygen supply (Wolin, 2009).

However, the mechanisms by which endogenous or exogenous nitrite is reduced to NO are still under discussion. One potential pathway occuring in blood is the reduction of nitrite by hemoglobin (Hb) in red blood cells (RBC). Cosby et al. suggested that nitrite-derived NO diffuses from the RBC into the smooth muscle cells of the vasculature and activates nitrite-mediated vasodilation (Cosby et al., 2003). Recently, however, it was suggested that not NO but another nitrogen species, N_2O_3, forms in RBCs diffuses into the tissues and induces vasodilation (Basu et al., 2007b). Lundberg et al. showed that the reduction of nitrite to NO depends on the predominant partial pressure of oxygen in the blood; lower oxygen levels facilitate NO release (Lundberg and Weitzberg, 2005). Hb seems to follow an allosteric regulation of nitrite reduction, showing the best nitrite reductase performance at 50% saturation with oxygen (Rassaf et al., 2007; van Faassen et al., 2009).

Another pathway of nitrite reduction other than the RBC pathway is mediated via parenchymal cells in tissues. Various

intracellular enzymes have been identified to possess nitrite reductase activity, for example xanthine oxidoreductase (XOR) (Webb et al., 2008) and NOS (van Faassen et al., 2009). Also mitochondria can rapidly reduce nitrite to NO (Kozlov et al., 1999). It has been shown that NO reduced from nitrite by mitochondria in turn reversibly inhibits mitochondrial respiration (Nohl et al., 2000). However, it is not known whether or not this NO pool may escape from mitochondria and activate other signaling pathways.

Apart from regulation of vascular tonus, NO plays an important role in the cardiovascular system to maintain cardiac function (Rastaldo et al., 2007) via activation of cGMP synthesis in a dose-dependent manner. Under physiologic conditions endothelial and neuronal NOS play an important role in cardiac function. The inhibition of NO synthesis catalyzed by NOS under normoxic conditions induces cardiac remodeling (hypertrophy), which is independent of the systemic hemodynamic effects of NO (Sanada et al., 2003). Nitrite represents a NOS-independent NO-source that becomes effective under hypoxic conditions. Nitrite, however, represents a NOS-independent NO-source that becomes effective under hypoxic conditions like I/R. Previously it was shown that the reduction of nitrite to NO in heart homogenate is nearly fully inhibited by myxothiazol, a specific inhibitor of the mitochondrial respiratory chain at complex III (Kozlov et al., 2005). However, the impact of this pathway on the bioactivation of nitrite in cardiomyocytes has not been addressed in the literature.

The aim of this study was to clarify the impact of mitochondria on nitrite reduction in HL-1 cardiomyocytes under hypoxic conditions.

MATERIALS AND METHODS

PREPARATION OF HL-1 CELLS AND RBC

HL-1 cardiomyocytes were used in this study. Cells were cultured under a 5% CO_2 atmosphere in Claycomb medium (Sigma, St. Louis, USA) supplemented with 10% fetal bovine serum (Lonza, Basel, Switzerland), 4 mM L-glutamine (Sigma, St. Louis, USA), 100 U/ml penicillin (Sigma, St. Louis, USA), 100 µg/ml streptomycin (Sigma, St. Louis, USA), and 100 µM norepinephrine (Sigma, St. Louis, USA). Cells were seeded in 24-well cell culture plates precoated with 25 µg/ml fibronectin and 0.02% gelatin solution and cultivated until confluent.

To isolate human RBC, whole blood was centrifuged at 1600 g for 10 min, plasma and buffy-coat discarded and the remaining RBC washed twice with phosphate buffered saline (PBS). RBC were then diluted with PBS accordingly and counted on a Cell-Dyn 3700 (Abbott, Switzerland) before use.

EXPERIMENTAL SETUP

Determination of nitrite-derived NO-release from HL-1 cells

Experiments were performed in a gas-tight glove box, which allowed to study nitrite reduction under various oxygen concentrations (from 21% to <1% O_2). All solutions were deoxygenated with nitrogen prior to experiment. Twenty-four-well cell culture plates with confluent HL-1 cells (approx. 250,000 cells/well) were transferred into the glove box containing nitrogen atmosphere. In selected experiments HL-1 cells had been preincubated under 21% oxygen for 1 h with either 10 µM myxothiazol, 10 mM potassium cynide, 1 mM allopurinol, 300 µM N-nitro-L-arginine methyl ester (L-NAME) or 500 µM methyrapone. The following procedures were performed inside the glove box: to measure NO-Hb, the cell medium was exchanged with diluted RBC in PBS and cells treated with 50 µM nitrite or PBS as control. For analysis of cGMP synthesis medium was exchanged with PBS, followed by addition of 50 µM nitrite or PBS. PBS contained 1 mM of the phosphodiesterase inhibitor (MacArthur et al., 2007) isobutylmethylxanthin (IBMX) to prevent cGMP degradation. Cells were then incubated under hypoxic conditions on a shaker at 37°C for 1 h. Afterwards, the supernatant was withdrawn for analyses of NO-Hb and cGMP, the remaining cells were lysed by sonification in 500 µl lysis reagent provided with the enzyme immunoassay for detection of cGMP (GE Healthcare, Fairfield, USA) and the lysates stored for quantification of intracellular nitrite and nitroso species. Protein content of the lysates was determined for normalization by BCA protein assay (Pierce, Rockford, USA). In selected experiments NO-gas was used as a positive control. Physiological saline was purged with NO gas (Messer, Austria) for 15 min. NO concentration was determined with a NO electrode (World Precision Instruments Ltd., USA) and was 1 mM in average.

EPR SPECTROSCOPY

The EPR spectra from frozen samples were recorded in a Miniscope MS 2000 (Magnettech Ltd., Berlin, Germany) at liquid nitrogen temperature with the following settings: microwave frequency 9.429 GHz, microwave power 30 mW, modulation frequency 100 kHz and modulation amplitude 6 G.

CONFOCAL MICROSCOPY

The detection of NO production in living cells was performed using the NO-sensitive fluorescent dye 4-Amino-5-methylamino-2′,7′-difluorofluorescein diacetate (DAF-FM diacetate; Molecular Probes, Carlsbad, CA). DAF-FM diacetate is nitrosated by NO and is a reasonable indication for NO. HL-1 cells or RBC were loaded with 10 µM DAF-FM diacetate and incubated for 30 min at 37°C. Afterwards, 50 µM of NaNO2 were added and cells were incubated for another 30 min at 37°C under anaerobic conditions in an incubator at <1% oxygen. Imaging was performed with an inverted confocal microscope (LSM 510, Zeiss, Germany) with excitation/emission maxima of 495/515 nm, 63× oil immersion objective and 2.0 scan zoom.

ANALYSIS OF NITRITE AND NITROSO SPECIES

Nitrite and nitroso species in cell lysates were measured using a triiodide-based reductive chemiluminescence method with a NO analyzer (model 280, Seivers, Boulder, USA). To determine the levels of nitrite and nitroso species two aliquots of each sample were analyzed, as previously described (MacArthur et al., 2007). The first aliquot was directly injected into the triiodide reagent to measure nitrite, the second was incubated for 10 min with acidified sulfanilamide (0.5% vol:vol) to eliminate nitrite before injected into the triiodide reagent. Since the second measurement represents the signal from nitroso species, the comparison of both peaks provides an accurate method for measuring nitrite.

cGMP MEASUREMENT

cGMP levels in HL-1 cells were measured by enzyme immunoassay (cGMP EIA; GE Healthcare, Fairfield, USA) according to protocol 3 of the manufacturer's instructions. Briefly, cell culture supernatants were aspirated and adherent cells lysed in the lysis reagent provided. Samples were acetylated prior to performing the assay. Optical density (405 nm) was measured by a plate reader (Tecan, Männedorf, Switzerland) and the concentration of cGMP was calculated from a standard curve produced from serial dilutions of acetylated cGMP solutions. All standards and samples were assayed in duplicate.

DATA PRESENTATION AND STATISTICS

Data represent mean ± SD. Significance was calculated using One-Way ANOVA test with *post-hoc* LSD (least significant difference) test.

RESULTS

Under hypoxic conditions NO reacts with Hb yielding nitrosyl complexes of hemoglobin (NO-Hb) with characteristic electron spin resonance spectra shown in the inset of **Figure 1A**. The baseline level of NO-Hb in RBC was doubled when RBC were incubated with nitrite, showing that RBC are well able to convert nitrite to NO. Co-culture with HL-1 cells led to a further significant increase in NO-Hb levels, indicating the significant portion of NO derived from HL-1 cells (**Figure 1A**). It also clearly demonstrated that the NO formed in HL-1 cells is released from the cells. Variation of the RBC:HL-1 ratio shows the relative contribution of RBC and HL-1 cells to NO formation (**Figure 1B**). A RBC:HL-1 ratio of 166:1 was chosen as it showed the highest difference between RBC and HL-1 derived NO. NO-Hb formation in both RBC and HL-1 cells was dependent on the partial pressure of oxygen (**Figure 1C**). The provision of free available NO, however, depends predominantly on parenchymal cells. The incubation of HL-1 cells with nitrite led to an increase in intracellular NO levels as revealed by confocal microscopy using the NO specific indicator dye DAF-2DA. In contrast, free NO was not detected in RBC as the fluorescence of RBC incubated with nitrite did not change compared to untreated control (**Figure 2A**).

Logically, the NO formed in cardiomyocytes has two major functions. A portion of NO diffusing out of cardiomyocytes may contribute to the regulation of vascular tonus and another portion may activate cGMP synthesis regulating myocardial contractility. The release of NO was determined by the formation of NO-Hb complexes in RBC co-cultured with HL-1 cells and cGMP levels were determined directly in HL-1 cells. To clarify the origin of nitrite-derived NO contributing to the formation of NO-Hb and cGMP synthesis, HL-cells were preincubated with various specific inhibitors, allowing definition of the impact of the respective enzymes. Regarding NO release and NO-Hb formation, all inhibitors used decreased the NO-Hb signal. However, the mitochondrial inhibitor myxothiazol had the most prominent effect, decreasing NO-Hb levels by 60%. Allopurinol, L-NAME and methyrapone, inhibitors of XOR, NOS and cytochrome P450, respectively, contributed to the formation of NO-Hb, although significantly less than mitochondria (**Figure 2B**).

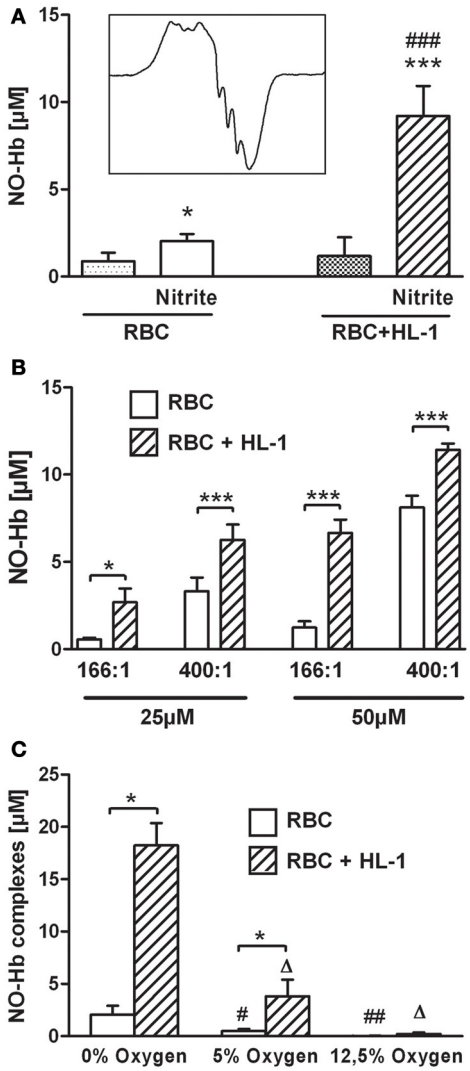

FIGURE 1 | (A) NO production from RBC and in co-culture with HL-1 cells under hypoxic conditions with and without 50 µM nitrite. **(A)** Both RBC and HL-1 cells are capable of nitrite reduction. Left set of bars shows the RBC-mediated release of NO from nitrite. Right set of bars represents data from co-culture of RBC with HL-cells in a RBC:HL-1 ratio of 166:1 ($^{*}p < 0.005$, $^{***}p < 0.001$ compared to the respective group without nitrite, $^{\#\#\#}p < 0.001$, compared to RBC with nitrite). Inset in 1 **(A)** shows typical EPR spectrum of NO-Hb complexes. **(B)** The relative contribution of both pathways depends on both nitrite concentrations and the RBC:HL-1 ratio. A ratio of 166:1 and a nitrite concentration of 50 µM were chosen for all other experiments as these conditions showed the highest difference inNO-signals with and without HL-1 cells. $^{*}p < 0.05$, $^{***}p < 0.001$ RBC vs. RBC + HL-1 of the same group. **(C)** Oxygen-dependence of NO-Hb signal. RBC and in co-culture with HL-1 cells were incubated with 50 µM nitrite under various oxygen concentrations. $^{*}p < 0.001$, NO-Hb signals with and without HL-1 cells. $^{\Delta}p < 0.001$, compared to RBC + HL-1 at 0% oxygen. $^{\#,\#\#}p < 0.05$ and $p < 0.01$, respectively, compared to RBC at 0% oxygen.

The impact of these enzymes on nitrite-dependent cGMP formation was investigated in a similar way. cGMP synthesis in HL-1 cells stimulated by nitrite-derived NO was fully prevented by myxothiazol while other inhibitors had no effect (**Figure 3A**). NO

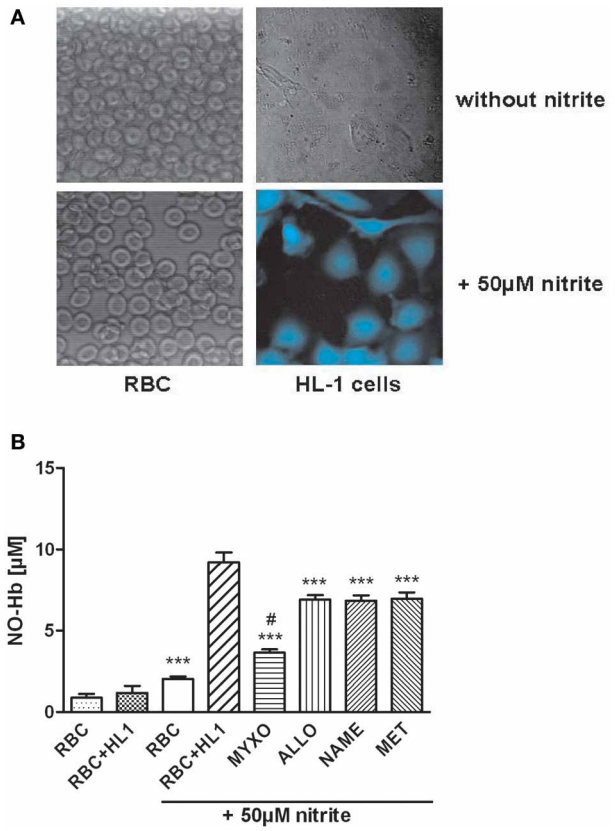

FIGURE 2 | (A) Analysis of free NO using a NO-specific dye and confocal microscopy. HL-1 cells or RBC were loaded with 10 μM DAF-FM and incubated for about 30 min at 37°C. Afterwards, 50 μM of $NaNO_2$ were added and cells were incubated for another 30 min at 37°C under anaerobic conditions. Free NO could only be detected in HL-1 cells but not in RBC. **(B)** Influence of various inhibitors on NO-Hb signals of RBC in co-culture with HL-1 cells determined by EPR analysis. Myxothiazol, an inhibitor of complex III of the respiratory chain, reduced NO-signal by 60%, while all inhibitors reduced NO-Hb levels by approx. 25%. $^{***}p < 0.001$, compared to HL-1 cells incubated with 50 μM nitrite. $^{\#}p < 0.05$, compared to RBC incubated with 50 μM nitrite.

gas-saturated saline, used as a positive control, led to significant increase in cGMP production. However, NO-mediated guanylyl cyclase (GC) activation was influenced by neither myxothiazol nor any of the other inhibitors (**Figure 3B**).

Chemoluminescence analysis showed that incubation of HL-1 cells with 50 μM nitrite led to a drastic increase in intracellular nitrite (**Figure 3C**) and nitroso species (**Figure 3D**) levels. In contrast to NO-Hb and cGMP, nitroso species formation was not sensitive to myxothiazol.

DISCUSSION

In the past years it has been demonstrated that nitrite represents a storage pool of NO which can be activated, especially under hypoxic conditions. As nitrite reduction occurs both in blood Hb and tissue, we investigated the process of exogenous nitrite reduction in monocultures of HL-1 cells and RBC and in a co-culture of these two cell types. Since Hb is itself a nitrite reductase, RBC were incubated with and without nitrite to determine the RBC-dependent nitrite reduction. The free radical NO binds efficiently to deoxy-Hb in RBC, yielding the characteristic triplet spectrum of this NO-Hb complex. The formation of NO-Hb complexes in RBC incubated with nitrite reflects diffusion of nitrite into RBC and it reduction to NO. It has been demonstrated in the literature that nitrite reduction is oxygen-dependent. **Figure 1C** shows NO-Hb signals at anaerobic conditions as well as at oxygen concentrations typical for arterial (12.5% O_2) and venous (5% O_2) blood. In both RBC and co-culture with HL-1 cells, NO-Hb signals are reduced with a decrease in oxygen. There are two explanations for this finding: first, activities of nitrite reductases decrease with increases in oxygen or, second, Hb becomes oxygenated and reacts with NO to form methemoglobin rather than NO-Hb. In any case, anaerobic conditions yield the highest amounts of nitrite-derived NO and thus, further experiments were performed under anaerobic conditions. In cardiomyocytes, the ability of nitrite to diffuse into HL-1 cells was confirmed directly by determination of intracellular nitrite levels in HL-1 cell lysates (**Figure 3D**).

It has previously been shown that NO diffuses from diverse parenchymal cells into the blood to form NO-Hb complexes in RBC, but NO bound to Hb does not diffuse back to parenchymal cells (Kozlov et al., 2001). Consequently, we assumed that determination of NO-Hb complexes in our model is a measure of total NO-production in RBC plus HL-1 cells. In fact, addition of HL-1 cells to a RBC suspension increased nitrite mediated NO-Hb formation due to an additional portion of NO reduced in HL-1 cells. An increase in the RBC:HL-1 ratio results in an increase of the NO portion formed in HL-1 cells and reduced the NO portion coming from RBC. This shows that both RBC- and HL-1 mediated pathways have a distinguishable contribution to total NO production determined by NO-Hb levels. Also, the difference in NO-Hb levels between coculture of HL-1 cells and Hb and Hb alone is the NO formed in HL-1 cells. In this experimental model we found that free NO is only detectable in cardiomyocytes but not in RBC. This was shown by confocal microscopy combined with using the fluorescent dye DAF used to determine free NO in RBC and HL-1 cells upon treatment with nitrite. Increased DAF fluorescence was clearly detected in HL-1 cells but not in RBC, suggesting that free NO only occurs in HL-1 cells. This suggests that NO is tightly bound to Hb inside RBC. The lack of free NO in RBC seems to be in contradiction to the fact that RBC-mediated nitrite reduction contributes to vasodilation. However, this contradiction was satisfactorily explained in the recent publication of Basu et al. who suggested that N_2O_3, not NO, is formed in RBC and is the active mediator of vasodilation (Basu et al., 2007a).

The intracellular mechanisms of nitrite bioactivation in HL-1 cells were investigated by using inhibitors of various enzymes with distinct nitrite reductase activity. Specific inhibitors for XOR, complex III of the mitochondrial electron transport chain, cytochrome P450 and NOS were used. Cells were incubated with inhibitors prior to the addition of RBC which served as NO detection reagent. Thus, the effects of these inhibitors on the NO-Hb signal were only HL-1 dependent. All inhibitors reduced NO release, seen as lowered NO-Hb levels, but to various extents. The mitochondria-specific inhibitor myxothiazol decreased NO

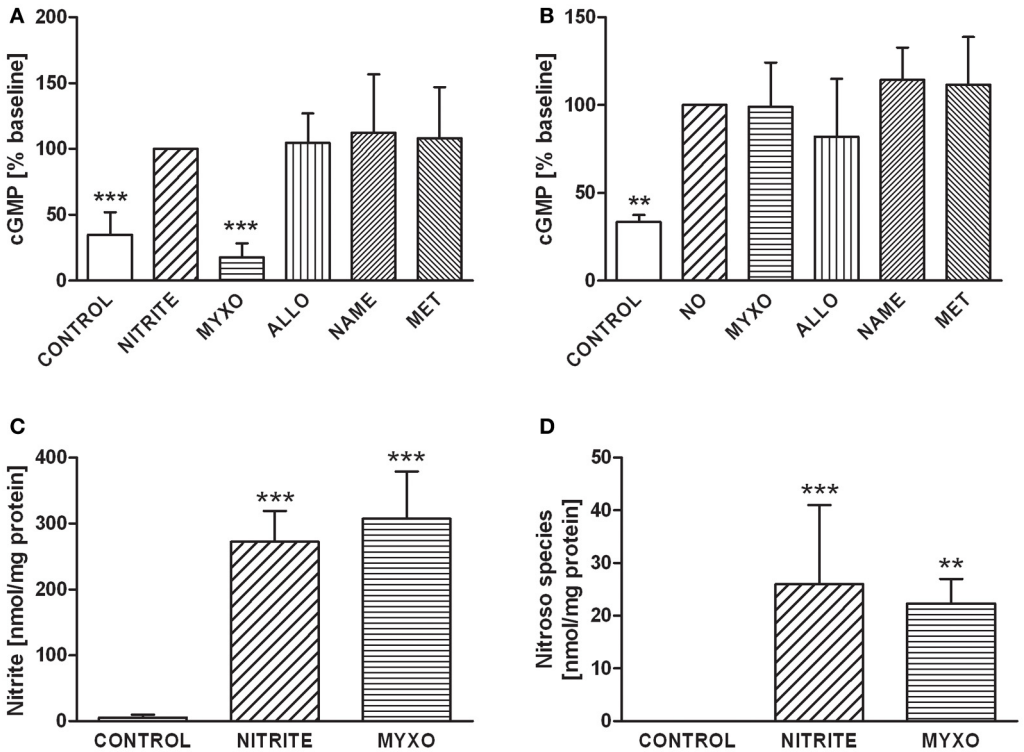

FIGURE 3 | (A) GMP levels in HL-1 incubated with 50 μM nitrite under hypoxic conditions. cGMP production was completely inhibited by myxothiazol, suggesting that NO derived from nitrite reduction in mitochondria is predominately responsible for cGMP synthesis. Controls are untreated HL-1 cells, Nitrite indicates HL-1 cells treated with 50 μM nitrite, all other groups were treated with nitrite and with one of the following inhibitors: Myxo, Myxothiazol; Allo, Allopurinol; NAME, N-nitro-L-arginine methyl ester; Met, Methyrapone. **(B)** cGMP levels in HL-1 cells incubated with 50 μM NO under hypoxic conditions. GC activation by NO-gas was not influenced by either myxothiazol or any other inhibitor, demonstrating that nitrite reduction via mitochondria is predominately responsible for cGMP synthesis. Controls are untreated HL-1 cells, NO indicates HL-1 cells treated with 50 μM nitritc oxide, all other groups were treated with NO and with one of the following inhibitors: Myxo, Myxothiazol; Allo, Allopurinol; NAME, N-nitro-L-arginine methyl ester; Met, Methyrapone. $^{**}p < 0.01$, $^{***}p < 0.001$. Intracellular levels of nitrite **(C)** and nitroso species **(D)** in HL-1 cells. Controls are untreated HL-1 cells, Nitrite indicates HL-1 cells treated with 50 μM nitrite, Myxo represents HL-1 cells incubated with 50 μM nitrite preincubated with myxothiazol. Cell lysates were analysed by a Sievers NOA280i chemiluminescence analyser using the tri-iodide method to determine nitrite. For analysis of nitroso species a second sample was treated with acidified sulfanilamide to eliminate nitrite. $^{***}p < 0.001$ vs. control.

signal by 60%. This is in line with the fact that mitochondria contribute to nitrite reductase activity in heart homogenates by approx. 80% (Kozlov et al., 2003). However, NO-Hb levels were not reduced to baseline levels of untreated cells, suggesting that there are additional pathway(s) of NO production. As allopurinol, NAME and methyrapone reduced NO-signals by 25% each, this indicates other active mechanisms. According to Dr. Claycomb, who established the HL-1 cell line, these cells should contain myoglobin (Mb) comparable to primary cardiomyocytes (private communication). Mb is a potent nitrite reductase in the heart (Shiva et al., 2007) whose impact was not investigated in this study. However, Shiva et al. used ferricyanide to oxidize Mb in heart homogenate which led to decreased NO production. Ferricyanide is an unspecific one electron acceptor interacting also with the respiratory chain of mitochondria (Krasnikov et al., 1997). Thus, both nitrite and ferricyanide are reduced accepting electrons from the respiratory chain. Consequently, the effects of ferricyanide may be due to the inhibition of nitrite reduction by the respiratory chain. Thus, ferricyanide might not be suitable to distinguish between Mb-mediated and mitochondria-mediated nitrite reduction. On the other hand there are specific inhibitors of the mitochondrial respiratory chain, which do not react with Mb, for instance myxothiazol. In our previous publication we have shown that myxothiazol nearly completely inhibits nitrite reduction to NO in heart homogenate. This suggests that mitochondria are responsible for nitrite reduction in heart homogenate.

Another situation is demonstrated in the paper of Totzeck et al. (2012). They showed that Mb in SMC is involved in nitrite reduction and vasodilation. This suggests that the data from heart homogenate reflect nitrite reduction in cardiomyocytes (the mayor cell type contributing to heart homogenate), which is likely relevant for the regulation of myocardial contractility and Mb in SMC for vascular tonus.

Beside Mb, several studies showed that XOR also is an important nitrite reductase in the heart. McNulty et al. showed that in RBC-free heart tissue, nitrite consumption could be blocked by 40% by allopurinol (McNulty et al., 2008) but

no mitochondria-specific inhibitor was tested in the study. One also has to keep in mind that allopurinol acts as an antioxidant as well, thus also inhibiting intracellular oxidative processes. Baker et al. demonstrated that both oxypuinol and diphenyleneiodonium (DPI), a non-specific flavoprotein inhibitor, inhibited nitrite-mediated cardioprotection (Baker et al., 2007). As DPI also inhibits mitochondrial complex I (Li and Trush, 1998), the reduction in cytoprotection might be due to reduced nitrite bioactivation by mitochondria. Irrespectively of the exact mechanism of allopurinol, we show that, in our model, mitochondria are the major contributor to the generation of diffusible NO.

Although mitochondria were only partially responsible for the generation of diffusible NO, they were the only NO source activating cGMP synthesis; myxothiazol completely inhibited cGMP synthesis and other inhibitors had no effect. This finding suggests that NO by mitochondria-mediated nitrite reduction is predominately responsible for cGMP synthesis in HL-1 cells. Zielinska et al. demonstrated that fluoroactetate, a metabolic inhibitor specifically affecting astrocytic mitochondria, inhibited cGMP synthesis by about 50% (Zielinska et al., 2007). An intracellular association of mitochondria and GC could explain that cGMP synthesis, but not NO-Hb signals, were completely blocked by mitochondrial inhibition.

To exclude the possibility that myxothiazol inhibited not only nitrite reduction, but also NO-mediated cGMP synthesis, we used pure NO as a control. GC activation by NO-gas was not influenced by either myxothiazol or any other inhibitor, showing the predominant contribution of mitochondria to nitrite bioactivation in cardiomyocytes under hypoxic conditions. These data suggest that the pathway responsible for stimulation of cGMP synthesis in cardiomyocytes was exclusively mitochondria-dependent. In addition, it has been shown that myxothiazol can also induce superoxide production in the mitochondrial matrix. Myxothiazol-derived superoxide may cause oxidation of NO produced in the mitochondria. However, myxothiazol did not inhibit cGMP production in NO-gas treated cells. These data may indicate that the nitrite reduction in the electron transfer chain occurs downstream of the myxothiazol binding site. This could point to complex IV, cytochrome c oxidase, which has recently been identified as a nitrite reductase (Castello et al., 2006).

Since NO has been cited to inhibit mitochondrial respiration nitrite reduction via complex IV the inhibition of this complex would initiate auto-regulation. Under hypoxic conditions nitrite reduction would continue until critical levels of NO will be reached to block the reaction at the same site.

We assume that this mitochondria-dependent increase in cGMP levels contributes to the regulation of myocardial contractility under hypoxic conditions and to cytoprotection (Cauwels et al., 2009). In contrast, formation of nitroso species upon nitrite treatment was not affected by myxothiazol. This suggests that nitroso compounds are formed from nitrite, not from NO within HL-1 cells.

In conclusion, in this study we showed *in vitro* that both RBC and HL-1 cardiomyocytes mediated the reduction of nitrite to NO under hypoxic conditions. RBC-mediated nitrite reduction did not contribute to cGMP synthesis in HL-1 cells. cGMP production in cardiomyocytes was completely inhibited by myxothiazol, a specific inhibitor of mitochondria, while inhibitors of XOR, NOS, and p450 had no effect. The effect of myxothiasol was not due to inhibition of cGMP synthesis itself, suggesting that mitochondria trigger nitrite-mediated cGMP synthesis in cardiomyocytes. Our data suggest that this pathway may be a key regulator of myocardial contractility, especially under hypoxic conditions.

ACKNOWLEDGMENTS

We thank Dr. Jack Lancaster Jr. for stimulating and helpful discussion and Dr. James Ferguson for editing the manuscript.

FUNDING

This work was supported by Austrian Science Fund (FWF) [grant P 21121-B11] and by City of Vienna Competence Team Tissue Engineering Bioreaktoren.

REFERENCES

Baker, J. E., Su, J., Fu, X., Hsu, A., Gross, G. J., Tweddell, J. S., et al. (2007). Nitrite confers protection against myocardial infarction: role of xanthine oxidoreductase, NADPH oxidase and K(ATP) channels. *J. Mol. Cell Cardiol.* 43, 437–444.

Basu, S., Grubina, R., Huang, J., Conradie, J., Huang, Z., Jeffers, A., et al. (2007a). Catalytic generation of N2O3 by the concerted nitrite reductase and anhydrase activity of hemoglobin. *Nat. Chem. Biol.* 3, 785–794.

Basu, S., Grubina, R., Huang, J., Conradie, J., Huang, Z., Jeffers, A., et al. (2007b). Catalytic generation of N2O3 by the concerted nitrite reductase and anhydrase activity of hemoglobin. *Nat. Chem. Biol.* 3, 785–794.

Bryan, N. S., Calvert, J. W., Gundewar, S., and Lefer, D. J. (2008). Dietary nitrite restores NO homeostasis and is cardioprotective in endothelial nitric oxide synthase-deficient mice. *Free Radic. Biol. Med.* 45, 468–474.

Calvert, J. W., and Lefer, D. J. (2009). Myocardial protection by nitrite. *Cardiovasc. Res.* 83, 195–203.

Castello, P. R., David, P. S., McClure, T., Crook, Z., and Poyton, R. O. (2006). Mitochondrial cytochrome oxidase produces nitric oxide under hypoxic conditions: implications for oxygen sensing and hypoxic signaling in eukaryotes. *Cell Metab.* 3, 277–287.

Cauwels, A., Buys, E. S., Thoonen, R., Geary, L., Delanghe, J., Shiva, S., et al. (2009). Nitrite protects against morbidity and mortality associated with TNF- or LPS-induced shock in a soluble guanylate cyclase-dependent manner. *J. Exp. Med.* 206, 2915–2924.

Cosby, K., Partovi, K. S., Crawford, J. H., Patel, R. P., Reiter, C. D., Martyr, S., et al. (2003). Nitrite reduction to nitric oxide by deoxyhemoglobin vasodilates the human circulation. *Nat. Med.* 9, 1498–1505.

Dezfulian, C., Raat, N., Shiva, S., and Gladwin, M. T. (2007). Role of the anion nitrite in ischemia-reperfusion cytoprotection and therapeutics. *Cardiovasc. Res.* 75, 327–338.

Dezfulian, C., Shiva, S., Alekseyenko, A., Pendyal, A., Beiser, D. G., Munasinghe, J. P., et al. (2009). Nitrite therapy after cardiac arrest reduces reactive oxygen species generation, improves cardiac and neurological function, and enhances survival via reversible inhibition of mitochondrial complex I. *Circulation* 120, 897–905.

Jung, K. H., Chu, K., Ko, S. Y., Lee, S. T., Sinn, D. I., Park, D. K., et al. (2006). Early intravenous infusion of sodium nitrite protects brain against *in vivo* ischemia-reperfusion injury. *Stroke* 37, 2744–2750.

Kozlov, A. V., Costantino, G., Sobhian, B., Szalay, L., Umar, F., Nohl, H., et al. (2005). Mechanisms of vasodilatation induced by nitrite instillation in intestinal lumen: possible role of hemoglobin. *Antioxid. Redox. Signal.* 7, 515–521.

Kozlov, A. V., Dietrich, B., and Nohl, H. (2003). Various intracellular compartments cooperate in the release of nitric oxide from glycerol trinitrate in liver. *Br. J. Pharmacol.* 139, 989–997.

Kozlov, A. V., Sobhian, B., Costantino, G., Nohl, H., Redl, H., and Bahrami, S. (2001). Experimental evidence suggesting that nitric oxide diffuses from tissue into blood but not from blood into tissue. *Biochim. Biophys. Acta* 1536, 177–184.

Kozlov, A. V., Staniek, K., and Nohl, H. (1999). Nitrite reductase activity is a novel function of mammalian mitochondria. *FEBS Lett.* 454, 127–130.

Krasnikov, B. F., Kuzminova, A. E., and Zorov, D. B. (1997). The Ca^{2+}-induced pore opening in mitochondria energized by succinate-ferricyanide electron transport. *FEBS Lett.* 419, 137–140.

Lepore, D. A., Kozlov, A. V., Stewart, A. G., Hurley, J. V., Morrison, W. A., and Tomasi, A. (1999). Nitric oxide synthase-independent generation of nitric oxide in rat skeletal muscle ischemia-reperfusion injury. *Nitric Oxide* 3, 75–84.

Li, Y., and Trush, M. A. (1998). Diphenyleneiodonium, an NAD(P)H oxidase inhibitor, also potently inhibits mitochondrial reactive oxygen species production. *Biochem. Biophys. Res. Commun.* 253, 295–299.

Lu, P., Liu, F., Yao, Z., Wang, C. Y., Chen, D. D., Tian, Y., et al. (2005). Nitrite-derived nitric oxide by xanthine oxidoreductase protects the liver against ischemia-reperfusion injury. *Hepatobiliary. Pancreat. Dis. Int.* 4, 350–355.

Lundberg, J. O., and Weitzberg, E. (2005). NO generation from nitrite and its role in vascular control. *Arterioscler. Thromb. Vasc. Biol.* 25, 915–922.

MacArthur, P. H., Shiva, S., and Gladwin, M. T. (2007). Measurement of circulating nitrite and S-nitrosothiols by reductive chemiluminescence. *J. Chromatogr. B Analyt. Technol. Biomed. Life Sci.* 851, 93–105.

McNulty, P. H., Scott, S., Kehoe, V., Kozak, M., Sinoway, L. I., and Li, J. (2008). Nitrite consumption in ischemic rat heart catalyzed by distinct blood-borne and tissue factors. *Am. J. Physiol. Heart Circ. Physiol.* 295, H2143–H2148.

Nohl, H., Staniek, K., Sobhian, B., Bahrami, S., Redl, H., and Kozlov, A. V. (2000). Mitochondria recycle nitrite back to the bioregulator nitric monoxide. *Acta Biochim. Pol.* 47, 913–921.

Perlman, D. H., Bauer, S. M., Ashrafian, H., Bryan, N. S., Garcia-Saura, M. F., Lim, C. C., et al. (2009). Mechanistic insights into nitrite-induced cardioprotection using an integrated metabolomic/proteomic approach. *Circ. Res.* 104, 796–804.

Rassaf, T., Flogel, U., Drexhage, C., Hendgen-Cotta, U., Kelm, M., and Schrader, J. (2007). Nitrite reductase function of deoxymyoglobin: oxygen sensor and regulator of cardiac energetics and function. *Circ. Res.* 100, 1749–1754.

Rastaldo, R., Pagliaro, P., Cappello, S., Penna, C., Mancardi, D., Westerhof, N., et al. (2007). Nitric oxide and cardiac function. *Life Sci.* 81, 779–793.

Sanada, S., Node, K., Minamino, T., Takashima, S., Ogai, A., Asanuma, H., et al. (2003). Long-acting Ca^{2+} blockers prevent myocardial remodeling induced by chronic NO inhibition in rats. *Hypertension* 41, 963–967.

Shiva, S., and Gladwin, M. T. (2009). Nitrite mediates cytoprotection after ischemia/reperfusion by modulating mitochondrial function. *Basic Res. Cardiol.* 104, 113–119.

Shiva, S., Huang, Z., Grubina, R., Sun, J., Ringwood, L. A., MacArthur, P. H., et al. (2007). Deoxymyoglobin is a nitrite reductase that generates nitric oxide and regulates mitochondrial respiration. *Circ. Res.* 100, 654–661.

Totzeck, M., Hendgen-Cotta, U. B., Luedike, P., Berenbrink, M., Klare, J. P., Steinhoff, H. J., et al. (2012). Nitrite regulates hypoxic vasodilation via myoglobin-dependent nitric oxide generation. *Circulation* 126, 325–334.

van Faassen, E. E., Bahrami, S., Feelisch, M., Hogg, N., Kelm, M., Kim-Shapiro, D. B., et al. (2009). Nitrite as regulator of hypoxic signaling in mammalian physiology. *Med. Res. Rev.* 29, 683–741.

Vanin, A. F., Bevers, L. M., Slama-Schwok, A., and van Faassen, E. E. (2007). Nitric oxide synthase reduces nitrite to NO under anoxia. *Cell Mol. Life Sci.* 64, 96–103.

Webb, A. J., Milsom, A. B., Rathod, K. S., Chu, W. L., Qureshi, S., Lovell, M. J., et al. (2008). Mechanisms underlying erythrocyte and endothelial nitrite reduction to nitric oxide in hypoxia: role for xanthine oxidoreductase and endothelial nitric oxide synthase. *Circ. Res.* 103, 957–964.

Wolin, M. S. (2009). Reactive oxygen species and the control of vascular function. *Am. J. Physiol Heart Circ. Physiol.* 296, H539–H549.

Zielinska, M., Fresko, I., Konopacka, A., Felipo, V., and Albrecht, J. (2007). Hyperammonemia inhibits the natriuretic peptide receptor 2 (NPR-2)-mediated cyclic GMP synthesis in the astrocytic compartment of rat cerebral cortex slices. *Neurotoxicology* 28, 1260–1263.

Zweier, J. L., Wang, P., Samouilov, A., and Kuppusamy, P. (1995). Enzyme-independent formation of nitric oxide in biological tissues. *Nat. Med.* 1, 804–809.

Conflict of Interest Statement: The authors declare that the research was conducted in the absence of any commercial or financial relationships that could be construed as a potential conflict of interest.

Received: 31 January 2013; paper pending published: 04 March 2013; accepted: 23 April 2013; published online: 20 May 2013.

*Citation: Dungel P, Teuschl AH, Banerjee A, Paier-Pourani J, Redl H and Kozlov AV (2013) Impact of mitochondria on nitrite metabolism in HL-1 cardiomyocytes. Front. Physiol. **4**:101. doi: 10.3389/fphys.2013.00101*

This article was submitted to Frontiers in Mitochondrial Research, a specialty of Frontiers in Physiology.

frontiers in PHYSIOLOGY

ORIGINAL RESEARCH ARTICLE
published: 30 July 2013
doi: 10.3389/fphys.2013.00183

Identification and characterization of CHCHD1, AURKAIP1, and CRIF1 as new members of the mammalian mitochondrial ribosome

Emine C. Koc[1]*†, Huseyin Cimen[1†], Beril Kumcuoglu[2], Nadiah Abu[2], Gurler Akpinar[2], Md. Emdadul Haque[3], Linda L. Spremulli[3] and Hasan Koc[4]*

[1] *Department of Biochemistry and Microbiology, Joan C. Edwards School of Medicine, Marshall University, Huntington, WV, USA*
[2] *Department of Biochemistry and Molecular Biology, Pennsylvania State University, University Park, PA, USA*
[3] *Department of Chemistry, University of North Carolina, Chapel Hill, NC, USA*
[4] *Department of Pharmaceutical Science and Research, School of Pharmacy, Marshall University, Huntington, WV, USA*

Edited by:
Sabzali Javadov, University of Puerto Rico School of Medicine, Puerto Rico

Reviewed by:
Nazareno Paolocci, Johns Hopkins University, USA
Nono Takeuchi, University of Tokyo, Japan

***Correspondence:**
Emine C. Koc, Department of Biochemistry and Microbiology, Joan C. Edwards School of Medicine, Marshall University, Robert C. Byrd Biotechnology Science Center, 1700 3rd Ave., Huntington, WV 25755, USA
e-mail: koce@marshall.edu;
Hasan Koc, Department of Pharmaceutical Science and Research, School of Pharmacy, Marshall University, One John Marshall Dr., Huntington, WV 25755, USA
e-mail: kocha@marshall.edu

† These authors have contributed equally to this work.

Defects in mitochondrial ribosomal proteins (MRPs) cause various diseases in humans. Because of the essential role of MRPs in synthesizing the essential subunits of oxidative phosphorylation (OXPHOS) complexes, identifying all of the protein components involved in the mitochondrial translational machinery is critical. Initially, we identified 79 MRPs; however, identifying MRPs with no clear homologs in bacteria and yeast mitochondria was challenging, due to limited availability of expressed sequence tags (ESTs) in the databases available at that time. With the improvement in genome sequencing and increased sensitivity of mass spectrometry (MS)-based technologies, we have established four previously known proteins as MRPs and have confirmed the identification of ICT1 (MRP58) as a ribosomal protein. The newly identified MRPs are MRPS37 (Coiled-coil-helix-coiled-coil-helix domain containing protein 1-CHCHD1), MRPS38 (Aurora kinase A interacting protein1, AURKAIP1), MRPS39 (Pentatricopeptide repeat-containing protein 3, PTCD3), in the small subunit and MRPL59 (CR-6 interacting factor 1, CRIF1) in the large subunit. Furthermore, we have demonstrated the essential roles of CHCHD1, AURKAIP1, and CRIF1in mitochondrial protein synthesis by siRNA knock-down studies, which had significant effects on the expression of mitochondrially encoded proteins.

Keywords: mitochondrial translation, MRPS37 (CHCHD1), MRPS38 (AURKAIP1), MRPS39 (PTCD3), MRPL58 (ICT1), MRPL59 (CRIF1), 55S, mitochondrial ribosomal proteins

INTRODUCTION

Mammalian mitochondria use oxidative phosphorylation (OXPHOS) to provide more than 90% of the ATP used for energy by cells. ATP production by this process depends on electron transport chain complexes and ATP synthase, components of which are encoded by both the nuclear and mitochondrial genomes. In mammals, mitochondrial DNA encodes the information for only 13 essential proteins required for OXPHOS, in addition to 22 tRNAs and 2 rRNAs. The 13 proteins encoded by the mitochondrial genome are synthesized on 55S ribosomes using the specialized translational system within the organelle.

Mammalian mitochondrial ribosomes (55S) consist of small (28S) and large (39S) subunits (O'Brien et al., 1993; Pel and Grivell, 1994). The 55S ribosome is composed of ∼80 mitochondrial ribosomal proteins (MRPs), and all of these proteins are encoded by nuclear genes and imported into mitochondria, where they are assembled into the ribosome with mitochondrially transcribed rRNAs (De Vries and Van Der Koogh-Schuuring, 1973; Pietromonaco et al., 1991; Koc et al., 2001a,b). About a decade ago, we and others identified almost all of the proteins present in these ribosomes using various proteomics techniques. This initial analysis indicated that the small subunit of the ribosome contains 29 proteins, whereas the large subunit has about 50 proteins (Goldschmidt-Reisin et al., 1998; Graack et al., 1999; Koc et al., 1999, 2001a,b; Suzuki et al., 2001). About half of the proteins in mammalian mitochondrial ribosomes have homologs in bacterial and yeast mitochondrial ribosomes and play a role either in the assembly and structure of ribosomes or in the initiation, elongation, or termination phases of mitochondrial translation (Smits et al., 2007; Christian and Spremulli, 2011; Koc and Koc, 2012). The functions and ribosomal locations of the mitochondrial-specific proteins are not known; however, they may replace some of the functions of bacterial ribosomal proteins that are not present in the mitochondrial ribosome. They may

Abbreviations: MRPS, Mitochondrial ribosomal small subunit protein; MRPL, Mitochondrial ribosomal large subunit protein; capLC-MS/MS, capillary liquid chromatography-nanoelectrospray ionization-tandem mass spectrometry.

also provide additional function(s) critical for protein synthesis or its regulation in mammalian mitochondria (Koc et al., 2001a,b). Although it is not possible to determine the exact locations of these mitochondrial-specific proteins without x-ray structural information, cryo-EM reconstruction studies indicate that they are distributed on the exterior surface of the ribosome (Sharma et al., 2003; Agrawal et al., 2011). It is clear that some of the mitochondrial-specific ribosomal proteins are located in functionally important regions of the ribosome, particularly at the mRNA entrance gate in the small subunit and at the polypeptide exit tunnel and central protuberance region of the large subunit, creating specific structures on the mitochondrial ribosome (Sharma et al., 2003; Agrawal et al., 2011).

In many instances, mitochondrial-specific ribosomal proteins were initially identified based on distinct biological functions that did not appear to be related to mitochondrial translation. For example, mitochondrial-specific MRPs such as MRPS29 (DAP3-death associated protein 3) and MRPS30 (PDCD9-programmed cell death protein 9) were originally identified on the basis of their involvement in apoptosis. MRPL37 and MRPL41 were also reported to be involved in apoptosis (Carim et al., 1999; Koc et al., 2001a,b; Levshenkova et al., 2004; Chintharlapalli et al., 2005; Yoo et al., 2005). Human mutations in MRPs have been reported and can have a variety of consequences (Galmiche et al., 2011; Smits et al., 2011). Major mutations in MRPs can lead to functional changes in mitochondrial translation and can be lethal (Miller et al., 2004; Jacobs and Turnbull, 2005; Saada et al., 2007; Galmiche et al., 2011; Rotig, 2011; Smits et al., 2011). Aberrantly expressed MRPs are also observed in many different tumors, including in breast cancer, gliomas, squamous cell carcinoma, and osteosarcoma (Bonnefoy et al., 2001; Koc et al., 2001b; Mariani et al., 2001; Miller et al., 2004; Lyng et al., 2006). Therefore, a complete list of mitochondrial ribosomal proteins will be fundamental to our understanding of the mitochondrial translational machinery and its contribution to mitochondrial ATP production in health and disease.

In the present study, we re-evaluated protein components of the mammalian mitochondrial ribosome using mass spectrometry (MS)-based proteomics and have established that five previously known mitochondrial proteins are components of the mitochondrial ribosome. These proteins are coiled-coil-helix-coiled-coil-helix domain containing protein 1 (CHCHD1), aurora kinase A interacting protein 1 (AURKAIP1), pentatricopeptide repeat-containing protein 3 (PTCD3), immature colon carcinoma transcript 1 protein (ICT1) and CR-6 interacting factor 1 [CRIF1, also known as growth arrest and DNA-damage-inducible proteins-interacting protein 1 (Gadd45GIP1)]. Three newly established mitochondrial ribosomal proteins (CHCHD1, AURKAIP1, and PTCD3) were assigned to the small subunit of the 55S ribosome, while ICT1 and CRIF1 were assigned to the large subunit. We further confirmed the specific roles for CHCHD1, AURKAIP1, and CRIF1 in mitochondrial translation by siRNA knock-down studies in human cell lines.

MATERIALS AND METHODS

PREPARATION OF BOVINE MITOCHONDRIAL RIBOSOMAL SUBUNITS

Mitochondrial ribosomes from bovine liver were prepared using a previously described method at high and low ionic strengths and at several different detergent concentrations (Matthews et al., 1982; Koc et al., 2001a,b; Spremulli, 2007). The high ionic strength and detergent concentrations used the standard conditions of 300 mM KCl and 1.6% Triton-X100 (Yang et al., 2010). For the preparation of mitochondrial ribosomes at low salt and detergent conditions, mitochondrial lysates were prepared in a buffer containing 50 mM Tris-HCl, pH 7.6, 40 mM KCl, 20 mM $MgCl_2$, 6 mM β-mercaptoethanol, 0.2% Triton X-100, and 1 mM phenylmethylsulfonyl fluoride (PMSF). The mitochondrial lysate (100 mg/mL) was layered onto a 34% sucrose cushion (40 mM KCl, 20 mM $MgCl_2$, 50 mM Tris-HCl, pH 7.6, 6 mM β-mercaptoethanol and 34% (w/w) sucrose). Samples were centrifuged at 35,000 rpm for 16 h at 4°C in a Beckman Type-50.2 rotor. The pellet was collected as crude mitochondrial ribosomes and resuspended in a buffer prepared with 40 mM KCl, 20 mM $MgCl_2$, 20 mM Tris-HCl pH 7.6, 1 mM dithiothreitol (DTT), and protease inhibitor cocktail from Sigma-Aldrich (containing 1.04 mM AEBSF, 0.8 μM Aprotinin, 40 μM Bestatin, 14 μM E-64, 20 μM Leupeptin, and 15 μM Pepstatin A as the final concentrations). Samples were then subjected to centrifugation through a 10–30% linear sucrose gradient in buffer containing 40 mM KCl, 20 mM $MgCl_2$, 50 mM Tris-HCl pH 7.6, and 1 mM DTT as described (Matthews et al., 1982; Koc et al., 2001a,b; Spremulli, 2007). Fractions containing 55S ribosomes were combined, and the ribosomes were collected by centrifugation at 40,000 rpm for 16 h. The concentration of Mg^{2+} in the preparations was reduced to 2 mM by dialysis in order to dissociate ribosomes into 28S and 39S subunits, and the samples were separated again on a linear 10–30% sucrose gradient containing 2 mM Mg^{2+} as described (Matthews et al., 1982; Koc et al., 2001a,b; Spremulli, 2007). Highly purified 28S and 39S subunits were collected by centrifugation at 40,000 rpm for 16 h.

IDENTIFICATION OF MITOCHONDRIAL RIBOSOMAL PROTEINS BY MASS SPECTROMETRY

To identify the proteins of mammalian mitochondrial ribosomes, approximately 0.5 A_{260} units of purified ribosomal 28S and 39S subunits and 55S samples were separated on SDS-PAGE, and corresponding protein bands were excised into at least thirty equal gel pieces. The pieces were processed by performing in-gel tryptic digestion using methods previously established in our laboratory (Miller et al., 2008, 2009; Soung et al., 2009). Tryptic digests were analyzed by capillary liquid chromatography-nanoelectrospray ionization-tandem mass spectrometry (capLC-MS/MS). Extracted tryptic peptides (3–5 μL) were injected into a peptide trap (Michrom peptide CapTrap, C8 like resin, 0.3 × 1 mm, 5 μm) over a 3 min interval at 10 μL/min for online desalting and concentration. With the use of a six-port switching valve, the peptide trap was then placed in-line with the analytical column, a PicoFrit column (0.075 × 150 mm) packed in-house with Wide Bore C18 reverse phase resin (Supelco Co., 5 μm, 300 Å). Tandem MS spectra of tryptic peptides were obtained by collision-induced dissociation (CID) in an LTQ linear ion trap mass spectrometer system (ThermoFinnigan) including a Surveyor HPLC pump and a Surveyor Micro AS autosampler.

MS/MS spectra were processed by Xcalibur 2.0 and searched against the nonredundant NCBI protein database and the Swiss-Prot and UnitProtKB databases using the Mascot server.

Additionally, the search was repeated using a bovine protein sequence database generated in-house. The protein information obtained from the database searches and the scores of mitochondrial ribosomal proteins that were observed in multiple bands were compared. To increase the data quality, proteins with a Mascot score lower than 45 were excluded from the list.

Ribosomal proteins were assigned to subunits according to their abundance in 28S and 39S fractions. The Exponentially Modified Protein Abundance Index (emPAI) score was calculated to compare the protein abundance in each sample (Ishihama et al., 2005). In brief, the ratio of the unique parent ion number observed in the analysis to the observable peptide number from *in silico* digestion is used as PAI in the formula: $\text{emPAI} = 10^{(\text{PAI})-1}$. The emPAI values were used to determine subunit distribution of each protein identified in 28S, 39S, and 55S samples.

PREPARATION OF CRUDE RIBOSOMES FROM HUMAN CELL LINES AND ISOLATED MITOCHONDRIA

HeLa cells were grown in Dulbecco's Modified Eagle's Medium (DMEM) media (Cellgro, Mediatech Inc.) supplemented with 10% (v/v) bovine calf serum (Hyclone Laboratories) and 100 IU/ml penicillin and 100 μg/ml streptomycin at 37°C and 5% CO_2 in a humidified atmosphere. For the whole cell lysate preparation, approximately 4×10^7 HeLa cells were combined and lysed in 2 mL of buffer containing 50 mM Tris-HCl, pH 7.6, 0.26 M sucrose, 60 mM KCl, 20 mM $MgCl_2$, 0.8 mM EDTA, 2 mM DTT, 0.05 mM spermine, 0.05 mM spermidine, 1.6% Triton X-100, and protease inhibitor cocktail from Sigma-Aldrich using a Dounce homogenizer (Wheaton). In order to isolate mitochondria, approximately 2×10^7 HeLa cells were resuspended in 1 mL of an isotonic mitochondrial buffer (MB) (210 mM mannitol, 70 mM sucrose, 1 mM EDTA, 10 mM HEPES-KOH pH 7.5), supplemented with protease inhibitors (1 mM PMSF and the protease cocktail from Sigma-Aldrich described above), and then homogenized in a Dounce homogenizer on ice. The suspension was centrifuged at 400 × g in a microcentrifuge (ThermoForma) at 4°C. The pellet was resuspended in another 1 mL of MB and the 400 × g centrifugation was repeated. Supernatants were combined and centrifuged at 10,000 × g at 4°C for 10 min to pellet mitochondria. The mitochondrial pellets were lysed in a buffer containing 0.26 M sucrose, 20 mM Tris-HCl, pH 7.6, 40 mM KCl, 20 mM $MgCl_2$, 0.8 mM EDTA, 0.05 mM spermine, 0.05 mM spermidine, 6 mM β-mercaptoethanol, and 1.6% Triton X-100 using a Dounce homogenizer.

To collect the crude ribosomes, whole cell and mitochondrial lysates (2 mL) were layered onto a 34% sucrose cushion (4 mL) in buffer (50 mM Tris-HCl, pH 7.6, 60 mM KCl, 20 mM $MgCl_2$, and 6 mM β-mercaptoethanol) and centrifuged in a Type 40 rotor (Beckman Coulter) at 40,000 rpm for 16 h. The post-ribosomal supernatant was fractionated into six separate layers (designated L1–L6) for analysis, and the pellet was collected as a crude ribosomal fraction. The crude ribosome preparations, which included mitochondrial and cytoplasmic ribosomes for whole cell lysates and only mitochondrial ribosomes for the mitochondrial lysates, were resuspended in 50 μL of Base Buffer III (50 mM Tris-HCl, pH 7.6, 60 mM KCl, 20 mM $MgCl_2$, 1 mM DTT) and protease inhibitor cocktail (Sigma-Aldrich). Ribosome suspensions were stored at −80°C for further analyses.

RNase A TREATMENT OF MITOCHONDRIAL RIBOSOMES

In order to confirm the direct or indirect interaction of new MRPs with the rRNA of the mitochondrial ribosome, approximately ∼5 A_{260} units of a crude preparation of ribosomes obtained from bovine liver were incubated in the absence or presence of 20 μg RNase A and loaded onto separate 10–30% linear sucrose gradients in buffer containing 40 mM KCl, 20 mM $MgCl_2$, 50 mM Tris-HCl, pH 7.6, and 1 mM DTT. After centrifugation, the proteins in equal volumes (25 μL) of gradient fractions were separated on 12% SDS-PAGE. The proteins were transferred to PVDF membranes and probed with corresponding antibodies as described below.

IMMUNOBLOTTING

Ribosome samples collected from HeLa cell and bovine mitochondria (including sucrose gradient fractions, purified 55S ribosomes, 28S subunits, and 39S subunits) were separated by 12% SDS-PAGE. Proteins were transferred to PVDF membranes, which were probed with rabbit polyclonal anti-CHCHD1 antibody at a 1:1000 dilution (Abcam), rabbit anti-AURKAIP1 antibody at a 1:1000 dilution (Sigma-Aldrich), goat anti-CRIF1 antibody at a 1:500 dilution (Santa Cruz Biotechnology), mouse monoclonal anti-MRPS29 (DAP3) and anti-HSP60 antibodies at 1:5000 dilutions (BD Transduction Laboratories), mouse anti-OXPHOS (MITOPROFILE®) at a 1:5000 dilution (Abcam Inc.), or rabbit polyclonal human anti-MRPL47 and mouse polyclonal human anti-MRPS18-2 antibodies at 1:5000 dilutions (produced in-house) for 16 h at 4°C. All of the secondary antibodies were used at 1:5000 dilutions, including donkey anti-goat IgG (Santa Cruz Biotechnology) for CRIF1; goat anti-mouse IgG (Pierce Biochemicals Inc.) for MRPS29, HSP60 and OXPHOS, and goat anti-rabbit IgG for CHCHD1, AURKAIP1, and MRPL47. The membranes were developed using SuperSignal West Pico Chemiluminescent substrate (Pierce Biochemicals Inc.) according to the protocol provided by the manufacturer.

[^{35}S]-METHIONINE PULSE LABELING OF MITOCHONDRIAL TRANSLATION PRODUCTS *IN VIVO*

Human embryonic kidney 293T (HEK293T) cell lines were cultured in DMEM (Cellgro, Mediatech Inc.) supplemented with 10% bovine calf serum (Hyclone), 100 IU/ml penicillin, and 100 μg/ml streptomycin at 37°C and 5% CO_2 in a humidified atmosphere. Cells were transfected with control siRNA (sc-44235) and mixtures of two to five target-specific siRNAs against CHCHD1 (sc-90488), AURKAIP1 (sc-72472), and CRIF1 (sc-97804) from Santa Cruz Biotechnology using Lipofectamine™ 2000 (Invitrogen) according to the protocol provided by the manufacturer. The transfected cells were grown in transfection medium for 2 days prior to labeling with [^{35}S]-methionine. It should be noted that the siRNA treated cells grew very poorly reflecting the importance of CHCHD1, AURKAIP1, and CRIF1 for cell growth and viability and suggesting that they play an essential role in the cell. Labeling experiments were performed in the presence of dialyzed serum (25 mM Tris-HCl, pH 7.4, 137 mM NaCl, and 10 mM KCl) and minimum essential DMEM medium, which does not contain methionine, glutamine, or cysteine, as indicated in our previous reports following the protocol

by Chomyn et al., with several modifications described by Leary et al. (Chomyn, 1996; Leary and Sasarman, 2009; Yang et al., 2010). Cells were incubated with emetine-containing medium for 5 min to arrest cytosolic protein synthesis, and 0.2 mCi/mL of [^{35}S]-methionine (Perkin Elmer) containing medium was then added to label the mitochondrially-encoded proteins. After a 2 h incubation, cells were lysed in buffer containing 50 mM Tris-HCl, pH 7.6, 150 mM NaCl, 1 mM EDTA, 1 mM EGTA, 0.1% SDS and 0.5% NP-40 supplemented with 1 mM PMSF and protease inhibitor cocktail (Sigma-Aldrich). Whole cell lysates (40 μg) were electrophoresed through 12% SDS-PAGE. The gels were dried on 3MM chromatography paper (Whatman), and the total intensities of the signals were quantified by phosphorimaging analyses (Jeffreys and Craig, 1976). The siRNA mediated knock-down efficiency of the corresponding mitochondrial ribosomal protein was confirmed with immunoblotting analysis of whole cell lysates or crude ribosomal fractions, prepared as stated above.

REVERSE TRANSCRIPTION POLYMERASE CHAIN REACTION (RT-PCR)

Total RNA was isolated from siRNA transfected HEK293T cells by using RNeasy Mini Kit from Qiagen. These RNA preparations were tested for mtDNA contamination using a minus reverse transcriptase control and shown to be free of mtDNA (data not shown). The cDNA was synthesized using the ThermoScript™ RT-PCR system (Invitrogen). The primers used were: CHCHD1 forward 5′- ACCTCTCATTCTAGCTAACCGCGT -3′, reverse 5′- AGACTCTCCCAGGGTTTCCTGTAT -3′; AURKAIP1 forward 5′- TCCACCGCAATCCTACCAGTGT -3′, reverse 5′- CG AACTTGATCTGCTTGCGTCTCA -3′; CRIF1 forward 5′- GAT GATTGTGAACTGGCAGCAGCA -3′, reverse 5′- CGCCTCCT TCTTCCGTTTCTGTTT -3′; ND6 forward 5′- GAGTGTGGGT TTAGTAATGGGGTTTGTGGGG -3′, reverse 5′- CCTATTCCC CCGAGCAATCTC -3′; COI forward 5′- ATTTAGCTGACTCG CCACACTCCA -3′, reverse 5′- TAGGCCGAGAAAGTGTTGTG GGAA -3′; COII forward 5′- ATGGCACATGCAGCGCAAGTA -3′, reverse 5′- CTATAGGGTAAATACGGGCCC-3′; ATP6 forward 5′- TAATACGACTCACTATAGATGAACGAAAATATGT -3′, reverse 5′- TTTTTTTTTTTTTTTTTTTTTTCATTGTTGGGT GGTGATTAG -3′; 12s rRNA forward 5′- AATAGGTTTGGT CCTAGCCTAGCC -3′, reverse 5′- GTTCGTCCAAGTGCACTT TCCAG -3′; MRPS29 forward 5′- ATGGACCGACACGGGTAT TGTACC -3′, reverse 5′- AAGGCCATGGGGAAATACAGTC -3′; MRPL47 forward 5′- AAACGGGGTACCGAGATGGCTGCG GCCGGTTTGGCCC -3′, reverse 5′- CCGCTCGAGTTAATGGT GATGGTGATGATGGACAAGACTTGACTTTTGGGC -3′; glyceraldehyde 3-phosphate dehydrogenase (GAPDH) forward 5′- GTCTTCACCACCATGGAGAAGG -3′, reverse 5′- ATGAGGTC CACCACCCTGTTGC -3′. Reactions were performed according to the instructions provided by the manufacturer. Samples were visualized using the ChemiDoc XRS system, employing Quantity One® 1D analysis software (Bio-Rad). The signal intensities obtained for control and siRNA knock-down samples were normalized to the GAPDH signals for the relative quantitation of RNA expression.

RESULTS AND DISCUSSION

IDENTIFICATION OF 55S RIBOSOMAL PROTEINS BY TANDEM MASS SPECTROMETRY

The majority of the protein components of mammalian mitochondrial ribosomes were identified by our group, as well as several other groups, a decade ago using proteomics strategies (Goldschmidt-Reisin et al., 1998; Graack et al., 1999; Koc et al., 1999, 2000, 2001a,b; O'Brien et al., 1999). However, due to the limited availability of bovine or rat protein and DNA sequence information, some of the ribosomal and ribosome-associated proteins were not detected or identified by matching the tandem MS data to the publicly available ESTs or protein databases available at the time. An analysis of the protein composition of a large macromolecular complex requires the preparation of that complex under conditions that are strong enough to remove contaminants, but that are gentle enough to prevent the loss of more loosely bound protein components. In order to re-evaluate their protein composition and to eliminate transiently associated proteins, mammalian mitochondrial ribosomes were purified under two different salt and detergent conditions from bovine liver (**Figure 1**) (Spremulli, 2007). The 10–30% linear sucrose gradient separation of mitochondrial ribosomes was carried out at 20 mM Mg^{2+} to collect 55S particles (**Figure 1**).

The protein compositions of the 55S samples prepared under the two different salt and detergent conditions were compared by SDS-PAGE (Figure S1). In general, the gel pattern was similar in both ribosomal preparations; however, the sample prepared at high salt and detergent concentrations contained relatively

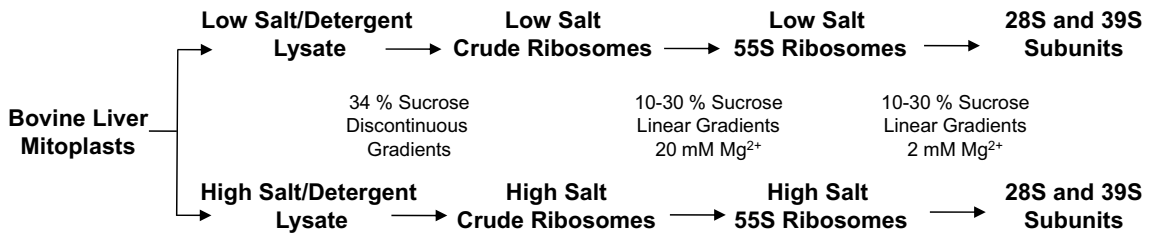

FIGURE 1 | Experimental scheme for the purification of mitochondrial ribosomes and 28S and 39S subunits. To obtain purified 55S ribosomes and 28S and 39S subunits using sequential linear sucrose gradients, bovine mitochondrial lysates were prepared at different ionic and detergent conditions to remove mitochondrial metabolic enzymes co-sedimenting with the mitochondrial ribosome. Experimental details are included in Materials and Methods.

lower amounts of high molecular weight proteins. The proteins in these bands may be subunits of the large enzyme complexes that co-sediment with the mitochondrial ribosome fractions (Figure S1). The gels were sliced into thirty fractions, and the in-gel tryptic digestion of each gel piece was analyzed by capLC-MS/MS. The peptide and protein contents of the gels were determined by matching MS/MS spectra to an in-house protein sequence database, which was generated by the combination of ∼30,000 bovine proteins found in the Swiss-Prot and UniProtKB databases.

A comprehensive list of the MRPs, the subunits of metabolic enzyme complexes, and the other proteins identified in our analyses is given in Tables S1 and S2. The list of the proteins that had not previously been identified as *bona fide* ribosomal proteins was created by excluding the known MRPs, mitochondrial metabolic pathway proteins, and oxidative phosphorylation proteins. In these analyses, CHCHD1, AURKAIP1, PTCD3, and CRIF1 were repeatedly found to be present in the mitoribosome with high confidence in both low and high salt and detergent preparations (**Tables 1**, S2, S3). It should be noted that CRIF1 and PTCD3 were known from previous studies to be associated with the ribosome (Davies et al., 2009; Kim et al., 2012). ICT1 (MRPL58) was also observed in these studies and was reported previously as a mitochondrial ribosomal protein (Richter et al., 2010). With the exception of large complexes of metabolic enzymes (specifically 2-oxoglutarate and pyruvate dehydrogenases and ATP synthase F1 subunits sedimenting with the ribosome), proteins consistently found in both low and high salt and detergent preparations of 55S ribosomes were considered as possible components of the mitochondrial translational machinery and ribosomal proteins (**Tables 1**, S1).

Table 1 | Peptide sequences of new mitochondrial ribosomal proteins identified from LC-MS/MS analyses of in-gel tryptic digestions of 28S, 39S, and 55S samples prepared at high salt conditions.

Name	Sequence	Score	m/z	Mr (expt)
CHCHD1	KPILKPNKPLILANHVGER	97	713.2	2136.7
	SIQEDLGELGSLPPR	112	805.7	1609.4
	SIQEDLGELGSLPPRK	85	870.4	1738.7
AURKAIP1	AGLKEAPPGWQTPK	74	740.7	14.79.4
	EAPPGWQTPK	83	556.7	1109.6
PTCD3	DEGADIAGTEEVVIPK	113	821.7	1641.5
	TWDKVAVLQALASTVHR	145	948.4	1894.9
	VAVLQALASTVHR	88	683	1364.1
	AGHQLGVTWR	63	563.4	1124.7
	AHTQALSMYTELLNNR	143	931.9	1861.7
	ADVHTFNSLIEATALVVNAK	150	1057.8	2113.7
	WNNILDLLK	54	564.9	1127.9
	QMVAQNVKPNLQTFNTILK	110	1094.5	2186.9
	GSSLIIYDIMDEITGK	118	878.3	1754.6
	FSPKDPDDDMFFQSAMR	72	723.6	2167.9
	DPDDDMFFQSAMR	102	788.2	1574.4
	DLELAYQVHGLLNTGDNR	124	1014.9	2027.9
	LEMIPQIWK	55	579.4	1156.8
	SDLKEEILMLMAR	91	775.4	1548.9
	EEILMLMAR	51	553.6	1105.2
	NELLNEFMDSAK	80	706.3	1410.5
	ASSSPAQAVEVVK	79	636.7	1271.4
	LTADFTLSQEQK	95	691	1379.9
	EALGDLTALTSDSESDSDSDTSKDK	90	863.8	2588.4
ICT1	QGNDDIPVDR	90	565.3	1128.5
	AGELILTSEYSR	79	670.4	1338.8
	GADTAWRVPGDAK	60	672.6	1343.2
	SAYSLDKLYPESR	95	766.3	1530.7
	FHLASADWIAEPVR	119	806.8	1611.5
	VPGDAKQGNDDIPVDR	69	565.6	1693.9
	DMIAEASQPATEPSKEDAALQK	124	1165.9	2329.9
CRIF1	HGAASGVDPGSLWPSR	115	797.5	1593.1
	AAAMAAAAAQDPADSETPDS	116	930.9	1859.8
	EQLLELEAEER	77	680.3	1358.6
	MPQMIENWR	54	602.9	1203.8
	FQELLQDLEK	62	632.3	1262.7

SUBUNIT ASSIGNMENTS OF RIBOSOME-ASSOCIATED PROTEINS BY LC-MS/MS

In order to categorize the newly observed proteins as either MRPs or proteins involved in translation, determining the subunit assignments of these proteins was essential. Sucrose gradient purified bovine 55S ribosomes prepared at high salt and detergent conditions (Figure S1) were sedimented on a second 10–30% linear sucrose gradient containing 2 mM Mg^{2+} to promote dissociation of the small (28S) and large (39S) subunits (**Figure 2A**). Proteins contained in the purified 28S, 39S, and 55S samples were separated by SDS-PAGE and stained with Coomassie Blue (**Figure 2A**). Although the amount of high molecular weight proteins found in the 55S ribosome preparation decreased, several remained associated with the 28S and 39S subunits in the second sucrose gradient (**Figure 2A**). The Coomassie Blue stained gel clearly showed the differential protein and MRP distribution in the 28S and 39S fractions, and the 55S fraction contains the protein bands observed in both 28S and 39S fractions (**Figure 2A**). Each lane was cut into thirty equal pieces. In-gel tryptic digestions were carried out, and the resulting peptides were analyzed by capLC-MS/MS. Database searches were performed as described for the analysis of 55S ribosomal proteins.

In general, the same set of proteins found in the 55S ribosomes was also identified in 28S and 39S subunits (Table S1). This table provides a complete list of the MRPs and the newly identified proteins, as well as their distributions in the 28S and 39S subunits. The proteins transiently associated with the 55S ribosome (including mitochondrial elongation factor EF-Tu, ribosome recycling factor (RRF), and a bacterial yBEB homolog, C7orf30) were released during either the 55S ribosome preparation or the dissociation of the ribosome into 28S and 39S subunits in the second sucrose gradient at 2 mM Mg^{2+} (Table S1). Four additional proteins not previously assigned as mitochondrial ribosomal proteins (CHCHD1, AURKAIP1, PTCD3, and CRIF1) were consistently observed in 28S or 39S subunits and in 55S ribosomes, making the determination of whether these proteins are *bona fide* ribosomal proteins or ribosome-associated

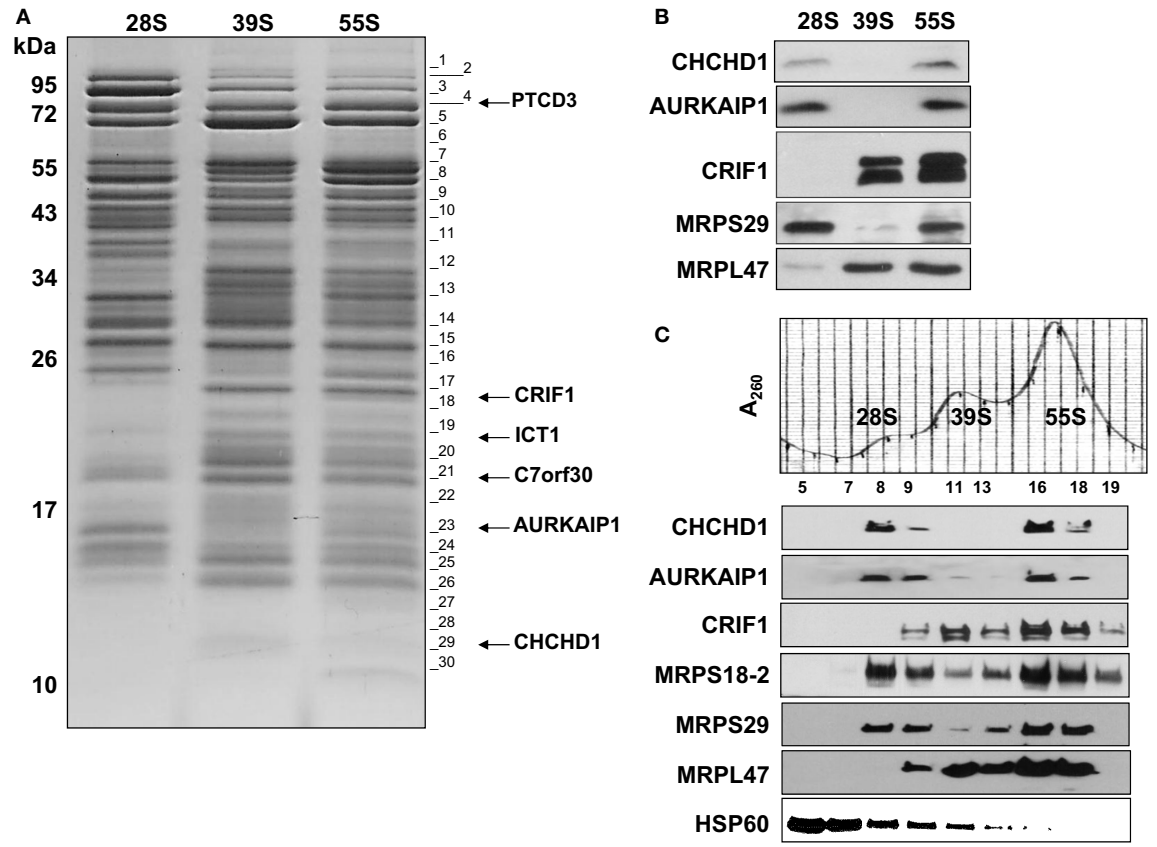

FIGURE 2 | Identification and detection of mitochondrial ribosomal proteins and their subunit association by capLC-MS/MS and immunoblotting analyses. (A) Purified mitochondrial (55S) ribosomes (~10 A_{260}) prepared in high salt conditions were dissociated into subunits by sedimentation through a second 10–30% linear sucrose gradient in the presence of 2 mM Mg^{2+} as described in **Figure 1**. After the sedimentation of the purified subunits, the same A_{260} units of 28S and 39S subunits and 55S ribosomes (~0.5) were separated on SDS-PAGE. The gel was cut into 30 pieces for in-gel digestion of protein bands with trypsin and the peptides were analyzed by capLC-MS/MS analysis to identify the proteins present. Gel fractions containing the peptides detected from newly identified MRPs are marked on the image. Proteins identified in these gel pieces are given in Tables S1, S2. **(B)** Purified 28S and 39S subunits (~0.2 A_{260}) were obtained from the dissociation of purified 55S ribosomes as described in Materials and Methods at 2 mM Mg^{2+}. Proteins present in these preparations were separated on 12% SDS-PAGE and analyzed by immunoblotting using CHCHD1, AURKAIP1, CRIF1, MRPS29, and MRPL47 antibodies to confirm subunit distribution of new MRPs. **(C)** To confirm the ribosome association of newly identified proteins, crude mitochondrial ribosomes prepared at high salt and detergent conditions were separated on a 10–30% linear sucrose gradient in the presence of 20 mM Mg^{2+} as described in **Figure 1**. Distribution of new proteins, CHCHD1, AURKAIP1, and CRIF1, were detected by immunoblotting analyses of sucrose gradient fractions containing dissociated ribosomal subunits (28S and 39S) and 55S ribosomes. Antibodies against two 28S subunit proteins, MRPS18B and MRPS29, and a 39S protein, MRPL47, were used to indicate the locations of the subunits and the 55S ribosome.

proteins critical. The relative molecular masses of these proteins were in good agreement with their expected molecular weights after the removal of mitochondrial import signals (**Figure 2A**) (Claros and Vincens, 1996). The Mascot scores obtained from database analyses of these peptides revealed that these proteins have clear subunit distributions in either the 28S or 39S subunit, except for ICT1 (Table S1). In addition to the Mascot scores obtained for each protein, the experimental emPAI scores determined as described by Ishihama et al. (Ishihama et al., 2005) were calculated to demonstrate the relative protein abundance in each subunit, using the ratio of peptides detected by capLC-MS/MS analyses to the number of observable peptides obtained from *in silico* digestion of a protein (**Tables 2**, S1, S3). The GenBank™ and Swiss-Prot access numbers of the newly identified MRPs used in the emPAI determination are listed in **Table 3**. The agreement between the emPAI scores for the 55S ribosome and either the 28S or 39S values for each protein clearly shows that these proteins were associated with the ribosome and its subunits under the conditions used in our experiments (**Table 2**). Variations in emPAI scores, specifically for PTCD3 and ICT1, could be due to discrepancies in the excision of gel slices, and the extraction of peptides in different samples, or the data dependent acquisition of peptides by the capLC-MS/MS system.

To confirm the subunit distribution determined by the emPAI scores, immunoblotting analyses of purified subunits and 55S ribosomes were performed using CHCHD1, AURKAIP1, and CRIF1 antibodies. Previous work had indicated that PTCD3 was associated with the small subunit, while CRIF1 and ICT1 interacted with the large subunit (Koc and Spremulli, 2003; Richter et al., 2010; Haque et al., 2011; Kim et al., 2012). In the

present analyses, CHCHD1 and AURKAIP1 signals overlapped with the MRPS29 signals, which were clearly detected in 28S and 55S fractions, indicating their association with the small subunit. CRIF1 was detected in 39S and 55S preparations, along with the large subunit protein MRPL47 (**Figures 2B,C**). The data obtained by capLC-MS/MS and immunoblotting analyses cooperatively suggest that CHCHD1 and AURKAIP1 are newly described components of the small subunit. Further, the data indicate that CRIF1 is not only associated with the large subunit, but also a *bona fide* component of the large subunit of the mitochondrial ribosome. Alignments of new MRPs across worm, fly, mouse, bovine, and human homologs (as well as yeast homologs of CHCHD1 and AURKAIP1) indicate the presence of evolutionarily conserved regions in these new proteins (Figure S2). Some of the characteristics of these new ribosomal proteins are described below.

CHCHD1

Although a signal peptide cleavage site was not predicted by MitoProt II, the probability of a mitochondrial localization of bovine CHCHD1 is 81% (Claros and Vincens, 1996). The accession numbers for CHCHD1 from various organisms, used in the alignment of the full length sequences, are given in **Table 3** (Figure S2). The full length bovine CHCHD1 is about 13.6 kDa. Mass spectrometry analysis of tryptic peptides extracted from the protein bands excised from 28S, 39S, and 55S lanes resulted in identification of CHCHD1 peptides in 28S and 55S samples, but not in 39S subunits (**Tables 1**, S1). Mammalian mitochondrial CHCHD1 has a homolog in the yeast mitochondrial ribosome, MRP10, as reported by Smits et al., which has about 20% sequence identity to the human protein (Graack et al., 1992; Jin et al., 1997). Similarly, the fly and worm homologs of CHCHD1 are also 20–25% identical to mammalian homologs, although their sequence identity to the yeast homolog is below 14% (Figure S2). The emPAI values calculated using CHCHD1 peptides clearly suggest that this protein is mainly associated with the small subunit of mitochondrial ribosomes (**Tables 2**, S3). The data presented here provide the first experimental evidence indicating that CHCHD1 is a component of the small subunit in mammalian mitochondria.

Table 2 | Relative distribution of new mitochondrial ribosomal proteins using emPAI (Exponentially Modified Protein Abundance Index) values calculated from peptides detected by LC-MS/MS analyses of proteins in 28S and 39S subunits and 55S ribosomes.

Subunit	CHCHD1	AURKAIP1	PTCD3	ICT1	CRIF1
28S	3.30	0.27	169.61	0.97	0.49
39S	ND	0.19	0.64	1.09	2.02
55S	3.14	0.27	22.77	0.86	2.11

Peptides (ion score cut off of ≥45) listed in Table S3 were used in emPAI calculations. ND; not detected.

AURKAIP1

AURKAIP1, also known as Aurora-A-interacting protein (AIP), was first described as a regulator of Aurora-A kinase, which is a Ser/Thr kinase involved in cell cycle progression and tumorigenesis (Kiat et al., 2002). The homology region found in AURKAIP1 homologs is termed DUF1713, and this region is found in the C-terminal domain of yeast COX24 (Figure S2). Yeast COX24 was described as one of the factors responsible for COI mRNA processing and translation (Barros et al., 2006). The calculated molecular mass of the full-length AURKAIP1 is 22.4 kDa; however, the mature protein migrates at about 16 kDa (**Figures 2B**, **3**). It is possible that AURKAIP1 has a longer signal peptide than the predicted signal peptide, which provides a 99% likelihood for the translocation of this protein into mitochondria. Translocation of AURKAIP1 into the mitochondria has also been experimentally validated by the Human Protein Atlas (HPA) project (Uhlen et al., 2010). AURKAIP1 was repeatedly detected in the capLC-MS/MS analyses of low and high salt preparations of bovine mitochondrial ribosomes and their subunits. The calculated emPAI values for peptides obtained from purified 28S and 39S preparations suggest the association of AURKAIP1 with the small subunit, considering that the emPAI value for the 28S subunit is 30% higher than that of the 39S subunit (**Tables 1**, **2**, S1, S3).

PTCD3

We first reported PTCD3 as an mRNA-binding protein associated with the 28S subunit and as a possible PET309 homolog, due to the presence of pentatricopeptide repeats (Koc and Spremulli, 2003). The association of PTCD3 with the small subunit and its essential role in mitochondrial translation has also been reported (Davies et al., 2009). Our data not only confirms the association of PTCD3 with the small subunit, but also provides evidence that it is a *bona fide* ribosomal protein. This idea was recently reinforced by the observation that PTCD3 is one of the 28S subunit proteins that interacts with mitochondrial initiation factor 3 (Haque et al., 2011). The full-length bovine PTCD3 is 77.8 kDa with a pI of 6.0; it is possibly the largest protein, and one of the most

Table 3 | GenBank™ and Swiss-Prot accession numbers of new mitochondrial ribosomal proteins found in various species.

MRP	Protein	Human	Bovine	Mouse	Fly	Worm
MRPS37	CHCHD1	Q96BP2	Q2HJE8	XP_852408	ABJ16982	AAB88317
MRPS38	AURKAIP1	Q9NWT8	Q0VCJ1	XM_843641	Q8IML6	Y54G9A
MRPS39	PTCD3	Q96EY7	Q2KI62	XP_532975	A1Z9A8	AAF60413
MRPL58	ICT1	Q14197	Q3T116	XP_533118	CAL26738	AAL06045
MRPL59	CRIF1	Q8TAE8	A1A4P4	XP_533898	AAM29650	CAB03171

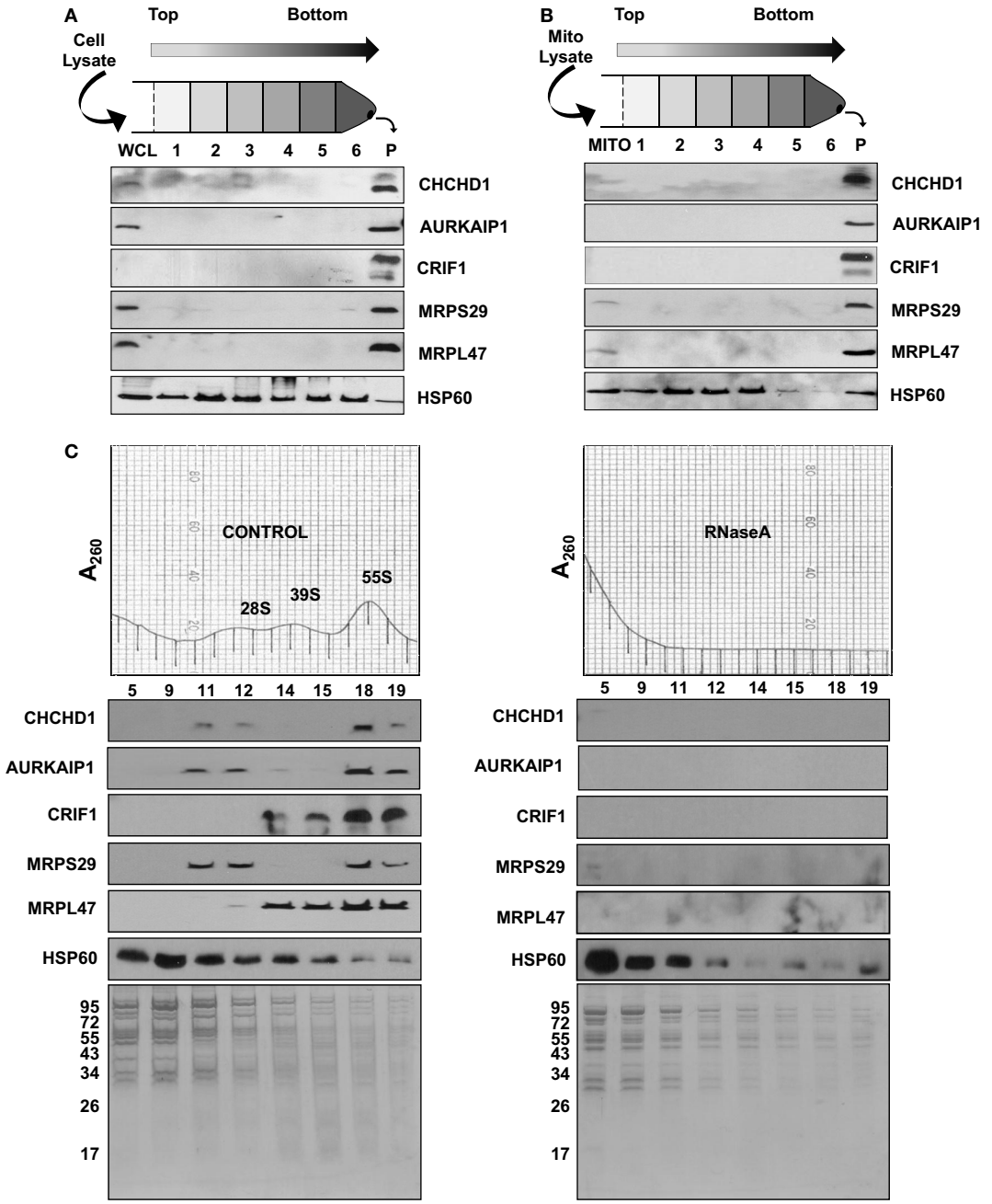

FIGURE 3 | Sedimentation of new MRPs with large complexes in human cell lines and mitochondria. (A) Whole cell lysate (WCL) and **(B)** mitochondrial lysate (MITO) obtained from human cell lines were layered on sucrose cushion preparations. After 16 h centrifugation, post-ribosomal supernatant layers (Layers 1 to 6) and the crude ribosome pellet (P) were collected and analyzed by immunoblotting probed with CHCHD1, AURKAIP1, CRIF1, MRPS29, MRPL47, and HSP60 antibodies. **(C)** To confirm the RNA-dependent association of new MRPs with mitochondrial ribosomes, the same amount of crude ribosomes, both Control and RNase A-treated, were sedimented on 10–30% sucrose gradients. Equal volumes of sucrose gradient fractions were separated on 12% SDS-PAGE. Sedimentation of new MRPs with ribosomal subunits and 55S ribosomes in the absence and presence of RNase A was analyzed by immunoblotting using CHCHD1, AURKAIP1, CRIF1, MRPS29, and MRPL47 antibodies. HSP60 immunoblotting and the Coomassie Blue stained gel are shown as controls for multimeric mitochondrial complexes sedimenting with the 55S ribosome in control and RNase A-treated gradients.

acidic components of the 55S ribosome. It is highly conserved among its animal mitochondrial homologs (Figure S2). PTCD3 is a larger protein and has a lower pI compared to the basic proteins of the mitochondrial ribosome, and nineteen unique peptides were detected in its capLC-MS/MS analyses (**Tables 1**, S3). In agreement with earlier observations, PTCD3 peptides were mainly detected in protein bands excised from 28S and 55S lanes (**Figure 2A** and Table S3). Its subunit localization is also

supported by the emPAI values shown in **Table 2**; specifically, the high experimental emPAI value for peptides identified in the 28S subunit sample, as well as in the 55S sample, indicates that PTCD3 is a ribosomal component associated with both the 28S subunit and 55S ribosomes (**Tables 2** and S3). The presence of a trace amount of PTCD3 in 39S preparations could be due to the presence of a small amount of 28S subunits in the large subunit fractions analyzed. This cross-contamination is common because there is a tendency for the 55S ribosome to dissociate somewhat during sucrose gradient centrifugation (Koc et al., 2001b). The high emPAI scores of the 28S subunit and 55S ribosomes enabled us to conclude that PTCD3 is a mitochondrial-specific MRP that is mainly associated with the 28S subunit.

ICT1

Our data confirm previous reports that ICT1 is a mitochondrial ribosomal protein. This protein belongs to the polypeptide release family of proteins, and it is the first example of an integral component of the large subunit providing peptidyl-tRNA hydrolase activity (Richter et al., 2010). ICT1 is essential for the hydrolysis of peptidyl-tRNAs on prematurely terminated mRNAs that lack a stop codon (Handa et al., 2010; Richter et al., 2010). It is a highly conserved protein among animals (Figure S2). Tryptic peptides detected by capLC-MS/MS analyses of protein bands are listed in **Tables 1** and S3. ICT1 peptides were detected in 28S, 39S, and 55S samples, which made the calculated emPAI values of the ICT1 in 28S and 39S subunits very close to each other (Table S3). The experimental emPAI scores were not sufficiently different to assign ICT1 to a particular subunit (**Table 2**). The human ICT1 was previously shown to be associated with the large subunit (Richter et al., 2010); however, our MS data do not clearly support association of ICT1 with the large subunit (**Table 2**). It is reasonable to suggest that ICT1 is located near the interface region of the large subunit, and that a fraction of ICT1 also sediments with the small subunit when the subunits are dissociated.

CRIF1

CR-6 interacting factor 1 (CRIF1), which is also known as growth arrest and DNA-damage-inducible proteins-interacting protein 1 (Gadd45GIP1), was identified as a transcriptional co-activator. The calculated molecular mass of the full-length bovine CRIF1 is 25.7 kDa. Its mitochondrial localization signal peptide is predicted to be in the first 28 amino acid residues, and it has a 90% possibility of mitochondrial localization (Figure S2). The calculated molecular mass for the mature CRIF1 is 22.9 kDa, and this value is in agreement with the migration of the protein in SDS-PAGE detected by capLC-MS/MS (**Figure 2A**). The emPAI values, calculated from five unique CRIF1 peptides detected in 39S and 55S samples, strongly suggest that the mitochondrial CRIF1 is a large subunit protein (**Tables 2** and S3).

SUBFRACTIONATION OF CHCHD1, AURKAIP1, AND CRIF1 WITH MITOCHONDRIAL RIBOSOMES

In the capLC-MS/MS analyses of highly purified bovine mitochondrial ribosomes and subunits presented above, we were able to assign the subunit in which the newly identified ribosomal proteins were present. Association of PTCD3 and ICT1 with the mitochondrial ribosome was reported in our earlier studies and by other groups (Koc and Spremulli, 2003; Richter et al., 2010). However, we are describing and characterizing CHCHD1, AURKAIP1, and CRIF1 as integral components of the mitochondrial ribosome for the first time. Ectopically expressed forms of CRIF1 and AURKAIP1 have been localized to the nucleus and cytosol and reported to be involved in the transcriptional activation and regulation of Aurora-A kinase in human cell lines, respectively (Kang et al., 2010). In order to evaluate their association with the mitochondrial ribosome, human whole cell and mitochondrial lysates were prepared under non-denaturing conditions and centrifuged through a 34% sucrose cushion, a step analogous to that used in the preparation of bovine liver mitochondrial ribosomes (**Figures 3A,B**). This process enriched the multimeric complexes resistant to high salt and non-ionic detergent treatments in the bottom layer and pellet, mainly as cytoplasmic 80S and mitochondrial 55S ribosomes. In immunoblotting analyses of post-ribosomal supernatant layers and crude ribosomal pellets obtained from the whole cell (**Figure 3A**) and mitochondrial lysates (**Figure 3B**), these MRPs were found mainly in the pellet along with two mitochondrial ribosomal proteins (MRPS29 and MRPL47), thus, confirming their co-localization with the mitochondrial ribosome or other large complexes in mitochondria.

Immunoblotting analyses and identification of these proteins in highly purified ribosomal subunits, 55S ribosomes (**Figure 2**), and crude ribosomes (**Figure 3B**) support their ribosome association; however, it is possible that these proteins could be associated with the large mitochondrial complexes that co-sediment with the ribosome but have nothing to do with mitochondrial translaiton. For example, we have observed that polypeptides of the oxoglutarate dehydrogenase complex can be detected in the 28S region of the gradient. To demonstrate that the proteins under study here are not simply co-sedimenting with the ribosome but are actually associated with the particle, RNase A-treatment of the 55S ribosome was carried out prior to loading the samples onto the sucrose gradients and immunoblotting analyses. RNase A-treatment destroys the integrity of the mitochondrial ribosome (**Figure 3C**), as it does other ribosomes, as indicated by the loss of the A_{260} from the 55S region of the sucrose gradient following nuclease treatment and the increase in the A_{260} near the top of the gradient. As shown in **Figure 3C**, the signals from the new MRPs overlapped with those from MRPS29 and MRPL47 in the control sucrose gradient fractions. When the ribosome sample was treated with RNase, signals from CHCHD1, AURKAIP1, and CRIF1 disappeared from the 55S region of the gradient as did the signals from the two control proteins, MRPS29 and MRPL47. This data indicates that these proteins are either assembled into the ribosome or strongly associated with the mitoribosome and are not simply co-fractioning with the 55S particles on the sucrose gradient. On the other hand, the HSP60 signal remained unchanged in these fractions, along with high molecular weight proteins which were subunits of the other multimeric complexes of mitochondria detected by Coomassie Blue stained SDS-PAGE (**Figure 3C**).

ROLE OF CHCHD1, AURKAIP1, AND CRIF1 IN MITOCHONDRIAL TRANSLATION

To investigate the role of newly identified MRPs in mitochondrial translation, we first transfected the HEK293 cells using control and specific siRNAs corresponding to CHCHD1, AURKAIP1, and CRIF1 mRNAs. The siRNA knock-down efficiency was determined by RT-PCR analyses using total RNA isolated from each cell line. In addition to the effect of siRNA knock-down on CHCHD1, AURKAIP1, and CRIF1 mRNA expression, we also determined the changes in expression of several nuclear encoded MRPs and mitochondrially encoded genes (**Figure 4A**). In specific siRNA knock-down cells, CHCHD1 and CRIF1 mRNA levels were reduced by 70% of the control siRNA knock-down cells, whereas the reduction in AURKAIP1 mRNA was about 85% (**Figure 4A**). Clearly, none of the nuclear encoded MRP mRNAs or the representative mitochondrially encoded mRNAs (ND6, COI, COII, ATP6, and 12S rRNA) were affected by the reduction in CHCHD1, AURKAIP1, or CRIF1 mRNAs (**Figure 4A**). Treatment with the specific siRNAs lead to the reduced expression (from 55 to 75%) of the corresponding CHCHD1, AURKAIP1, and CRIF1 proteins, as confirmed by immunoblotting analyses of whole cell lysates and ribosomes enriched from knock-down cell

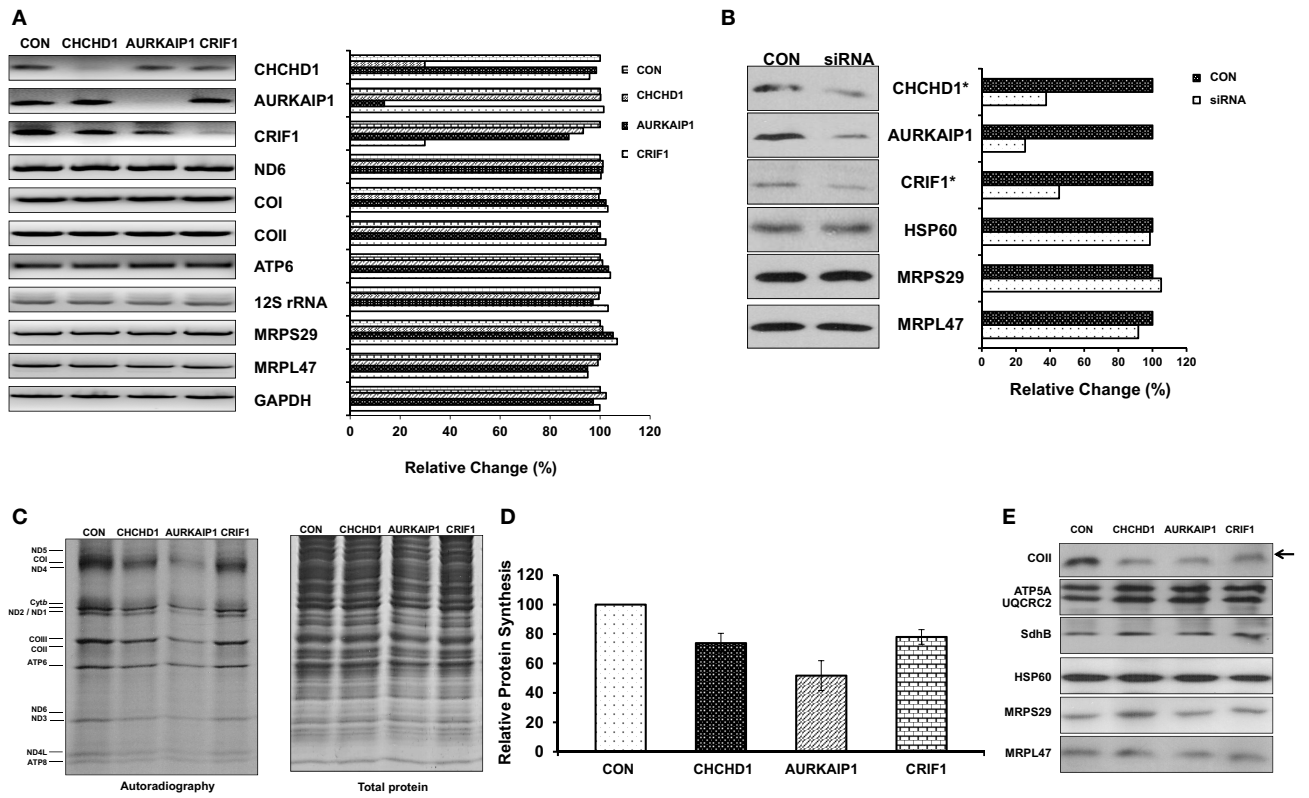

FIGURE 4 | Role of CHCHD1, AURKAIP1, and CRIF1 knock-down on mitochondrial protein synthesis. (A) Transcript levels of CHCHD1, AURKAIP1, and CRIF1 were shown as an indication of knock-down efficiency in cell lines transfected with control siRNA and siRNAs for corresponding new MRPs. Mitochondrial encoded ND6, COI, COII, ATP6, and 12S rRNA, and nuclear encoded MRPS29 and MRPL47 were examined by RT-PCR reactions in the same samples. RT-PCR reactions with GAPDH were performed as a positive control and relative quantitation of signal intensities was calculated based on GAPDH mRNA levels (or siRNA control cell line) in each knock-down cell line. **(B)** Expression levels of new MRPs in control siRNA and MRP-specific siRNA transfected HEK293T cell lysates and total crude ribosome fractions (*) were analyzed by immunoblotting using antibodies against AURKAIP1, CHCHD1, CRIF1, MRPS29, MRPL47, and HSP60. Immunoblotting analyses with HSP60, MRPS29, and MRPL47 antibodies were used as loading controls for total protein and total ribosome content using whole cell lysates obtained from control and AURKAIP1 siRNA knock-down cells. Similar results were obtained with immunoblotting analyses of total crude ribosome fractions from CHCHD1 and CRIF1 siRNA knock-down cell lines using HSP60, MRPS29, and MRPL47 antibodies (data not shown). **(C)** *De novo* synthesis of mitochondrial proteins was evaluated in control siRNA and the siRNA of corresponding MRPs transfected HEK293T cells by pulse labeling of proteins in the presence of [^{35}S]-methionine and a cytosolic translation inhibitor, emetine. A representative electrophoretic pattern of the *de novo* synthesized translational products is presented. ND1, −2, −3, −4, −4L, −5, and −6 are subunits of Complex I; Cyt*b* is a subunit of Complex III; COI, −II, and −III are subunits of Complex IV; ATP6 and ATP8 are subunits of Complex V. Coomassie blue staining of the same gel was performed to ensure equal protein loading in the gel. **(D)** The combined intensities of the 13 mitochondrially-encoded proteins from each lane were used as an overall quantitation of mitochondrial protein synthesis from three separate experiments. **(E)** Immunoblotting analysis of whole cell lysates prepared from control siRNA and MRP specific siRNA transfected HEK293T cells was performed to examine the steady state levels of the mitochondrial encoded subunit of Complex IV (COII) and nuclear encoded subunits of Complex V (ATP5A), III (UQCRC2), and II (SDHB). The arrow shows the reduced translation of mitochondrial encoded protein COII in cell lines transfected with CHCHD1, AURKAIP1, and CRIF1 specific siRNAs. The same PVDF was reprobed with MRPS29, MRPL47, and HSP60 antibodies to ensure equal loading.

lines using corresponding antibodies (**Figure 4B**). Since changes in the expression of the newly identified MRPs by siRNAs had no effect on the expression of mitochondrially encoded mRNAs and rRNAs, the newly identified proteins are not directly involved in transcription or RNA processing in mammalian mitochondria. Furthermore, the presence of normal amounts of the 12S rRNA indicates that there is no defect in the synthesis or assembly of the mitoribosome suggesting that CHCHD1, AURKAIP1, and CRIF1 are unlikely to be proteins involved in ribosome assembly.

Given the association of new MRPs with the mitochondrial ribosome, we next examined the role of CHCHD1, AURKAIP1, and CRIF1 knock-downs on the *de novo* synthesis of mitochondrially-encoded proteins by [^{35}S]-methionine labeling in the presence of the cytosolic protein synthesis inhibitor emetine. In this analysis, only the thirteen essential subunits of the OXPHOS complexes synthesized by the mitochondrial translational machinery were labeled by [^{35}S]-methionine (**Figure 4C**). In cells transfected with CHCHD1, AURKAIP1, and CRIF1 siRNAs, relative mitochondrial protein synthesis was decreased by 27, 48, and 22%, respectively, whereas the total protein content of the cell lysates was comparable (**Figures 4C,D**). Clearly, the inhibition of protein synthesis in knock-down cells was due to a reduction in expression of new MRPs, because reprobing the same membrane with MRPS29, MRPL47, and HSP60 antibodies displayed no significant difference in ribosomal or mitochondrial protein levels (**Figure 4E**). Although a considerable amount of new MRPs remained in siRNA knock-down cells (**Figure 4B**), the 22–48% reduction in overall mitochondrial translation is significant. In addition to the decrease in pulse labeling of mitochondrially encoded proteins, the steady state levels of the mitochondrially encoded subunit of Complex IV, COII, was also reduced in cells transfected with MRP-specific siRNAs, as detected by immunoblotting analysis (**Figure 4E**). On the other hand, the nuclear encoded subunits of oxidative phosphorylation complexes, such as Complex V subunit ATP5A, Complex III subunit Core II subunit (UQCRC2), and Complex II SDHB subunit, remained unchanged (**Figure 4E**). Altogether, these observations strongly suggest that CHCHD1, AURKAIP1, and CRIF1 all have essential roles in mitochondrial protein synthesis as components of the small and large subunits of the 55S ribosome.

NOMENCLATURE

The two-dimensional gel analysis of bovine mitochondrial ribosomes lead to the prediction of as many as 33 ribosomal proteins in the 28S subunit and 52 ribosomal proteins in the 39S subunit (Koc et al., 2001a,b). These proteins were designated S1 through S33 for the 28S subunit and L1 through L52 for the 39S subunit, in order of decreasing molecular weights (Pietromonaco et al., 1991). Later, we and several other groups identified 29 and 49 MRPs in the small and large subunits, respectively, using proteomic analyses (Goldschmidt-Reisin et al., 1998; Graack et al., 1999; Koc et al., 1999, 2001a,b; Suzuki et al., 2001; Yang et al., 2010). To provide consistency for designation of the same proteins in different organisms, we adopted a system of nomenclature in which proteins with prokaryotic homologues are given the same number as the corresponding ribosomal protein in *E. coli*. Proteins without bacterial homologs are given the next available number. Bacterial ribosomes have proteins designated S1 through S21 in the 28S subunit and L1 through L36 in the large subunit. Additionally, previously identified mammalian ribosomal proteins without bacterial homologs were designated S22 through S36 for the 28S subunit and L37 through L57 for the 39S subunit, including a new number for MRP63 (MRPL57), because its association with the 39S subunit was not previously known (**Table 4**) (Kenmochi et al., 2001). As a result, we proposed that the newly identified small subunit proteins (CHCHD1, AURKAIP1, and PTCD3) be named MRPS37, MRPS38, and MRPS39 and that ICT1 and CRIF1, as newly identified large subunit proteins, be designated as MRPL58 and MRPL59, respectively (**Table 4**). Here, the adaptation of the new MRP numbers is absolutely critical for their classification as mitochondrial ribosomal proteins and for further investigation of their roles in mitochondrial translation and biogenesis.

POTENTIAL ROLES OF NEW MITOCHONDRIAL RIBOSOMAL PROTEINS IN TRANSLATION

Ribosomal proteins have roles in ribosome assembly, substrate binding, and different stages of translation, such as initiation, elongation, and termination. Furthermore, they are likely to interact with the nascent chain and facilitate their insertion into the respiratory chain complexes in the mitochondrial inner membrane. The MRPs with bacterial homologs are expected to have conserved functions in ribosome structure and translation. For the mammalian mitochondrial-specific proteins without known homologs in other ribosomes, it is highly challenging to identify and assign whether a ribosome-associated protein is a genuine ribosomal protein or a factor transiently associated with the ribosome. In fact, a recent bioinformatics survey of the evolutionarily conserved ribosomal proteins failed to identify several additional components of the mammalian mitochondrial ribosome (Smits et al., 2007). The criteria used in this study, however, allowed us to characterize the newly identified proteins as mitochondrial-specific ribosomal proteins. One issue that arises in these studies is to assess whether a protein observed in the ribosome preparations is a *bona fide* ribosomal protein or represents a protein transiently associated with the ribosome. Several criteria can be applied in making this determination. First, the newly assigned protein must have a distribution that parallels that of known ribosomal proteins and changes in accordance with the distribution of ribosomal proteins as the subunits are associated or dissociated. The proteins should also be associated with the ribosomal particles when they are prepared under a variety of salt and detergent conditions. This criterion is met by the newly assigned proteins under study here. Second, the majority of the protein should be present in fractions containing the ribosome, and there should be little or no free pool of the protein. This criterion is met by the majority of the known MRPs, although there are exceptions, including MRPL12, which is known to have a free pool of protein that may interact with RNA polymerase. Examination of the distribution of the new MRPs classified here indicates that this criterion is also met. Proteins involved in processes such as ribosome assembly generally show a distribution in which only a portion of the total protein is found in the ribosome fraction. For

Table 4 | List of mammalian mitochondrial ribosomal proteins with their bacterial homologs.

28S proteins	30S proteins	New class	39S proteins	50S proteins	New class	50S proteins
Missing	S1	MRPS22	MRPL1	L1	MRPL33	L33
MRPS2	S2	MRPS23	MRPL2	L2	MRPL34	L34
MRPS24	S3	MRPS24	MRP-L3	L3	MRPL35	L35
Missing	S4	MRPS25	MRPL4	L4	MRPL36	L36
MRPS5	S5	MRPS26	Missing	L5	MRPL37	
MRPS6	S6	MRPS27	Missing	L6	MRPL38	
MRPS7	S7	MRPS28	MRPL12	L7/L12	MRPL39	
Missing	S8	MRPS29	MRPL9	L9	MRPL40	
MRPS9	S9	MRPS30	MRPL10	L10	MRPL41	
MRPS10	S10	MRPS31	MRPL11	L11	MRPL42	
MRPS11	S11	MRPS32 (MRPL42)	MRPL13	L13	MRPL43	
MRP-S12	S12	MRPS33	MRPL14	L14	MRPL44	
Missing	S13	MRPS34	MRPL15	L15	MRPL45	
MRPS14	S14	MRPS35	MRPL16	L16	MRPL46	
MRPS15	S15	MRPS36	MRPL17	L17	MRPL48	
MRPS16	S16	MRPS37 (CHCHD1)	MRPL18	L18	MRPL49	
MRPS17	S17	MRPS38 (AURKAIP1)	MRPL19	L19	MRPL50	
MRPS18-1	S18	MRPS39 (PTCD3)	MRPL20	L20	MRPL51	
MRPS18-2	S18		MRPL21	L21	MRPL52	
MRPS18-3	S18		MRPL22	L22	MRPL53	
Missing	S19		MRPL23	L23	MRPL54	
Missing	S20		MRPL24	L24	MRPL55	
MRPS21	S21		Missing	L25	MRPL56	
			MRPL27	L27	MRPL57 (RP_63)	
			MRPL28	L28	MRPL58 (ICT1)	
			MRPL47	L29	MRPL59 (CRIF1)	
			MRPL30	L30		
			Missing	L31		
			MRPL32	L32		

example, less than half of C7orf30, which is involved in the assembly of the large subunit, is observed associated with ribosomes (Rorbach et al., 2012). Similarly, a significant fraction of ERAL1 involved in the assembly of the small subunit is also observed in the non-ribosomal fraction of mitochondria (Dennerlein et al., 2010).

Third, the preparations studied should have few peptide signals from proteins that are known to be transiently associated with the ribosome. In our analysis, slight signals were detected from elongation factor Tu and C7orf30. However, no peptides were detected from many other proteins known to be associated with the ribosome, including elongation factor G, initiation factor 2, initiation factor 3, OXA1L, ObgH1, and Mtg1. Thus, the bulk of the evidence indicates that CHCHD1, CRIF1, and AURKAIPI are, indeed, ribosomal proteins.

With the newly identified MRPs, the number of mammalian mitochondrial ribosomal proteins is brought to 31 for the small subunit and is increased to 51 for the large subunit (Koc et al., 2000, 2001a,b; Suzuki et al., 2001; O'Brien et al., 2005) (**Table 4**). It is not feasible to assign specific roles for the majority of mitochondrial-specific proteins without structural information and their relative locations in the ribosome; however, many of them have been shown to be essential for mitochondrial protein synthesis and function. For instance, the yeast homologue of MRPS37 (CHCHD1), MRP10, was discovered to be indispensable for mitochondrial translation. A respiratory defect caused by a null mutant of *MRP10* was recovered by the reintroduction of the *MRP10* gene into a wild-type mitochondrial DNA background (Jin et al., 1997). Similarly, MRPS38 (AURKAIP1) is a possible homolog of yeast COX24p, which is involved in the processing and translation of COX I mRNA (Barros et al., 2006). However, we observed an overall reduction in the expression of all 13 mitochondrially encoded proteins in AURKAIP1 knockdown cell lines (**Figure 4C**), suggesting that this protein plays a general role in mitochondrial translation that is not limited to the synthesis of cytochrome oxidase. Further, no changes in the level of COI mRNA were observed in the AURKAIP1 knockdown cell line (**Figure 4A**). This observation clearly supports the fact that mammalian mitochondrial genes do not contain introns to be processed, unlike the mitochondrially encoded genes in yeast. MRPS37 and MRPS38 are ribosomal small subunit proteins that are clearly involved in translation; however, their specific roles in mammalian mitochondrial translation remain to be discovered.

The siRNA knock-down of MRPS39 (PTCD3) decreased the activities of Complex III and Complex IV, possibly by directly affecting mRNA binding to the mitochondrial ribosome, as shown in our cross-linking experiments (Haque et al., 2011). In fact, PTCD3 was identified as one of the mRNA-binding proteins and $IF3_{mt}$ interacting proteins located near the mRNA-binding path of the small subunit in crosslinking studies (Davies et al., 2009). Although the majority of the MRPs forming the platform of the mRNA-binding path in the 28S subunit are bacterial homologs (such as MRPS7, MRPS11, MRPS18, and MRPS21), the shoulder region and the mRNA-gate of the 28S subunit are mainly formed by mitochondrial-specific MRPs (Smits et al., 2007; Christian and Spremulli, 2011; Koc and Koc, 2012). Therefore, it is possible that MRPS39 is one of the proteins that forms the mRNA-binding path and interacts with the 5′-ends of mitochondrial mRNAs.

MRPL58 was initially identified as immature colon carcinoma transcript 1 (ICT1) because it was one of the transcripts differentially expressed in colorectal tumors that deviate from the normal maturation pathway in colon epithelium (Van Belzen et al., 1995, 1998). Later, it was discovered to be an unusual member of a release factor family involved in termination of mitochondrial translation, possessing a codon-independent peptidyl-tRNA hydrolase activity associated with the mitochondrial ribosome (Richter et al., 2010). It was also recently reported that MRPL58 is essential for cell viability, because its knock-down resulted in reduced cytochrome *c* oxidase activity and eventually lead to apoptotic cell death (Handa et al., 2010).

The other new large subunit protein, MRPL59 (CRIF1), has been identified as a transcription co-factor that controls the G1/S phase of the cell cycle (Chung et al., 2003). It also negatively regulates the stability of a transcription factor, nuclear respiratory factor 2, that stimulates the expression of many mitochondrial proteins and proteins involved in oxidative damage (Kang et al., 2010). The majority of these studies were performed using the protein tagged at its amino terminus as the ectopically expressed form of CRIF1; therefore, it is possible that the majority of the tagged CRIF1 did not get incorporated into the 55S ribosome, due to the masking of the mitochondrial targeting signal. This form of the expressed protein could subsequently be translocated into the nucleus. Another explanation could be that a very small fraction of CRIF1 is located in the nucleus to manifest its function as a transcription co-factor. However, when the tag is placed at protein's carboxy terminus, this protein is targeted to mitochondria (Chung et al., 2003). Recently, it has been reported to interact with mitochondrial ATAD3 and the ribosome, confirming its mitochondrial localization and assignment as a ribosomal large subunit protein (He et al., 2012; Kim et al., 2012). Endogenous levels of CRIF1 have been shown to be dramatically reduced in epithelial cell cancers in thyroid and breast tissue, in agreement with the possible mitochondrial dysfunction reported in many different cancer types. In this study, we provided very strong evidence for CRIF1 being a *bona fide* ribosomal protein and an essential component of the mitochondrial translation machinery.

Given that the mitochondrial translational machinery and its components are essential for the expression of OXPHOS subunits, studies related to the identification of new components of the translational machinery and their specific roles in translation have the utmost importance in understanding energy production by OXPHOS. A completed picture of the mitochondrial translation machinery will be important to assess mitochondrial dysfunction manifested not only in neurodegenerative diseases, aging, diabetes, and cancer, but also in acute and chronic cardiovascular diseases.

FUNDING SOURCES

This work was supported by the National Institutes of Health [R01GM32734 to Linda L. Spremulli, R01GM071034 to Emine C. Koc].

SUPPLEMENTARY MATERIAL

The Supplementary Material for this article can be found online at: http://www.frontiersin.org/Mitochondrial_Research/10.3389/fphys.2013.00183/abstract

REFERENCES

Agrawal, R. K., Sharma, M. R., Yassin, A., Lahiri, I., and Spremulli, L. L. (2011). *Structure and Function of Organaller Ribosomes as Revealed by Cryo-EM in Ribosomes: Structure, Functions and Dynamics*, eds M. Rodnina, W. Wintermeyer, and R. Green (New York, NY: Springer Wien), 83–96.

Barros, M. H., Myers, A. M., Van Driesche, S., and Tzagoloff, A. (2006). COX24 codes for a mitochondrial protein required for processing of the COX1 transcript. *J. Biol. Chem.* 281, 3743–3751. doi: 10.1074/jbc.M510778200

Bonnefoy, N., Bsat, N., and Fox, T. D. (2001). Mitochondrial Translation of Saccharomyces cerevisiae COX2 mRNA Is Controlled by the Nucleotide Sequence Specifying the Pre-Cox2p Leader Peptide. *Mol. Cell. Biol.* 21, 2359–2372. doi: 10.1128/MCB.21.7.2359-2372.2001

Carim, L., Sumoy, L., Nadal, M., Estivill, X., and Escarceller, M. (1999). Cloning, expression, and mapping of PDCD9, the human homolog of Gallus gallus pro-apoptotic protein p52. *Cytogenet. Cell Genet.* 87, 85–88. doi: 10.1159/000015397

Chintharlapalli, S. R., Jasti, M., Malladi, S., Parsa, K. V., Ballestero, R. P., and Gonzalez-Garcia, M. (2005). BMRP is a Bcl-2 binding protein that induces apoptosis. *J. Cell Biochem.* 94, 611–626. doi: 10.1002/jcb.20292

Chomyn, A. (1996). *In vivo* labeling and analysis of human mitochondrial translation products. *Methods Enzymol.* 264, 197–211. doi: 10.1016/S0076-6879(96)64020-8

Christian, B. E., and Spremulli, L. L. (2011). Mechanism of protein biosynthesis in mammalian mitochondria. *Biochim. Biophys. Acta* 1819, 1035–1054.

Chung, H. K., Yi, Y. W., Jung, N. C., Kim, D., Suh, J. M., Kim, H., et al. (2003). CR6-interacting factor 1 interacts with Gadd45 family proteins and modulates the cell cycle. *J. Biol. Chem.* 278, 28079–28088. doi: 10.1074/jbc.M212835200

Claros, M. G., and Vincens, P. (1996). Computational method to predict mitochondrially imported proteins and their targeting sequences. *Eur. J. Biochem.* 241, 770–786. doi: 10.1111/j.1432-1033.1996.00779.x

Davies, S. M., Rackham, O., Shearwood, A. M., Hamilton, K. L., Narsai, R., Whelan, J., et al. (2009). Pentatricopeptide repeat domain protein 3 associates with the mitochondrial small ribosomal subunit and regulates translation. *FEBS Lett.* 583, 1853–1858. doi: 10.1016/j.febslet.2009.04.048

De Vries, H., and Van Der Koogh-Schuuring, R. (1973). Physicochemical properties of isolated 55-S mitochondrial ribosomes from rat-liver. *Biochem. Biophys. Res. Comm.* 54, 308–314. doi: 10.1016/0006-291X(73)90924-8

Dennerlein, S., Rozanska, A., Wydro, M., Chrzanowska-Lightowlers, Z. M., and Lightowlers, R. N. (2010). Human ERAL1 is a mitochondrial RNA chaperone involved in the assembly of the 28S small mitochondrial ribosomal subunit. *Biochem. J.* 430, 551–558. doi: 10.1042/BJ20100757

Galmiche, L., Serre, V., Beinat, M., Assouline, Z., Lebre, A. S., Chretien, D., et al. (2011). Exome sequencing identifies MRPL3 mutation in mitochondrial cardiomyopathy. *Hum. Mutat*. 32, 1225–1231. doi: 10.1002/humu.21562

Goldschmidt-Reisin, S., Kitakawa, M., Herfurth, E., Wittmann-Liebold, B., Grohmann, L., and Graack, H.-R. (1998). Mammalian mitochondrial ribosomal proteins: N-terminal amino acid sequencing, characterization, and identification of corresponding gene sequences. *J. Biol. Chem*. 273, 34828–34836. doi: 10.1074/jbc.273.52.34828

Graack, H.-R., Bryant, M., and O'Brien, T. W. (1999). Identification of mammalian mitochondrial ribosomal proteins (MRPs) by N-terminal sequencing of purified bovine MRPs and comparison to data bank sequences: the large subribosomal particle. *Biochemistry* 38, 16569–16577. doi: 10.1021/bi991543s

Graack, H.-R., Grohman, L., Kitakawa, M., Schafer, K., and Kruft, V. (1992). YmL9, a nucleus-encoded mitochondrial ribosomal protein of yeast, is homologous to L3 ribosomal proteins from all natural kingdoms and photosynthetic organelles. *Eur. J. Biochem*. 206, 373–380. doi: 10.1111/j.1432-1033.1992.tb16937.x

Handa, Y., Hikawa, Y., Tochio, N., Kogure, H., Inoue, M., Koshiba, S., et al. (2010). Solution structure of the catalytic domain of the mitochondrial protein ICT1 that is essential for cell vitality. *J. Mol. Biol*. 404, 260–273. doi: 10.1016/j.jmb.2010.09.033

Haque, M. E., Koc, H., Cimen, H., Koc, E. C., and Spremulli, L. L. (2011). Contacts between mammalian mitochondrial translational initiation factor 3 and ribosomal proteins in the small subunit. *Biochim. Biophys. Acta* 1814, 1779–1784. doi: 10.1016/j.bbapap.2011.09.013

He, J., Cooper, H. M., Reyes, A., Di Re, M., Sembongi, H., Litwin, T. R., et al. (2012). Mitochondrial nucleoid interacting proteins support mitochondrial protein synthesis. *Nucleic Acids Res*. 40, 6109–6121. doi: 10.1093/nar/gks266

Ishihama, Y., Oda, Y., Tabata, T., Sato, T., Nagasu, T., Rappsilber, J., et al. (2005). Exponentially modified protein abundance index (emPAI) for estimation of absolute protein amount in proteomics by the number of sequenced peptides per protein. *Mol. Cell. Proteomics* 4, 1265–1272. doi: 10.1074/mcp.M500061-MCP200

Jacobs, H. T., and Turnbull, D. M. (2005). Nuclear genes and mitochondrial translation: a new class of genetic disease. *Trends Genet* 21, 312–314. doi: 10.1016/j.tig.2005.04.003

Jeffreys, A. J., and Craig, I. W. (1976). Analysis of proteins synthesized in mitochondria of cultured mammalian cells. An assessment of current approaches and problems in interpretation. *Eur. J. Biochem*. 68, 301–311. doi: 10.1111/j.1432-1033.1976.tb10789.x

Jin, C., Myers, A. M., and Tzagoloff, A. (1997). Cloning and characterization of MRP10, a yeast gene coding for a mitochondrial ribosomal protein. *Curr. Genet*. 31, 228–234. doi: 10.1007/s002940050199

Kang, H. J., Hong, Y. B., Kim, H. J., and Bae, I. (2010). CR6-interacting factor 1 (CRIF1) regulates NF-E2-related factor 2 (NRF2) protein stability by proteasome-mediated degradation. *J. Biol. Chem*. 285, 21258–21268. doi: 10.1074/jbc.M109.084590

Kenmochi, N., Suzuki, T., Uechi, T., Magoori, M., Kuniba, M., Higa, S., et al. (2001). The human mitochondrial ribosomal protein genes: mapping of 54 genes to the chromosomes and implications for human disorders. *Genomics* 77, 65–70. doi: 10.1006/geno.2001.6622

Kiat, L. S., Hui, K. M., and Gopalan, G. (2002). Aurora-A kinase interacting protein (AIP), a novel negative regulator of human Aurora-A kinase. *J. Biol. Chem*. 277, 45558–45565. doi: 10.1074/jbc.M206820200

Kim, S. J., Kwon, M. C., Ryu, M. J., Chung, H. K., Tadi, S., Kim, Y. K., et al. (2012). CRIF1 is essential for the synthesis and insertion of oxidative phosphorylation polypeptides in the mammalian mitochondrial membrane. *Cell Metab*. 16, 274–283. doi: 10.1016/j.cmet.2012.06.012

Koc, E. C., Blackburn, K., Burkhart, W., and Spremulli, L. L. (1999). Identification of a mammalian mitochondrial homolog of ribosomal protein S7. *Biochem. Biophys. Res. Comm*. 266, 141–146. doi: 10.1006/bbrc.1999.1785

Koc, E. C., Burkhart, W., Blackburn, K., Moseley, A., Koc, H., and Spremulli, L. L. (2000). A proteomics approach to the identification of mammalian mitochondrial small subunit ribosomal proteins. *J. Biol. Chem*. 275, 32585–32591. doi: 10.1074/jbc.M003596200

Koc, E. C., Burkhart, W., Blackburn, K., Moseley, A., and Spremulli, L. L. (2001a). The small subunit of the mammalian mitochondrial ribosome: Identification of the full complement of ribosomal proteins present. *J. Biol. Chem*. 276, 19363–19374.

Koc, E. C., Burkhart, W., Blackburn, K., Schlatzer, D. M., Moseley, A., and Spremulli, L. L. (2001b). The large subunit of the mammalian mitochondrial ribosome: Analysis of the complement of ribosomal protein present. *J. Biol. Chem*. 276, 43958–43969.

Koc, E. C., and Koc, H. (2012). Regulation of mammalian mitochondrial translation by post-translational modifications. *Biochim. Biophys. Acta* 1819, 1055–1066. doi: 10.1016/j.bbagrm.2012.03.003

Koc, E. C., and Spremulli, L. L. (2003). RNA-binding proteins of mammalian mitochondria. *Mitochondrion* 2, 277–291. doi: 10.1016/S1567-7249(03)00005-9

Leary, S. C., and Sasarman, F. (2009). Oxidative phosphorylation: synthesis of mitochondrially encoded proteins and assembly of individual structural subunits into functional holoenzyme complexes. *Methods Mol. Biol*. 554, 143–162. doi: 10.1007/978-1-59745-521-3_10

Levshenkova, E. V., Ukraintsev, K. E., Orlova, V. V., Alibaeva, R. A., Kovriga, I. E., Zhugdernamzhilyn, O., et al. (2004). The structure and specific features of the cDNA expression of the human gene MRPL37. *Bioorg. Khim*. 30, 499–506.

Lyng, H., Brovig, R. S., Svendsrud, D. H., Holm, R., Kaalhus, O., Knutstad, K., et al. (2006). Gene expressions and copy numbers associated with metastatic phenotypes of uterine cervical cancer. *BMC Genomics* 7:268. doi: 10.1186/1471-2164-7-268

Mariani, L., Beaudry, C., Mcdonough, W. S., Hoelzinger, D. B., Kaczmarek, E., Ponce, F., et al. (2001). Death-associated protein 3 (Dap-3) is overexpressed in invasive glioblastoma cells *in vivo* and in glioma cell lines with induced motility phenotype in vitro. *Clin. Cancer Res*. 7, 2480–2489.

Matthews, D. E., Hessler, R. A., Denslow, N. D., Edwards, J. S., and O'Brien, T. W. (1982). Protein composition of the bovine mitochondrial ribosome. *J. Biol. Chem*. 257, 8788–8794.

Miller, C., Saada, A., Shaul, N., Shabtai, N., Ben-Shalom, E., Shaag, A., et al. (2004). Defective mitochondrial translation caused by a ribosomal protein (MRPS16) mutation. *Ann. Neurol*. 56, 734–738.

Miller, J. L., Cimen, H., Koc, H., and Koc, E. C. (2009). Phosphorylated proteins of the mammalian mitochondrial ribosome: implications in protein synthesis. *J. Proteome Res*. 8, 4789–4798. doi: 10.1021/pr9004844

Miller, J. L., Koc, H., and Koc, E. C. (2008). Identification of phosphorylation sites in mammalian mitochondrial ribosomal protein DAP3. *Protein Sci*. 17, 251–260. doi: 10.1110/ps.073185608

O'Brien, T. W., Denslow, N. D., Faunce, W., Anders, J., Liu, J., and O'Brien, B. (1993). "Structure and function of mammalian mitochondrial ribosomes," in *The Translational Apparatus: Structure, Function Regulation and Evolution*, eds K. Nierhaus, F. Franceschi, A. Subramanian, V. Erdmann, and B. Wittmann-Liebold (New York, NY: Plenum Press), 575–586.

O'Brien, T. W., Fiesler, S., Denslow, N. D., Thiede, B., Wittmann-Liebold, B., Mouge, E., et al. (1999). Mammalian mitochondrial ribosomal proteins: amino acid sequences, characterization and identification of corresponding gene sequences. *J. Biol. Chem*. 274, 36043–36051. doi: 10.1074/jbc.274.51.36043

O'Brien, T., W., O'Brien, B., J., and Norman, R. A. (2005). Nuclear MRP genes and mitochondrial disease. *Gene* 354, 147–151. doi: 10.1016/j.gene.2005.03.026

Pel, H., and Grivell, L. (1994). Protein synthesis in mitochondria. *Mol. Biol. Rep*. 19, 183–194. doi: 10.1007/BF00986960

Pietromonaco, S., Denslow, N., and O'Brien, T. W. (1991). Proteins of mammalian mitochondrial ribosomes. *Biochimie* 73, 827–836. doi: 10.1016/0300-9084(91)90062-6

Richter, R., Rorbach, J., Smith, P. M., Wessels, H. J., Huynen, M. A., Smeitink, J. A., et al. (2010). A functional peptidyl-tRNA hydrolase, ICT1, has been recruited into the human mitochondrial ribosome. *EMBO J*. 29, 1116–1125. doi: 10.1038/emboj.2010.14

Rorbach, J., Gammage, P. A., and Minczuk, M. (2012). C7orf30 is necessary for biogenesis of the large subunit of the mitochondrial ribosome. *Nucleic Acids Res*. 40, 4097–4109. doi: 10.1093/nar/gkr1282

Rotig, A. (2011). Human diseases with impaired mitochondrial protein synthesis. *Biochim.*

Biophys. Acta 1807, 1198–1205. doi: 10.1016/j.bbabio.2011.06.010

Saada, A., Shaag, A., Arnon, S., Dolfin, T., Miller, C., Fuchs-Telem, D., et al. (2007). Antenatal mitochondrial disease caused by mitochondrial ribosomal protein (MRPS22) mutation. *J. Med. Genet*. 44, 784–786. doi: 10.1136/jmg.2007.053116

Sharma, M. R., Koc, E. C., Datta, P. P., Booth, T. M., Spremulli, L. L., and Agrawal, R. K. (2003). Structure of the mammalian mitochondrial ribosome reveals an expanded functional role for its component proteins. *Cell* 115, 97–108. doi: 10.1016/S0092-8674(03)00762-1

Smits, P., Saada, A., Wortmann, S. B., Heister, A. J., Brink, M., Pfundt, R., et al. (2011). Mutation in mitochondrial ribosomal protein MRPS22 leads to Cornelia de Lange-like phenotype, brain abnormalities and hypertrophic cardiomyopathy. *Eur. J. Hum. Genet.* 19, 394–399. doi: 10.1038/ejhg.2010.214

Smits, P., Smeitink, J. A., Van Den Heuvel, L. P., Huynen, M. A., and Ettema, T. J. (2007). Reconstructing the evolution of the mitochondrial ribosomal proteome. *Nucleic Acids Res*. 35, 4686–4703. doi: 10.1093/nar/gkm441

Soung, G. Y., Miller, J. L., Koc, H., and Koc, E. C. (2009). Comprehensive analysis of phosphorylated proteins of Escherichia coli ribosomes. *J. Proteome Res*. 8, 3390–3402. doi: 10.1021/pr900042e

Spremulli, L. L. (2007). Large-scale isolation of mitochondrial ribosomes from mammalian tissues. *Methods Mol. Biol*. 372, 265–275. doi: 10.1007/978-1-59745-365-3_19

Suzuki, T., Terasaki, M., Takemoto-Hori, C., Hanada, T., Ueda, T., Wada, A., et al. (2001). Structural Compensation for the deficit of rrna with proteins in the mammalian mitochondrial ribosome. Systematic analysis of protein components of the large ribosomal subunit from mammalian mitochondria. *J. Biol. Chem*. 276, 21724–21736.

Uhlen, M., Oksvold, P., Fagerberg, L., Lundberg, E., Jonasson, K., Forsberg, M., et al. (2010). Towards a knowledge-based Human Protein Atlas. *Nat Biotechnol*. 28, 1248–1250. doi: 10.1038/nbt1210-1248

Van Belzen, N., Diesveld, M. P., Van Der Made, A. C., Nozawa, Y., Dinjens, W. N., Vlietstra, R., et al. (1995). Identification of mRNAs that show modulated expression during colon carcinoma cell differentiation. *Eur. J. Biochem*. 234, 843–848. doi: 10.1111/j.1432-1033.1995.843_a.x

Van Belzen, N., Dinjens, W. N., Eussen, B. H., and Bosman, F. T. (1998). Expression of differentiation-related genes in colorectal cancer: possible implications for prognosis. *Histol. Histopathol*. 13, 1233–1242.

Yang, Y., Cimen, H., Han, M. J., Shi, T., Deng, J. H., Koc, H., et al. (2010). NAD^+-dependent deacetylase SIRT3 regulates mitochondrial protein synthesis by deacetylation of the ribosomal protein MRPL10. *J. Biol. Chem*. 285, 7417–7429. doi: 10.1074/jbc.M109.053421

Yoo, Y. A., Kim, M. J., Park, J. K., Chung, Y. M., Lee, J. H., Chi, S. G., et al. (2005). Mitochondrial ribosomal protein L41 suppresses cell growth in association with p53 and p27Kip1. *Mol. Cell. Biol*. 25, 6603–6616. doi: 10.1128/MCB.25.15.6603-6616.2005

Conflict of Interest Statement: The authors declare that the research was conducted in the absence of any commercial or financial relationships that could be construed as a potential conflict of interest.

Received: 28 February 2013; accepted: 26 June 2013; published online: 30 July 2013.

*Citation: Koc EC, Cimen H, Kumcuoglu B, Abu N, Akpinar G, Haque ME, Spremulli LL and Koc H (2013) Identification and characterization of CHCHD1, AURKAIP1, and CRIF1 as new members of the mammalian mitochondrial ribosome. Front. Physiol. **4**:183. doi: 10.3389/fphys.2013.00183*

This article was submitted to Frontiers in Mitochondrial Research, a specialty of Frontiers in Physiology.

frontiers in
PHYSIOLOGY

MINI REVIEW ARTICLE
published: 11 April 2013
doi: 10.3389/fphys.2013.00076

Mitochondrial permeability transition and cell death: the role of cyclophilin D

***Sabzali Javadov*[1]* and *Andrey Kuznetsov*[2]**

[1] *Department of Physiology, School of Medicine, University of Puerto Rico, San Juan, PR, USA*
[2] *Cardiac Surgery Research Laboratory, Department of Cardiac Surgery, Innsbruck Medical University, Innsbruck, Austria*

Edited by:
Fabio DiLisa, Universita di Padova, Italy

Reviewed by:
Samarjit Das, Johns Hopkins University, USA
Eric Fontaine, Joseph Fourier University, France

***Correspondence:**
Sabzali Javadov, Department of Physiology, School of Medicine, University of Puerto Rico, San Juan, PR 00936-5067, USA.
e-mail: sabzali.javadov@upr.edu

Mitochondria serve as a "powerhouse" which provides near 90% of ATP necessary for cell life. However, recent studies provide strong evidence that mitochondria also play a central role in cell death. Mitochondrial permeability transition (mPT) at high conductance in response to oxidative or other cellular stresses is accompanied by pathological and non-specific mPT pore (mPTP) opening in the inner membrane of mitochondria. Mitochondrial PTP can serve as a target to prevent cell death under pathological conditions such as cardiac and brain ischemia/reperfusion injury and diabetes. On the other hand, mPTP can be used as an executioner to specifically induce cell death thus blocking tumorigenesis in cancer diseases. Despite many studies, the molecular identity of the mPTP remains unclear. Cyclophilin D (CyP-D) plays an essential regulatory role in pore opening. This review will discuss direct and indirect mechanisms underlying CyP-D interaction with a target protein of the mPTP complex. Understanding of the mechanisms of mPTP opening will be helpful to further develop new pharmacological agents targeting mitochondria-mediated cell death.

Keywords: mitochondria, permeability transition pore, cyclophilin D, cell death

MITOCHONDRIAL PERMEABILITY TRANSITION AND CELL DEATH

Studies over the past 30 years demonstrated that, in addition to their role in cell life, mitochondria are the main executioners of cell death in response to oxidative stress. Accumulation of ROS along with Ca^{2+} overload induces is mitochondrial permeability transition (mPT) that is associated with non-selective pathological PT pore (mPTP) opening in the inner membrane of mitochondria (IMM). Opening of the mPTP is accompanied by loss of the mitochondrial membrane potential and proton gradient across the IMM. At low electrochemical potential, F_{0F1}-ATPase induces ATP hydrolysis in an attempt to maintain the mitochondrial membrane potential, and adenine nucleotide translocase (ANT) functions in a "reverse mode", transporting ATP to the matrix. Mitochondrial PT can occur at low and high conductance leading to reversible of irreversible consequences. Reversible mPTPs are permeable to ions and solutes with the molecular mass <300 Da, and do not induce notable matrix swelling (Brenner and Moulin, 2012). This mode may be important in regulation of mitochondrial Ca^{2+} homeostasis since mitochondrial Ca^{2+} efflux is inhibited by the immunosupressor cyclosporine A (CsA) in various cells including cardiomyocytes (Altschuld et al., 1992). Furthermore, the low-conductance mode can initiate mitochondrial depolarization spikes generating and conveying calcium signals (waves) from one mitochondrion to another (Ichas et al., 1997). In a high conductance mode, solutes, water, and ions with the molecular mass up to ∼1.5 kD enter through the mPTP thus enhancing colloid-osmotic pressure in the matrix. This causes rupture of the outer membrane of the mitochondria (OMM) leading to cell death via apoptosis and/or necrosis depending on the ATP level in cells. Opening of the mPTP is regulated by ions (P_i, H^+, Ca^{2+}, Mg^{2+}), ROS, adenine nucleotides, ubiquinones (Halestrap et al., 1998; Bernardi, 1999; Crompton, 1999), and many other factors.

CYCLOPHILIN D IS THE ONLY DEFINED mPTP COMPONENT

Although mPT induction has been broadly accepted as a well-known phenomenon the molecular identity of the mPTP still remains elusive. Initially three proteins, ANT in the IMM, voltage-dependent anion channel (VDAC or porin) in the OMM, and cyclophilin D (CyP-D) in the matrix were proposed as the main structural components of the mPTP. In addition, the benzodiazepine receptor, hexokinase, creatine kinase, Bcl2, phosphate carrier (PiC), and other proteins may play regulatory roles in pore opening (Weiss et al., 2003). Later, genetic studies conducted in knock-out mice demonstrated that mitochondria containing neither VDAC nor ANT were still susceptible to Ca^{2+}-induced mPTP induction therefore excluding the role of these proteins as the essential structural components of the mPTP (Kokoszka et al., 2004; Basso et al., 2005; Baines et al., 2007). However, mitochondria isolated from Cyp-$D^{-/-}$ mice were more resistant to mPTP opening than wild-type mice and exhibited mPT induction at higher [Ca^{2+}], and less cell death in response to oxidative stress (Baines et al., 2005; Nakagawa et al., 2005). In addition, mPTP-mediated cell death preferably occurred through necrosis rather than apoptosis as CyP-$D^{-/-}$ cells were resistant to necrotic stimuli but demonstrated similar sensitivity to apoptotic factors as wild-type cells (Nakagawa et al., 2005). It must be noted that although genetic studies revealed VDAC and ANT as the non-essential pore components, many questions related to the role of these proteins in mPT induction remain unresolved. Recently, PiC was identified as an essential component of the mPTP although

studies on PiC knock-out mice are still required to validate these data (Varanyuwatana and Halestrap, 2012). The presence of a large number of proteins in the IMM and the dynamic structure of the pore complex apparently make difficult to uncover its molecular identity. Here we will focus on CyP-D, which on the basis of multiple genetic and biochemical studies has been accepted as a key regulator and component of the pore opening. CyP-D belongs to cyclophilins known as peptidyl-prolyl cis–trans isomerases, a family of proteins that catalyze the *cis-trans* isomerization of peptydyl-prolyl bonds, and possess chaperone activity to regulate protein folding. There are seven major cyclophilin isoforms found in subcellular compartments including the cytoplasm (CyP-D, CyP-NK, CyP-40), endo(sarco)plasmic reticulum (CyP-B, CyP-C), nucleus (CyP-E), and mitochondria (CyP-D) (Lee and Kim, 2010). Notably, individual cyclophilins can have distinct effects on cell survival under pathological conditions. Studies performed on various cancer models and tissue samples from patients demonstrated that overexpression of CyP-A stimulates cancer cell growth (reviewed in Lee and Kim, 2010). On the other hand, expression of CyP-D, a soluble matrix protein, is associated with mPTP opening and cell death during ischemia/reperfusion in the heart and brain. CyP-D is a nuclear encoded protein widely expressed in all mammalian tissues. It contains a mitochondrial targeting presequence which is cleaved after its translocation into the matrix (Connern and Halestrap, 1992). Homozygous CyP-D knock-out mice exhibit normal phenotype (Basso et al., 2005; Nakagawa et al., 2005) although develop insulin resistance (Rieusset et al., 2012). In addition to its role in pore opening, CyP-D has been shown to catalyze folding of newly imported proteins in the matrix of mitochondria (Matouschek et al., 1995). Recent studies on human SH-SY5Y neuroblastoma cells demonstrated that CyP-D can also act as a redox sensor in mitochondria of mammalian cells (Linard et al., 2009), and regulate Ca^{2+} exchange between endoplasmic reticulum and mitochondria (Rieusset et al., 2012).

THE ROLE OF CyP-D IN PORE OPENING

The mechanisms of interaction of CyP-D with a target protein(s) in the IMM and the induction of conformational changes of the target protein to form the mPTP complex remain unrevealed. Importantly, the translocation of CyP-D from the matrix to the IMM and its interaction with a target protein to induce pore opening in response to oxidative stress can occur through both *direct* and *indirect* mechanisms (**Figure 1**). *Direct binding* of CyP-D to a target protein in the IMM can be triggered by activation of the latter in response to oxidative stress. Oxidative stress can induce conformational changes of the target protein by chemical modification and/or alterations in the inner membrane topography due to increased matrix swelling. Most, if not all, previous studies were focused on ANT as a target protein interacting with CyP-D to initiate the pore opening. Initial studies provided strong evidence that Ca^{2+}-triggered conformational change of the ANT is a key step in mPTP opening which is facilitated by CyP-D binding. GST-CyP-D pull-down and co-immunoprecipitation studies on isolated mitochondria revealed CsA-sensitive binding of CyP-D to ANT (Crompton et al., 1998; Woodfield et al., 1998). Also, oxidative stress sensitizes the mPTP to [Ca^{2+}] by antagonizing adenine nucleotide binding, and enhances CyP-D binding to the ANT (McStay et al., 2002). Chemical modifications of three cysteine residues (Cys56, Cys159, and Cys256) in ANT in response both to oxidative stress and thiol reagents were shown to be associated with a conformational change of the exchanger (Majima et al., 1993).

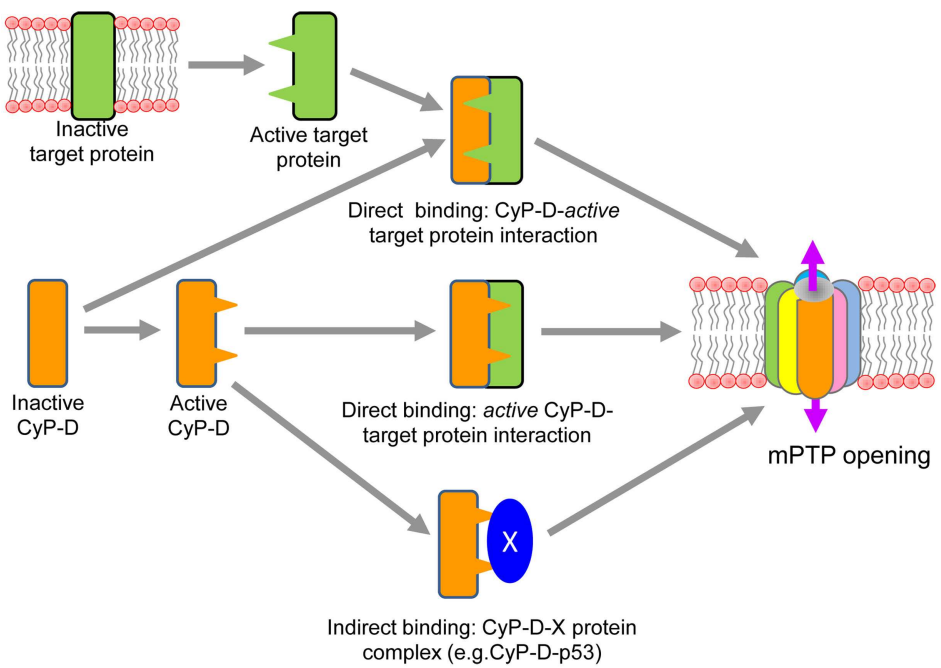

FIGURE 1 | Proposed direct and indirect mechanisms of CyP-D interaction with a target protein of the mPTP complex.

Two distinct thiol groups have been identified to participate in the modulation of mPTP activity (Costantini et al., 1996), and cysteine residues in the ANT may represent these thiol groups that regulate the binding affinity of the ANT for CyP-D and ADP (Halestrap et al., 1997). Consequently, oxidative stress or thiol reagents have been shown to induce cross-linking of two matrix facing cysteine residues (Cys56 and Cys159) of ANT that modulate mPTP activity through the CyP-D-ANT interaction (Halestrap and Brenner, 2003). Direct binding of CyP-D to a target protein in the IMM can also occur through activation of the former. In fact, Cys203 residue of Cyp-D has been shown to play a crucial role in oxidative stress induced activation of mPTP in mouse embryonic fibroblasts (Nguyen et al., 2011). CyP-D can be activated in the matrix due to post-translational modification, which may facilitate its translocation to the IMM and initiate mPT (**Figure 1**). Moreover, CyP-D can undergo post-transitional modifications (phosphorylation, nitrosylation, acetylation, etc.) on specific site(s) which would increase its activity to interact with a target protein. However, at present, there are rather few studies directly showing post-translational modifications of CyP-D. Recent studies also discovered that acetylation of CyP-D due to inhibition of the mitochondrial isoform of sirtuins, SIRT 3, a NAD^+ dependent deacetylase, increased interaction of CyP-D with ANT (Shulga and Pastorino, 2010). Furthermore, CyP-D acetylation was associated with reduced SIRT3 expression and increased pore opening in heart failure induced by transverse aortic constriction (Hafner et al., 2010) and myocardial infarction (Parodi-Rullan et al., 2012) in rodents. In addition, significant fraction of GSK-3beta has been shown to be co-localized with CyP-D in mitochondria, suggesting thus a potential regulatory role for GSK-3beta in pore opening. Active GSK is shown to phosphorylate CyP-D in an ERK1/2-dependent manner, and phospho-CyP-$D^{Ser/Thr}$ promoted depolarization of mitochondria and pore opening (Rasola et al., 2010). Conversely, pharmacological inhibition of GSK-3beta prevented the phosphorylation of CyP-D, which may lead to the inhibition of the mPT in murine tubular epithelial cells (Bao et al., 2012). Post-translational modification of CyP-D induced by nitrosylation may also be important in regulating of the mPTP. *In vitro* studies using proteins and cells revealed that both NO and $ONOO^-$ can affect ANT and increase mPT in a CsA-sensitive manner (Vieira et al., 2001), suggesting a key role of nitrosylation in the activation of pore opening. Nitric oxide can induce or inhibit the mPT depending on its concentration in the cell (Burwell and Brookes, 2008). Recent studies demonstrated that treatment of heart homogenates with GSNO resulted in S-nitrosylation of CyP-D on cysteine-203 (Kohr et al., 2011). Increased nitration of CyP-D as well as VDAC and ANT on tyrosine was found in mitochondria of neurons after cortical injury which was associated with elevated ROS production and cell death (Martin et al., 2011). However, it is not clear yet how nitrosylated CyP-D interacts with the target protein to induce mPT. Recent *in vitro* studies demonstrated that CyP-D association to the lateral stalk of F_{0F1}-ATP synthase modulates the activity of the complex, and the ATP synthase-CyP-D interactions were modulated by P_i and CsA, respectively, increasing and decreasing CyP-D binding to the enzyme (Giorgio et al., 2009). Interestingly, P_i was specifically required for PTP desensitization by CsA or by CyP-D ablation (Basso et al., 2008) as well as for inhibition of mPTP by blocking the complex I (Li et al., 2012).

Indirect binding of CyP-D to a target protein(s) in the IMM can occur through its interaction with other proteins in the matrix. Most recent studies demonstrated that in response to oxidative stress induced by brain ischemia/reperfusion injury p53, a tumor suppressor protein, accumulates in the mitochondrial matrix and triggers mPTP opening and necrosis by physical interaction with CyP-D (Vaseva et al., 2012). Conversely, reduction of p53 levels or treatment of mice with CsA prevented the p53-Cyp-D complex opening which was associated with effective stroke protection (Vaseva et al., 2012). Likely, p53 triggers translocation of CyP-D to the IMM and therefore facilitates the pore opening through interaction with a pore protein(s). However, the study demonstrated no regulation of calcium-dependent MPTP opening by p53. It is not clear how p53-CyP-D interaction senses and induces mPTP opening in a Ca^{2+}-independent manner (Karch and Molkentin, 2012). Notably, binding of CyP-D to a matrix protein in cancer cells may have an opposite effect, leading to inhibition of the mPTP. Also, it has been demonstrated that abundant expression of Hsp60 in mitochondria of tumor cells is associated with increased levels of the Hsp60-CyP-D complexes and reduced mPTP opening (Ghosh et al., 2010). Conversely, Hsp90 antagonists directed to mitochondria caused severe mitochondrial dysfunction and selective tumor cell death inhibiting the interaction of Hsp90 with CyP-D (Kang et al., 2007). Likewise, interaction of CyP-D with Bcl2 has been shown to exert an anti-apoptotic effect, and CsA, disrupted the CyP-D-Bcl2 interaction. The anti-apoptotic effect of CyP-D in some cancer cells which overexpress the protein can be explained by CyP-D-Bcl2 interaction to suppress apoptosis in these cells (Eliseev et al., 2009).

Thus, accumulating data suggest that activation of CyP-D and its interaction with the mPTP complex can occur through different mechanisms including (i) post-translational modification of the protein, (ii) direct interaction with an active target protein, and/or (iii) indirectly via binding to a matrix protein.

CONCLUSION

Irreversible mPTP opening acts as a target and executioner of cell death under pathological conditions such as cardiac and brain ischemia/reperfusion, diabetes, and cancer. Although mPT is a well-known phenomenon, the molecular identity of the mPTP complex is still unidentified. Existing studies provide strong evidence that CyP-D plays a regulatory role in mPT, and understanding the mechanism(s) of CyP-D activation and its interaction with the mPTP complex is important in developing new pharmacological agents to modulate mitochondria-mediated cell death.

ACKNOWLEDGMENTS

This study was supported by the National Heart, Lung, And Blood Institute of the National Institutes of Health through Research Grant SC1HL118669 (Sabzali Javadov) and by a research grant from the Austrian Science Fund (FWF): [P 22080-B20] (Andrey Kuznetsov).

REFERENCES

Altschuld, R. A., Hohl, C. M., Castillo, L. C., Garleb, A. A., Starling, R. C., and Brierley, G. P. (1992). Cyclosporin inhibits mitochondrial calcium efflux in isolated adult rat ventricular cardiomyocytes. *Am. J. Physiol.* 262, H1699–H1704.

Baines, C. P., Kaiser, R. A., Purcell, N. H., Blair, N. S., Osinska, H., Hambleton, M. A., et al. (2005). Loss of cyclophilin D reveals a critical role for mitochondrial permeability transition in cell death. *Nature* 434, 658–662.

Baines, C. P., Kaiser, R. A., Sheiko, T., Craigen, W. J., and Molkentin, J. D. (2007). Voltage-dependent anion channels are dispensable for mitochondrial-dependent cell death. *Nat. Cell Biol.* 9, 550–555.

Bao, H., Ge, Y., Zhuang, S., Dworkin, L. D., Liu, Z., and Gong, R. (2012). Inhibition of glycogen synthase kinase-3beta prevents NSAID-induced acute kidney injury. *Kidney Int.* 81, 662–673.

Basso, E., Fante, L., Fowlkes, J., Petronilli, V., Forte, M. A., and Bernardi, P. (2005). Properties of the permeability transition pore in mitochondria devoid of Cyclophilin D. *J. Biol. Chem.* 280, 18558–18561.

Basso, E., Petronilli, V., Forte, M. A., and Bernardi, P. (2008). Phosphate is essential for inhibition of the mitochondrial permeability transition pore by cyclosporin A and by cyclophilin D ablation. *J. Biol. Chem.* 283, 26307–26311.

Bernardi, P. (1999). Mitochondrial transport of cations: channels, exchangers, and permeability transition. *Physiol. Rev.* 79, 1127–1155.

Brenner, C., and Moulin, M. (2012). Physiological roles of the permeability transition pore. *Circ. Res.* 111, 1237–1247.

Burwell, L. S., and Brookes, P. S. (2008). Mitochondria as a target for the cardioprotective effects of nitric oxide in ischemia-reperfusion injury. *Antioxid. Redox Signal.* 10, 579–599.

Connern, C. P., and Halestrap, A. P. (1992). Purification and N-terminal sequencing of peptidyl-prolyl cis-trans-isomerase from rat liver mitochondrial matrix reveals the existence of a distinct mitochondrial cyclophilin. *Biochem. J.* 284(Pt 2), 381–385.

Costantini, P., Chernyak, B. V., Petronilli, V., and Bernardi, P. (1996). Modulation of the mitochondrial permeability transition pore by pyridine nucleotides and dithiol oxidation at two separate sites. *J. Biol. Chem.* 271, 6746–6751.

Crompton, M. (1999). The mitochondrial permeability transition pore and its role in cell death. *Biochem. J.* 341(Pt 2), 233–249.

Crompton, M., Virji, S., and Ward, J. M. (1998). Cyclophilin-D binds strongly to complexes of the voltage-dependent anion channel and the adenine nucleotide translocase to form the permeability transition pore. *Eur. J. Biochem.* 258, 729–735.

Eliseev, R. A., Malecki, J., Lester, T., Zhang, Y., Humphrey, J., and Gunter, T. E. (2009). Cyclophilin D interacts with Bcl2 and exerts an anti-apoptotic effect. *J. Biol. Chem.* 284, 9692–9699.

Ghosh, J. C., Siegelin, M. D., Dohi, T., and Altieri, D. C. (2010). Heat shock protein 60 regulation of the mitochondrial permeability transition pore in tumor cells. *Cancer Res.* 70, 8988–8993.

Giorgio, V., Bisetto, E., Soriano, M. E., Dabbeni-Sala, F., Basso, E., Petronilli, V., et al. (2009). Cyclophilin D modulates mitochondrial F_{0F1}-ATP synthase by interacting with the lateral stalk of the complex. *J. Biol. Chem.* 284, 33982–33988.

Hafner, A. V., Dai, J., Gomes, A. P., Xiao, C. Y., Palmeira, C. M., Rosenzweig, A., et al. (2010). Regulation of the mPTP by SIRT3-mediated deacetylation of CypD at lysine 166 suppresses age-related cardiac hypertrophy. *Aging (Albany NY)* 2, 914–923.

Halestrap, A. P., and Brenner, C. (2003). The adenine nucleotide translocase: a central component of the mitochondrial permeability transition pore and key player in cell death. *Curr. Med. Chem.* 10, 1507–1525.

Halestrap, A. P., Kerr, P. M., Javadov, S., and Woodfield, K. Y. (1998). Elucidating the molecular mechanism of the permeability transition pore and its role in reperfusion injury of the heart. *Biochim. Biophys. Acta* 1366, 79–94.

Halestrap, A. P., Woodfield, K. Y., and Connern, C. P. (1997). Oxidative stress, thiol reagents, and membrane potential modulate the mitochondrial permeability transition by affecting nucleotide binding to the adenine nucleotide translocase. *J. Biol. Chem.* 272, 3346–3354.

Ichas, F., Jouaville, L. S., and Mazat, J. P. (1997). Mitochondria are excitable organelles capable of generating and conveying electrical and calcium signals. *Cell* 89, 1145–1153.

Kang, B. H., Plescia, J., Dohi, T., Rosa, J., Doxsey, S. J., and Altieri, D. C. (2007). Regulation of tumor cell mitochondrial homeostasis by an organelle-specific Hsp90 chaperone network. *Cell* 131, 257–270.

Karch, J., and Molkentin, J. D. (2012). Is p53 the long-sought molecular trigger for cyclophilin D-regulated mitochondrial permeability transition pore formation and necrosis? *Circ. Res.* 111, 1258–1260.

Kohr, M. J., Aponte, A. M., Sun, J., Wang, G., Murphy, E., Gucek, M., et al. (2011). Characterization of potential *S*-nitrosylation sites in the myocardium. *Am. J. Physiol. Heart Circ. Physiol.* 300, H1327–1335.

Kokoszka, J. E., Waymire, K. G., Levy, S. E., Sligh, J. E., Cai, J., Jones, D. P., et al. (2004). The ADP/ATP translocator is not essential for the mitochondrial permeability transition pore. *Nature* 427, 461–465.

Lee, J., and Kim, S. S. (2010). An overview of cyclophilins in human cancers. *J. Int. Med. Res.* 38, 1561–1574.

Li, B., Chauvin, C., De Paulis, D., De Oliveira, F., Gharib, A., Vial, G., et al. (2012). Inhibition of complex I regulates the mitochondrial permeability transition through a phosphate-sensitive inhibitory site masked by cyclophilin D. *Biochim. Biophys. Acta* 1817, 1628–1634.

Linard, D., Kandlbinder, A., Degand, H., Morsomme, P., Dietz, K. J., and Knoops, B. (2009). Redox characterization of human cyclophilin D: identification of a new mammalian mitochondrial redox sensor? *Arch. Biochem. Biophys.* 491, 39–45.

Majima, E., Koike, H., Hong, Y. M., Shinohara, Y., and Terada, H. (1993). Characterization of cysteine residues of mitochondrial ADP/ATP carrier with the SH-reagents eosin 5-maleimide and N-ethylmaleimide. *J. Biol. Chem.* 268, 22181–22187.

Martin, L. J., Adams, N. A., Pan, Y., Price, A., and Wong, M. (2011). The mitochondrial permeability transition pore regulates nitric oxide-mediated apoptosis of neurons induced by target deprivation. *J. Neurosci.* 31, 359–370.

Matouschek, A., Rospert, S., Schmid, K., Glick, B. S., and Schatz, G. (1995). Cyclophilin catalyzes protein folding in yeast mitochondria. *Proc. Natl. Acad. Sci. U.S.A.* 92, 6319–6323.

McStay, G. P., Clarke, S. J., and Halestrap, A. P. (2002). Role of critical thiol groups on the matrix surface of the adenine nucleotide translocase in the mechanism of the mitochondrial permeability transition pore. *Biochem. J.* 367, 541–548.

Nakagawa, T., Shimizu, S., Watanabe, T., Yamaguchi, O., Otsu, K., Yamagata, H., et al. (2005). Cyclophilin D-dependent mitochondrial permeability transition regulates some necrotic but not apoptotic cell death. *Nature* 434, 652–658.

Nguyen, T. T., Stevens, M. V., Kohr, M., Steenbergen, C., Sack, M. N., and Murphy, E. (2011). Cysteine 203 of cyclophilin D is critical for cyclophilin D activation of the mitochondrial permeability transition pore. *J. Biol. Chem.* 286, 40184–40192.

Parodi-Rullan, R., Barreto-Torres, G., Ruiz, L., Casasnovas, J., and Javadov, S. (2012). Direct renin inhibition exerts an anti-hypertrophic effect associated with improved mitochondrial function in post-infarction heart failure in diabetic rats. *Cell. Physiol. Biochem.* 29, 841–850.

Rasola, A., Sciacovelli, M., Chiara, F., Pantic, B., Brusilow, W. S., and Bernardi, P. (2010). Activation of mitochondrial ERK protects cancer cells from death through inhibition of the permeability transition. *Proc. Natl. Acad. Sci. U.S.A.* 107, 726–731.

Rieusset, J., Fauconnier, J., Paillard, M., Belaidi, E., Tubbs, E., Chauvin, M. A., et al. (2012). Disruption of cyclophilin D-mediated calcium transfer from the ER to mitochondria contributes to hepatic ER stress and insulin resistance. *Hepatology.* doi:10.1002/hep.26189. [Epub ahead of print].

Shulga, N., and Pastorino, J. G. (2010). Ethanol sensitizes mitochondria to the permeability transition by inhibiting deacetylation of cyclophilin-D mediated by sirtuin-3. *J. Cell. Sci.* 123, 4117–4127.

Varanyuwatana, P., and Halestrap, A. P. (2012). The roles of phosphate and the phosphate carrier in the mitochondrial permeability transition pore. *Mitochondrion* 12, 120–125.

Vaseva, A. V., Marchenko, N. D., Ji, K., Tsirka, S. E., Holzmann, S., and Moll, U. M. (2012). p53 opens the mitochondrial permeability transition pore to trigger necrosis. *Cell* 149, 1536–1548.

Vieira, H. L., Belzacq, A. S., Haouzi, D., Bernassola, F., Cohen, I., Jacotot, E., et al. (2001). The adenine nucleotide translocator: a target of nitric oxide, peroxynitrite, and 4-hydroxynonenal. *Oncogene* 20, 4305–4316.

Weiss, J. N., Korge, P., Honda, H. M., and Ping, P. (2003). Role of the mitochondrial permeability transition in myocardial disease. *Circ. Res.* 93, 292–301.

Woodfield, K., Ruck, A., Brdiczka, D., and Halestrap, A. P. (1998). Direct demonstration of a specific interaction between cyclophilin-D and the adenine nucleotide translocase confirms their role in the mitochondrial permeability transition. *Biochem. J.* 336(Pt 2), 287–290.

Conflict of Interest Statement: The authors declare that the research was conducted in the absence of any commercial or financial relationships that could be construed as a potential conflict of interest.

Received: 25 January 2013; accepted: 21 March 2013; published online: 11 April 2013.

*Citation: Javadov S and Kuznetsov A (2013) Mitochondrial permeability transition and cell death: the role of cyclophilin D. Front. Physiol. **4**:76. doi: 10.3389/fphys.2013.00076*

This article was submitted to Frontiers in Mitochondrial Research, a specialty of Frontiers in Physiology.

frontiers in PHYSIOLOGY

ORIGINAL RESEARCH ARTICLE
published: 16 May 2013
doi: 10.3389/fphys.2013.00112

nNOS(+) striatal neurons, a subpopulation spared in Huntington's Disease, possess functional NMDA receptors but fail to generate mitochondrial ROS in response to an excitotoxic challenge

Lorella M. T. Canzoniero[1], Alberto Granzotto[2], Dorothy M. Turetsky[3], Dennis W. Choi[4], Laura L. Dugan[5,6] and Stefano L. Sensi[2,7,8]*

[1] Department of Biological and Environmental Science, University of Sannio, Benevento, Italy
[2] Molecular Neurology Unit, Center of Excellence on Aging, University "G. d'Annunzio", Chieti, Italy
[3] Department of Biochemistry and Microbiology, Oklahoma State University, Tulsa, OK, USA
[4] Department of Neurology, Stony Brook University, Stony Brook, NY, USA
[5] Department of Medicine, University of California San Diego, San Diego, CA, USA
[6] Department of Neuroscience, University of California San Diego, San Diego, CA, USA
[7] Department of Neuroscience and Imaging, University "G. d'Annunzio", Chieti, Italy
[8] Departments of Neurology and Pharmacology, Institute for Memory Impairments and Neurological Disorders, University of California Irvine, Irvine, CA, USA

Edited by:
Andrey V. Kuznetsov, Innsbruck Medical University, Austria

Reviewed by:
Fadi G. Akar, Mount Sinai School of Medicine, USA
Junhui Sun, National Heart Lung and Blood Institute/National Institutes of Health, USA

***Correspondence:**
Stefano L. Sensi, Molecular Neurology Unit, Center of Excellence on Aging, University "G. d'Annunzio", Chieti, Italy, Via dei Vestini, 31, Chieti, 66100, Italy.
e-mail: ssensi@uci.edu

Huntington's disease (HD) is a neurodegenerative condition characterized by severe neuronal loss in the cortex and striatum that leads to motor and behavioral deficits. Excitotoxicity is thought to be involved in HD and several studies have indicated that NMDA receptor (NMDAR) overactivation can play a role in the selective neuronal loss found in HD. Interestingly, a small subset of striatal neurons (less than 1% of the overall population) is found to be spared in post-mortem HD brains. These neurons are medium-sized aspiny interneurons that highly express the neuronal isoform of nitric oxide synthase (nNOS). Intriguingly, neurons expressing large amounts of nNOS [hereafter indicated as nNOS(+) neurons] show reduced vulnerability to NMDAR-mediated excitotoxicity. Mechanisms underlying this reduced vulnerability are still largely unknown and may shed some light on pathogenic mechanisms involved in HD. One untested possibility is that nNOS(+) neurons possess fewer or less functioning NMDARs. Employing single cell calcium imaging we challenged this hypothesis and found that cultured striatal nNOS(+) neurons show NMDAR-evoked responses that are identical to the ones observed in the overall population of neurons that express lower levels of nNOS [nNOS(−) neurons]. NMDAR-dependent deregulation of intraneuronal Ca^{2+} is known to generate high levels of reactive oxygen species of mitochondrial origin (mt-ROS), a crucial step in the excitotoxic cascade. With confocal imaging and dihydrorhodamine (DHR; a ROS-sensitive probe) we compared mt-ROS levels generated by NMDAR activation in nNOS(+) and (−) cultured striatal neurons. DHR experiments revealed that nNOS(+) neurons failed to produce significant amounts of mt-ROS in response to NMDA exposure, thereby providing a potential mechanism for their reduced vulnerability to excitotoxicity and decreased vulnerability in HD.

Keywords: NADPH diaphorase, excitotoxicity, reactive oxygen species, nitric oxide synthase, Huntington's disease

INTRODUCTION

Excitotoxicity is a major pathogenic component of several neurodegenerative disorders, including Alzheimer's disease, Parkinson's disease, amyotrophic lateral sclerosis, and Huntington's disease (HD) (Choi, 2005; Lau and Tymianski, 2010; Spalloni et al., 2013). HD is an autosomal dominant neurodegenerative condition characterized by severe behavioral, cognitive, and movement disorders (Ross and Tabrizi, 2011). Inheritance of the huntingtin (Htt) protein showing a pathogenic expansion of a glutamine stretch (polyQ repeats >35) (Macdonald et al., 1993) leads to massive cortical and striatal neuronal loss (Halliday et al., 1998; Cattaneo et al., 2005; Guo et al., 2012). Reasons for this sub-regional selectivity of the neurodegenerative process are not completely understood, although several mechanisms have been proposed. In that respect, evidence indicates that polyQ Htt promotes HD pathology through deregulation of vesicle trafficking (Difiglia et al., 1995; Qin et al., 2004), alteration of BDNF transport (Gauthier et al., 2004), disruption of microtubules (Trushina et al., 2003), interference with NMDA receptor (NMDAR) and synaptic activity (Zeron et al., 2004) as well as disruption of mitochondrial functioning and morphology (Rockabrand et al., 2007; Costa and Scorrano, 2012).

Excitotoxicity is a phenomenon driven by excessive synaptic accumulation of glutamate and associated with dysregulation of intraneuronal Ca^{2+} ($[Ca^{2+}]_i$) homeostasis (Choi, 2005). A major feature of excitotoxicity is the NMDAR/Ca^{2+}-dependent enhanced generation of nitric oxide (NO) and other reactive oxygen species (ROS) [reviewed in Forder and Tymianski (2009) and Szydlowska and Tymianski (2010)].

A subpopulation of striatal neurons (accounting for less than 1% of the overall population) expresses high levels of the enzyme nicotinamide adenine dinucleotide phosphate-diaphorase (NADPH-d) that is the neuronal isoform of nitric oxide synthase (nNOS) (Hope et al., 1991). Intriguingly, these neurons expressing large amount of nNOS [hereafter called nNOS(+) neurons] are not affected by NMDAR-dependent toxicity and spared in the striatum of HD patients (Ferrante et al., 1985; Koh et al., 1986; Koh and Choi, 1988). The molecular and biochemical determinants of this decreased vulnerability are still not completely known. A possible simple explanation for the phenomenon is that nNOS(+) neurons have fewer or less active NMDARs. To test this hypothesis, we employed single cell Ca^{2+} imaging and assessed differences in NMDAR-evoked rises in $[Ca^{2+}]_i$ in striatal cultures, and compared responses obtained in nNOS(+) and the overall population of striatal neurons that express lower levels of the enzyme and hereafter called nNOS(−) neurons.

Mitochondrial function is critical to maintaining $[Ca^{2+}]_i$ homeostasis (Pizzo et al., 2012). Mutant Htt promotes mitochondrial dysfunction and we have previously shown that specific Htt domains are crucial to drive its mitochondrial localization and promote dysfunction (Rockabrand et al., 2007).

Ca^{2+} overload in mitochondria promotes generation of free radicals in the organelles (Dugan et al., 1995; Reynolds and Hastings, 1995), a step that has been shown to be instrumental in the initiation of the excitotoxic cascade (White and Reynolds, 1995, 1996; Nicholls and Budd, 1998; Stout et al., 1998; Nicholls and Budd, 2000; Nicholls and Ward, 2000; Votyakova and Reynolds, 2001; Nicholls, 2002, 2004; Nicholls et al., 2003, 2007; Rintoul et al., 2003; Reynolds et al., 2004; Vesce et al., 2004; Votyakova and Reynolds, 2005). Thus, we also tested whether exposure to NMDA in striatal cultures generated different levels of mitochondrial ROS (mt-ROS) in nNOS(+) neurons compared to the overall population of nNOS(−) cells.

MATERIALS AND METHODS

CHEMICALS

Tissue culture media and sera were purchased from GIBCO (Life Technologies). Fluorescent calcium (fura-2 AM, and fluo-4FF AM) and ROS (dihydrorhodamine, DHR) indicators were purchased from Molecular Probes (Life Technologies). All other chemicals, unless otherwise specified, were purchased from Sigma-Aldrich.

NEURONAL STRIATAL CULTURES

All the procedures involving animals were approved by the institutional Ethics Committee (Ce.S.I.) and performed accordingly to institutional guidelines and in compliance with national and international laws and policies.

Striatal cell cultures were prepared from fetal (E15 or E16) Swiss–Webster or CD1 mice. Striatal tissues were dissected in ice-cold dissecting medium and then placed in trypsin (0.25%) for 10 min at 37°C. Tissues were centrifuged, supernatant discarded, and pellet mechanically dissociated with a glass Pasteur pipette. Cells were then resuspended in plating medium containing either: (for mixed cultures) Eagle's Minimal Essential Medium (with 20 mM glucose, 26.2 mM $NaHCO_3$) supplemented with L-glutamine (2 mM), 5% fetal calf serum, and 5% horse serum (Hyclone), or (for near-pure neuronal cultures) Neurobasal Medium supplemented with L-Glutamine (0.5 mM), 5% fetal bovine serum, 5% horse serum, 1× B27, and 0.2% penicillin/streptomycin.

To prepare mixed cultures, cell suspensions were diluted and plated onto an astrocytes layer on 35 mm culture dishes with a glass bottom (Mat-Tek). Cells were fed twice a week with a growth medium (containing 10% horse serum, and 2 mM L-glutamine) and after 12 days *in vitro* (DIV) with a serum-free medium supplemented with 2 mM L-glutamine.

For near-pure neuronal cultures, cells suspensions were diluted and plated onto laminin/poly-DL-lysine coated glass coverslips. Three days after plating, non-neuronal cell growth was inhibited by adding 10 μM of cytosine arabinofuranoside. Twice a week, 25% of the medium was replaced with equal amounts of fresh Neurobasal medium.

Striatal neurons were used between 12 to 17 DIV.

IMAGING STUDIES

Ca^{2+} imaging employing fura-2 was performed using a Nikon Diaphot inverted microscope equipped with a Xenon lamp, a 40× Nikon epifluorescence oil immersion objective (N.A.: 1.3), and a CCD camera (Quantex). Fluo-4FF experiments were instead performed using a Nikon Eclipse TE300 inverted microscope equipped with a Xenon lamp, a 40× Nikon epifluorescence oil immersion objective (N.A.: 1.3) and a 12-bit Orca CCD camera (Hamamatsu). DHR experiments were performed with a confocal microscope (Noran Odyssey) equipped with an argon-ion laser, an inverted microscope (Nikon Diaphot), and a 60× Nikon oil-immersion objective (N.A.: 1.4). Fura-2 ratios and DHR confocal images (and relative bright field images) were digitized and analyzed using Image-1 system (Universal Imaging) or Metamorph imaging software (Universal Imaging), respectively. Fluo-4FF images were acquired and analyzed with Metafluor 6.0 software (Molecular Devices).

$[Ca^{2+}]_i$ Measurements

Striatal cultures were loaded for 30 min in the dark with fura-2 AM (5 μM) or fluo-4FF AM (5 μM) plus 0.2% Pluronic F-127 in HEPES-buffered saline solution (HCSS) (120 mM NaCl, 5.4 mM KCl, 0.8 mM $MgCl_2$, 20 mM HEPES, 15 mM glucose, 1.8 mM $CaCl_2$, 10 mM NaOH, pH 7.4), washed, and incubated for further 30 min in HCSS. In fura-2 experiments $[Ca^{2+}]_i$ was determined using the ratio method described by Grynkiewicz et al. (1985). Fura-2 (Ex λ: 340, 380 nm, Em λ: 510 nm) calibrated values were obtained by determining R_{min} and R_{max} using: EGTA (10 mM) and ionomycin (10 μM) in 0 Ca^{2+} buffer for R_{min}, and Ca^{2+} (10 mM) with ionomycin (10 μM) for R_{max}. Fura-2 K_d

was set at 225 nM. Results are reported as mean $[Ca^{2+}]_i$ nM ± SEM. In fluo-4FF (Ex λ: 490 nm, Em λ: 510 nm) fluorescence changes of each cell (F_x) were normalized to basal fluorescence intensity (F_0). Results are expressed as mean F_x/F_0 ± SEM values. In all experiments, NMDA (50 μM + 10 μM glycine) was applied for 20 s and then removed through a rapid perfusion system.

ROS Production Measurements

Cells were loaded with DHR (5 μM) in the dark in a 37°C/5% CO_2 incubator for 30 min and then studied with confocal imaging. DHR was excited at 488 nm and emission collected at >515 nm. In order to minimize DHR photo-oxidation, laser beam was used to less than 5% of full power and image acquisition intervals minimized to ≤ 2 s every 5 min. DHR was maintained in the buffer throughout all the imaging session to maintain probe equilibration between the inside and outside of cells.

NMDA exposure was performed by adding NMDA (50 μM + 10 μM glycine) to the baseline HCSS solution for 5 min. NMDARs activation was then halted by addition of 10 μM MK-801 and neurons imaged for additional 25 min.

NADPH-DIAPHORASE STAINING

To identify what we call nNOS(+) neurons we employed the NADPH-d staining procedure (Koh et al., 1986). To that aim, after $Ca^{2+}{}_i$ or DHR experiments, cultures were rinsed three times in ice-cold TBS and fixed for 30 min at 4°C in 4% paraformaldehyde/0.1 M PBS buffer. After fixation, dishes were washed with TBS and staining solution applied for 1 h at 37°C. NADPH-d staining solution contained: 0.1 mM Tris/HCl, 0.2% Triton X-100, 1.2 mM sodium azide, 0.2 mM nitrotetrazolium blue, and 1 mM NADPH, pH 7.2. The staining solution was removed and cultures rinsed with TBS. After staining, dishes were re-inserted in the microscope stage and fields re-matched with those previously imaged with fura-2, fluo-4FF, and DHR. nNOS(+) neurons identified as NADPH-d (+) under bright-field illumination were then evaluated for their responses in the imaging experiments.

STATISTICAL ANALYSIS

Grubbs' test was performed to detect outliers, the significance level was set at $\alpha = 0.05$ (no nNOS(+) were found to be significant outliers). Statistical analysis was performed using the Student's *t*-test for unpaired data. Results were considered statistically significant at $p < 0.05$.

RESULTS

$[Ca^{2+}]_i$ RISES UPON NMDA EXPOSURE IN nNOS(+) AND (−) STRIATAL NEURONS

In this set of experiment, we tested whether nNOS(+) possess functional NMDARs and evaluated NMDAR-dependent $[Ca^{2+}]_i$ increases as an indirect parameter of receptor activity. $[Ca^{2+}]_i$ rises upon NMDA exposure were investigated with single cell Ca^{2+} imaging. This indirect assay is the only possible way to study NMDAR activity in specific nNOS(+) neurons. A more direct approach would have been to investigate NMDAR-evoked currents with patch clamp electrophysiology. Unfortunately, this approach is highly unfeasible given the extremely low density (<1%) of nNOS(+) neurons in our striatal cultures along with the absence of any suitable marker to identify these neurons when in culture, two factors making very unlikely the possibility of successfully patching on to these cells in adequate numbers.

Striatal cultures loaded with fura-2, a high affinity Ca^{2+} probe ($K_d = 225$ nM), were exposed to NMDA (50 μM + 10 μM glycine) and $[Ca^{2+}]_i$ elevation assessed during and after the challenge. In this set of experiments, we observed that NMDAR-dependent $[Ca^{2+}]_i$ rises occurring in nNOS(+) were not statistically different from those found in the overall population of nNOS(−) neurons (**Figures 1A,B**). To dissect and possibly reveal more subtle differences in $[Ca^{2+}]_i$ handling between nNOS(+) and (−) neurons, we analyzed peak amplitudes, areas under the curve (an index of the overall cytosolic Ca^{2+} load) and recovery phase time (τ) of the $[Ca^{2+}]_i$ changes (**Figures 1C–E**). None of these parameters showed statistically significant differences between the two neuronal populations. Analysis of baseline $[Ca^{2+}]_i$ levels also showed no differences between nNOS(+) and (−) neurons at rest (data not shown).

In the fura-2 data set we noticed that some neurons showed $[Ca^{2+}]_i$ responses in the micromolar range. Fura-2 is a high affinity Ca^{2+} probe, a technical limitation that leads to underestimating peak $[Ca^{2+}]_i$ rises for values above 1 μM (Hyrc et al., 1997). We therefore repeated the same set of experiments with the low affinity Ca^{2+} indicator fluo-4FF, a probe that, with a K_d of 9.7 μM, is suitable for the detection of $[Ca^{2+}]_i$ changes occurring in the 1 μM to 1 mM range. Fluo-4FF experiments confirmed that NMDAR-dependent $[Ca^{2+}]_i$ increases are identical in nNOS(+) and (−) neurons (**Figures 2A–E**). Of note, different from fura-2 experiments, in the fluo-4FF data set we observed a decreased recovery time in all neurons, a phenomenon that likely reflects the lower affinity of the probe for Ca^{2+}.

Finally, we assessed whether nNOS(+) neurons show differences in $[Ca^{2+}]_i$ response via other glutamatergic ionotropic receptors (i.e., AMPARs). To that aim, fura-2 loaded striatal neurons were exposed to kainate (50 μM) and $[Ca^{2+}]_i$ levels analyzed in terms of agonist-evoked peak levels as well as overall cytosolic cation loads (as indicated by evaluation of the area under the curve of fura-2 signals). Even in this set of experiments, we did not observe significant differences between nNOS(+) and (−) striatal neurons (data not shown).

In summary, Ca^{2+} imaging experiments indicated that nNOS(+) neurons possess fully functional NMDARs.

ROS GENERATION UPON NMDA EXPOSURE IN nNOS(+) AND (−) NEURONS

Aberrant Ca^{2+} entry through NMDARs results in cytosolic Ca^{2+} overload, dissipation of the mitochondrial inner membrane potential, opening of the permeability transition pore, and production of mt-ROS (Rizzuto et al., 2012). ROS are major contributors to excitotoxicity (Choi, 1992a,b; Dugan and Choi, 1994; Sayre et al., 2008). As mentioned above, NADPH diaphorase is the neuronal nNOS enzyme (Hope et al., 1991). Thus, nNOS(+) neurons are likely to be chronically exposed to an intracellular

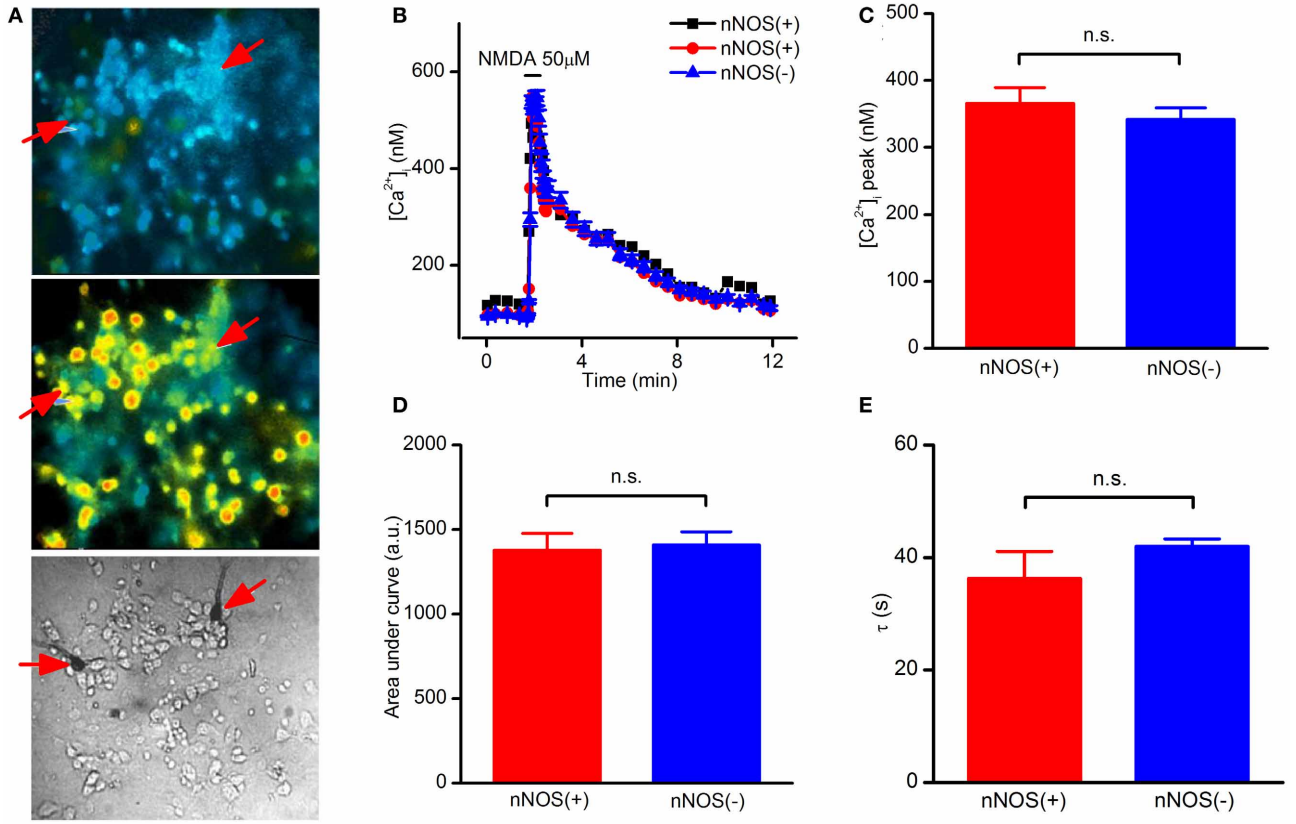

FIGURE 1 | NMDAR-dependent $[Ca^{2+}]_i$ rises in striatal cultured neurons evaluated with a high affinity Ca^{2+}-sensitive probe. (A) Fluorescence images of fura-2 loaded striatal neurons before (top), and upon NMDA exposure (middle). Bright field image (bottom) showing stained nNOS(+), indicated by arrows, and nNOS(−)neurons. **(B)** Time course of NMDAR-dependent $[Ca^{2+}]_i$ rises, traces of a single experiment [NOS(+) ($n = 2$) and nNOS(−) ($n = 47$)], representative of 20 independent experiments. **(C)** Average $[Ca^{2+}]_i$ peak amplitude in the two neuronal populations ($p = 0.42$). **(D)** $[Ca^{2+}]_i$ dynamics expressed as area under the curve ($p = 0.70$). **(E)** Recovery phase following NMDA exposure ($p = 0.43$). Results are expressed as mean values ± SEM; nNOS(+) $n = 22$; nNOS(−) $n = 560$.

environment that is constantly confronted (and needs to be equipped to deal) with the presence of high NO levels.

To investigate mt-ROS levels generated by NMDAR activation, striatal neurons were first loaded with the ROS sensitive probe DHR (Henderson and Chappell, 1993) and fluorescent changes evaluated before, during, and after NMDA exposure with confocal microscopy. Native DHR is uncharged, not fluorescent, and passively diffuses through membranes. Once in the presence of ROS, DHR is oxidized to the cationic fluorescent product, rhodamine 123, allowing the investigation of mitochondrial ROS production (Dugan et al., 1995).

In this set of experiments DHR-loaded neurons, after acquisition of baseline fluorescence levels, were exposed to NMDA (50 + 10 μM glycine) for 5 min, NMDAR activation was then halted by addition of the receptor antagonist (MK-801; 10 μM) and fluorescence changes evaluated up to 30 min. Confocal DHR imaging revealed that NMDA application failed to promote significant fluorescence changes in nNOS(+) neurons while (−) neurons showed significant signal rises (**Figure 3**).

Thus, DHR experiments revealed that NMDA exposure fails to elicit production of mt-ROS in nNOS(+) striatal neurons.

DISCUSSION

nNOS(+) neurons are spared from NMDAR-driven excitotoxicity, a phenomenon that has puzzled the field for many years (Beal et al., 1986; Koh and Choi, 1988; Kumar, 2004; El Ghazi et al., 2012). Our study offers two major findings that may help to unravel the mechanisms underlying the decreased vulnerability of these neurons and offer additional insight for their increased survival in the context of HD.

Firstly, nNOS(+) striatal neurons possess fully functional NMDARs and respond to receptor activation with $[Ca^{2+}]_i$ rises that do not differ for amplitude and temporal dynamics to the ones observed in the overall population of nNOS(−) neurons. Secondly, in nNOS(+) neurons, NMDAR activation does not lead to generation of mt-ROS, thereby occluding a critical downstream event of their excitotoxic cascade.

NMDAR-dependent deregulation of intraneuronal $[Ca^{2+}]_i$ levels upon prolonged or excessive glutamate exposure is the event that starts excitotoxicity (Choi, 1992a,b, 2005). Thus, the reduced vulnerability of nNOS(+) neurons to excitotoxic challenges could have been easily explained by reduced expression or functioning of NMDARs in this subpopulation.

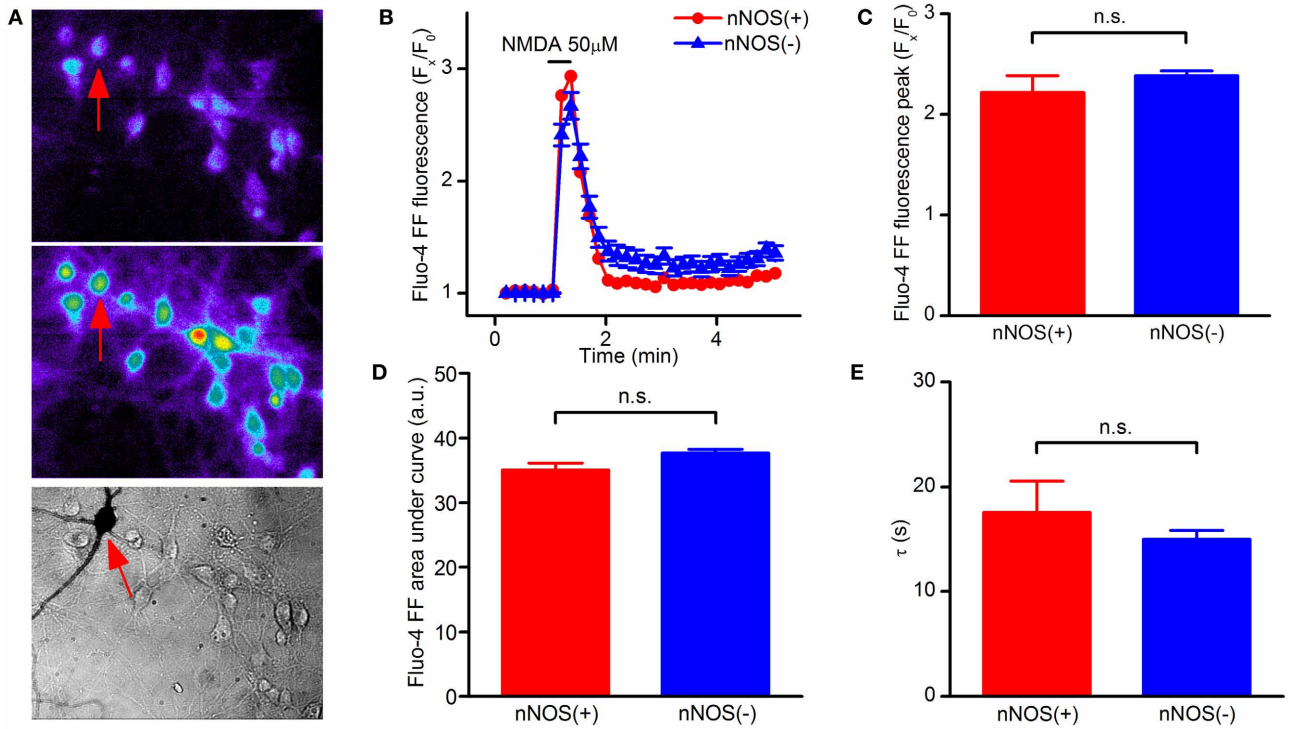

FIGURE 2 | NMDAR-dependent $[Ca^{2+}]_i$ rises in striatal cultured neurons evaluated with a low affinity Ca^{2+}-sensitive probe. (A) Fluorescence images of fluo4-FF loaded striatal neurons before (top) and upon NMDA exposure (middle). Bright field image (bottom) showing stained nNOS(+), indicated by arrows, and nNOS(−) neurons. **(B)** Time course of NMDAR-dependent $[Ca^{2+}]_i$ rises, traces of a single experiment [nNOS(+) ($n = 1$) and nNOS(−) ($n = 18$)], representative of 12 independent experiments. **(C)** Average Ca_i^{2+} peak amplitude in the two neuronal populations ($p = 0.36$). **(D)** $[Ca^{2+}]_i$ dynamics expressed as area under the curve ($p = 0.24$). **(E)** Recovery phase following NMDA exposure ($p = 0.43$). Results are expressed as mean values ± SEM; nNOS(+) $n = 13$; nNOS(−) $n = 165$.

Our data lend us to hypothesize an alternative view and finally demonstrate that these neurons are most likely resistant not because they differ in number or functionality of NMDARs but, on the contrary, because they are able to set in motion protective events acting downstream to block a key step in the injurious cascade set in motion by NMDAR activation: the intraneuronal raise of mt-ROS levels.

ROS play important roles in several biological functions and are critical mediators of physiological or death signaling (Huang and McNamara, 2012; Ray et al., 2012). Upon excitotoxic conditions, NMDAR-driven production of high levels of cytosolic and mitochondrial ROS as well as nitrosative species leads to neuronal death (Floyd, 1999; Droge, 2002; Lau and Tymianski, 2010). Neurons maintain a redox homeostasis and counteract these oxidative and nitrosative hits by employing several endogenous scavenging mechanisms (Greenlund et al., 1995) like superoxide dismutases, catalases, and glutathione peroxidases.

As nNOS(+) neurons express high levels of nNOS (Hope et al., 1991) and are thereby producing large amounts of NO, it is conceivable that they are primed to deal with an oxidizing intracellular environment and possess an enhanced capability to neutralize this challenge.

Landmark findings support this idea and, in fact, indicate that nNOS(+) express high levels of manganese superoxide dismutase (MnSOD) (Gonzalez-Zulueta et al., 1998). MnSOD, a mitochondrial enzyme, neutralizes free radicals. The enzyme confers resistance against NMDA- and NO-mediated toxicity both *in vivo* and *in vitro* by preventing the generation of toxic peroxynitrite originating from the NO and O_2^- interaction (Beckman and Koppenol, 1996; Gonzalez-Zulueta et al., 1998; Brown, 2010). Thus, our data suggest a conceptual framework in which enhanced MnSOD activity in nNOS(+) neurons might lead to the reduced ROS generation that we find upon NMDA exposure and provides potential explanation for their decreased vulnerability to NMDAR-mediated neuronal death.

Our results are providing support for the idea that mitochondria play a strategic role in the phenomenon. We acknowledge that future experiments are needed to clarify whether increased MnSOD activity is indeed play a major role in the neuroprotective pathway. We show that NMDA exposure produces $[Ca^{2+}]_i$ levels that are similar in nNOS(+) and (−) striatal neurons. We also show that these excitotoxic Ca^{2+} rises fail to promote significant ROS raises in the mitochondria of nNOS(+) neurons. Thus, in nNOS(+) neurons, the behavior of mitochondria, critical actors of the excitotoxic cascade, differ.

Two major arguments support this assumption. In the Ca^{2+} imaging experiments we have shown that nNOS(+) neurons face the same NMDAR-driven Ca^{2+} overload. If one has to fit

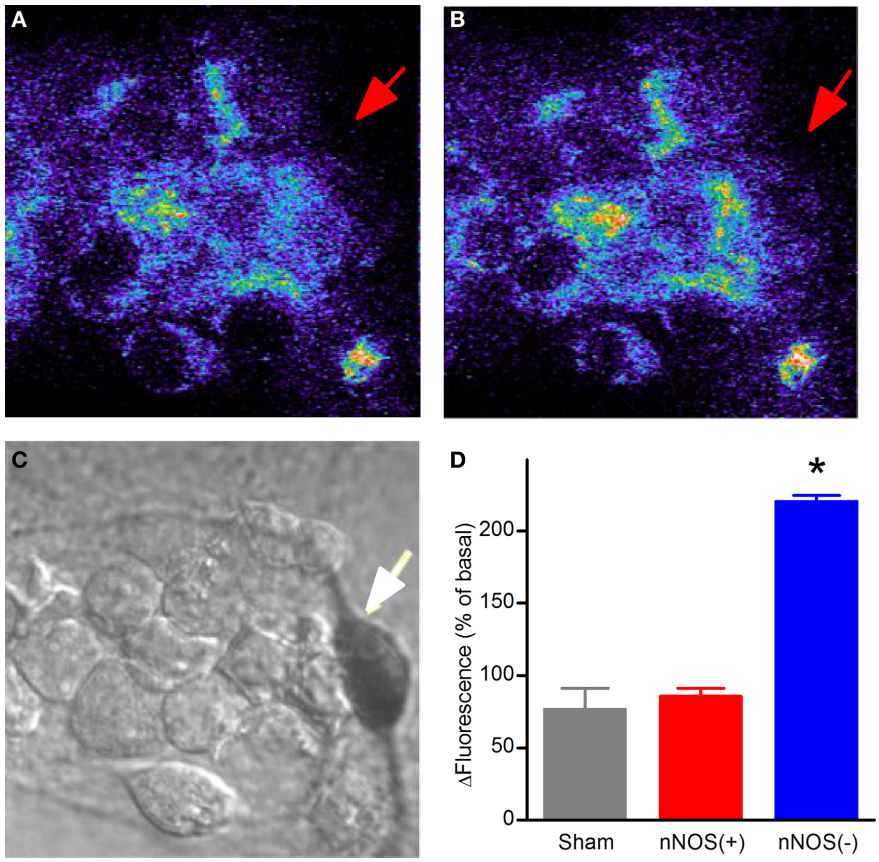

FIGURE 3 | NMDAR-dependent mitochondrial ROS production in striatal cultured neurons. (A) Confocal images of basal levels of fluorescence of DHR-loaded neurons prior to NMDA stimulation. **(B)** DHR fluorescence 25 min after a 5 min NMDA exposure. **(C)** Bright field image showing stained nNOS(+), indicated by arrow, and nNOS(−) neurons. **(D)** Quantification of DHR fluorescence increases 25 min after NMDA exposure (*$p < 0.001$). Results are expressed as mean % of $F_x/F_0 \pm$ SEM; nNOS(+) $n = 19$; nNOS(−) $n = 142$ from 18 independent experiments.

these data and the DHR results in a comprehensive conceptual framework, it can be hypothesized that either: (1) mitochondria of nNOS(+) neurons are allowing less Ca^{2+} uptake (thereby decreasing the overall generation of Ca^{2+}-dependent mt-ROS) or (2) nNOS(+) neurons have developed ways to counteract the generation of mt-ROS.

When considering the first hypothesis, it should be underlined that our Ca^{2+} imaging experiments take in account and report changes of cation levels occurring in the cytosol, a phenomenon that is the net result of simultaneous and concerted activities of many Ca^{2+} homeostatic systems (Pizzo et al., 2012; Rizzuto et al., 2012). The fact that we observed similar NMDAR-driven Ca^{2+} loads in the two neuronal subpopulations could, in theory, be explained by compensatory mechanisms occurring in nNOS(+) neurons that prevent Ca^{2+} overloads in mitochondria. For this mechanism to work, one has to infer that these cells may have enhanced expression and/or functioning of the plasma-membrane Ca^{2+}-ATPases (PMCA), a key pathway for Ca^{2+} extrusion, a possibility that we have not tested yet. Differences in activity of the other major cellular system for Ca^{2+} extrusion, the plasmatic Na^{+}-Ca^{2+} exchanger (NCX), are unlikely as excitotoxic conditions (like the one used in our setting) favor either a NCX reverse operational mode (thereby leading the exchanger to serve as pathway for Ca^{2+} entry) (Orrenius et al., 2003) or NCX functional blockade by calpain-mediated cleavage of the exchanger (Bano et al., 2005).

Enhanced functioning of intracellular Ca^{2+} stores (i.e., the endoplasmic reticulum; ER) is also unlikely to work to decrease Ca^{2+} rises in nNOS(+) neurons. Accordingly to the "hot spot" hypothesis proposed by Rizzuto et al. (1998), Ca^{2+} overload in the ER is a detrimental source for ROS generation as the cation eventually exits the ER and is taken up by mitochondria located in the ER vicinity, thereby providing the driving force for production of mt-ROS. Thus, if nNOS(+) neurons do overdrive the ER to maintain Ca^{2+} homeostasis such compensatory mechanism should be counterbalanced by enhanced levels of mt-ROS, the opposite of what we observed in our nNOS(+) neurons.

The idea that mitochondria of nNOS(+) sequester equal amounts of Ca^{2+} but respond to this hit with a decreased generation of ROS is strongly suggested by previous findings (Gonzalez-Zulueta et al., 1998) that indicate a major role for MnSOD in promoting protection against NMDAR-mediated oxidative stress in nNOS(+) neurons. Within this framework, we do speculate

that the observed reduction of ROS levels in nNOS(+) neurons may be due to higher scavenging capabilities of this neuronal subpopulation.

In summary, our data offer complementary data that substantiate a major role for mitochondria in promoting the reduced vulnerability to NMDA in nNOS(+) striatal neurons. Given the role played by polyQ Htt in affecting mitochondrial functioning, this mechanism can be particularly relevant in the context of the neuronal loss occurring in the striatum of HD patients and provide targets for therapeutic intervention.

ACKNOWLEDGMENTS

Stefano L. Sensi is supported by funds from the Italian Department of Education (PRIN 2008 and 2010).

REFERENCES

Bano, D., Young, K. W., Guerin, C. J., Lefeuvre, R., Rothwell, N. J., Naldini, L., et al. (2005). Cleavage of the plasma membrane Na+/Ca2+ exchanger in excitotoxicity. *Cell* 120, 275–285.

Beal, M. F., Kowall, N. W., Ellison, D. W., Mazurek, M. F., Swartz, K. J., and Martin, J. B. (1986). Replication of the neurochemical characteristics of Huntington's disease by quinolinic acid. *Nature* 321, 168–171.

Beckman, J. S., and Koppenol, W. H. (1996). Nitric oxide, superoxide, and peroxynitrite: the good, the bad, and ugly. *Am. J. Physiol.* 271, C1424–C1437.

Brown, G. C. (2010). Nitric oxide and neuronal death. *Nitric Oxide* 23, 153–165.

Cattaneo, E., Zuccato, C., and Tartari, M. (2005). Normal huntingtin function: an alternative approach to Huntington's disease. *Nat. Rev. Neurosci.* 6, 919–930.

Choi, D. W. (1992a). Excitotoxic cell death. *J. Neurobiol.* 23, 1261–1276.

Choi, D. W. (1992b). Bench to bedside: the glutamate connection. *Science* 258, 241–243.

Choi, D. W. (2005). Neurodegeneration: cellular defences destroyed. *Nature* 433, 696–698.

Costa, V., and Scorrano, L. (2012). Shaping the role of mitochondria in the pathogenesis of Huntington's disease. *EMBO J.* 31, 1853–1864.

Difiglia, M., Sapp, E., Chase, K., Schwarz, C., Meloni, A., Young, C., et al. (1995). Huntingtin is a cytoplasmic protein associated with vesicles in human and rat brain neurons. *Neuron* 14, 1075–1081.

Droge, W. (2002). Free radicals in the physiological control of cell function. *Physiol. Rev.* 82, 47–95.

Dugan, L. L., and Choi, D. W. (1994). Excitotoxicity, free radicals, and cell membrane changes. *Ann. Neurol.* 35(Suppl.), S17–S21.

Dugan, L. L., Sensi, S. L., Canzoniero, L. M., Handran, S. D., Rothman, S. M., Lin, T. S., et al. (1995). Mitochondrial production of reactive oxygen species in cortical neurons following exposure to N-methyl-D-aspartate. *J. Neurosci.* 15, 6377–6388.

El Ghazi, F., Desfeux, A., Brasse-Lagnel, C., Roux, C., Lesueur, C., Mazur, D., et al. (2012). NO-dependent protective effect of VEGF against excitotoxicity on layer VI of the developing cerebral cortex. *Neurobiol. Dis.* 45, 871–886.

Ferrante, R. J., Kowall, N. W., Beal, M. F., Richardson, E. P. Jr., Bird, E. D., and Martin, J. B. (1985). Selective sparing of a class of striatal neurons in Huntington's disease. *Science* 230, 561–563.

Floyd, R. A. (1999). Antioxidants, oxidative stress, and degenerative neurological disorders. *Proc. Soc. Exp. Biol. Med.* 222, 236–245.

Forder, J. P., and Tymianski, M. (2009). Postsynaptic mechanisms of excitotoxicity: involvement of postsynaptic density proteins, radicals, and oxidant molecules. *Neuroscience* 158, 293–300.

Gauthier, L. R., Charrin, B. C., Borrell-Pages, M., Dompierre, J. P., Rangone, H., Cordelieres, F. P., et al. (2004). Huntingtin controls neurotrophic support and survival of neurons by enhancing BDNF vesicular transport along microtubules. *Cell* 118, 127–138.

Gonzalez-Zulueta, M., Ensz, L. M., Mukhina, G., Lebovitz, R. M., Zwacka, R. M., Engelhardt, J. F., et al. (1998). Manganese superoxide dismutase protects nNOS neurons from NMDA and nitric oxide-mediated neurotoxicity. *J. Neurosci.* 18, 2040–2055.

Greenlund, L. J., Deckwerth, T. L., and Johnson, E. M. Jr. (1995). Superoxide dismutase delays neuronal apoptosis: a role for reactive oxygen species in programmed neuronal death. *Neuron* 14, 303–315.

Grynkiewicz, G., Poenie, M., and Tsien, R. Y. (1985). A new generation of Ca2+ indicators with greatly improved fluorescence properties. *J. Biol. Chem.* 260, 3440–3450.

Guo, Z., Rudow, G., Pletnikova, O., Codispoti, K. E., Orr, B. A., Crain, B. J., et al. (2012). Striatal neuronal loss correlates with clinical motor impairment in Huntington's disease. *Mov. Disord.* 27, 1379–1386.

Halliday, G. M., McRitchie, D. A., Macdonald, V., Double, K. L., Trent, R. J., and McCusker, E. (1998). Regional specificity of brain atrophy in Huntington's disease. *Exp. Neurol.* 154, 663–672.

Henderson, L. M., and Chappell, J. B. (1993). Dihydrorhodamine 123: a fluorescent probe for superoxide generation? *Eur. J. Biochem.* 217, 973–980.

Hope, B. T., Michael, G. J., Knigge, K. M., and Vincent, S. R. (1991). Neuronal NADPH diaphorase is a nitric oxide synthase. *Proc. Natl. Acad. Sci. U.S.A.* 88, 2811–2814.

Huang, Y. Z., and McNamara, J. O. (2012). Neuroprotective effects of reactive oxygen species mediated by BDNF-independent activation of TrkB. *J. Neurosci.* 32, 15521–15532.

Hyrc, K., Handran, S. D., Rothman, S. M., and Goldberg, M. P. (1997). Ionized intracellular calcium concentration predicts excitotoxic neuronal death: observations with low-affinity fluorescent calcium indicators. *J. Neurosci.* 17, 6669–6677.

Koh, J. Y., and Choi, D. W. (1988). Vulnerability of cultured cortical neurons to damage by excitotoxins: differential susceptibility of neurons containing NADPH-diaphorase. *J. Neurosci.* 8, 2153–2163.

Koh, J. Y., Peters, S., and Choi, D. W. (1986). Neurons containing NADPH-diaphorase are selectively resistant to quinolinate toxicity. *Science* 234, 73–76.

Kumar, U. (2004). Characterization of striatal cultures with the effect of QUIN and NMDA. *Neurosci. Res.* 49, 29–38.

Lau, A., and Tymianski, M. (2010). Glutamate receptors, neurotoxicity and neurodegeneration. *Pflugers Arch.* 460, 525–542.

Macdonald, M. E., Ambrose, C. M., Duyao, M. P., Myers, R. H., Lin, C., Srinidhi, L., et al. (1993). A novel gene containing a trinucleotide repeat that is expanded and unstable on Huntington's disease chromosomes. *Cell* 72, 971–983.

Nicholls, D. G. (2002). Mitochondrial function and dysfunction in the cell: its relevance to aging and aging-related disease. *Int. J. Biochem. Cell Biol.* 34, 1372–1381.

Nicholls, D. G. (2004). Mitochondrial dysfunction and glutamate excitotoxicity studied in primary neuronal cultures. *Curr. Mol. Med.* 4, 149–177.

Nicholls, D. G., and Budd, S. L. (1998). Mitochondria and neuronal glutamate excitotoxicity. *Biochim. Biophys. Acta* 1366, 97–112.

Nicholls, D. G., and Budd, S. L. (2000). Mitochondria and neuronal survival. *Physiol. Rev.* 80, 315–360.

Nicholls, D. G., Johnson-Cadwell, L., Vesce, S., Jekabsons, M., and Yadava, N. (2007). Bioenergetics of mitochondria in cultured neurons and their role in glutamate excitotoxicity. *J. Neurosci. Res.* 85, 3206–3212.

Nicholls, D. G., Vesce, S., Kirk, L., and Chalmers, S. (2003). Interactions between mitochondrial bioenergetics and cytoplasmic calcium in cultured cerebellar granule cells. *Cell Calcium* 34, 407–424.

Nicholls, D. G., and Ward, M. W. (2000). Mitochondrial membrane potential and neuronal glutamate excitotoxicity: mortality and millivolts. *Trends Neurosci.* 23, 166–174.

Orrenius, S., Zhivotovsky, B., and Nicotera, P. (2003). Regulation of cell death: the calcium-apoptosis link. *Nat. Rev. Mol. Cell Biol.* 4, 552–565.

Pizzo, P., Drago, I., Filadi, R., and Pozzan, T. (2012). Mitochondrial Ca(2)(+) homeostasis: mechanism, role, and tissue specificities. *Pflugers Arch.* 464, 3–17.

Qin, Z. H., Wang, Y., Sapp, E., Cuiffo, B., Wanker, E., Hayden, M. R., et al. (2004). Huntingtin bodies sequester vesicle-associated proteins by a polyproline-dependent interaction. *J. Neurosci.* 24, 269–281.

Ray, P. D., Huang, B. W., and Tsuji, Y. (2012). Reactive oxygen species (ROS) homeostasis and redox regulation in cellular signaling. *Cell. Signal.* 24, 981–990.

Reynolds, I. J., and Hastings, T. G. (1995). Glutamate induces the production of reactive oxygen species in cultured forebrain neurons following NMDA receptor activation. *J. Neurosci.* 15, 3318–3327.

Reynolds, I. J., Malaiyandi, L. M., Coash, M., and Rintoul, G. L. (2004). Mitochondrial trafficking in neurons: a key variable in neurodegeneration? *J. Bioenerg. Biomembr.* 36, 283–286.

Rintoul, G. L., Filiano, A. J., Brocard, J. B., Kress, G. J., and Reynolds, I. J. (2003). Glutamate decreases mitochondrial size and movement in primary forebrain neurons. *J. Neurosci.* 23, 7881–7888.

Rizzuto, R., De Stefani, D., Raffaello, A., and Mammucari, C. (2012). Mitochondria as sensors and regulators of calcium signalling. *Nat. Rev. Mol. Cell Biol.* 13, 566–578.

Rizzuto, R., Pinton, P., Carrington, W., Fay, F. S., Fogarty, K. E., Lifshitz, L. M., et al. (1998). Close contacts with the endoplasmic reticulum as determinants of mitochondrial Ca2+ responses. *Science* 280, 1763–1766.

Rockabrand, E., Slepko, N., Pantalone, A., Nukala, V. N., Kazantsev, A., Marsh, J. L., et al. (2007). The first 17 amino acids of Huntingtin modulate its sub-cellular localization, aggregation and effects on calcium homeostasis. *Hum. Mol. Genet.* 16, 61–77.

Ross, C. A., and Tabrizi, S. J. (2011). Huntington's disease: from molecular pathogenesis to clinical treatment. *Lancet Neurol.* 10, 83–98.

Sayre, L. M., Perry, G., and Smith, M. A. (2008). Oxidative stress and neurotoxicity. *Chem. Res. Toxicol.* 21, 172–188.

Spalloni, A., Nutini, M., and Longone, P. (2013). Role of the N-methyl-d-aspartate receptors complex in amyotrophic lateral sclerosis. *Biochim. Biophys. Acta* 1832, 312–322.

Stout, A. K., Raphael, H. M., Kanterewicz, B. I., Klann, E., and Reynolds, I. J. (1998). Glutamate-induced neuron death requires mitochondrial calcium uptake. *Nat. Neurosci.* 1, 366–373.

Szydlowska, K., and Tymianski, M. (2010). Calcium, ischemia and excitotoxicity. *Cell Calcium* 47, 122–129.

Trushina, E., Heldebrant, M. P., Perez-Terzic, C. M., Bortolon, R., Kovtun, I. V., Badger, J. D. 2nd., et al. (2003). Microtubule destabilization and nuclear entry are sequential steps leading to toxicity in Huntington's disease. *Proc. Natl. Acad. Sci. U.S.A.* 100, 12171–12176.

Vesce, S., Kirk, L., and Nicholls, D. G. (2004). Relationships between superoxide levels and delayed calcium deregulation in cultured cerebellar granule cells exposed continuously to glutamate. *J. Neurochem.* 90, 683–693.

Votyakova, T. V., and Reynolds, I. J. (2001). DeltaPsi(m)-dependent and -independent production of reactive oxygen species by rat brain mitochondria. *J. Neurochem.* 79, 266–277.

Votyakova, T. V., and Reynolds, I. J. (2005). Ca2+-induced permeabilization promotes free radical release from rat brain mitochondria with partially inhibited complex I. *J. Neurochem.* 93, 526–537.

White, R. J., and Reynolds, I. J. (1995). Mitochondria and Na+/Ca2+ exchange buffer glutamate-induced calcium loads in cultured cortical neurons. *J. Neurosci.* 15, 1318–1328.

White, R. J., and Reynolds, I. J. (1996). Mitochondrial depolarization in glutamate-stimulated neurons: an early signal specific to excitotoxin exposure. *J. Neurosci.* 16, 5688–5697.

Zeron, M. M., Fernandes, H. B., Krebs, C., Shehadeh, J., Wellington, C. L., Leavitt, B. R., et al. (2004). Potentiation of NMDA receptor-mediated excitotoxicity linked with intrinsic apoptotic pathway in YAC transgenic mouse model of Huntington's disease. *Mol. Cell. Neurosci.* 25, 469–479.

Conflict of Interest Statement: The authors declare that the research was conducted in the absence of any commercial or financial relationships that could be construed as a potential conflict of interest.

Received: 17 January 2013; accepted: 30 April 2013; published online: 16 May 2013.

Citation: Canzoniero LMT, Granzotto A, Turetsky DM, Choi DW, Dugan LL and Sensi SL (2013) nNOS(+) striatal neurons, a subpopulation spared in Huntington's Disease, possess functional NMDA receptors but fail to generate mitochondrial ROS in response to an excitotoxic challenge. Front. Physiol. ***4****:112. doi: 10.3389/fphys.2013.00112*

This article was submitted to Frontiers in Mitochondrial Research, a specialty of Frontiers in Physiology.

frontiers in
PHYSIOLOGY

PERSPECTIVE ARTICLE
published: 28 June 2013
doi: 10.3389/fphys.2013.00151

Metabolic control analysis of respiration in human cancer tissue

Tuuli Kaambre[1]*, Vladimir Chekulayev[1], Igor Shevchuk[1], Kersti Tepp[1], Natalja Timohhina[1], Minna Varikmaa[1], Rafaela Bagur[2], Aleksandr Klepinin[1], Tiia Anmann[1], Andre Koit[1], Andrus Kaldma[1], Rita Guzun[2], Vahur Valvere[3,4] and Valdur Saks[1,2]

[1] Laboratory of Bioenergetics, National Institute of Chemical Physics and Biophysics, Tallinn, Estonia
[2] Laboratory of Fundamental and Applied Bioenergetics, Joseph Fourier University, Grenoble, France
[3] Oncology and Hematology Clinic at the North Estonia Medical Centre, Tallinn, Estonia
[4] Competence Centre for Cancer Research, Tallinn, Estonia

Edited by:
Sabzali Javadov, University of Puerto Rico School of Medicine, Puerto Rico

Reviewed by:
Sonia C. Cortassa, Johns Hopkins University, USA
Miguel A. Aon, Johns Hopkins University School of Medicine, USA

***Correspondence:**
Tuuli Kaambre, Laboratory of Bioenergetics, National Institute of Chemical Physics and Biophysics, Akadeemia tee 23, 12618 Tallinn, Estonia
e-mail: tuuli.kaambre@kbfi.ee

Bioenergetic profiling of cancer cells is of great potential because it can bring forward new and effective therapeutic strategies along with early diagnosis. Metabolic Control Analysis (MCA) is a methodology that enables quantification of the flux control exerted by different enzymatic steps in a metabolic network thus assessing their contribution to the system's function. Our main goal is to demonstrate the applicability of MCA for *in situ* studies of energy metabolism in human breast and colorectal cancer cells as well as in normal tissues. We seek to determine the metabolic conditions leading to energy flux redirection in cancer cells. A main result obtained is that the adenine nucleotide translocator exhibits the highest control of respiration in human breast cancer thus becoming a prospective therapeutic target. Additionally, we present evidence suggesting the existence of mitochondrial respiratory supercomplexes that may represent a way by which cancer cells avoid apoptosis. The data obtained show that MCA applied *in situ* can be insightful in cancer cell energetic research.

Keywords: metabolic control analysis, respiratory chain, breast and colorectal cancer, Warburg effect, OXPHOS

INTRODUCTION

Oncologic diseases such as breast and colorectal cancers are still one of the main causes of premature death among people. The low efficiency of contemporary medicine in the treatment of these malignancies is largely mediated by a poor understanding of the processes involved in metastatic dissemination of cancer cells as well as the unique energetic properties of mitochondria from tumors. Current knowledge supports the idea that human breast and colorectal cancer cells exhibit increased rates of glucose consumption displaying a Warburg phenotype, i.e., elevated glycolysis even in the presence of oxygen (Warburg and Dickens, 1930; Warburg, 1956; Izuishi et al., 2012). Notwithstanding, there are some evidences that in these malignancies mitochondrial oxidative phosphorylation (OXPHOS) is the main source of ATP rather than glycolysis. Cancer cells have been classified according to their pattern of metabolic remodeling depending of the relative balance between aerobic glycolysis and OXPHOS (Bellance et al., 2012). The first type of tumor cells is highly glycolytic, the second OXPHOS deficient and the third type of tumors display enhanced OXPHOS. Recent studies strongly suggest that cancer cells can utilize lactate, free fatty acids, ketone bodies, butyrate and glutamine as key respiratory substrates eliciting metabolic remodeling of normal surrounding cells toward aerobic glycolysis—"reverse Warburg" effect (Whitaker-Menezes et al., 2011; Salem et al., 2012; Sotgia et al., 2012; Witkiewicz et al., 2012). In normal cells, the OXPHOS system is usually closely linked to phosphotransfer systems, including various creatine kinase (CK) isotypes, which ensure a safe operation of energetics over a broad functional range of cellular activities (Dzeja and Terzic, 2003). However, our current knowledge about the function of CK/creatine (Cr) system in human breast and colorectal cancer is insufficient. In some malignancies, for example sarcomas the CK/Cr system was shown to be strongly down regulated (Bera et al., 2008; Patra et al., 2008). Our previous studies showed that the mitochondrial-bound CK (MtCK) activity was significantly decreased in HL-1 tumor cells (Monge et al., 2009), as compared to normal parent cardiac cells where the OXPHOS is the main ATP source of and the CK system is a main energy carrier. In the present study, we estimated the role of MtCK in maintaining energy homeostasis in human colorectal cancer cells.

Understanding the control and regulation of energy metabolism requires analytical tools that take into account the existing interactions between individual network components and their impact on systemic network function. Metabolic Control Analysis (MCA) is a theoretical framework relating the properties of metabolic systems to the kinetic characteristics of their individual enzymatic components (Fell, 2005). An experimental approach of MCA has been already successfully applied to the studies of OXPHOS in isolated mitochondria (Tager et al., 1983; Kunz et al., 1999; Rossignol et al., 2000) and in skinned muscle fibers (Kuznetsov et al., 1997; Tepp et al., 2010).

Recent work from Moreno-Sanchez and Westerhoff's groups has applied MCA to investigate the control of glycolytic flux

and mitochondrial respiration in different types of tumor cells growing in culture. A main conclusion of these studies is that the significance of OXPHOS in bioenergetics of cancer cells should be re-evaluated and experimentally determined for each particular type of neoplasm (Marin-Hernandez et al., 2006; Moreno-Sanchez et al., 2007, 2008, 2010). These findings also indicated that MCA may be a very useful approach for studying *in situ* mitochondrial respiration and energy fluxes.

In the present work we applied MCA for *in situ* studies the energy metabolism in human cancer cells. Using oxygraphy and MCA in permeabilized human breast and colorectal cancer cells (Kuznetsov et al., 1997) we quantitatively characterized the control exerted by the different components of the respiratory chain and the ATP synthasome (Tepp et al., 2011).

MATERIALS AND METHODS

PATIENTS AND TISSUE SAMPLING

Bioenergetic proiling was performed on post-operation material derived from patients with human breast (HBC) and colorectal cancers (HCC). Thirty two patients 50–71 year-old were in the HBC group with local or locally advanced disease at pathological stage IA-IIIB (T1-4N0-2M0) and eighteen patients, 63–82 year-old in HCC group with pathological stage (T2-3 N1-M0). Tumor differentiation was into well, moderately, and poorly differentiated adenocarcinoma.

Immediately after the surgery the human samples were placed into pre-cooled Mitomedium-B solution, dissected into small fiber bundles and permeabilized with 50 μg/ml saponin (Kuznetsov et al., 2008). Control experiments showed that this procedure has no effect on the integrity of mitochondrial membranes and that the stimulatory effect on respiration by added cytochrome-c is absent (Kuznetsov et al., 2008; Kaambre et al., 2012).

HIGH-RESOLUTION RESPIROMETRY

Mitochondrial respiration of tissue samples was measured at 25°C under continuous magnetic stirring with an Oxygraph-2 k, (Oroboros Instruments, Innsbruck, Austria) 5 mM glutamate, 2 mM malate and 10 mM succinate were used as respiratory substrates. In permeabilized tumor and muscle fibers, the mitochondrial respiration was activated by exogenously added ADP. The flux control coefficients (FCC) for permeabilized human samples were determined with direct activation of respiration by ADP (state 3 respiration). The presence of MtCK in permeabilized human cancer samples was assayed as described earlier (Monge et al., 2009; Kaambre et al., 2012).

METABOLIC CONTROL ANALYSIS

By applying the principles of MCA, it is possible to quantify the degree of the control, exerted by an enzymatic or transport step through FCC. FCC is defined as the ratio of the fractional change in the steady-state flux with respect to an infinitesimal variation in the biochemical activity that caused the change in flux (Fell, 1997). In the present study FCC was assessed by stepwise titration of the respiratory activity of the system with the specific inhibitors for each step from the respiratory chain and ATP synthasome complexes. Control coefficients are determined from the initial slope of the titration curve and the ratio of inhibitor concentration at maximal flux inhibition over the uninhibited flux.

FCC-values were quantified according to a graphical method (Groen et al., 1982; Fell, 2005) modified by Small (Small and Fell, 1990) and results obtained were compared with the computer estimated coefficients (Gellerich et al., 1990; Small and Fell, 1990). Previous studies indicated that similar values can be obtained with either methods, but special attention should be paid to systems with branched pathways or direct channeling due to possible unreliable estimates (Kholodenko et al., 1993; Kholodenko and Westerhoff, 1993; Tepp et al., 2011).

RESULTS AND DISCUSSION

BIOENERGETIC PROFILING OF HUMAN CANCER AND MCA

First, we evaluated the impact of Cr, ADP, mitochondrial-bound hexokinase (HK) and CK reactions on OXPHOS in permeabilized human tumor samples. It has been proposed that in cancer cells the binding of HK-2 to the mitochondrial voltage-dependent anion channel (VDAC) mediates their Warburg behavior further suggesting that this enzyme could be used as a target for antineoplastic therapy (Pedersen, 2008). We found that affecting mitochondria-bound CK and HK only produces minor effects on mitochondrial respiration in HCC cells. Indeed, the addition of 10 mM Cr and 5 mM glucose with 0.2 mM ATP (in the presence of phosphoenolpyruvate-pyruvate kinase ADP trapping system) had no effect on the rates of oxygen consumption by these cells. Similar effects were also registered in HBC cells (Kaambre et al., 2012). From these results, it appears that MtCK does not play a significant role in HBC and HCC cells *in situ*. The role of another CK isoforms in maintaining of energy homeostasis in these cancer cells will be examined in future work. The data obtained suggest that mitochondrial, but not glycolytic ATP, plays a key role in maintaining life processes in HCC and HBC cells. In contrast to HCC cells, a marked stimulatory effect on mitochondrial respiration by glucose addition (in the presence of exogenous MgATP) was observed in saponized HL-1 tumor cells that display a glycolytic phenotype (Eimre et al., 2008; Monge et al., 2009). Furthermore, we found that adding respiratory substrates and 2 mM ADP to HCC and HBC fibers resulted in a notable increase in O2 consumption rate (**Table 1**).

Due to the absence of MtCK in HCC cells, we further analyzed OXPHOS in these cells upon direct activation of respiration with exogenous ADP. In order to evaluate the functionality of individual respiratory complexes of the electron transport chain (ETC) in HCC and HBC cells, the rates of O_2 consumption were measured after sequential addition of specific substrates and inhibitors in the following order: 2 mM ADP, 10 μM rotenone, 10 mM succinate, 10 μM antimycin A, 5 mM ascorbate with 1 mM tetramethyl-p-phenylenediamine (TMPD). We found that the addition of 2 mM ADP activates mitochondrial respiration by ∼3.2 and 3.3 times in HCC and HBC samples, respectively (**Table 1**). Our studies showed that these human malignancies have a functionally active Krebs cycle as well as the ETC. Accordingly ADP stimulated respiration of human breast and colorectal tumors was found to be strongly depressed

Table 1 | Values of basal (V_o) and maximal respiration rate (V_{max}, in the presence of 2 mM ADP) and apparent Michaelis Menten constant (K_m) for ADP in permeabilized human breast and colorectal cancer samples as well as health tissue.

Tissues	$V_o^{\#}$	V_o(succ)	K_m^{app}ADP, μM	V_{max}	RCI	Source
Colorectal cancer	1.4 ± 0.21	2.62 ± 0.34*	34.2 ± 11.1	4.51 ± 0.47*	3.2 ± 0.8	Our data
Control tissue	1.19 ± 0.17	1.61 ± 0.24	46.3 ± 15.5	2.56 ± 0.32	2.2 ± 0.6	Our data
Breast cancer	0.33 ± 0.03	0.56 ± 0.04	114.8 ± 13.6	1.09 ± 0.04	3.3 ± 0.4	Kaambre et al., 2012
Control breast tissue	0.02 ± 0.01	0.10 ± 0.02	–	–	–	Kaambre et al., 2012
Rat soleus	2.19 ± 0.30	–	354 ± 46	12.2 ± 0.5	5.6 ± 1.0	Kuznetsov et al., 1996; Monge et al., 2009
Rat gastrocnemius white	1.23 ± 0.13	–	14.4 ± 2.6	4.10 ± 0.25	3.3 ± 0.6	Kuznetsov et al., 1996; Monge et al., 2009

*# Respiration rate is expressed in nmol O_2/min/mg dry weight; V_o—in the presence of 2 mM malate and 5 mM glutamate as respiratory substrates; V_o(succ)—in the presence of 2 mM malate, 5 mM glutamate, and 10 mM succinate; RCI—respiratory control index is the ratio of V_{max} value to V_o; *$p < 0.05$ as compared to control tissue; data are expressed as mean ± standard error of the mean(SEM).*

upon addition of 10 μM rotenone (an inhibitor of Complex-I), antimycin (an inhibitor of Complex-III), 1 mM NaCN (an inhibitor of Complex-IV) and, on the contrary, it was strongly (>5 times) activated in the presence of ascorbate with TMPD, indicating the presence of active cytochrome-c-oxidase (data not shown). Apparently, the activity of Complex-II in HCC exceeds that in normal tissue, as the addition of succinate to permeabilized fibers led to a stronger stimulation of respiration than in control tissue, although it has been reported that SDHD gene expression is reduced in ∼80% colorectal cancers (Habano et al., 2003).

The results shown in **Table 1** demonstrate that the respiratory activity of breast and colorectal cancers differ significantly that of normal adjacent tissues. Both tumors exhibited respiratory rates close to tissue from rat skeletal muscles (**Table 1**). These data may indicate the presence of a "reverse Warburg" effect, which depends on the properties of the tumor microenvironment. The microenvironment (e.g., substrate availability) is a strong determinant of mitochondrial content and activity in tumors, which could play an important role in the definition of tumors bioenergetic profile (Bellance et al., 2012; Jose and Rossignol, 2013).

When we analyzed respiration as a function of exogenously added ADP, we found that mitochondria from human breast and colorectal cancer cells exhibit an increased affinity toward exogenously added ADP compared with normal oxidative type tissues. The apparent Michaelis Menten constants (K_m) for MgADP were determined as 114.8 ± 13.6 μM and 34.2 ± 11.1 μM for breast and colorectal cancer, respectively (**Table 1**). These values are significantly lower as compared to rat soleus (K_m = 354 ± 46 μM) or isolated cardiomyocytes [K_m = 360 μM (Anmann et al., 2006)], but this value is still higher than the apparent K_m for isolated mitochondria (10–20 μM). The observed difference in the metabolic regulation of respiration could be linked to a decreased expression or absence of some cytoskeletal proteins (Appaix et al., 2003; Saks et al., 2010; Guzun et al., 2012). It has been shown that in normal oxidative muscle, βII-tubulin can bind to VDAC and thereby strongly limit the permeability of mitochondrial outer membrane to adenine nucleotides (Rostovtseva et al., 2008; Guzun et al., 2011). In addition to βII-tubulin, candidate proteins are desmin, microtubule-associated proteins, other isoforms of tubulin and plectin (Appaix et al., 2003; Guzun et al., 2012).

We used MCA to quantitate the control exerted by the different ETC complexes and the ATP synthasome on the respiratory flux in human colorectal and breast carcinomas. FCCs were determined in permeabilized human fibers using the inhibitor titration method in ADP-stimulated respiration.

In HBC cells, the main rate-controlling steps of respiration were Complex IV ($FCC = 0.74$), ATP synthase ($FCC = 0.61$), and phosphate carrier ($FCC = 0.60$). The highest control was exerted by adenine nucleotide translocase (ANT), $FCC = 1.02$ (Kaambre et al., 2012). Our preliminary data for HCC showed high FCCs for: Complex-I ($FCC = 0.62$), Complex-III ($FCC = 0.73$), and Complex-IV ($FCC = 0.58$).

The FCC was calculated graphically as shown in **Figure 1** and as explained in Methods. In the case of HCC, the FCC-values for PIC was calculated as 0.52 (graphic method) (Groen et al., 1982) and 0.47 [according to the Small equation (Small, 1993)]. Although both these methods gave similar values, the use of the Small equation for calculating of FCC(s) was preferred over the graphical one because it is more robust and less subjective. Further investigations are needed to determine the FCC-values for other respiratory chain complexes in HCC and in healthy colon tissue.

In the case of HBC, the summation of the determined FCC(s) for all steps evaluated in the ATP synthasome and ETC complexes was found to be around 4. This value significantly exceeds the theoretically expected summation for linear pathways (value 1). According to Lenaz et al. (2010), a sum of FCC(s) exceeding 1 indicates the existence of supramolecular association of the respiratory complexes that was confirmed by electron microscopy, native gel electrophoresis and single particle image processing (Lenaz and Genova, 2009, 2010). Although more studies are needed to elucidate this important matter, supercomplex formation would allow to explain, at least in part, the high intrinsic resistance to apoptotic stimuli that tumor cells exhibit, namely via suppression of cytochrome-c release. The formation of respiratory supercomplexes could occur not only in HBC but also in HCC cells.

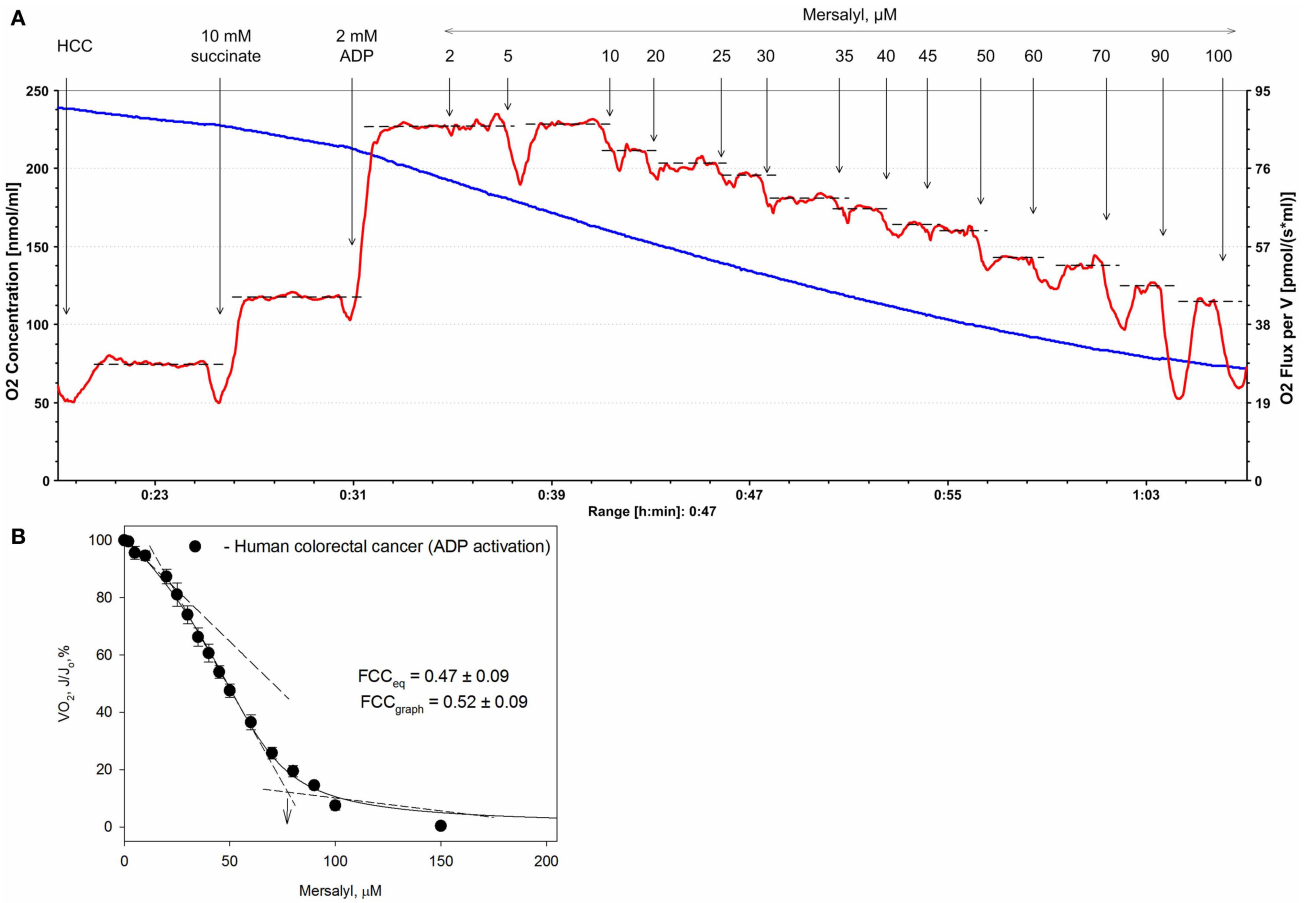

FIGURE 1 | Representative traces of change in the rate of oxygen consumption by permeabilized human colorectal cancer (HCC) fibers after their titration with increasing concentrations of mersalyl, an inhibitor of inorganic phosphate carrier (panel A). The values of respiration rate obtained were plotted vs. mersalyl concentration (panel **B**) and from the plot the corresponding flux control coefficient was calculated. Bars are ±SEM.

CONCLUSION

In this work we show that MCA can be applied to *in situ* quantitative analysis of respiration in cancerous and normal tissues obtained from small amounts of biopsy material. *In situ* studies have the advantage of preserving the cellular ultrastructure such as the cytoskeleton thus enabling the study of their role in controlling energetics in cancer cells. It is important to emphasize that the use of MCA for studying mitochondrial function *in situ* allows us to avoid changes in microenvironment that happen during the isolation procedure. Our studies were performed on cells from tissue samples isolated from patients. This may represent a limitation because recently it has been emphasized that the bioenergetic profile of tumors cells depends largely, among other factors, on the stage of tumor growth and its degree of vascularization (Moreno-Sanchez et al., 2007). Large number of studies were performed on tumor cell cultures, which exhibit a strong dependency on glycolysis, but there might be a strong impact of the artificial culture conditions on energy metabolism (Jose and Rossignol, 2013). One example of the impact of cell culture, the so-called "culture shock," modulates the activity of some genes, which possibly upregulate glycolysis (Gnaiger and Kemp, 1990; Gstraunthaler et al., 1999). This specificity underscores the importance of examining tumor cell behavior in their natural environment.

We quantified the control of respiration in two different types of human cancer cells. The main result obtained is that the ANT exerts a high flux control, implicating the role of adenine nucleotide exchange between mitochondrial and cytoplasmic compartments as a key energetic trait in cancer cells. This result may be important for cancer therapy. Possible suppression of ANT2 and/or overexpression of ANT1 and ANT3 isoforms in cancer cells may induce their death via apoptosis (Jang et al., 2008). We also show that HCC cells exhibit increased respiratory rates as compared to adjacent normal cells suggesting the presence of "reverse Warburg" effect (Whitaker-Menezes et al., 2011). The novel concept of reverse Warburg in cancer metabolism denotes that tumor cells provoke aerobic glycolysis in the tumor stroma thus lactate secretion from cancer-associated fibroblasts. Secreted lactate then fuels OXPHOS in epithelial cancer cells, by acting as a paracrine onco-metabolite. Our data suggest a new strategy for HCC treatment; namely, by

inhibitors of some monocarboxylate transporters (Queiros et al., 2012).

From our MCA studies it can be inferred the presence of respiratory supercomplexes in mitochondria from cancer cells. Recent investigations have shown that respiratory chain complexes I, III and IV can interact to form supercomplexes (respirasomes) (Acín-Pérez et al., 2008; Lenaz and Genova, 2010; Dudkina et al., 2011). Future studies using MCA should unravel how the FCC-value depend upon structural organization of the respirasomes and how exactly the respiratory chain is organized in tumor cells.

Further development in the area of metabolic flux analysis and cellular bioenergetics is important to link future studies on tumor metabolomics to clinical research.

ACKNOWLEDGMENTS

This work was supported by grants Nos. 8987 from the Estonian Science Foundation, SF0180114Bs08 from Estonia Ministry of Education, and by the project "Aid for research and development in health care technology" of Archimedes foundation No. 3.2.1001.11-0027.

REFERENCES

Acín-Pérez, R., Fernández-Silva, P., Peleato, M. L., Perez-Martos, A., and Enriquez, J. A. (2008). Respiratory active mitochondrial supercomplexes. *Mol. Cell.* 32, 529–539. doi: 10.1016/j.molcel.2008.10.021

Anmann, T., Guzun, R., Beraud, N., Pelloux, S., Kuznetsov, A. V., Kogerman, L., et al. (2006). Different kinetics of the regulation of respiration in permeabilized cardiomyocytes and in HL-1 cardiac cells. Importance of cell structure/organization for respiration regulation. *Biochim. Biophys. Acta* 1757, 1597–1606. doi: 10.1016/j.bbabio.2006.09.008

Appaix, F., Kuznetsov, A. V., Usson, Y., Kay, L., Andrienko, T., Olivares, J., et al. (2003). Possible role of cytoskeleton in intracellular arrangement and regulation of mitochondria. *Exp. Physiol.* 88, 175–190. doi: 10.1113/eph8802511

Bellance, N., Pabst, L., Allen, G., Rossignol, R., and Nagrath, D. (2012). Oncosecretomics coupled to bioenergetics identifies alpha-amino adipic acid, isoleucine and GABA as potential biomarkers of cancer: differential expression of c-Myc, Oct1 and KLF4 coordinates metabolic changes. *Biochim. Biophys. Acta* 1817, 2060–2071. doi: 10.1016/j.bbabio.2012.07.004

Bera, S., Wallimann, T., Ray, S., and Ray, M. (2008). Enzymes of creatine biosynthesis, arginine and methionine metabolism in normal and malignant cells. *FEBS J.* 275, 5899–5909. doi: 10.1111/j.1742-4658.2008.06718.x

Dzeja, P. P., and Terzic, A. (2003). Phosphotransfer networks and cellular energetics. *J. Exp. Biol.* 206, 2039–2047. doi: 10.1242/jeb.00426

Dudkina, N. V., Kudryashev, M., Stahlberg, H., and Boekema, E. J. (2011). Interaction of complexes I, III, and IV within the bovine respirasome by single particle cryoelectron tomography. *Proc. Natl. Acad. Sci. U.S.A.* 108, 15196–15200. doi: 10.1073/pnas.1107819108

Eimre, M., Paju, K., Pelloux, S., Beraud, N., Roosimaa, M., Kadaja, L., et al. (2008). Distinct organization of energy metabolism in HL-1 cardiac cell line and cardiomyocytes. *Biochim. Biophys. Acta* 1777, 514–524. doi: 10.1016/j.bbabio.2008.03.019

Fell, D. (1997). *Understanding the Control of Metabolism.* London; Miami: Portland Press.

Fell, D. (2005). "Metabolic control analysis" in *Systems Biology*, eds L. Alberghina and H. V. Westerhoff (Berlin: Springer-Verlag), 69–80.

Gellerich, F. N., Kunz, W. S., and Bohnensack, R. (1990). Estimation of flux control coefficients from inhibitor titrations by non-linear regression. *FEBS Lett.* 274, 167–170. doi: 10.1016/0014-5793(90)81355-R

Gnaiger, E., and Kemp, R. B. (1990). Anaerobic metabolism in aerobic mammalian cells: information from the ratio of calorimetric heat flux and respirometric oxygen flux. *Biochim. Biophys. Acta* 1016, 328–332. doi: 10.1016/0005-2728(90)90164-Y

Groen, A. K., Wanders, R. J., Westerhoff, H. V., Van Der Meer, R., and Tager, J. M. (1982). Quantification of the contribution of various steps to the control of mitochondrial respiration. *J. Biol. Chem.* 257, 2754–2757.

Gstraunthaler, G., Seppi, T., and Pfaller, W. (1999). Impact of culture conditions, culture media volumes, and glucose content on metabolic properties of renal epithelial cell cultures. Are renal cells in tissue culture hypoxic? *Cell. Physiol. Biochem.* 9, 150–172. doi: 10.1159/000016312

Guzun, R., Gonzalez-Granillo, M., Karu-Varikmaa, M., Grichine, A., Usson, Y., Kaambre, T., et al. (2012). Regulation of respiration in muscle cells *in vivo* by VDAC through interaction with the cytoskeleton and MtCK within mitochondrial interactosome. *Biochim. Biophys. Acta* 1818, 1545–1554. doi: 10.1016/j.bbamem.2011.12.034

Guzun, R., Karu-Varikmaa, M., Gonzalez-Granillo, M., Kuznetsov, A. V., Michel, L., Cottet-Rousselle, C., et al. (2011). Mitochondria-cytoskeleton interaction: distribution of beta-tubulins in cardiomyocytes and HL-1 cells. *Biochim. Biophys. Acta* 1807, 458–469. doi: 10.1016/j.bbabio.2011.01.010

Habano, W., Sugai, T., Nakamura, S., Uesugi, N., Higuchi, T., Terashima, M., et al. (2003). Reduced expression and loss of heterozygosity of the SDHD gene in colorectal and gastric cancer. *Oncol. Rep.* 10, 1375–1380.

Izuishi, K., Yamamoto, Y., Sano, T., Takebayashi, R., Nishiyama, Y., Mori, H., et al. (2012). Molecular mechanism underlying the detection of colorectal cancer by 18F-2-fluoro-2-deoxy-D-glucose positron emission tomography. *J. Gastrointest. Surg.* 16, 394–400. doi: 10.1007/s11605-011-1727-z

Jang, J. Y., Choi, Y., Jeon, Y. K., and Kim, C. W. (2008). Suppression of adenine nucleotide translocase-2 by vector-based siRNA in human breast cancer cells induces apoptosis and inhibits tumor growth *in vitro* and *in vivo*. *Breast Cancer Res.* 10:R11. doi: 10.1186/bcr1857

Jose, C., and Rossignol, R. (2013). Rationale for mitochondria-targeting strategies in cancer bioenergetic therapies. *Int. J. Biochem. Cell. Biol.* 45, 123–129. doi: 10.1016/j.biocel.2012.07.005

Kaambre, T., Chekulayev, V., Shevchuk, I., Karu-Varikmaa, M., Timohhina, N., Tepp, K., et al. (2012). Metabolic control analysis of cellular respiration *in situ* in intraoperational samples of human breast cancer. *J. Bioenerg. Biomembr.* 44, 539–558. doi: 10.1007/s10863-012-9457-9

Kholodenko, B. N., Demin, O. V., and Westerhoff, H. V. (1993). 'Channelled' pathways can be more sensitive to specific regulatory signals. *FEBS Lett.* 320, 75–78. doi: 10.1016/0014-5793(93)81661-I

Kholodenko, B. N., and Westerhoff, H. V. (1993). Metabolic channelling and control of the flux. *FEBS Lett.* 320, 71–74. doi: 10.1016/0014-5793(93)81660-R

Kunz, W. S., Kuznetsov, A. V., Clark, J. F., Tracey, I., and Elger, C. E. (1999). Metabolic consequences of the cytochrome c oxidase deficiency in brain of copper-deficient Mo(vbr) mice. *J. Neurochem.* 72, 1580–1585. doi: 10.1046/j.1471-4159.1999.721580.x

Kuznetsov, A. V., Tiivel, T., Sikk, P., Kaambre, T., Kay, L., Daneshrad, Z., et al. (1996). Striking differences between the kinetics of regulation of respiration by ADP in slow-twitch and fast-twitch muscles *in vivo*. *Eur. J. Biochem.* 241, 909–915. doi: 10.1111/j.1432-1033.1996.00909.x

Kuznetsov, A. V., Veksler, V., Gellerich, F. N., Saks, V., Margreiter, R., and Kunz, W. S. (2008). Analysis of mitochondrial function *in situ* in permeabilized muscle fibers, tissues and cells. *Nat. Protoc.* 3, 965–976. doi: 10.1038/nprot.2008.61

Kuznetsov, A. V., Winkler, K., Kirches, E., Lins, H., Feistner, H., and Kunz, W. S. (1997). Application of inhibitor titrations for the detection of oxidative phosphorylation defects in saponin-skinned muscle fibers of patients with mitochondrial diseases. *Biochim. Biophys. Acta* 1360, 142–150. doi: 10.1016/S0925-4439(96)00072-5

Lenaz, G., and Genova, M. L. (2009). Structural and functional organization of the mitochondrial respiratory chain: a dynamic super-assembly. *Int. J. Biochem. Cell. Biol.* 41, 1750–1772. doi: 10.1016/j.biocel.2009.04.003

Lenaz, G., and Genova, M. L. (2010). Structure and organization of mitochondrial respiratory complexes: a new understanding of an old subject. *Antioxid. Redox. Signal.* 12, 961–1008. doi: 10.1089/ars.2009.2704

Lenaz, G., Baracca, A., Barbero, G., Bergamini, C., Dalmonte, M. E., Del Sole, M., et al. (2010). Mitochondrial respiratory chain

super-complex I-III in physiology and pathology. *Biochim. Biophys. Acta* 1797, 633–640. doi: 10.1016/j.bbabio.2010.01.025

Marin-Hernandez, A., Rodriguez-Enriquez, S., Vital-Gonzalez, P. A., Flores-Rodriguez, F. L., Macias-Silva, M., Sosa-Garrocho, M., et al. (2006). Determining and understanding the control of glycolysis in fast-growth tumor cells. Flux control by an over-expressed but strongly product-inhibited hexokinase. *FEBS J.* 273, 1975–1988. doi: 10.1111/j.1742-4658.2006.05214.x

Monge, C., Beraud, N., Tepp, K., Pelloux, S., Chahboun, S., Kaambre, T., et al. (2009). Comparative analysis of the bioenergetics of adult cardiomyocytes and non-beating HL-1 cells: respiratory chain activities, glycolytic enzyme profiles, and metabolic fluxes. *Can. J. Physiol. Pharmacol.* 87, 318–326. doi: 10.1139/Y09-018

Moreno-Sanchez, R., Rodriguez-Enriquez, S., Marin-Hernandez, A., and Saavedra, E. (2007). Energy metabolism in tumor cells. *FEBS J.* 274, 1393–1418. doi: 10.1111/j.1742-4658.2007.05686.x

Moreno-Sanchez, R., Saavedra, E., Rodriguez-Enriquez, S., Gallardo-Perez, J. C., Quezada, H., and Westerhoff, H. V. (2010). Metabolic control analysis indicates a change of strategy in the treatment of cancer. *Mitochondrion* 10, 626–639. doi: 10.1016/j.mito.2010.06.002

Moreno-Sanchez, R., Saavedra, E., Rodriguez-Enriquez, S., and Olin-Sandoval, V. (2008). Metabolic control analysis: a tool for designing strategies to manipulate metabolic pathways. *J. Biomed. Biotechnol.* 2008, 597913. doi: 10.1155/2008/597913

Patra, S., Bera, S., Sinharoy, S., Ghoshal, S., Ray, S., Basu, A., et al. (2008). Progressive decrease of phosphocreatine, creatine and creatine kinase in skeletal muscle upon transformation to sarcoma. *FEBS J.* 275, 3236–3247. doi: 10.1111/j.1742-4658.2008.06475.x

Pedersen, P. L. (2008). Voltage dependent anion channels (VDACs): a brief introduction with a focus on the outer mitochondrial compartment's roles together with hexokinase-2 in the "Warburg effect" in cancer. *J. Bioenerg. Biomembr.* 40, 123–126. doi: 10.1007/s10863-008-9165-7

Queiros, O., Preto, A., Pacheco, A., Pinheiro, C., Azevedo-Silva, J., Moreira, R., et al. (2012). Butyrate activates the monocarboxylate transporter MCT4 expression in breast cancer cells and enhances the antitumor activity of 3-bromopyruvate. *J. Bioenerg. Biomembr.* 44, 141–153. doi: 10.1007/s10863-012-9418-3

Rossignol, R., Letellier, T., Malgat, M., Rocher, C., and Mazat, J. P. (2000). Tissue variation in the control of oxidative phosphorylation: implication for mitochondrial diseases. *Biochem. J.* 347(Pt 1), 45–53. doi: 10.1042/0264-6021:3470045

Rostovtseva, T. K., Sheldon, K. L., Hassanzadeh, E., Monge, C., Saks, V., Bezrukov, S. M., et al. (2008). Tubulin binding blocks mitochondrial voltage-dependent anion channel and regulates respiration. *Proc. Natl. Acad. Sci. U.S.A.* 105, 18746–18751. doi: 10.1073/pnas.0806303105

Saks, V., Guzun, R., Timohhina, N., Tepp, K., Varikmaa, M., Monge, C., et al. (2010). Structure-function relationships in feedback regulation of energy fluxes *in vivo* in health and disease: mitochondrial interactosome. *Biochim. Biophys. Acta* 1797, 678–697. doi: 10.1016/j.bbabio.2010.01.011

Salem, A. F., Whitaker-Menezes, D., Lin, Z., Martinez-Outschoorn, U. E., Tanowitz, H. B., Al-Zoubi, M. S., et al. (2012). Two-compartment tumor metabolism: autophagy in the tumor microenvironment and oxidative mitochondrial metabolism (OXPHOS) in cancer cells. *Cell Cycle* 11, 2545–2556. doi: 10.4161/cc.20920

Small, J. R. (1993). Flux control coefficients determined by inhibitor titration: the design and analysis of experiments to minimize errors. *Biochem. J.* 296(Pt 2), 423–433.

Small, J. R., and Fell, D. A. (1990). Covalent modification and metabolic control analysis. Modification to the theorems and their application to metabolic systems containing covalently modifiable enzymes. *Eur. J. Biochem.* 191, 405–411. doi: 10.1111/j.1432-1033.1990.tb19136.x

Sotgia, F., Whitaker-Menezes, D., Martinez-Outschoorn, U. E., Flomenberg, N., Birbe, R. C., Witkiewicz, A. K., et al. (2012). Mitochondrial metabolism in cancer metastasis: visualizing tumor cell mitochondria and the "reverse Warburg effect" in positive lymph node tissue. *Cell Cycle* 11, 1445–1454. doi: 10.4161/cc.19841

Tager, J. M., Wanders, R. J., Groen, A. K., Kunz, W., Bohnensack, R., Kuster, U., et al. (1983). Control of mitochondrial respiration. *FEBS Lett.* 151, 1–9. doi: 10.1016/0014-5793(83)80330-5

Tepp, K., Shevchuk, I., Chekulayev, V., Timohhina, N., Kuznetsov, A. V., Guzun, R., et al. (2011). High efficiency of energy flux controls within mitochondrial interactosome in cardiac intracellular energetic units. *Biochim. Biophys. Acta* 1807, 1549–1561. doi: 10.1016/j.bbabio.2011.08.005

Tepp, K., Timohhina, N., Chekulayev, V., Shevchuk, I., Kaambre, T., and Saks, V. (2010). Metabolic control analysis of integrated energy metabolism in permeabilized cardiomyocytes - experimental study. *Acta Biochim. Pol.* 57, 421–430.

Warburg, O. (1956). On the origin of cancer cells. *Science* 123, 309–314. doi: 10.1126/science.123.3191.309

Warburg, O. H., and Dickens, F. (1930). *The Metabolism of Tumours.* London: Constable.

Whitaker-Menezes, D., Martinez-Outschoorn, U. E., Lin, Z., Ertel, A., Flomenberg, N., Witkiewicz, A. K., et al. (2011). Evidence for a stromal-epithelial "lactate shuttle" in human tumors: MCT4 is a marker of oxidative stress in cancer-associated fibroblasts. *Cell Cycle* 10, 1772–1783. doi: 10.4161/cc.10.11.15659

Witkiewicz, A. K., Whitaker-Menezes, D., Dasgupta, A., Philp, N. J., Lin, Z., Gandara, R., et al. (2012). Using the "reverse Warburg effect" to identify high-risk breast cancer patients: stromal MCT4 predicts poor clinical outcome in triple-negative breast cancers. *Cell Cycle* 11, 1108–1117. doi: 10.4161/cc.11.6.19530.

Conflict of Interest Statement: The authors declare that the research was conducted in the absence of any commercial or financial relationships that could be construed as a potential conflict of interest.

Received: 25 January 2013; paper pending published: 25 February 2013; accepted: 05 June 2013; published online: 28 June 2013.

*Citation: Kaambre T, Chekulayev V, Shevchuk I, Tepp K, Timohhina N, Varikmaa M, Bagur R, Klepinin A, Anmann T, Koit A, Kaldma A, Guzun R, Valvere V and Saks V (2013) Metabolic control analysis of respiration in human cancer tissue. Front. Physiol. **4**:151. doi: 10.3389/fphys.2013.00151*

This article was submitted to Frontiers in Mitochondrial Research, a specialty of Frontiers in Physiology.

frontiers in
PHYSIOLOGY

ORIGINAL RESEARCH ARTICLE
published: 17 April 2013
doi: 10.3389/fphys.2013.00074

Diminished exercise capacity and mitochondrial *bc1* complex deficiency in tafazzin-knockdown mice

Corey Powers, Yan Huang, Arnold Strauss and Zaza Khuchua*

Division of Molecular Cardiovascular Biology, Cincinnati Children's Medical Center, Cincinnati, OH, USA

Edited by:
Sabzali Javadov, University of Puerto Rico School of Medicine, Puerto Rico

Reviewed by:
Lawrence J. Prochaska, Wright State University, USA
John Hollander, West Virginia University School of Medicine, USA
Andrey V. Kozlov, Ludwig Boltzmann Institute for Experimental and Clinical Traumatology, Austria

***Correspondence:**
Zaza Khuchua, Division of Molecular Cardiovascular Biology, Cincinnati Children's Hospital Medical Center,240 Albert Sabin Way, S4.236,Cincinnati, OH 45229, USA.
e-mail: zaza.khuchua@cchmc.org

The phospholipid, cardiolipin, is essential for maintaining mitochondrial structure and optimal function. Cardiolipin-deficiency in humans, Barth syndrome, is characterized by exercise intolerance, dilated cardiomyopathy, neutropenia, and 3-methyl-glutaconic aciduria. The causative gene is the mitochondrial acyl-transferase, tafazzin, that is essential for remodeling acyl chains of cardiolipin. We sought to determine metabolic rates in tafazzin-deficient mice during resting and exercise, and investigate the impact of cardiolipin-deficiency on mitochondrial respiratory chain activities. Tafazzin-knockdown in mice markedly impaired oxygen consumption rates during an exercise, without any significant effect on resting metabolic rates. CL-deficiency resulted in significant reduction of mitochondrial respiratory reserve capacity in neonatal cardiomyocytes that is likely to be caused by diminished activity of complex-III, which requires CL for its assembly and optimal activity. Our results may provide mechanistic insights of Barth syndrome pathogenesis.

Keywords: Barth syndrome, tafazzin, complex-III, cardiolipins, exercise intolerance, mouse models

INTRODUCTION

Phospholipids are building blocks of biological membranes. The mitochondrial inner membrane contains a unique phospholipid – cardiolipin that constitutes about 20% of total phospholipids (Schlame et al., 2005). The predominant form of CL in mammals is tetra-linoleoyl cardiolipin, or L4CL, which contains 4 linoleic acyl side chains (C18:2, *n*−6) (Schlame et al., 1993). L4CL is especially enriched in mitochondria of cardiac and skeletal muscles. CL is essential for assembly of respiratory chain (RC) complexes and their optimal activities (Fry and Green, 1981; Zhang et al., 2002, 2005; Pfeiffer et al., 2003; Acehan et al., 2011).

One of the clues to the importance of L4CL in mitochondrial function was provided when it was recognized that L4CL is markedly deficient in the mitochondria of patients with Barth syndrome (BTHS) (MIM 302060) (Valianpour et al., 2002). BTHS is a rare X-linked recessive genetic disorder caused by mutations in tafazzin gene on the X-chromosome. Taz is a mitochondrial transacylase required for CL remodeling and formation of L4CL. BTHS is characterized by dilated cardiomyopathy, exercise intolerance, chronic fatigue, skeletal muscle weakness, and cyclic or intermittent neutropenia.

Tafazzin-knockdown (Taz-KD) creates a mouse model of BTHS that resulted in marked reduction of L4CL both in cardiac and skeletal muscles (Acehan et al., 2010; Soustek et al., 2010). Prenatal loss of taz-deficient embryos due to cardiac abnormalities was reported at E12.5–E14.5 (Phoon et al., 2012). Transmission electron microscopy revealed mitochondrial damage and excessive mitophagy in striated muscles, consistent with findings in human BTHS samples (Acehan et al., 2010; Soustek et al., 2010).

Currently it is unknown how cardiolipin-deficiency affects principal energy-producing systems, such as RC complexes, in mammalian mitochondria. In the current study, we examine the impact of CL-deficiency on exercise capacity, oxygen utilization, respiratory exchange ratio (RER), and energy expenditure at rest and during exercise in Taz-KD mice. In addition, Taz-KD drastically diminishes mitochondrial respiratory reserve capacity, which is caused by reduced activity of mitochondrial RC complex III in CL-depleted mitochondria.

MATERIALS AND METHODS

ANIMAL PROCEDURES

All animal studies were approved by our Institutional Animal Care and Use Committee. Animals were housed in micro-isolator cages with temperature-controlled conditions under a 14/10 h light/dark cycle with free access to drinking water and food. Taz-KD was induced by introduction of doxycycline, as described previously (Acehan et al., 2010). Genotyping was performed by PCR analysis of tail genomic DNA (Acehan et al., 2010). Only males were used in experiments.

EXERCISE ON TREADMILL AND OPEN-CIRCUIT CALORIMETRY

Metabolic rates were measured at rest and during exercise as described by G. Faldt et al. (2004). The resting oxygen consumption and carbon dioxide production rates (VO_2 and VCO_2, respectively) were measured at 31°C (thermoneutrality) every 10 min using the Oxymax system (Columbus Instrument, Columbus, OH, USA) for 24 h and normalized to mouse body weight. Normalized VO_2 and VCO_2 values at cold (+5°C) were measured every 10 min during a 5 h-period. Measurements were performed in metabolic chambers without food, but with free access to water. Fresh air was delivered into chambers with an electric pump.

Mice were exercised on a sealed motorized treadmill that had adjustable speed and inclination and was equipped with an electric shock-delivering grid. Electric shock intensity was set to 1 mA. Fresh air was delivered with an electric pump. Gas samples from the treadmill chamber were collected every 30 s and analyzed by the Oxymax system for measurement of VO_2 and VCO_2. RER, also known as the respiratory quotient, was calculated as VO_2/VCO_2. Open-circuit calorimetry results were calculated using Clax software (Columbus Instrument, Columbus, OH, USA).

CULTURE OF CARDIOMYOCYTES AND MITOCHONDRIAL RESPIRATION MEASUREMENT

All reagents were purchased from Sigma Aldrich (St. Louis, MO, USA), unless otherwise noted. Neonatal cardiac myocytes were isolated from the hearts of 1 day old WT and Taz-KD neonatal mice as previously described (Khuchua et al., 1998). Viable cells were counted with a hemocytometer and plated at 20,000–50,000 cells/well density on laminin-coated XF24 plates. Cells were cultured for 48–72 h in a CO_2 incubator at 37°C. The cardiomyocytes genotype in each well was determined by PCR-genotyping of tail samples from the corresponding carcass. One hour before measurements on an XF24 extracellular flux analyzer (Seahorse Bioscience, Billerica, MA, USA), cells were removed from the CO_2 incubator and placed at 37°C in normal atmosphere, and media was replaced with 500 μl FX assay media composed of 143 mM NaCl, 5.4 mM KCl, 0.8 mM $MgSO_4$, 0.91 mM Na_2HPO_4, 2 mM glutamine, 2 mg/ml BSA, and 15 mg/L phenol red, pH 7.4. Stock solutions (X10) of oligomycin, FCCP, and rotenone were prepared in FX assay media and loaded into injection ports A, B, and C, respectively. Measurements were obtained at 37°C.

ISOLATION OF MITOCHONDRIA

Mitochondria were isolated from fresh adult mouse cardiac muscle. Animals were euthanized using ketamine (100 mg/kg), and hearts were quickly excised and placed in ice-cold 0.9% NaCl solution. All procedures were performed on ice. Blood was removed by washing, and hearts were minced with fine scissors. Minced tissues were transferred into Dounce glass-Teflon homogenizer and washed three times with 4 ml of ice-cold mitochondria isolation media (MIM) composed of 0.3 M sucrose, 10 mM Tris-HCl (pH 7.4), and 1 mM EDTA. One ml of ice-cold 0.025% trypsin-EDTA solution (Gibco) was added to each sample, gently mixed and incubated on ice for 7 min. Trypsin activity was quenched by addition of 3 ml of MIM with 4 mg/ml BSA. Tissues were gently homogenized with a Teflon pestle using a motorized drive. Homogenates were centrifuged at 1000 × *g* for 5 min at 4°C. Supernatants were transferred into new tubes and mitochondria sedimented by centrifugation at 8000 × *g* for 10 min at 4°C. Mitochondrial pellets were washed three times with MIM containing 2 mg/ml BSA and finally resuspended in 50 μl MIM with 2 mg/ml BSA (Roche). Mitochondrial protein concentration was determined using the DC protein assay (BioRad). Mitochondrial preparations were aliquoted, frozen in liquid nitrogen, and stored at −80°C.

ENZYMATIC ACTIVITIES

Activities of mitochondrial RC complexes were determined spectrophotometrically using Shimadzu UV-1700 spectrophotometer in digitonin-treated isolated mitochondria as described earlier (Barrientos, 2002; Wibom et al., 2003) and normalized to citrate synthase (CS) activities.

For pretreatment, 10 μl frozen mitochondrial pellet (approximately 200 μg) was resuspended in 90 μl of 20 mM Tris-HCl, 120 mM KCl, 2 mg/ml digitonin (Life Technologies), 0.5 mg/ml BSA, and kept on ice.

NADH: coenzyme Q (complex I)

C-I assay mixture contained following final composition: 10 μl pretreated mitochondria, 0.97 ml of 5 mM KH_2PO_4 (pH 7.5), 5 mM $MgCl_2$, 0.24 mM CoQ1, 0.5 mM KCN, 1 mg/ml BSA, and 2.4 μg/ml antimycin A. Reaction was initiated with 0.02 mM NADH and reduction of absorbance at 340 nm was recorded with spectrophotometer before and after addition of rotenone (final concentration 2 μg/ml).

NADH: cytochrome c reductase (complex I + III)

Ten microliters of pretreated mitochondria were incubated for 5 min at 30°C in 0.98 ml of 5 mM KH_2PO_4 (pH 7.5), 5 mM $MgCl_2$, 0.24 mM CoQ1, 0.5 mM KCN, 1 mg/ml BSA, 0.12 mM cytochrome *c* (oxidized form). Reaction was initiated with 0.02 mM NADH and increase of absorbance at 550 nm was recorded with spectrophotometer before and after addition of antimycin A (final concentration 2 μg/ml).

Cytochrome c oxidase (complex IV)

Non-enzymatic oxidation of cytochrome c was followed at 550 nm in 0.99 ml of 50 mM KH_2PO_4 (pH 7.5), 2 μg/ml rotenone, and 0.03 mM reduced cytochrome *c*. Reduced cytochrome *c* was prepared using ascorbate (Birch-Machin et al., 1994). Ten microliters of pretreated mitochondria were added to reaction buffer and enzyme-catalyzed cytochrome c oxidation was measured before and after addition of 0.20 mM KCN.

Mitochondria ATPse activity (Complex V)

C-V assay media containing 50 mM Tris (pH 8.0), 5 mg/ml BSA, 20 mM $MgCl_2$, 50 mM KCl, 15 μM FCCP, 5 μM antimycin A, 10 mM phosphoenol pyruvate, 2.5 mM ATP, 2 U/ml of lactate dehydrogenase and pyruvate kinase, and 0.02 mM NADH. Reaction was initiated by adding 10 μl of pretreated mitochondria and reaction was followed by reduction of NADH absorbance at 340 nm before and after addition 2 μM of oligomycin.

Citrate synthase

Citrate synthase activity was measured at 412 nm. CS assay media contained 0.1 mM 5,5′-dithiobis (2-nitrobenzoic acid); 3-carboxy-4-nitrophenyl disulfide (DTNB), 0.25% Triton X-100, 0.5 mM oxaloacetate, 0.31 mM acetyl CoA, 50 mM Tris-HCl, pH 8.0. CS activity was calculated by increasing absorbance at 412 nm using extinction coefficient for TNB 13.6 $mM^{-1} \times cm^{-1}$.

STATISTICAL ANALYSIS

Differences between groups were assessed for significance by unpaired Student's *t*-test with the assumption of equal variances. Results were considered statistically significant if the *P* value

was <0.05. Results are expressed as arithmetic means ± SEM. Statistical calculations were performed using the Prism program (GraphPad Software, San Diego, CA, USA).

RESULTS

ENERGY EXPENDITURE AND RER DURING REST AND FORCED EXERCISE ON TREADMILL

Impaired ability to withstand physiological and environmental stressors, such as physical exercise or cold exposure, is a common feature for many mitochondrial myopathies. Exercise intolerance is one of the main clinical manifestations of BTHS in humans and has been linked to reduced ability of CL-deficient mitochondria to extract and utilize oxygen from blood (Spencer et al., 2011). Cold-intolerance has been reported in mouse models of fatty acid oxidation deficiency (Exil et al., 2006) and uncoupling protein knockout mice (Enerback et al., 1997). We investigated whether the mitochondrial abnormalities in striated muscles in Taz-KD model affect the ability of mice to withstand physiological and environmental stressors, such as physical exercise and cold environment. We were particularly interested if intolerance to stressors became manifest prior to the cardiac phenotype that becomes apparent at 7–8 months of age. Therefore, for exercise and indirect calorimetry experiments, we selected 4–5 month old WT and Taz-deficient male littermates. Metabolic indices in WT and Taz-KD mice were analyzed at rest and during exercise using an open-circuit indirect calorimetry.

First, we analyzed the resting metabolic rate at thermoneutrality (+31°C) and in the cold (+5°C). Mice were placed in the temperature-controlled metabolic chambers without food but with free access to water. Oxygen consumption and CO_2 production rates were measured every 10 min in small gas samples taken from the chamber using an online open-circuit indirect calorimetry system. Analysis showed that there were no differences in the resting oxygen consumption rates (VO_2) between Taz-KD and WT groups at +31°C. Exposure to cold significantly increased VO_2 in both experimental groups, but, again, values did not differ between WT and Taz-KD mice (**Figure 1A**). These results demonstrate that thermogenic capacity is not affected by CL-deficiency and that Taz-KD mice can adjust well and tolerate a cold environment. Monitoring of oxygen consumption during a 24-h-period at +31°C revealed that VO_2 values follow periodic oscillating patterns, as shown on **Figure 1B**. Similarly, oscillating patterns of VO_2 were observed in WT mice, when placed in cold environment (**Figure 1C**). In contrast, Taz-KD mice VO_2 oscillation amplitudes were significantly less than those for WT controls.

Next, we subjected mice to forced exercise on a treadmill. After initial resting on the treadmill for 30 min to acclimate the animals, the test was started with a 10% incline and 5 m/min speed. Speed was increased step-wise by 5 m/min every 5 min to a final speed of 25 m/min. Thus, the duration of an exercise session was 36.8 min and the distance traveled was 507.4 m. Taz-KD mice repeatedly failed to stay on the belt at 15 m/min and 10% inclination, and none of the Taz-KD mice were able to sustain running when the treadmill speed more than 20 m/min. In contrast, WT control mice had no difficulty maintaining exercise at this speed. Because Taz-KD mice could not sustain exercise on the treadmill at 10% incline, we reduced the incline to 5%, and mice of both experimental groups were able to tolerate this workload during the entire 36.8 min session.

Indirect calorimetric analysis revealed that VO_2 values sharply rose with increased workload in Taz-KD animals, while those for WT mice remained relatively steady (**Figure 2A**). Paradoxically, with further increases of running speed, VO_2 values for Taz-KD mice declined, but WT mice VO_2 continued to rise with increasing workload (**Figure 2A**). Analysis revealed a sudden drop of RER values during exercise with increasing speed (**Figure 2B**). This drop of RER values was common for all tested WT mice. Surprisingly this phenomenon is either absolutely absent or significantly subtler in Taz-KD mice (**Figure 2B**). Blood glucose and lactate were analyzed at the end of exercise sessions. Blood glucose levels were not significantly different between WT and Taz-KD groups (**Figure 2C**); however, lactate was significantly elevated in blood samples of Taz-KD mice compared to WT controls (**Figure 2D**), indicative of impaired aerobic energy metabolism in Taz-deficient mice.

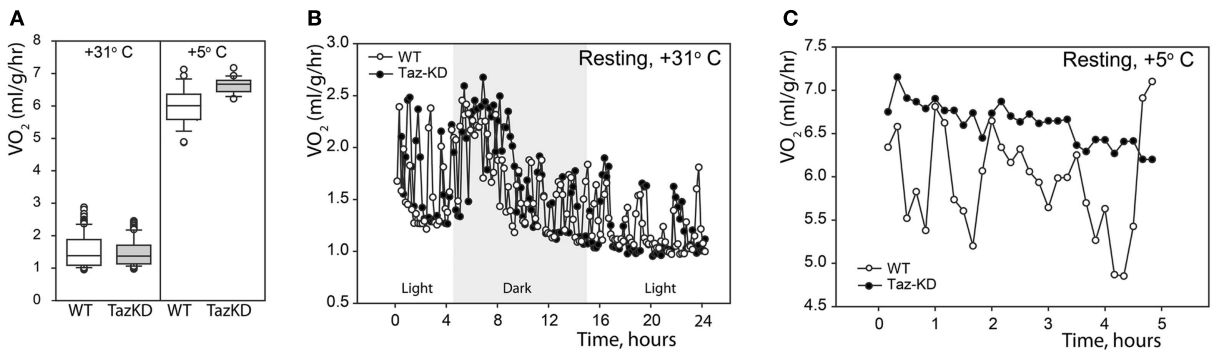

FIGURE 1 | Resting physiological indices of Taz-KD and WT mice at thermoneutrality (+31°C) and in the cold (+5°C). (A) Whisker box plot of normalized oxygen consumption rates of WT (white) and Taz-KD (gray) mice at +31 and +5°C. **(B)** Representative plot of normalized oxygen consumption of WT and Taz-KD mice during a 24-h period at +31°C. Dark and light cycles are shown. **(C)** Representative plot of normalized oxygen consumption of WT and Taz-KD mice during a 5-h period at +5°C.

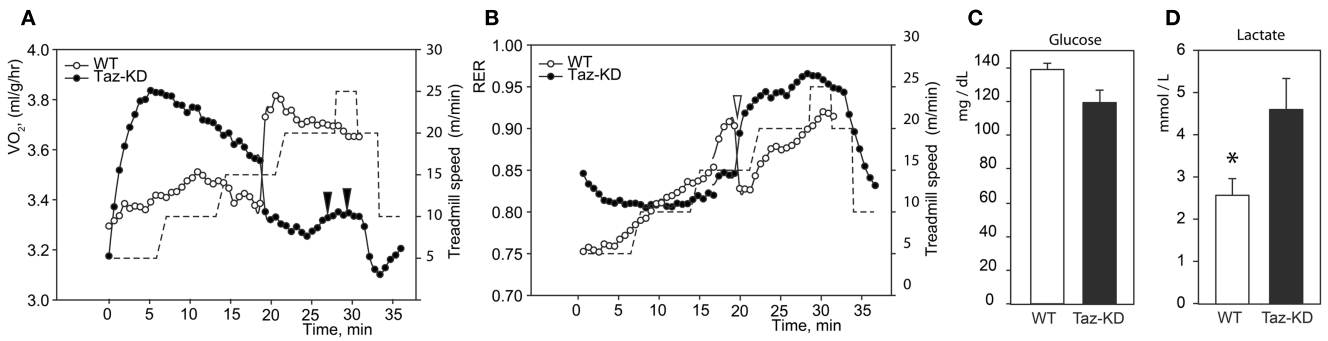

FIGURE 2 | Representative recordings of physiological parameters of Taz-KD and WT mice during forced exercise on a treadmill. (A,B) O_2 consumption rate and respiration exchange ratio (RER) were monitored continuously during the entire session of forced exercise. Taz-KD mice repeatedly failed to stay on treadmill [black arrowheads on **(A)**], while WT controls remained on the treadmill belt during the entire test. Sudden drops of RER values were present in all tested WT mice [white arrowhead on **(B)**] and were totally absent or substantially blunted in Taz-KD mice. Treadmill speed is shown with dashed line [right hand axis of **(A,B)**]. Blood glucose **(C)** and lactate **(D)** levels were measured in WT and Taz-KD mice immediately after completion of exercise testing ($n = 4$). $^*P < 0.05$.

METABOLIC PROFILING OF NEONATAL CARDIOMYOCYTES

Previously, we demonstrated that L4CL content is greatly reduced in Taz-deficient cardiac mitochondria (Acehan et al., 2010). Reduction of L4CL is likely to affect enzymatic activities of the electron transport chain. To further characterize defects of mitochondrial metabolism within the context of intact cells, we prepared primary cultures of neonatal cardiomyocytes from WT and Taz-KD mice. We analyzed mitochondrial oxygen consumption rate (OCR) and extracellular acidification rate (ECAR) in cultured neonatal cardiomyocytes using the XF24 Seahorse bioanalyzer (**Figure 3**). First, basal respiration rates of cardiomyocytes were determined (**Figure 3A**). Following the measurements of basal OCR values, oligomycin, a complex V inhibitor, was introduced into the respiration media to distinguish ATP-linked respiration from the proton leak. As shown on **Figure 3A**, basal respiration rates and proton leak values were not different between WT and taz-deficient cardiomyocytes. Following oligomycin injection, maximal, or uncoupled respiration rate was determined by injecting wells with 3.8 μM FCCP. Taz-KD cardiomyocytes exhibited approximately 40% lower maximal respiration values than WT controls; presumably signifying reduced activities of ETC complexes in CL-deficient mitochondria.

Coincident with this decrease in mitochondrial oxygen consumption, we noted that the basal ECAR in Taz-KD cardiomyocytes was higher than in WT controls, consistent with an increased reliance on glycolysis (**Figures 3C,D**). This metabolic shift away from aerobic respiration and toward cytosolic glycolysis in CL-deficient cardiomyocytes probably indicates a compensatory remodeling of cellular metabolism in order to maintain cellular energy homeostasis in the setting of dysfunctional mitochondria.

MEASUREMENT OF ACTIVITIES OF INDIVIDUAL MITOCHONDRIAL RC COMPLEXES

Reduction of maximal respiration rates in Taz-KD cells suggest that the mitochondrial oxidative phosphorylation system is damaged and that activities of RC complexes are compromised in CL-depleted mitochondria. However, it is not clear which RC complex is most affected by CL-insufficiency.

We examined activities of individual mitochondrial complexes in cardiac mitochondria. Mitochondrial fractions were isolated from doxycyline-fed WT and Taz-KD mice of 3–4 months of age. Mitochondria were solubilized with digitonin. Enzymatic activities of complex I (NADH-dehydrogenase), complex I–III segment, complex IV (cytochrome c oxidase), and complex V (mitochondrial ATPase) were measured spectrophotometrically. Activities of mitochondrial RC complexes were normalized to CS activities for each mitochondrial preparation.

We found that rotenone-sensitive complex-I, cyanide-sensitive complex IV, and oligomycin-sensitive complex V activities were not significantly affected by CL-deficiency in Taz-KD cardiac mitochondria. In contrast, activity of RC segment complex I–III (cytochrome *c* oxidoreductase or C-I–C-III) was reduced in Taz-KD mitochondria by 40% (**Table 1**, **Figure 4A**), suggesting that mitochondrial complex III activity is diminished in CL-deficient mitochondria.

DISCUSSION

In the present study, we investigated mechanisms of exercise intolerance in a mouse model of BTHS. Exercise intolerance has been recognized as one of the hallmarks of human BTHS. It has been suggested that exercise intolerance in BTHS patients is caused by diminished extraction/utilization of oxygen by skeletal muscle and impaired cardiac contractile reserve (Spencer et al., 2011). However, molecular mechanisms underlying the effects of CL-deficiency on mitochondrial function in muscle cells remain unknown.

We demonstrated that CL-deficiency in Taz-deficient mice had no significant effect on resting metabolism in either warm or cold environments. Both WT and Taz-KD mice equally responded to cold stress by robustly increasing oxygen consumption. Cold-intolerance has been described in genetic models with defects in mitochondrial energy-producing systems. However, our results demonstrated that Taz-KD mice did not show any signs of distress

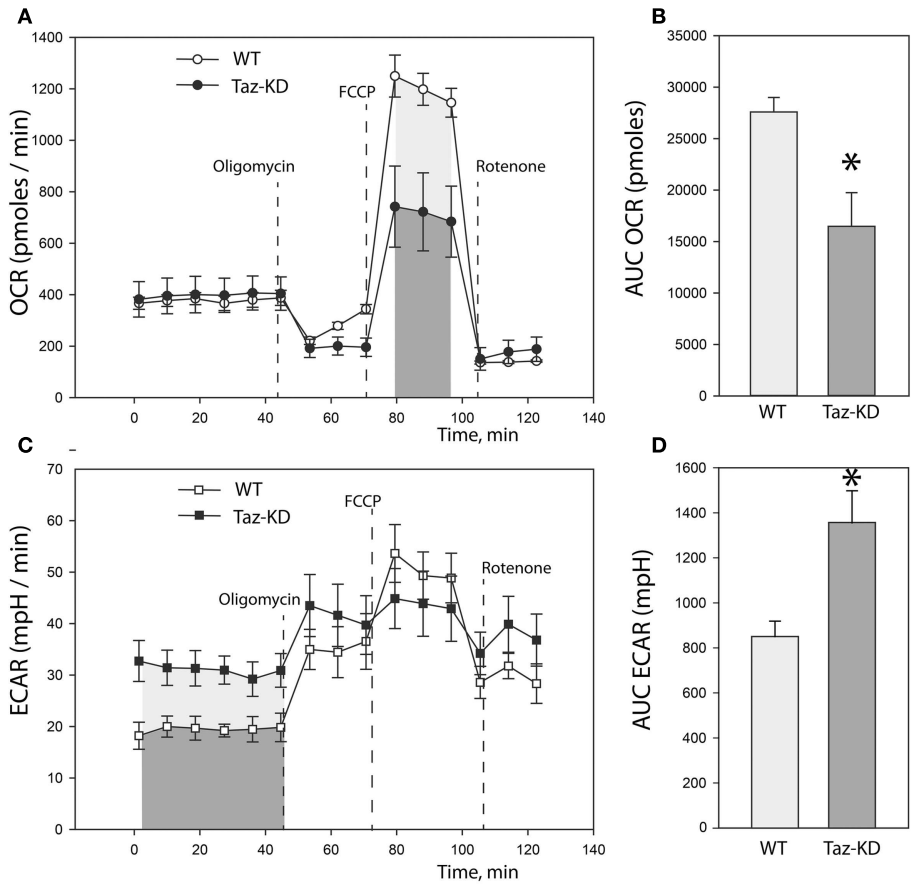

FIGURE 3 | Metabolic profiling of neonatal cardiomyocytes from WT and Taz-KD mice. (A) Basal and stimulated mitochondrial oxygen consumption rates (OCR) in cultured cardiomyocytes. OCR traces are expressed as pmol O_2 per min in WT and Taz-KD cardiomyocytes and normalized to cell number. Vertical dashed lines indicate the times of addition of oligomycin (2 μM), FCCP (3.7 μM), and rotenone (2 μM). **(B)** Total oxygen consumption (reserve capacity) is significantly lower in Taz-KD cardiomyocytes compared with the WT controls (*$p < 0.007$). Mitochondrial reserve capacity was determined by calculating the total area under the curve (AUC) of FCCP-stimulated respiration trace [shaded areas on **(A)**]. **(C)** Extracellular acidification rates (ECAR) of WT and Taz-KD neonatal cardiomyocytes. ECAR rates, expressed as mpH per min in WT and Taz-KD cardiomyocytes and normalized to cell numbers. **(D)** ECAR values at basal conditions were significantly higher for Taz-KD cardiomyocytes (*$p < 0.002$), consistent with an increase reliance of Taz-KD cells on glycolysis. Extracellular acidification values were determined by calculating AUC of ECAR tracing at basal metabolic state [shaded areas on **(C)**]. The differences in means in **(B,D)** were assessed by Tukey's post-hoc test.

Table 1 | Enzymatic activities of mitochondrial respiratory chain complexes in WT and Taz-KD mitochondria.

	WT	Taz-KD	
Complex I	0.215 ± 0.020 (n = 6)	0.227 ± 0.028 (n = 4)	ns
Complex I – III	1.289 ± 0.393 (n = 5)	0.574 ± 0.105 (n = 5)	$P < 0.05$
Complex IV	4.382 ± 0.085 (n = 6)	3.960 ± 0.269 (n = 4)	ns
Complex V	0.357 ± 0.059 (n = 3)	0.388 ± 0.084 (n = 3)	ns

Values are normalized to citrate synthase activities and presented as a mean ± SEM (n, number of assays; ns, not statistically significant).

while exposed to cold environment (+5°C) for more than 5 h. More detailed analysis of metabolic parameters in a warm environment revealed that OCR of WT control mice follow periodic oscillating patterns, perhaps reflecting murine circadian activities (**Figure 1B**). Similar oscillating patterns of O_2 consumption rates were observed in WT mice when placed in cold environment (**Figure 1C**). In contrast, in Taz-KD mice VO_2 oscillation was either completely absent or amplitudes were significantly reduced as compared to WT controls. These results may be indicative that mechanisms of dynamic regulation of whole-body metabolism are affected by CL-deficiency in mitochondria.

When subjected to forced exercise on treadmill, Taz-KD mice performed far more poorly than WT littermates. Taz-KD mice were not able to sustain a high-intensity exercise (20 m/min at 10% inclining) even for 30 s, while WT control littermates remained on the belt at this level of intense exercise. Open-circuit calorimetry during aerobic exercise on the treadmill revealed that, in response to step-wise increasing intensity of workload, mice progressively move metabolic reliance from mixed substrates (fat, carbohydrates, and amino acids) toward the carbohydrates. This shift in fuel preference is reflected as a gradual

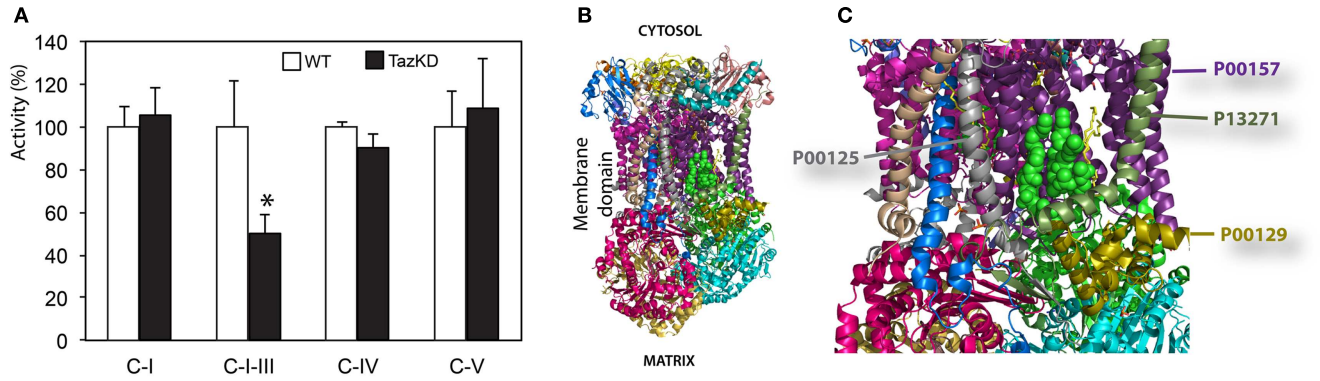

FIGURE 4 | Impaired complex-III activity in CL-deficient mitochondria. (A) Activities of individual respiratory chain complexes in isolated cardiac mitochondria of WT and Taz-KD mice. **(B)** The structure of bovine *bc1* complex (C-III) with bound phospholipid molecules (PDB entry 2AO6). Different polypeptides are shown with various colors. Sides facing cytosol and mitochondrial matrix sides are shown. **(C)** magnified view of phospholipids moiety in mitochondrial *bc1* complex. Two cardiolipin molecules are illustrated with green balls. Phosphatidyl-ethanolamine molecules are shown as yellow sticks. Polypeptides in close proximity to phospholipid molecules are shown: cytochrome c1 (P00125, gray), cytochrome b (P00157, purple), subunit 8, or ubiquinone-binding protein QP-C (P13271, dark olive) and subunit 7 (P00129, gold).

increase of RER values from 0.75 to 0.95 or higher with increasing workload. With further increases in running speed, RER values for Taz-KD mice sharply dropped, which indicates that WT mice dynamically shifted their reliance on metabolic substrates from predominantly carbohydrates (RER $\geq$ 0.9) to mixed substrates (RER $\leq$ 0.8). This switch, which was common for all tested WT mice, can be related to the "second wind" phenomenon in athletes (Bank and Chance, 1994). Surprisingly, this phenomenon is either absolutely absent or significantly reduced in Taz-KD mice. The "second wind" phenomenon is affected in humans with various inborn metabolic defects (Haller and Vissing, 2002, 2004; Vissing et al., 2005). Absence of a "second wind" may be further evidence that mechanisms of dynamic regulation of metabolism in response to energy demands are deficient in Taz-KD mice. Open calorimetry results are in good agreement with recently published data suggesting that BTHS patients have difficulties extracting oxygen from blood and/or utilizing it when performing an exercise on cycle ergometer (Spencer et al., 2011).

Cardiolipin molecules are associated with all RC complexes. Cardiolipin is essential for interactions of RC complexes and assembly of supercomplexes (Zhang et al., 2005). Metabolic profiling of neonatal cardiomyocytes revealed that CL-deficiency had no apparent effect on basal oxygen consumption level; however, maximal uncoupled respiration rate was markedly reduced in Taz-KD cardiomyocytes compared to WT controls. Reduction of maximal respiration rate in Taz-KD cells can be caused by diminished activity of mitochondrial complex-III in CL-depleted mitochondria. Mitochondrial complex III (C-III), also called cytochrome *bc1* complex, is composed of 11 subunits (PDB: 2A06), of which of only one, cytochrome *b*, is encoded by the mitochondrial genome. C-III catalyzes the transfer of electrons from reduced coenzyme Q to cytochrome c, with a concomitant translocation of protons across the inner mitochondrial membrane (Benit et al., 2009; Wenz et al., 2009; Gil Borlado et al., 2010). Bovine cardiac C-III contains four structurally incorporated CL molecules (Huang et al., 2005). The head groups of one cardiolipin molecule bind at the interface of cytochrome b (P00157) and subunit 7 (P00129) and might be important for the structural integrity of the complex (**Figures 4B,C**). Cardiolipin is essential for super-complex formation between C-III and C-IV in yeast mitochondria (Zhang et al., 2005). CL molecules may also participate in forming the environment necessary to promote substrate diffusion from the membrane to the active site and/or substrate exchange between sites of quinine/quinol catalysis within the complex (Palsdottir and Hunte, 2004).

Mitochondrial DNA (mtDNA) mutations in cytochrome *b (MT-CYB)* gene constitute a major cause of complex III deficiency and underlie a wide range of neuromuscular disorders (Gil Borlado et al., 2010), with exercise intolerance as a major symptom (Andreu et al., 1999). Ischemia-reperfusion injury in rat heart causes reduction of C-III with concomitant decrease of CL content in mitochondria (Petrosillo et al., 2003).

Reduced C-III activity perhaps may not be the only factor that results in diminished maximal respiration in Taz-KD cells. Other factors, such as limited lateral diffusion of electron-transporting carriers and destabilization of RC supercomplexes in CL-depleted mitochondria, cannot be entirely excluded. It has been demonstrated that CL is required for the assembly of supramolecular complexes of complex-V (ATP synthase complex) (Acehan et al., 2011). In a recent publication (Kiebish et al., 2013) it has been shown that Taz-knockdown affects C-III activity in cardiac mitochondria without any effects on C-I, C-II, and C-IV activities. However, in contrast with our studies the authors observed a relatively small, but statistically significant deficiency in C-V activity in Taz-KD cardiac mitochondria. This discrepancy with our results may be explained by differences in temperatures of C-V assays. In our experiments, we measured C-V activity at 30°C, while Kiebish et al. at 37°C. It is plausible that C-V deficiency is not perceptible at 30°C, but manifests at higher temperature. Moreover, in our

C-V assay, we measured ATP hydrolysis rate, the reverse reaction to ATP synthesis. It is possible that the presence of CL is critical for the ATP synthase reaction, but has less effect on ATP hydrolysis.

Possible enhanced production of reactive oxygen species (ROS) in CL-deficient mitochondria and increased ROS-mediated damage of mtDNA may be additional pathogenic factors in developing of phenotype in Taz-KD mice and BTHS patients.

In summary, we report exercise intolerance in Taz-KD mice with markedly impaired oxygen utilization capability at high workload, but without apparent deficiencies at rest. CL-deficiency resulted in significant reductions of maximal uncoupled mitochondrial respiration rate, or mitochondrial reserve in Taz-KD neonatal cardiomyocytes. Reduction of mitochondrial reserve in Taz-KD cardiomyocytes is likely caused by diminished activity of complex-III, which requires CL for its assembly and optimal activity. Our results provide a mechanistic insight of pathogenesis of BTHS and may be useful for designing potential therapeutic interventions, such as increasing the mitochondrial RC efficiency by supplementations with vitamins K_2 and C (Argov et al., 1986; Vos et al., 2012).

ACKNOWLEDGMENTS

This study was partially supported by Cincinnati Children's Research Foundation, National Institute of Health grant RO1HL108867 (Zaza Khuchua).

REFERENCES

Acehan, D., Malhotra, A., Xu, Y., Ren, M., Stokes, D. L., and Schlame, M. (2011). Cardiolipin affects the supramolecular organization of ATP synthase in mitochondria. *Biophys. J.* 100, 2184–2192.

Acehan, D., Vaz, F., Houtkooper, R. H., James, J., Moore, V., Tokunaga, C., et al. (2010). Cardiac and skeletal muscle defects in a mouse model of human Barth syndrome. *J. Biol. Chem.* 286, 899–908.

Andreu, A. L., Hanna, M. G., Reichmann, H., Bruno, C., Penn, A. S., Tanji, K., et al. (1999). Exercise intolerance due to mutations in the cytochrome b gene of mitochondrial DNA. *N. Engl. J. Med.* 341, 1037–1044.

Argov, Z., Bank, W. J., Maris, J., Eleff, S., Kennaway, N. G., Olson, R. E., et al. (1986). Treatment of mitochondrial myopathy due to complex III deficiency with vitamins K3 and C: A 31P-NMR follow-up study. *Ann. Neurol.* 19, 598–602.

Bank, W., and Chance, B. (1994). An oxidative defect in metabolic myopathies: diagnosis by noninvasive tissue oximetry. *Ann. Neurol.* 36, 830–837.

Barrientos, A. (2002). In vivo and in organello assessment of OXPHOS activities. *Methods* 26, 307–316.

Benit, P., Lebon, S., and Rustin, P. (2009). Respiratory-chain diseases related to complex III deficiency. *Biochim. Biophys. Acta* 1793, 181–185.

Birch-Machin, M. A., Briggs, H. L., Saborido, A. A., Bindoff, L. A., and Turnbull, D. M. (1994). An evaluation of the measurement of the activities of complexes I-IV in the respiratory chain of human skeletal muscle mitochondria. *Biochem. Med. Metab. Biol.* 51, 35–42.

Enerback, S., Jacobsson, A., Simpson, E. M., Guerra, C., Yamashita, H., Harper, M. E., et al. (1997). Mice lacking mitochondrial uncoupling protein are cold-sensitive but not obese. *Nature* 387, 90–94.

Exil, V. J., Gardner, C. D., Rottman, J. N., Sims, H., Bartelds, B., Khuchua, Z., et al. (2006). Abnormal mitochondrial bioenergetics and heart rate dysfunction in mice lacking very-long-chain acyl-CoA dehydrogenase. *Am. J. Physiol.* 290, H1289–H1297.

Faldt, J., Wernstedt, I., Fitzgerald, S. M., Wallenius, K., Bergstrom, G., and Jansson, J. O. (2004). Reduced exercise endurance in interleukin-6-deficient mice. *Endocrinology* 145, 2680–2686.

Fry, M., and Green, D. E. (1981). Cardiolipin requirement for electron transfer in complex I and III of the mitochondrial respiratory chain. *J. Biol. Chem.* 256, 1874–1880.

Gil Borlado, M. C., Moreno Lastres, D., Gonzalez Hoyuela, M., Moran, M., Blazquez, A., Pello, R., et al. (2010). Impact of the mitochondrial genetic background in complex III deficiency. *PLoS ONE* 5:e12801. doi:10.1371/journal.pone.0012801

Haller, R. G., and Vissing, J. (2002). Spontaneous "second wind" and glucose-induced second "second wind" in McArdle disease: oxidative mechanisms. *Arch. Neurol.* 59, 1395–1402.

Haller, R. G., and Vissing, J. (2004). No spontaneous second wind in muscle phosphofructokinase deficiency. *Neurology* 62, 82–86.

Huang, L. S., Cobessi, D., Tung, E. Y., and Berry, E. A. (2005). Binding of the respiratory chain inhibitor antimycin to the mitochondrial bc1 complex: a new crystal structure reveals an altered intramolecular hydrogen-bonding pattern. *J. Mol. Biol.* 351, 573–597.

Khuchua, Z. A., Qin, W., Boero, J., Cheng, J., Payne, R. M., Saks, V. A., et al. (1998). Octamer formation and coupling of cardiac sarcomeric mitochondrial creatine kinase are mediated by charged N-terminal residues. *J. Biol. Chem.* 273, 22990–22996.

Kiebish, M. A., Yang, K., Liu, X., Mancuso, D. J., Guan, S., Zhao, Z., et al. (2013). Dysfunctional cardiac mitochondrial bioenergetic, lipidomic, and signaling in a murine model of Barth syndrome. *J. Lipid Res.* PMID: 23410936. [Epub ahead of print].

Palsdottir, H., and Hunte, C. (2004). Lipids in membrane protein structures. *Biochim. Biophys. Acta* 1666, 2–18.

Petrosillo, G., Ruggiero, F. M., Di Venosa, N., and Paradies, G. (2003). Decreased complex III activity in mitochondria isolated from rat heart subjected to ischemia and reperfusion: role of reactive oxygen species and cardiolipin. *FASEB J.* 17, 714–716.

Pfeiffer, K., Gohil, V., Stuart, R. A., Hunte, C., Brandt, U., Greenberg, M. L., et al. (2003). Cardiolipin stabilizes respiratory chain supercomplexes. *J. Biol. Chem.* 278, 52873–52880. [Epub October 5, 2003 52815].

Phoon, C. K., Acehan, D., Schlame, M., Stokes, D., Edelman-Novemsky, I., Yu, D., et al. (2012). Tafazzin knockdown in mice leads to a developmental cardiomyopathy with early diastolic dysfunction preceding myocardial noncompaction. *J. Am. Heart Assoc.* doi:10.1161/JAHA.111.000455

Schlame, M., Brody, S., and Hostetler, K. Y. (1993). Mitochondrial cardiolipin in diverse eukaryotes. Comparison of biosynthetic reactions and molecular acyl species. *Eur. J. Biochem.* 212, 727–735.

Schlame, M., Ren, M., Xu, Y., Greenberg, M. L., and Haller, I. (2005). Molecular symmetry in mitochondrial cardiolipins. *Chem. Phys. Lipids* 138, 38–49.

Soustek, M. S., Falk, D., Mah, C., Toth, M., Schlame, M., Lewin, A., et al. (2010). Characterization of a transgenic shRNA induced murine model of tafazzin deficiency. *Hum. Gene Ther.* 22, 865–871.

Spencer, C. T., Byrne, B. J., Bryant, R. M., Margossian, R., Maisenbacher, M., Breitenger, P., et al. (2011). Impaired cardiac reserve and severely diminished skeletal muscle O2 utilization mediate exercise intolerance in Barth syndrome. *Am. J. Physiol.* 301, H2122–H2129.

Valianpour, F., Wanders, R. J., Overmars, H., Vreken, P., Van Gennip, A. H., Baas, F., et al. (2002). Cardiolipin deficiency in X-linked cardioskeletal myopathy and neutropenia (Barth syndrome, MIM 302060): a study in cultured skin fibroblasts. *J. Pediatr.* 141, 729–733.

Vissing, J., Quistorff, B., and Haller, R. G. (2005). Effect of fuels on exercise capacity in muscle phosphoglycerate mutase deficiency. *Arch. Neurol.* 62, 1440–1443.

Vos, M., Esposito, G., Edirisinghe, J. N., Vilain, S., Haddad, D. M., Slabbaert, J. R., et al. (2012). Vitamin K2 is a mitochondrial electron carrier that rescues pink1 deficiency. *Science* 336, 1306–1310.

Wenz, T., Hielscher, R., Hellwig, P., Schagger, H., Richers, S., and Hunte, C. (2009). Role of phospholipids in respiratory cytochrome bc(1) complex catalysis and supercomplex formation. *Biochim. Biophys. Acta* 1787, 609–616.

Wibom, R., Hagenfeldt, L., and von Dobeln, U. (2003). Measurement of ATP production and respiratory chain enzyme activities in mitochondria isolated from small muscle biopsy samples. *Anal. Biochem.* 317, 139–151.

Zhang, M., Mileykovskaya, E., and Dowhan, W. (2002). Gluing the respiratory chain together. Cardiolipin is required for supercomplex formation in the inner mitochondrial membrane. *J. Biol. Chem.* 277, 43553–43556.

Zhang, M., Mileykovskaya, E., and Dowhan, W. (2005). Cardiolipin is essential for organization of complexes III and IV into a supercomplex in intact yeast mitochondria. *J. Biol. Chem.* 280, 29403–29408.

Conflict of Interest Statement: The authors declare that the research was conducted in the absence of any commercial or financial relationships that could be construed as a potential conflict of interest.

Received: 28 January 2013; paper pending published: 25 February 2013; accepted: 21 March 2013; published online: 17 April 2013.

Citation: Powers C, Huang Y, Strauss A and Khuchua Z (2013) Diminished exercise capacity and mitochondrial bc1 complex deficiency in tafazzinknockdown mice. Front. Physiol. 4:74. doi:10.3389/fphys.2013.00074

This article was submitted to Frontiers in Mitochondrial Research, a specialty of Frontiers in Physiology.

frontiers in
PHYSIOLOGY

ORIGINAL RESEARCH ARTICLE
published: 15 May 2013
doi: 10.3389/fphys.2013.00103

Protection of rat skeletal muscle fibers by either L-carnitine or coenzyme Q10 against statins toxicity mediated by mitochondrial reactive oxygen generation

P. G. La Guardia[1], L. C. Alberici[1], F. G. Ravagnani[1], R. R. Catharino[2] and A. E. Vercesi[1]*

[1] *Departamento de Patologia Clínica, Faculdade de Ciências Médicas, Universidade Estadual de Campinas, Campinas, Brazil*
[2] *Innovare Biomarkers Laboratory, Faculdade de Ciências Médicas, Universidade Estadual de Campinas, Campinas, Brazil*

Edited by:
Andrey V. Kuznetsov, Innsbruck Medical University, Austria

Reviewed by:
Mei-ling A. Joiner, University of Iowa, USA
Andrey V. Kozlov, L. Boltzmann Institute for Traumatology, Austria

***Correspondence:**
A. E. Vercesi, Departamento de Patologia Clínica, Faculdade de Ciências Médicas, Universidade Estadual de Campinas, Campinas, SP, CEP-13083-887, Brazil.
e-mail: anibal@unicamp.br

Mitochondrial redox imbalance has been implicated in mechanisms of aging, various degenerative diseases and drug-induced toxicity. Statins are safe and well-tolerated therapeutic drugs that occasionally induce myotoxicity such as myopathy and rhabdomyolysis. Previous studies indicate that myotoxicity caused by statins may be linked to impairment of mitochondrial functions. Here, we report that 1-h incubation of permeabilized rat soleus muscle fiber biopsies with increasing concentrations of simvastatin (1–40 μM) slowed the rates of ADP-or FCCP-stimulated respiration supported by glutamate/malate in a dose-dependent manner, but caused no changes in resting respiration rates. Simvastatin (1 μM) also inhibited the ADP-stimulated mitochondrial respiration supported by succinate by 24% but not by TMPD/ascorbate. Compatible with inhibition of respiration, 1 μM simvastatin stimulated lactate release from soleus muscle samples by 26%. Co-incubation of muscle samples with 1 mM L-carnitine, 100 μM mevalonate or 10 μM coenzyme Q10 (Co-Q10) abolished simvastatin effects on both mitochondrial glutamate/malate-supported respiration and lactate release. Simvastatin (1 μM) also caused a 2-fold increase in the rate of hydrogen peroxide generation and a decrease in Co-Q10 content by 44%. Mevalonate, Co-Q10 or L-carnitine protected against stimulation of hydrogen peroxide generation but only mevalonate prevented the decrease in Co-Q10 content. Thus, independently of Co-Q10 levels, L-carnitine prevented the toxic effects of simvastatin. This suggests that mitochondrial respiratory dysfunction induced by simvastatin, is associated with increased generation of superoxide, at the levels of complexes-I and II of the respiratory chain. In all cases the damage to these complexes, presumably at the level of 4Fe-4S clusters, is prevented by L-carnitine.

Keywords: statins, skeletal muscle mitochondrial dysfunction, myotoxicity, L-carnitine, coenzyme Q10

INTRODUCTION

Statins are natural (fungal-derived) or synthetic inhibitors of the enzyme HMG-CoA reductase that catalyzes the conversion of 3-hydroxy-3-methylglutaryl coenzyme-A (HMG-CoA) into mevalonic acid, the rate-limiting step in cholesterol synthesis (Endo, 1992). High plasma levels of cholesterol are well established as independent risk factor for coronary heart disease (Sirvent et al., 2005a) that can be significantly reduced by statins treatment (Tobert et al., 1982). The efficacy and tolerability of statins are well documented (Tobert et al., 1982; Sirvent et al., 2005b). Although this treatment normally lowers morbidity and mortality (LIPID Study Group, 1998) about 10% of the patients (Bruckert et al., 2005) develop myophatic symptoms and approximately one in 7.5 million patients develop fatal rhabdomyolysis (Venero and Thompson, 2009). Myopathic symptoms caused by statins, such as muscle cramps, myalgia, weakness and exercise intolerance can occur with or without increase in plasma creatine kinase levels (Sirvent et al., 2005a).

Statins block cholesterol synthesis early in its metabolic pathway therefore they also decrease the production of both ubiquinone (Co-Q10) and other important metabolites including dolichols and other prenylated isoprenoids required for muscle cell functions (Sirvent et al., 2008). Co-Q10 is an important respiratory chain electron transporter that also displays antioxidant properties in its reduced form (ubiquinol). Although the molecular mechanisms underlying statins induced myotoxicity are not well established the most popular hypothesis proposes that it is mediated by inhibition of mitochondrial respiration as a consequence of Co-Q10 depletion (Ghirlanda et al., 1993; Laaksonen et al., 1995; Thibault et al., 1996; Miyake et al., 1999; Rundek et al., 2004; Paiva et al., 2005; Littarru and Langsjoen, 2007; Mabuchi et al., 2007; Young et al., 2011; Bookstaver et al., 2012). In addition, several studies using isolated mitochondria or intact cells propose that statins promote cell death mediated by mitochondrial dysfunctions associated with alterations in calcium homeostasis, inhibition of beta-oxidation, inhibition of complex I

of the electron transport chain and mitochondrial oxidative stress (Sirvent et al., 2005b; Yasuda et al., 2005; Kaufmann et al., 2006; Velho et al., 2006; Oliveira et al., 2008; Skottheim et al., 2008; Itagaki et al., 2009; Kwak et al., 2012).

Data from our group (Velho et al., 2006) showed that statins stimulate Ca^{2+} induced mitochondrial permeability transition (MPT) *in vitro*, in mitochondria isolated from control mice liver or in liver mitochondria isolated from mice treated with lovastatin (100 mg/kg daily via gavage, during 15 days). In addition, Sacher et al. (2005) reported that simvastatin or lovastatin (1–100 μM) activate the mitochondrial pathway of apoptosis in primary human skeletal muscle cells obtained from skeletal muscle biopsies of healthy individuals. With respect to the mechanisms of cell death induced by statins, we have previously shown that, at low concentrations (≤10 μM), simvastatin induces apoptosis in PC3 prostate cancer cells. At these low concentrations mevalonate but not cyclosporine A, an inhibitor of MPT, prevented cell death (Oliveira et al., 2008). At higher concentrations (≥60 μM) simvastatin-induced necrosis was sensitive to cyclosporine A but not to mevalonate, indicating that, at high concentrations, the toxicity of statins is not solely the result of HMG-CoA reductase inhibition. In addition, cell necrosis was preceded by a threefold increase in the concentration of cytosolic free Ca^{2+} and MPT (Oliveira et al., 2008). More recently Costa et al. (2013) provided evidence that simvastatin-induced MPT and cell necrosis were inhibited by L-carnitine and piracetam in a dose-dependent fashion; when combined, L-carnitine and piracetam acted at concentrations significantly lower than they act individually. These results shed new light into both the cytotoxic mechanisms of high statins concentrations and the mechanisms underlying the protection against MPT and cell death by the compounds L-carnitine and piracetam (Costa et al., 2013).

L-carnitine, beyond the physiological functions on fatty acids transport across the inner mitochondrial membrane, has the properties to scavenge reactive oxygen (Gulcin, 2006; Mescka et al., 2011) and to bind Fe^{2+} (Gulcin, 2006) a transition metal, supposed to participate in the mitochondrial oxidative stress that leads to MPT (Castilho et al., 1995). Therefore, the aims of this study were double: first, to analyze the events leading to simvastatin induced skeletal muscle toxicity, at low concentrations (1 μM), and second, to better understand the mechanism underlying mitochondrial protection against reactive oxygen by L-carnitine or Co-Q10.

The results presented here indicate that simvastatin induced inhibition of respiration is mediated by the attack of mitochondrially generated superoxide radicals to the respiratory chain complexes I and II probably at the level of 4Fe-4S clusters. In addition, both L-carnitine and Co-Q10 act directly as radical scavenger in the protection against simvastatin-induced oxidative damage to skeletal muscle mitochondria.

MATERIALS AND METHODS

CHEMICALS AND REAGENTS

For all experiments, the reagents used were of analytical grade. Adenosine 5′-diphosphate monopotassium salt dihydrate (ADP), adenosine 5′-triphosphate monopotassium salt dihydrate (ATP), bovine serum albumin (BSA), dimethyl sulfoxide (DMSO), ethylene-bis(oxyethylenenitrilo)tetraacetic acid (EGTA), oligomycin, L-glutamic acid, L-malic acid, carbonyl cyanide 4-(trifluoromethoxy) phenylhydrazone (FCCP), 4-(2-hydroxyethyl)piperazine-1-ethanesulfonic acid (HEPES) Phospho-creatine, taurine, (2-[N-Morpholino] ethanesulfonic acid) monohydrate, ascorbic acid, oxaloacetic acid, imidazole, K-lactobionate, simvastatin, ubiquinone, β-Nicotinadenineamine dinucleotide were obtained from Sigma-Aldrich (St. Louis, MO, USA). The ADP, glutamate and malate solutions were prepared by dissolving the acids in water and adjusting the pH to 7.2 with KOH.

ANIMALS

Wistar female rats with 10–12 weeks of age had access to standard laboratory rodent chow diet and water *ad libitum* and were housed at 22 ± 2°C on a 12 h light-dark cycle. The experiments were approved by the Committee for Ethics in Animal Experimentation at the university and are in accordance with the Guide for the Care and Use of Laboratory Animals published by the National Academy of Sciences.

SKELETAL MUSCLE SAMPLE PREPARATION

Soleus muscle tissues were harvested from rats and placed in ice-cold relaxing solution [containing 10 mM Ca-EGTA buffer (2.77 mM of CaK_2EGTA + 7.23 mM K_2EGTA) free concentration of calcium 0.1 mmol/L, 20 mmol/L imidazole, 50 mmol/L K^+/4-morpholinoethanesulfonic acid, 0.5 mmol/L dithiothreitol, 7 mmol/L $MgCl_2$, 5 mmol/L ATP, 15 mmol/L phosphocreatine, pH 7.1]. Two to three milligram of soleus skeletal muscle were utilized and individual fiber bundles were separated with 2 forceps. Samples were permeabilized for 30 min in ice-cold relaxing solution with saponin (50 μg/mL) gently stirred and washed 3 times with MiR05 medium (60 mmol/L potassium lactobionate, 0.5 mmol/L EGTA, 3 mmol/L $MgCl_2$, 20 mmol/L taurine, 10 mmol/L KH_2PO_4, 20 mmol/L HEPES, 110 mmol/L sucrose, 1 g/L BSA, pH 7.1) at 4°C. Samples were dried with filter paper and weighted (Kuznetsov et al., 2008).

OXYGEN CONSUMPTION MEASUREMENTS

Oxygen consumption in permeabilized skeletal muscle tissues was measured in a medium MiR05 at 37°C, in the presence of 10 mM glutamate and 5 mM malate, or 5 mM succinate, or 50 μM TMPD plus 2 mM ascorbate plus 1 μM antimycin A using a high resolution oxygraph OROBOROS (Innsbruck, Austria). Simvastatin or Dimetilsulfóxido (DMSO) was incubated by 1 h. 400 μM ADP, 1 μg/mL oligomycin, and 0.2 μM FCCP were added during experiments (Kuznetsov et al., 2008).

CITRATE SYNTHASE (CS) ACTIVITY

The conversion of oxaloacetate and acetyl-CoA to citrate and SH-CoA catalyzed by citrate synthase was monitored by measuring the colorimetric product thionitrobenzoic acid (Shepherd and Garland, 1969). Soleus skeletal muscle homogenates (0.5–0.75 mg/mL, wet weight) were incubated at 30°C in a buffer containing 50 mM tris-HCl (pH 8.0), 0.1% Triton X-100, 250 μM oxaloacetate, 50 μM acetyl-CoA,

and 100 μM 5,5′-dithiobis(2-nitrobenzoic acid). The increase in absorbance at 412 nm was monitored for 6 min using a microplate reader (Power Wave XS 2, BioTek Instruments, Winooski, VT, USA).

LACTATE ASSAY

Lactate production was monitored by means of changes in NADH fluorescence. Medium containing 50 mM hydroxylamine, 50 mM tris, pH10.0, 800 μM NAD^+, 40 U lactate dehydrogenase and an aliquot of medium MiR05 containing the non-permeabilized sample prior incubation with simvastatin or DMSO for 1 h, at 25°C. Calibration was made by addition of know concentrations of lactate. A Hitachi F4500 spectrofluorometer operating at excitation and emission wavelengths of 366 and 450 nm, respectively, was used to measure the changes in NADH fluorescence.

HYDROGEN PEROXIDE RELEASE

Soleus skeletal muscle samples (∼20 mg) were pre incubated with simvastatin or DMSO for 1 h in medium MiR05 plus 10 μM Amplex red (Molecular Probes, Invitrogen, Carlsbad, CA) and 1 U/mL horseradish peroxidase. Calibration was made by addition of known concentrations of hydrogen peroxide. Changes in fluorescence were monitored using a spectrofluorometer (Hitachi F4500) operated at excitation and emission wavelengths of 563 and 587 nm, respectively (Anderson and Neufer, 2006).

SAMPLES FOR COENZYME Q10 ASSAY

Standard coenzyme Q10 (≥98%purity) was purchased from Sigma-Aldrich (USA). HPLC-grade water was prepared using a MilliQTM System (Millipore Corporation). Methanol HPLC-grade was purchase from Merck Chemicals (Germany), Ethanol analytical grade and perchloric acid were purchased from F. MAIA (Brazil). Benzene (light petroleum) was purchased from VETEC (Brazil). Samples from soleus skeletal muscle (around 100 mg) from Wistar rats were prepared as previously described by Redfearn and Whittaker (1966) with modifications (Redfearn and Whittaker, 1966). Briefly, muscle tissue samples were homogenized in medium containing 1 mL of MiR05 medium, 1 mL of 0.6 M perchloric acid, and 3 mL of cold methanol. The homogenates were vortexed during 30 s, 5 mL of benzene were added and the samples were vortexed again for 30 s. The samples were centrifuged at 5000× g for 10 min (room temperature). The upper phase was collected and dried under nitrogen flux. The precipitate obtained was dissolved in 50 μL of hexane.

HPLC ASSAY FOR COENZYME Q

Coenzyme Q10 was determined using a chromatographic system Shimadzu LC (Japan) in conjunction with a SPD-10A UV-Visible set to 275 nm. Twenty microliters of the samples in hexane were injected into the analytical column (Luna 250 × 4.6 mm; C18 (2) 100A; 5 μm particle size; Phenomenex®) maintained at 25°C. Coenzyme Q10 was eluted from the column at a flow rate of 1.4 mL/min using a isocratic mode linear gradient of methanol:ethanol (65:35). Lower and upper limits of detection for total coenzyme Q10 were confirmed at the following concentrations: 0.167 μmol/L and 150 μmol/L. The lower and upper limits of linearity were observed at the following concentrations: 0.5 μmol/L and 50.0 μmol/L.

STATISTICAL ANALYSES

The results of experiments performed in at least five independent experiments are displayed as means ± S.E.D and significance was assessed by ANOVA, followed by the Tukey post-test, or student-*t* test with significance level set at $p < 0.05$ using Sigma Stat 3.1 (Systat, San Jose, CA, USA).

RESULTS

INHIBITION BY SIMVASTATIN OF ADP- OR FCCP-STIMULATED OXYGEN CONSUMPTION SUPPORTED BY COMPLEX I SUBSTRATES IN SKELETAL MUSCLE FIBERS

In order to investigate the effects of simvastatin on soleus skeletal muscle mitochondrial respiration "*in vitro*" we incubated the permeabilized bundles for 1 h in the standard incubation medium (MiR05) containing increasing concentrations (1, 15, or 40 μM) of simvastatin or 0.1% DMSO as control. Oxygen consumption supported by 10 mM glutamate plus 5 mM malate was monitored before and after the sequential additions of 400 μM ADP, 1 μg/mL oligomycin, and 0.2 μM FCCP. **Figure 1** shows that simvastatin promoted a dose dependent inhibition of ADP- and FCCP-stimulated respiration but did not affect the rate of resting respiration (data not shown). The inhibition caused by 1 μM simvastatin was 25 and 27% for ADP- and FCCP-stimulated respiration, respectively. The inhibition peaked at 57% in the presence of 40 μM simvastatin for both ADP- and FCCP-stimulated respiration.

Considering that typically prescribed daily oral doses of statins 20–80 mg (Kwak et al., 2012) generate concentration peaks in skeletal muscle in the range of 2–5 μM, we choose the concentration of 1 μM simvastatin to perform the next experiments.

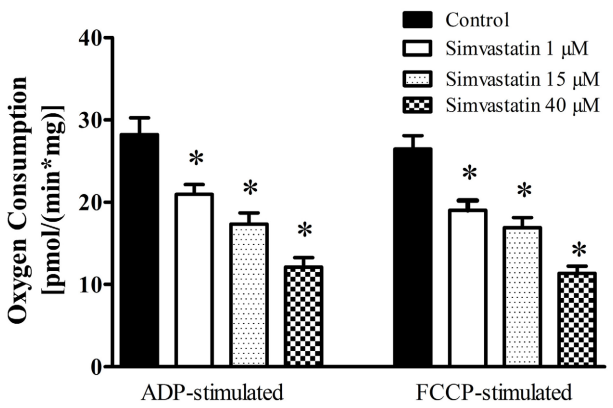

FIGURE 1 | Inhibition by simvastatin of ADP- or FCCP-stimulated oxygen consumption supported by complex I substrates in skeletal muscle. Skeletal muscle samples were incubated in MiR05 medium in the presence of 1, 15, and 40 μM simvastatin, or DMSO for 1 h. ADP (400 μM) or 1 μg/mL oligomycin plus 0.2 μM FCCP were added where indicated. Respiration was supported by 10 mM glutamate plus 5 mM malate. *$p < 0.05$ vs. control by one-way analysis of variance. N = at least 6 independent experiments.

INHIBITION BY SIMVASTATIN OF ADP-STIMULATED OXYGEN CONSUMPTION SUPPORTED BY SUCCINATE

The results on respiratory complex II inhibition by statins reported in the literature are controversial (Sirvent et al., 2005a, 2012; Bouitbir et al., 2012a). Here we analyzed the effect of 1 μM simvastatin on succinate or TMPD/ascorbate supported respiration. One hour incubation of the skeletal muscle preparation with 1 μM simvastatin caused 24% inhibition of ADP-stimulated respiration supported by succinate but did not significantly change the rate of TMPD/ascorbate supported respiration (**Figure 2A**). In addition, the citrate synthase activity assay applied to skeletal muscle tissue incubated during 1 h in the presence of 1 μM simvastatin indicated that mitochondrial density and number were not changed by the statin treatment (**Figure 2B**).

INHIBITION BY 1 μM SIMVASTATIN OF ADP- OR FCCP-STIMULATED OXYGEN CONSUMPTION SUPPORTED BY COMPLEX I SUBSTRATES WAS PREVENTED BY MEVALONATE, Co-Q10 OR L-carnitine

The first step to elucidate the mechanism of simvastatin induced skeletal muscle respiration inhibition was the co-incubation with mevalonate, the product of the reaction catalyzed by the enzyme HMG-CoA reductase. **Figures 3A,B** show that 100 μM mevalonate protected against simvastatin-induced inhibition of complex I substrates supported respiration stimulated by ADP or FCCP, respectively. The next step was the co-incubation with coenzyme Q10, another product of cholesterol *de novo* biosynthesis. It can be seen that 10 μM Co-Q10 similarly to mevalonate significantly protected against the inhibition of complex I respiration stimulated by ADP- or FCCP (**Figures 3A,B**). L-carnitine is another compound reported to protect skeletal muscle or tumor

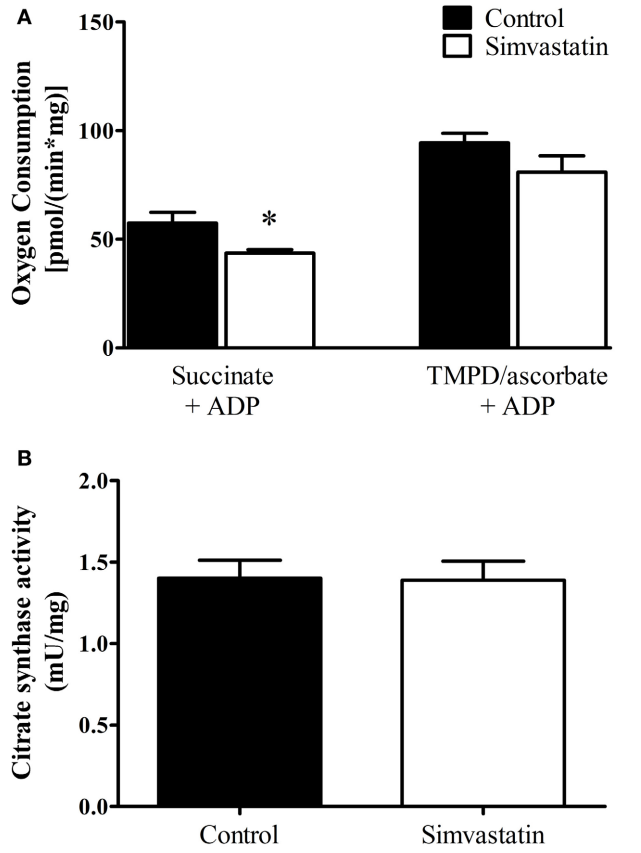

FIGURE 2 | Inhibition by 1 μM simvastatin of ADP-stimulated oxygen consumption supported by succinate but not by TMPD/ascorbate. **(A)** Skeletal muscle samples were incubated in MiR05 medium in the presence of 1 μM simvastatin, or DMSO for 1 h. ADP (400 μM) or 1 μg/mL oligomycin plus 0.2 μM FCCP were respectively added. The respiration was supported by 5 mM succinate or 5 μM TMPD plus 2 mM ascorbate plus 1 μM antimycin A. **(B)** Skeletal muscle homogenates were incubated at 30°C in a buffer containing 50 mM tris-HCl (pH 8.0), 0.1% Triton X-100, 250 μM oxaloacetate, 50 μM acetyl-CoA, and 100 μM 5, 5′-dithiobis(2-nitrobenzoic acid) to assay citrate synthase activity. Prior preparation of homogenates, skeletal muscle samples were incubated by 1 h in MiR05 medium in presence of 1 μM simvastatin. $^*p < 0.05$ vs. control by student *t*-test. $N =$ at least 5 independent experiments.

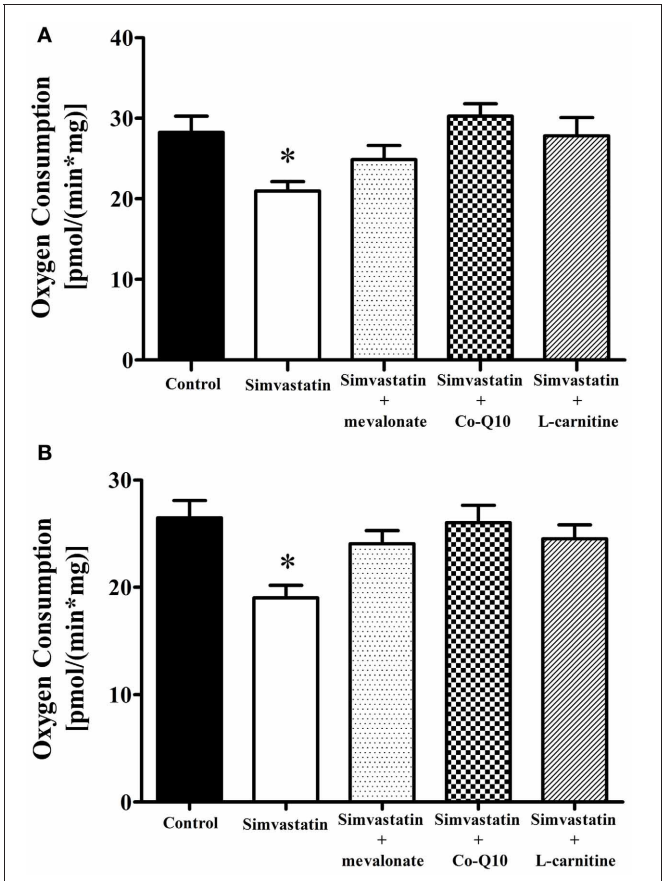

FIGURE 3 | Inhibition by 1 μM simvastatin of (A) ADP or (B) FCCP-stimulated oxygen consumption supported by complex I substrates was prevented by mevalonate, Co-Q10 or L-carnitine. Skeletal muscle samples were incubated in MiR05 medium in the presence of 1 μM simvastatin, or DMSO for 1 h containing 100 μM mevalonate, 10 μM coenzyme Q10, or 1 mM L-carnitine. ADP (400 μM) or 1 μg/mL oligomycin plus 0.2 μM FCCP were added and oxygen consumption was supported by 10 mM glutamate plus 5 mM malate. Since the control and 1 μM simvastatin bars were not statically different in **Figure 1** and panel **(A)**, we used a general averages for controls and 1 μM simvastatin in both figures. $^*p < 0.05$ vs control by one-way analysis of variance. $N =$ at least 6 independent experiments.

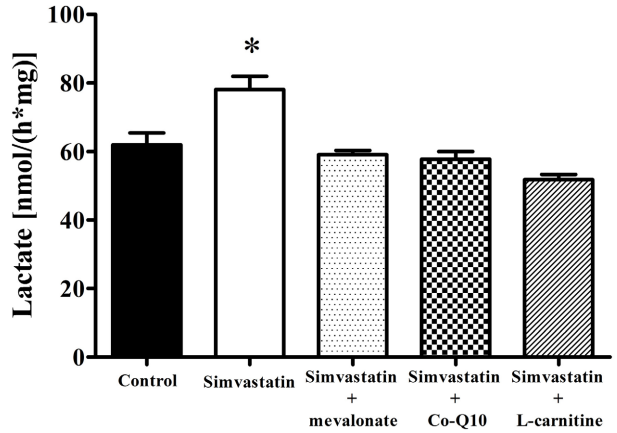

FIGURE 4 | Increase in lactate production by 1 μM simvastatin was prevented by mevalonate, Co-Q10 or L-carnitine in skeletal muscle. An aliquot of MiR05 medium containing non-permeabilized skeletal muscle samples pre incubated by 1 h with 1 μM simvastatin or DMSO, or coincubated with 100 μM mevalonate, 10 μM coenzyme Q10 or 1 mM L-carnitine was added to a medium containing 50 mM hidroxilamine, 50 mM tris, 800 μM NAD^+, 40 U lactate dehydrogenase, pH 10 at 25°C, for spectrofluorimetric assay of lactate release. $^*p < 0.05$ vs. control by one-way analysis of variance. N = at least 5 independent experiments.

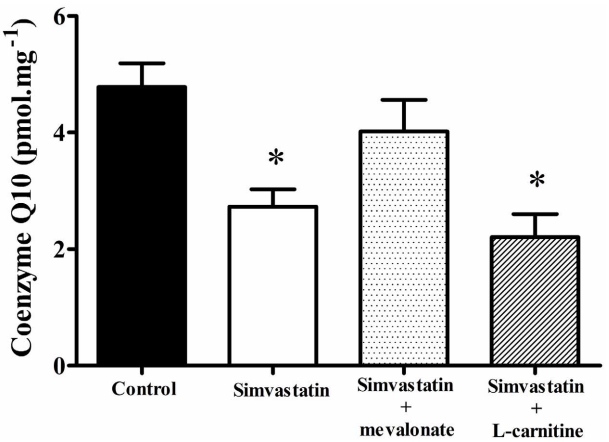

FIGURE 5 | Determination of coenzyme Q10 in skeletal muscle incubated with 1 μM simvastatin alone or in the presence of mevalonate or L-carnitine. Permeabilized skeletal muscle samples were incubated in MiR05 medium in the presence of 1 μM simvastatin, or DMSO for 1 h in the presence of 100 μM mevalonate, 10 μM coenzyme Q10, or 1 mM L-carnitine. After tissue homogenization, extraction was performed utilizing perchloric acid and cold methanol. Coenzyme Q10 was measured with a Shimadzu HPLC. $^*p < 0.05$ vs. control by one-way analysis of variance. N = at least 9 independent experiments.

cells against simvastatin induced toxicity (Arduini et al., 2004; Costa et al., 2013). **Figures 3A,B**, respectively, show that 1 mM L-carnitine protected against inhibition of complex I respiration stimulated by ADP or FCCP.

INCREASE IN LACTATE PRODUCTION BY 1 μM SIMVASTATIN WAS PREVENTED BY MEVALONATE, Co-Q10 OR L-carnitine IN SKELETAL MUSCLE FIBERS

Treatment of hypercholesterolemic patients with statins has been reported (De Pinieux et al., 1996) to increase lactate/pyruvate ratio in blood serum. In fact, this ratio can be used as a non-invasive test to detect impairment or toxic effects on mitochondrial energy linked metabolism (Robinson, 1989; Munnich et al., 1992; Chariot et al., 1994). Here we present data showing that 1 h incubation of skeletal muscle tissue with 1 μM simvastatin caused an increase of 26% in lactate production (**Figure 4**) that was abolished by the co-incubation of simvastatin with each of the compounds 100 μM mevalonate, 10 μM Co-Q10, or 1 mM L-carnitine.

DECREASE IN COENZYME Q10 BY 1 μM SIMVASTATIN WAS PREVENTED BY MEVALONATE BUT NOT BY L-carnitine IN SKELETAL MUSCLE FIBERS

In order to ascertain the possible role of ubiquinone in the mechanism of statins induced mitochondrial dysfunction (Ghirlanda et al., 1993; Laaksonen et al., 1995; Thibault et al., 1996; Miyake et al., 1999; Rundek et al., 2004; Paiva et al., 2005; Littarru and Tiano, 2010) we assayed the Co-Q10 content in permeabilized skeletal muscle tissues after 1 h incubation with 1 μM simvastatin. **Figure 5** shows that under the same experimental conditions in which the statin promotes inhibition of respiration the reduced levels of Co-Q10 were about 40% decreased relative to the control experiment. Interestingly, 100 μM mevalonate but not 1 mM L-carnitine prevented the decrease in Co-Q10 content. Therefore, we hypothesized that either L-carnitine or Co-Q10 protected against simvastatin-induced inhibition of respiration by acting as antioxidants. Accordingly, this inhibition of respiration was not mediated by the ability of Co-Q10 to transfer electrons from complex I and II to complex III, but rather by the action of Co-Q10 as a free radical scavenger. In order to ascertain this possibility we next investigated the effects of simvastatin alone or in co-incubation with 100 μM mevalonate, 10 μM Co-Q10, or 1 mM L-carnitine on hydrogen peroxide production by skeletal muscle fibers mitochondria.

INCREASE IN HYDROGEN PEROXIDE BY 1 μM SIMVASTATIN WAS PREVENTED BY MEVALONATE, Co-Q10 OR L-carnitine IN SKELETAL MUSCLE FIBERS

Literature data also report that statin treatment may increase the rates of superoxide and hydrogen peroxide production in muscular cells (Kwak et al., 2012) and in muscle tissues from patients (Bouitbir et al., 2012b). In this study we assayed hydrogen peroxide and found that 1 h incubation of skeletal muscle tissues with 1 μM simvastatin promoted an increase of about 103% in the rate of hydrogen peroxide production compared to the controls. Similarly to what happens with respiration and lactate production, this increase in H_2O_2 was abolished by co-incubation of simvastatin with 100 μM mevalonate, 10 μM Co-Q10, or 1 mM L-carnitine (**Figure 6**).

DISCUSSION

The present work provides evidence that 1 h incubation of skeletal muscle fibers with 1 μM simvastatin promotes mitochondrial

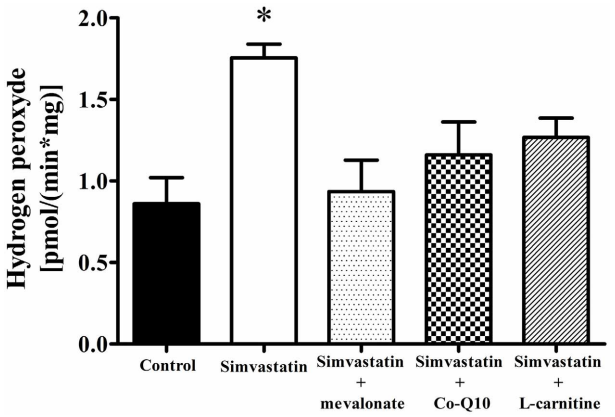

FIGURE 6 | Increase in hydrogen peroxide release by 1 μM simvastatin was prevented by mevalonate, Co-Q10 or L-carnitine in skeletal muscle. Permeabilized skeletal muscle samples were incubated, for 1 h, in medium MiR05 containing 1 μM simvastatin or DMSO, 10 μM Amplex red, 1 U/mL horseradish peroxidase, 10 mM glutamate, 5 mM malate, or simultaneous incubated with 100 μM mevalonate, 10 μM coenzyme Q10 or 1 mM L-carnitine. Changes in fluorescence were monitored on a spectrofluorometer. $^*p < 0.05$ vs. control by one-way analysis of variance. $N =$ at least 5 independent experiments.

dysfunction associated with inhibition of respiration, decrease in the content of Co-Q10 and increased rates of hydrogen peroxide production.

Most literature data on statins toxicity was obtained from *in vivo* or *in vitro* experiments using different animal models and higher doses than those found in the serum of hypercholesterolemic patients (Sacher et al., 2005; Sirvent et al., 2005a; Kaufmann et al., 2006; Nadanaciva et al., 2007). Here we analyzed the mechanisms underlying mitochondrial dysfunctions associated with the lowest simvastatin concentration (1 μM) that significantly inhibited respiration supported by complex I and II linked substrates, under our experimental conditions. Although the assays were made *in vitro* using muscle biopsies, the present findings may be relevant to the understanding of statins toxicity *in vivo* that produces a variety of myophatic symptoms including myalgia, muscle cramps, and rarely rhabdomyolysis. These symptoms are more frequent in patients treated with high statin doses (80 mg/daily) and are increased by factors or conditions that increase serum and muscle statin concentrations (grape fruit juice, hypothyroidism, diabetes mellitus, advanced age, liver, and kidney diseases), and factors that increase muscle susceptibility to injury such as alcohol consumption, drug abuse, heavy exercise, and some muscle diseases (Venero and Thompson, 2009).

In the present study we did not find significant difference in resting respiration between statin treatment and controls. In contrast, a significant inhibition of both phosphorylating and uncoupled respiration, relative to the controls (**Figure 1**) suggests that mitochondrial number and density were normal and that the maximal respiratory capacity of skeletal muscle was decreased by simvastatin. This interpretation is supported by the citrate synthase assay (**Figure 2**) and is in line with those by Kwak et al. (2012) using myotube cells treated with simvastatin.

Increase in lactate levels, decrease in ATP production, and stimulated glycolysis have also been associated with inhibition of muscle respiration by statins impairment of mitochondrial functions (Robinson, 1989; Munnich et al., 1992; Chariot et al., 1994). Here we show that both inhibition of respiration and increase in lactate production were prevented by co-incubation of simvastatin with L-carnitine, mevalonate or Co-Q10; compounds known to protect against statins toxicity (Arduini et al., 2004; Sacher et al., 2005; Kettawan et al., 2007; Oliveira et al., 2008; Costa et al., 2013). These results are consistent with literature data (Kaufmann et al., 2006; Sirvent et al., 2008) proposing that simvastatin-induced inhibition of oxygen consumption in skeletal muscle is mediated by inhibition of Co-Q10 synthesis. On these grounds, the present results suggest that L-carnitine might also be protecting against the decrease in Co-Q10.

Co-Q10 is a mobile carrier that collects electrons from complex I and II transferring them to complex III and, in addition, in its reduced form (ubiquinol) acts as a potent antioxidant (Graham et al., 2009; Deichmann et al., 2010; Figueira et al., 2013). Supplementation with Co-Q10 has demonstrated effectiveness in ameliorating neurodegenerative diseases, cerebellar ataxia, heart failure, and muscular symptoms (Kaikkonen et al., 2002; Naini et al., 2003; Mabuchi et al., 2007; Littarru and Tiano, 2010). Therefore, we assayed the Co-Q10 content in skeletal muscle tissue treated with 1 μM simvastatin. In agreement with literature data (Ghirlanda et al., 1993; Laaksonen et al., 1995; Thibault et al., 1996; Miyake et al., 1999; Rundek et al., 2004; Paiva et al., 2005; Littarru and Langsjoen, 2007) our results indicate that simvastatin significantly decreased the content of the reduced form of Co-Q10. Interestingly, the co-incubation with L-carnitine, in contrast to the co-incubation with mevalonate that also protects against simvastatin-induced inhibition of respiration, did not protect against Co-Q10 depletion. This indicates that the decreased content of Co-Q10 is limiting the rate of mitochondrial respiration in the presence of simvastatin mainly due to its property to remove or scavenging free radicals and not due to its property to transfer electrons from complexes I and II to complex III. As a matter of fact, Panov et al. (2005) provided evidence that inhibition of respiration by superoxide, at the levels of complex I and complex II, may result from damage to 4Fe-4S clusters. Indeed, complex I has six and complex II has one 4Fe-4S clusters rendering these structures highly sensitive to the damaging effects of superoxide. Accordingly, previous data indicate that enzymes containing 4Fe-4S clusters are particularly vulnerable to damaging by superoxide or peroxinitrite radicals (Flint et al., 1993; Radi et al., 1994; Fridovich, 1995; Bouton et al., 1996; Panov et al., 2005; Demicheli et al., 2007).

L-carnitine is known to protect against mitochondrial dysfunctions associated with oxidative stress caused by a series of conditions such as aging, ischemia reperfusion, inflammation, degenerative diseases, carcinogenesis and drug toxicity, *in vivo* or *in vitro* (Moretti et al., 2002; Binienda, 2003; Kumaran et al., 2004, 2005; Sener et al., 2004; Virmani et al., 2004; Binienda et al., 2005; Keil et al., 2006; Yapar et al., 2007; Shen et al., 2008; Silva-Adaya et al., 2008; Elinos-Calderon et al., 2009; Vamos et al., 2010; Ye et al., 2010; Zhang et al., 2010). Given the properties of L-carnitine to scavenge reactive oxygen

(Gulcin, 2006; Mescka et al., 2011) and to bind Fe^{2+} (Gulcin, 2006), we propose that this molecule may directly interact with 4Fe-4S clusters protecting the respiratory complexes I and II against the attack by the superoxide radical. This proposition is not in contrast to the results reported by Benati et al. (2010) showing that simvastatin decreases the capacity of macrophages to phagocyte and kill bacteria by impairment of oxidative burst, a rather different mechanism not involving the mitochondrial respiratory chain.

In addition, it is noteworthy to remind that 60 μM simvastatin-induced MPT and cell necrosis were sensitive to L-carnitine or piracetam in a dose-dependent fashion and mediated by additive mechanisms (Costa et al., 2013). In the present work we observed that piracetam did not affect the inhibition of respiration or the increase in H_2O_2 production induced by 1 μM simvastatin (results not shown). These results suggest that in the previous work (Costa et al., 2013) the role of piracetam on the protection against high simvastatin concentrations (60 μM) was mediated by the ability of the compound to protect against Ca^{2+}-induced alterations in membrane fluidity (Keil et al., 2006). This occurs via unspecific interactions of piracetam with the polar head groups of biological membranes (Keil et al., 2006). Indeed, Ca^{2+} binding to inner membrane cardiolipin causes important alterations in the lipid organization that favors the burst of mitochondrial ROS that triggers Ca^{2+}-induced MPT (Grijalba et al., 1999).

CONCLUSIONS

Considering that the three compounds (mevalonate, Co-Q10, or L-carnitine) that prevented the inhibition of respiration by simvastatin also protected against stimulation of hydrogen peroxide generation, we may conclude that reactive oxygen is the common denominator in the mechanism of respiration inhibition by statins. In addition, the lack of protection against Co-Q10 depletion by L-carnitine indicates that this compound as well as Co-Q10 acts directly as radical scavenger in the protection against simvastatin-induced oxidative damage to skeletal muscle mitochondria.

ACKNOWLEDGMENTS

The authors would like to thank Dr. Roger F. Castilho and Dr. Helena C. F. Oliveira for critical reading of this manuscript. This work was supported by Fundação de Amparo à Pesquisa do Estado de São Paulo (FAPESP), Conselho Nacional de Desenvolvimento Científico e Tecnológico (CNPq), Instituto Nacional de Ciência e Tecnologia (INCT) em Diabetes e Obesidade (CNPq/FAPESP), and Coordenação de Aperfeiçoamento de Pessoal de Nível Superior (CAPES).

REFERENCES

Anderson, E. J., and Neufer, P. D. (2006). Type II skeletal myofibers possess unique properties that potentiate mitochondrial H(2)O(2) generation. *Am. J. Physiol. Cell Physiol.* 290, C844–C851.

Arduini, A., Peschechera, A., Giannessi, F., and Carminati, P. (2004). Improvement of statin-associated myotoxicity by L-carnitine. *J. Thromb. Haemost.* 2, 2270–2271.

Benati, D., Ferro, M., Savino, M. T., Ulivieri, C., Schiavo, E., Nuccitelli, A., et al. (2010). Opposite effects of simvastatin on the bactericidal and inflammatory response of macrophages to opsonized *S. aureus*. *J. Leukoc. Biol.* 87, 433–442.

Binienda, Z. K. (2003). Neuroprotective effects of L-carnitine in induced mitochondrial dysfunction. *Ann. N.Y. Acad. Sci.* 993, 289–295. discussion: 345–349.

Binienda, Z., Przybyla-Zawislak, B., Virmani, A., and Schmued, L. (2005). L-carnitine and neuroprotection in the animal model of mitochondrial dysfunction. *Ann. N.Y. Acad. Sci.* 1053, 174–182.

Bookstaver, D. A., Burkhalter, N. A., and Hatzigeorgiou, C. (2012). Effect of coenzyme Q10 supplementation on statin-induced myalgias. *Am. J. Cardiol.* 110, 526–529.

Bouitbir, J., Charles, A. L., Echaniz-Laguna, A., Kindo, M., Daussin, F., Auwerx, J., et al. (2012a). Opposite effects of statins on mitochondria of cardiac and skeletal muscles: a 'mitohormesis' mechanism involving reactive oxygen species and PGC-1. *Eur. Heart J.* 33, 1397–1407.

Bouitbir, J., Daussin, F., Charles, A. L., Rasseneur, L., Dufour, S., Richard, R., et al. (2012b). Mitochondria of trained skeletal muscle are protected from deleterious effects of statins. *Muscle Nerve* 46, 367–373.

Bouton, C., Raveau, M., and Drapier, J. C. (1996). Modulation of iron regulatory protein functions. Further insights into the role of nitrogen- and oxygen-derived reactive species. *J. Biol. Chem.* 271, 2300–2306.

Bruckert, E., Hayem, G., Dejager, S., Yau, C., and Begaud, B. (2005). Mild to moderate muscular symptoms with high-dosage statin therapy in hyperlipidemic patients–the PRIMO study. *Cardiovasc. Drugs Ther.* 19, 403–414.

Castilho, R. F., Kowaltowski, A. J., Meinicke, A. R., and Vercesi, A. E. (1995). Oxidative damage of mitochondria induced by Fe(II)citrate or t-butyl hydroperoxide in the presence of Ca2+: effect of coenzyme Q redox state. *Free Radic. Biol. Med.* 18, 55–59.

Chariot, P., Monnet, I., Mouchet, M., Rohr, M., Lefaucheur, J. P., Dubreuil-Lemaire, M. L., et al. (1994). Determination of the blood lactate:pyruvate ratio as a noninvasive test for the diagnosis of zidovudine myopathy. *Arthritis Rheum.* 37, 583–586.

Costa, R. A. P., Fernandes, M. P., Souza-Pinto, N. C. D., and Vercesi, A. E. (2013). Protective effects of L-carnitine and piracetam against mitochondrial permeability transition and PC3 cell necrosis induced by simvastatin. *Eur. J. Pharmacol.* 701, 82–86.

Deichmann, R., Lavie, C., and Andrews, S. (2010). Coenzyme q10 and statin-induced mitochondrial dysfunction. *Ochsner J.* 10, 16–21.

Demicheli, V., Quijano, C., Alvarez, B., and Radi, R. (2007). Inactivation and nitration of human superoxide dismutase (SOD) by fluxes of nitric oxide and superoxide. *Free Radic. Biol. Med.* 42, 1359–1368.

De Pinieux, G., Chariot, P., Ammi-Said, M., Louarn, F., Lejonc, J. L., Astier, A., et al. (1996). Lipid-lowering drugs and mitochondrial function: effects of HMG-CoA reductase inhibitors on serum ubiquinone and blood lactate/pyruvate ratio. *Br. J. Clin. Pharmacol.* 42, 333–337.

Elinos-Calderon, D., Robledo-Arratia, Y., Perez-De La Cruz, V., Pedraza-Chaverri, J., Ali, S. F., and Santamaria, A. (2009). Early nerve ending rescue from oxidative damage and energy failure by L: -carnitine as post-treatment in two neurotoxic models in rat: recovery of antioxidant and reductive capacities. *Exp. Brain Res.* 197, 287–296.

Endo, A. (1992). The discovery and development of HMG-CoA reductase inhibitors. *J. Lipid Res.* 33, 1569–1582.

Figueira, T. R., Barros, M. H., Camargo, A. A., Castilho, R. F., Ferreira, J. C., Kowaltowski, A. J., et al. (2013). Mitochondria as a source of reactive oxygen and nitrogen species: from molecular mechanisms to human health. *Antioxid. Redox Signal.* 18, 2029–2074.

Flint, D. H., Tuminello, J. F., and Emptage, M. H. (1993). The inactivation of Fe-S cluster containing hydro-lyases by superoxide. *J. Biol. Chem.* 268, 22369–22376.

Fridovich, I. (1995). Superoxide radical and superoxide dismutases. *Annu. Rev. Biochem.* 64, 97–112.

Ghirlanda, G., Oradei, A., Manto, A., Lippa, S., Uccioli, L., Caputo, S., et al. (1993). Evidence of plasma CoQ10-lowering effect by HMG-CoA reductase inhibitors: a double-blind, placebo-controlled study. *J. Clin. Pharmacol.* 33, 226–229.

Graham, D., Huynh, N. N., Hamilton, C. A., Beattie, E., Smith, R. A., Cocheme, H. M., et al. (2009). Mitochondria-targeted antioxidant MitoQ10 improves endothelial function and attenuates cardiac hypertrophy. *Hypertension* 54, 322–328.

Grijalba, M. T., Vercesi, A. E., and Schreier, S. (1999). Ca2+-induced increased lipid packing and domain formation in submitochondrial particles. A possible early step in the mechanism of Ca2+-stimulated generation of reactive oxygen species by the respiratory chain. *Biochemistry* 38, 13279–13287.

Gulcin, I. (2006). Antioxidant and antiradical activities of L-carnitine. *Life Sci.* 78, 803–811.

Itagaki, M., Takaguri, A., Kano, S., Kaneta, S., Ichihara, K., and Satoh, K. (2009). Possible mechanisms underlying statin-induced skeletal muscle toxicity in L6 fibroblasts and in rats. *J. Pharmacol. Sci.* 109, 94–101.

Kaikkonen, J., Tuomainen, T. P., Nyyssonen, K., and Salonen, J. T. (2002). Coenzyme Q10 absorption, antioxidative properties, determinants, and plasma levels. *Free Radic. Res.* 36, 389–397.

Kaufmann, P., Torok, M., Zahno, A., Waldhauser, K. M., Brecht, K., and Krahenbuhl, S. (2006). Toxicity of statins on rat skeletal muscle mitochondria. *Cell. Mol. Life Sci.* 63, 2415–2425.

Keil, U., Scherping, I., Hauptmann, S., Schuessel, K., Eckert, A., and Muller, W. E. (2006). Piracetam improves mitochondrial dysfunction following oxidative stress. *Br. J. Pharmacol.* 147, 199–208.

Kettawan, A., Takahashi, T., Kongkachuichai, R., Charoenkiatkul, S., Kishi, T., and Okamoto, T. (2007). Protective effects of coenzyme q(10) on decreased oxidative stress resistance induced by simvastatin. *J. Clin. Biochem. Nutr.* 40, 194–202.

Kumaran, S., Savitha, S., Anusuya Devi, M., and Panneerselvam, C. (2004). L-carnitine and DL-alpha-lipoic acid reverse the age-related deficit in glutathione redox state in skeletal muscle and heart tissues. *Mech. Ageing Dev.* 125, 507–512.

Kumaran, S., Subathra, M., Balu, M., and Panneerselvam, C. (2005). Supplementation of L-carnitine improves mitochondrial enzymes in heart and skeletal muscle of aged rats. *Exp. Aging Res.* 31, 55–67.

Kuznetsov, A. V., Veksler, V., Gellerich, F. N., Saks, V., Margreiter, R., and Kunz, W. S. (2008). Analysis of mitochondrial function *in situ* in permeabilized muscle fibers, tissues and cells. *Nat. Protoc.* 3, 965–976.

Kwak, H. B., Thalacker-Mercer, A., Anderson, E. J., Lin, C. T., Kane, D. A., Lee, N. S., et al. (2012). Simvastatin impairs ADP-stimulated respiration and increases mitochondrial oxidative stress in primary human skeletal myotubes. *Free Radic. Biol. Med.* 52, 198–207.

Laaksonen, R., Jokelainen, K., Sahi, T., Tikkanen, M. J., and Himberg, J. J. (1995). Decreases in serum ubiquinone concentrations do not result in reduced levels in muscle tissue during short-term simvastatin treatment in humans. *Clin. Pharmacol. Ther.* 57, 62–66.

LIPID (The Long-Term Intervention with Pravastatin in Ischaemic Disease) Study Group. (1998). Prevention of cardiovascular events and death with pravastatin in patients with coronary heart disease and a broad range of initial cholesterol levels. *N. Engl. J. Med.* 339, 1349–1357.

Littarru, G. P., and Langsjoen, P. (2007). Coenzyme Q10 and statins: biochemical and clinical implications. *Mitochondrion* 7(Suppl.), S168–S174.

Littarru, G. P., and Tiano, L. (2010). Clinical aspects of coenzyme Q10 an update. *Nutrition* 26, 250–254.

Mabuchi, H., Nohara, A., Kobayashi, J., Kawashiri, M. A., Katsuda, S., Inazu, A., et al. (2007). Effects of CoQ10 supplementation on plasma lipoprotein lipid, CoQ10 and liver and muscle enzyme levels in hypercholesterolemic patients treated with atorvastatin: a randomized double-blind study. *Atherosclerosis* 195, e182–e189.

Mescka, C., Moraes, T., Rosa, A., Mazzola, P., Piccoli, B., Jacques, C., et al. (2011). *In vivo* neuroprotective effect of L-carnitine against oxidative stress in maple syrup urine disease. *Metab. Brain Dis.* 26, 21–28.

Miyake, Y., Shouzu, A., Nishikawa, M., Yonemoto, T., Shimizu, H., Omoto, S., et al. (1999). Effect of treatment with 3-hydroxy-3-methylglutaryl coenzyme A reductase inhibitors on serum coenzyme Q10 in diabetic patients. *Arzneimittelforschung* 49, 324–329.

Moretti, S., Famularo, G., Marcellini, S., Boschini, A., Santini, G., Trinchieri, V., et al. (2002). L-carnitine reduces lymphocyte apoptosis and oxidant stress in HIV-1-infected subjects treated with zidovudine and didanosine. *Antioxid. Redox Signal.* 4, 391–403.

Munnich, A., Rustin, P., Rotig, A., Chretien, D., Bonnefont, J. P., Nuttin, C., et al. (1992). Clinical aspects of mitochondrial disorders. *J. Inherit. Metab. Dis.* 15, 448–455.

Nadanaciva, S., Dykens, J. A., Bernal, A., Capaldi, R. A., and Will, Y. (2007). Mitochondrial impairment by PPAR agonists and statins identified via immunocaptured OXPHOS complex activities and respiration. *Toxicol. Appl. Pharmacol.* 223, 277–287.

Naini, A., Lewis, V. J., Hirano, M., and Dimauro, S. (2003). Primary coenzyme Q10 deficiency and the brain. *Biofactors* 18, 145–152.

Oliveira, K. A., Zecchin, K. G., Alberici, L. C., Castilho, R. F., and Vercesi, A. E. (2008). Simvastatin inducing PC3 prostate cancer cell necrosis mediated by calcineurin and mitochondrial dysfunction. *J. Bioenerg. Biomembr.* 40, 307–314.

Paiva, H., Thelen, K. M., Van Coster, R., Smet, J., De Paepe, B., Mattila, K. M., et al. (2005). High-dose statins and skeletal muscle metabolism in humans: a randomized, controlled trial. *Clin. Pharmacol. Ther.* 78, 60–68.

Panov, A., Dikalov, S., Shalbuyeva, N., Taylor, G., Sherer, T., and Greenamyre, J. T. (2005). Rotenone model of Parkinson disease: multiple brain mitochondria dysfunctions after short term systemic rotenone intoxication. *J. Biol. Chem.* 280, 42026–42035.

Radi, R., Rodriguez, M., Castro, L., and Telleri, R. (1994). Inhibition of mitochondrial electron transport by peroxynitrite. *Arch. Biochem. Biophys.* 308, 89–95.

Redfearn, E. R., and Whittaker, P. A. (1966). The determination of the oxidation-reduction states of ubiquinone (coenzyme Q) in rat-liver mitochondria. *Biochim. Biophys. Acta* 118, 413–418.

Robinson, B. H. (1989). Lacticacidemia. Biochemical, clinical, and genetic considerations. *Adv. Hum. Genet.* 18, 151–179; 371–372.

Rundek, T., Naini, A., Sacco, R., Coates, K., and Dimauro, S. (2004). Atorvastatin decreases the coenzyme Q10 level in the blood of patients at risk for cardiovascular disease and stroke. *Arch. Neurol.* 61, 889–892.

Sacher, J., Weigl, L., Werner, M., Szegedi, C., and Hohenegger, M. (2005). Delineation of myotoxicity induced by 3-hydroxy-3-methylglutaryl CoA reductase inhibitors in human skeletal muscle cells. *J. Pharmacol. Exp. Ther.* 314, 1032–1041.

Sener, G., Paskaloglu, K., Satiroglu, H., Alican, I., Kacmaz, A., and Sakarcan, A. (2004). L-carnitine ameliorates oxidative damage due to chronic renal failure in rats. *J. Cardiovasc. Pharmacol.* 43, 698–705.

Shen, W., Liu, K., Tian, C., Yang, L., Li, X., Ren, J., et al. (2008). Protective effects of R-alpha-lipoic acid and acetyl-L-carnitine in MIN6 and isolated rat islet cells chronically exposed to oleic acid. *J. Cell. Biochem.* 104, 1232–1243.

Shepherd, D., and Garland, P. B. (1969). The kinetic properties of citrate synthase from rat liver mitochondria. *Biochem. J.* 114, 597–610.

Silva-Adaya, D., Perez-De La Cruz, V., Herrera-Mundo, M. N., Mendoza-Macedo, K., Villeda-Hernandez, J., Binienda, Z., et al. (2008). Excitotoxic damage, disrupted energy metabolism, and oxidative stress in the rat brain: antioxidant and neuroprotective effects of L-carnitine. *J. Neurochem.* 105, 677–689.

Sirvent, P., Bordenave, S., Vermaelen, M., Roels, B., Vassort, G., Mercier, J., et al. (2005a). Simvastatin induces impairment in skeletal muscle while heart is protected. *Biochem. Biophys. Res. Commun.* 338, 1426–1434.

Sirvent, P., Mercier, J., Vassort, G., and Lacampagne, A. (2005b). Simvastatin triggers mitochondria-induced Ca2+ signaling alteration in skeletal muscle. *Biochem. Biophys. Res. Commun.* 329, 1067–1075.

Sirvent, P., Fabre, O., Bordenave, S., Hillaire-Buys, D., Raynaud De Mauverger, E., Lacampagne, A., et al. (2012). Muscle mitochondrial metabolism and calcium signaling impairment in patients treated with statins. *Toxicol. Appl. Pharmacol.* 259, 263–268.

Sirvent, P., Mercier, J., and Lacampagne, A. (2008). New insights into mechanisms of statin-associated myotoxicity. *Curr. Opin. Pharmacol.* 8, 333–338.

Skottheim, I. B., Gedde-Dahl, A., Hejazifar, S., Hoel, K., and Asberg, A. (2008). Statin induced myotoxicity: the lactone forms are more potent than the acid forms in human skeletal muscle cells *in vitro*. *Eur. J. Pharm. Sci.* 33, 317–325.

Thibault, A., Samid, D., Tompkins, A. C., Figg, W. D., Cooper, M. R., Hohl, R. J., et al. (1996). Phase I study of lovastatin, an inhibitor of the mevalonate pathway, in patients with cancer. *Clin. Cancer Res.* 2, 483–491.

Tobert, J. A., Hitzenberger, G., Kukovetz, W. R., Holmes, I. B., and Jones, K. H. (1982). Rapid and substantial lowering of human serum cholesterol by mevinolin (MK-803), an inhibitor of

hydroxymethylglutaryl-coenzyme A reductase. *Atherosclerosis* 41, 61–65.

Vamos, E., Voros, K., Vecsei, L., and Klivenyi, P. (2010). Neuroprotective effects of L-carnitine in a transgenic animal model of Huntington's disease. *Biomed. Pharmacother.* 64, 282–286.

Velho, J. A., Okanobo, H., Degasperi, G. R., Matsumoto, M. Y., Alberici, L. C., Cosso, R. G., et al. (2006). Statins induce calcium-dependent mitochondrial permeability transition. *Toxicology* 219, 124–132.

Venero, C. V., and Thompson, P. D. (2009). Managing statin myopathy. *Endocrinol. Metab. Clin. North Am.* 38, 121–136.

Virmani, A., Gaetani, F., Binienda, Z., Xu, A., Duhart, H., and Ali, S. F. (2004). Role of mitochondrial dysfunction in neurotoxicity of MPP+: partial protection of PC12 cells by acetyl-L-carnitine. *Ann. N.Y. Acad. Sci.* 1025, 267–273.

Yapar, K., Kart, A., Karapehlivan, M., Atakisi, O., Tunca, R., Erginsoy, S., et al. (2007). Hepatoprotective effect of L-carnitine against acute acetaminophen toxicity in mice. *Exp. Toxicol. Pathol.* 59, 121–128.

Yasuda, N., Matzno, S., Iwano, C., Nishikata, M., and Matsuyama, K. (2005). Evaluation of apoptosis and necrosis induced by statins using fluorescence-enhanced flow cytometry. *J. Pharm. Biomed. Anal.* 39, 712–717.

Ye, J., Li, J., Yu, Y., Wei, Q., Deng, W., and Yu, L. (2010). L-carnitine attenuates oxidant injury in HK-2 cells via ROS-mitochondria pathway. *Regul. Pept.* 161, 58–66.

Young, J. M., Molyneux, S. L., Reinheimer, A. M., Florkowski, C. M., Frampton, C. M., Scott, R. S., et al. (2011). Relationship between plasma coenzyme Q10, asymmetric dimethylarginine and arterial stiffness in patients with phenotypic or genotypic familial hypercholesterolemia on long-term statin therapy. *Atherosclerosis* 218, 188–193.

Zhang, Z., Zhao, M., Wang, J., Ding, Y., Dai, X., and Li, Y. (2010). [Effect of acetyl-L-carnitine on the insulin resistance of L6 cells induced by tumor necrosis factor-alpha]. *Wei Sheng Yan Jiu* 39, 152–154.

Conflict of Interest Statement: The authors declare that the research was conducted in the absence of any commercial or financial relationships that could be construed as a potential conflict of interest.

Received: 29 January 2013; accepted: 23 April 2013; published online: 15 May 2013.

*Citation: La Guardia PG, Alberici LC, Ravagnani FG, Catharino RR and Vercesi AE (2013) Protection of rat skeletal muscle fibers by either L-carnitine or coenzyme Q10 against statins toxicity mediated by mitochondrial reactive oxygen generation. Front. Physiol. **4**:103. doi: 10.3389/fphys.2013.00103*

This article was submitted to Frontiers in Mitochondrial Research, a specialty of Frontiers in Physiology.

frontiers in PHYSIOLOGY

ORIGINAL RESEARCH ARTICLE
published: 07 June 2013
doi: 10.3389/fphys.2013.00138

Experimental data suggesting that inflammation mediated rat liver mitochondrial dysfunction results from secondary hypoxia rather than from direct effects of inflammatory mediators

Adelheid Weidinger[1], Peter Dungel[1], Martin Perlinger[1], Katharina Singer[1], Corina Ghebes[1], J. Catharina Duvigneau[2], Andrea Müllebner[2], Ute Schäfer[3], Heinz Redl[1] and Andrey V. Kozlov[1]*

[1] Ludwig Boltzmann Institute for Experimental and Clinical Traumatology, Vienna, Austria
[2] Institute for Medical Chemistry, University of Veterinary Medicine Vienna, Vienna, Austria
[3] Department of Neurosurgery, Medical University Graz, Graz, Austria

Edited by:
Andrey V. Kuznetsov, Innsbruck Medical University, Austria

Reviewed by:
Hartmut Jaeschke, University of Kansas Medical Center, US Minor Outlying Islands
Enrico Calzia, Universität Ulm, Germany
Vladimir Veksler, University Paris-XI, France

***Correspondence:**
Andrey V. Kozlov, Ludwig Boltzmann Institute for Experimental and Clinical Traumatology, Donaueschingenstrasse 13, A-1200 Vienna, Austria
e-mail: andrey.kozlov@trauma.lbg.ac.at

Systemic inflammatory response (SIR) comprises both direct effects of inflammatory mediators (IM) and indirect effects, such as secondary circulatory failure which results in tissue hypoxia (HOX). These two key components, SIR and HOX, cause multiple organ failure (MOF). Since HOX and IM occur and interact simultaneously *in vivo*, it is difficult to clarify their individual pathological impact. To eliminate this interaction, precision cut liver slices (PCLS) were used in this study aiming to dissect the effects of HOX and IM on mitochondrial function, integrity of cellular membrane, and the expression of genes associated with inflammation. HOX was induced by incubating PCLS or rat liver mitochondria at $pO_2 < 1\%$ followed by reoxygenation (HOX/ROX model). Inflammatory injury was stimulated by incubating PCLS with IM (IM model). We found upregulation of inducible nitric oxide synthase (iNOS) expression only in the IM model, while heme oxygenase 1 (HO-1) expression was upregulated only in the HOX/ROX model. Elevated expression of interleukin 6 (IL-6) was found in both models reflecting converging pathways regulating the expression of this gene. Both models caused damage to hepatocytes resulting in the release of alanine aminotransferase (ALT). The leakage of aspartate aminotransferase (AST) was observed only during the hypoxic phase in the HOX/ROX model. The ROX phase of HOX, but not IM, drastically impaired mitochondrial electron supply via complex I and II. Additional experiments performed with isolated mitochondria showed that free iron, released during HOX, is likely a key prerequisite of mitochondrial dysfunction induced during the ROX phase. Our data suggests that mitochondrial dysfunction, previously observed in *in vivo* SIR-models, is the result of secondary circulatory failure inducing HOX rather than the result of a direct interaction of IM with liver cells.

Keywords: liver, reoxygenation, lipopolysaccharide, cytokine, iNOS, IL-6, HO-1, free iron

INTRODUCTION

Trauma, sepsis, and several types of shock are accompanied by two key pathological events. These are drastic elevation of levels of inflammatory mediators (IM), predominantly cytokines (Clarkson et al., 2005), and secondary circulatory failure causing tissue hypoxia (HOX) (Legrand et al., 2010). Systemic inflammatory response syndrome (SIRS) can be induced by either damage-associated molecular pattern molecules (DAMPs) or pathogen-associated molecular pattern molecules (PAMPs) causing non-infectious and infectious inflammatory responses that are associated with elevated IM levels. In ischemia, immune activation is mainly mediated by DAMPs, whereas in infectious diseases it is triggered by PAMPs. Cytokines, such as tumor necrosis factor alpha (TNF-α), interleukin 6 (IL-6), and interferon gamma (IFN-γ), contribute to the inflammatory response by activating pathological intracellular signaling cascades which result in cellular dysfunction and death. While TNF-α is the most potent activator of death pathways, IL-6 is one of the key regulators of the inflammatory response in the liver. It activates acute phase response, increasing the synthesis of C-reactive protein, fibrinogen, and serum amyloid A, among others. Additionally, IL-6 production has also been suggested as a common feature of ischemic injury (Kielar et al., 2005) and particularly of liver ischemia (Tacchini et al., 2006). The inducible nitric oxide synthase (iNOS) is typically upregulated by IM, predominantly by TNF-α and IFN-γ, and plays an important role in the onset of inflammatory response. Upregulation of iNOS has also been demonstrated in hepatic ischemia reperfusion models

(Isobe et al., 1999). Nitric oxide (NO), a product of iNOS activity, modulates mitochondrial function and stimulates cGMP-dependent signaling. Heme oxygenase 1 (HO-1) is a member of the heat shock protein family (HSP32), catalyzing enzymatic degradation of heme, resulting in the release of equivalent amounts of biliverdin, carbon monoxide, and ferrous ion (Tenhunen et al., 1968). Upregulation of HO-1 has been shown in both conditions, inflammation (Bauer et al., 2003) and impaired circulation (Duvigneau et al., 2010). Meanwhile, it is well documented that both hypoxia/reoxygenation (HOX/ROX) and IM activate multiple transcription factors that regulate IL-6, iNOS, and HO-1 expression. However, it is less clear which condition has the major impact on the early upregulation of either gene. Furthermore, both HOX (Shiva et al., 2007) and IM (Singer et al., 2004) are often associated with impaired mitochondrial function. HOX/ischemia (Rouslin et al., 1990) as well as inflammatory response (Duvigneau et al., 2008) has been shown to decrease ATP levels. Damage to mitochondria is critical for many cellular functions, as mitochondria are involved in a variety of other processes, e.g., innate immune signaling (West et al., 2011), ROS production (Murphy, 2009) and programmed cell death (Skulachev, 1999). There is a body of literature documenting the release of alanine aminotransferase (ALT) and aspartate aminotransferase (AST) following liver ischemia (Lin et al., 2009) and SIRS (Izeboud et al., 2004). In the event of cell lysis, hepatocellular enzymes are released and can be determined in blood or in the incubation medium in *in vitro* experiments (Lerche-Langrand and Toutain, 2000). ALT is mainly present in the cytoplasm of hepatocytes whereas AST is mostly localized in mitochondria but also in the cytoplasm. Therefore, release of ALT predominantly indicates increased permeability of the cytoplasmic membrane, while the increased AST levels reflect both increased permeability of the cytoplasmic membrane and mitochondrial damage. It is difficult to differentiate *in vivo* between the pathological impact of IM and hypoxia on tissue functions because of systemic interactions. However, it is important to gain better understanding of the exact pathological mechanisms leading to organ dysfunction in order to develop efficient therapeutic strategies. Precision cut liver slices (PCLS) are a reliable *in vitro* model of liver tissue, maintaining cell–cell and cell-extracellular matrix interactions without the influence of systemic processes (Lerche-Langrand and Toutain, 2000). We applied this model to dissect the effects of IM and HOX on liver cells. We hypothesized that the above described changes in gene expression and cellular function/integrity could partially be exclusively attributed to either HOX/ROX or IM. Consequently, determination of these markers will help to understand the dynamics of disease and choose an adequate therapeutic strategy. Therefore, the main objective of this study was to investigate whether or not mitochondrial dysfunction, disintegrity of cellular membranes and the expression of genes associated with SIRS can be assigned to either HOX- or IM-dependent pathways.

MATERIALS AND METHODS

CHEMICALS

All reagents were obtained from Sigma-Aldrich (Vienna, Austria) unless otherwise noted.

ANIMALS

Adult male Sprague-Dawley rats (300–350 g) were purchased from the Animal Research Laboratories, Himberg, Austria. All animal procedures were approved by the local legislative committee and conducted according to National Institute of Health guidelines.

WHITE BLOOD CELLS (WBC) ISOLATION AND CONDITIONED MEDIUM GENERATION

Eight rats were anesthetized with isoflurane (Abbott, Vienna, Austria), heparin (600 U/kg, Ebewe, Unterach, Austria) was injected and whole full blood was withdrawn from the vena cava and transferred into 50 ml flasks. Red blood cells were lysed with Schwinzer lysis buffer (0.16 M NH_4Cl, 0.27 mM EDTA, 10 mM $KHCO_3$) for 15 min at 4°C. WBC were pelleted by centrifugation (10 min, 400 g, 4°C) and washed twice in RPMI 1640 medium. Cell pellets were resuspended to 1×10^6 cells/ml in RPMI 1640 medium. IM were generated by incubation of WBC with lipopolysaccharide (LPS, *E. coli* Serotype 026:B6, 6 μg/ml) for 24 h at 37°C. Finally, the cell suspension was centrifuged, the supernatant, now containing WBC-derived cytokines (conditioned medium), was pooled and stored at −80°C. The cytokine pattern of the conditioned medium determined by Myriad RBMTM (Austin, TX, USA) is shown in **Table 1**.

PREPARATION OF PCLS

Rats were anesthetized with isoflurane and sacrificed by decapitation. The liver was extracted and placed into ice cold custodiol solution (Koehler Chemie, Bensheim, Germany) until slice preparation. Cylindrical tissue cores of 6 mm diameter were punched from the left lateral liver lobe and embedded in 3% agarose gel. Slices of 250 μm thickness were cut using a microtome (compresstome VF-300, Precisionary Instruments Inc., Greenville, NC, USA) at room temperature. Slices were incubated in ice cold Ringer solution (Fresenius Kabi, Graz, Austria) for 25 min in order to wash out intracellular compounds released due to the preparation procedure.

Table 1 | Selected cytokines present in control and conditioned medium (CM).

Cytokine	Lower limit of detection	Control	CM
C-reactive protein, [μg/mL]	0.017	ND[a]	0.078
Interferon γ, [pg/mL]	4.6	ND	4.6
Interleukin-1 α, [pg/mL]	36	ND	288.5
Interleukin-10, [pg/mL]	45	ND	74.7
Interleukin-11, [pg/mL	27	ND	94.5
Interleukin-2, [pg/mL]	12	ND	12
Interleukin-7, [ng/mL]	0.015	ND	0.08
Tumor necrosis factor α, [ng/mL]	0.010	ND	0.59
Monocyte chemotactic protein 1, [pg/mL]	0.996	ND	1335

[a] *ND, not detectable.*

EXPERIMENTAL MODELS BASED ON PCLS

In the HOX/ROX-model, HOX was induced by incubating PCLS in glass vials under nitrogen flow at $pO_2 < 1\%$ followed by subsequent ROX with medium equilibrated with air oxygen. HOX/ROX medium was supplemented with the glycolysis inhibitor 2-deoxy-D-glucose (DOG, 10 mM). Duration of the hypoxic and ROX phases is indicated in figure legends. Normoxic control samples (NOX) were incubated in the HOX/ROX medium which was equilibrated with air during the whole incubation period. Inflammatory injury (IM-model) was simulated by incubation of PCLS in 6 well plates (Costar, Corning, USA) containing 1 mL conditioned medium. Corresponding controls were incubated in normal, not preconditioned, RPMI 1640 medium (NM) with or without LPS (6 μg/ml).

PREPARATION OF ISOLATED MITOCHONDRIA

Liver mitochondria were isolated by four consecutive centrifugation steps as previously described (Dungel et al., 2011). The final pellet was resuspended in buffer containing 0.25 M saccharose, 10 mM Tris, 0.5 mM ethylenediaminetetraacetic acid, and 5 mg/mL fatty acid-free bovine serum albumin (pH 7.2, 25°C). The protein concentration was analyzed using the Biuret method.

DETERMINATION OF ENDOGENOUS FREE IRON IN LIVER SECTIONS

Liver sections were cut (2 × 2 × 10 mm) to fit to the EPR spectrometer cavity and subjected to hypoxia for 1 h under nitrogen. Sections were processed as previously described (Kozlov et al., 1992) to determine endogenous free iron following formation of nitrosyl iron complexes.

MITOCHONDRIAL RESPIRATION

Respiratory parameters of mitochondria were monitored using a high resolution respirometer (Oxygraph-2k, Oroboros Instruments, Innsbruck, Austria). Isolated mitochondria/PCLS were incubated in buffer containing 105 mM KCl, 5 mM KH_2PO_4, 20 mM Tris-HCL, 0.5 mM EDTA, and 5 mg/mL fatty acid-free bovine serum albumin (pH 7.2, 25°C). State 2 respiration was stimulated by the addition of either 5 mM glutamate/5 mM malate or 10 mM succinate and 1 ng/ml rotenone. Transition to state 3 respiration was induced by addition of adenosine diphosphate (ADP, 1 mM). In experiments with isolated mitochondria, 20 μM $FeSO_4$ and/or 20 μM desferrioxamine B (Desferal, Novartis, Vienna, Austria) were added to a number of samples before the onset of hypoxia. Mitochondrial function was determined before hypoxia [baseline (BL)], immediately after hypoxia and after 15 min of ROX. To determine mitochondrial function after hypoxia, mitochondria, incubated under hypoxic conditions, were moved in buffer equilibrated with air. Measurements were started immediately and were completed 2 min later.

LIVER ENZYME ASSAY

ALT and AST levels were analyzed in the incubation medium after PCLS incubations using a Cobas c 111 reader (Roche, Basel, Switzerland). Samples were taken at different time points as indicated in figure legends.

cDNA SYNTHESIS AND RT-PCR

RNA was isolated from snap frozen PCLS using illustra RNAspin Mini RNA Isolation Kit (GE Healthcare, Buckinghamshire, UK). The amount of extracted RNA was determined spectrophotometrically at 260 nm and purity was assessed by the 260/280 nm ratio on an Eppendorf BioPhotometer plusUV/Vis (Eppendorf, Hamburg, Germany). RNA integrity was controlled by microcapillary gel analyzes using Agilent Bioanalyzer 2001 System and RNA6000 nano LabChip Kit (Agilent Technologies, Santa Clara, CA, USA). 1 μg of total RNA was used for cDNA synthesis. cDNA was generated using Superscript™ II RNAse H- reverse transcriptase (200U/reaction; Invitrogen; Carlsbad, CA, USA) and anchored oligo-dT-primers (3.5 μmol/L final concentration). Successful cDNA generation was checked by conventional PCR using GAPDH specific primers, as described elsewhere (Duvigneau et al., 2003). Equal aliquots from each cDNA were pooled to generate an internal standard (IS) which was used as reference for the quantification. Analysis of gene expression was performed by means of qPCR. Primer pairs for the analysis of HO-1 are described elsewhere (Duvigneau et al., 2008). Primer paires for the analysis of IL6 and iNOS were newly designed. Further details regarding settings and validation of the qPCR assays in adhering to MIQE guidelines can be found in the supplementary material (**Table S1**; **Figure S1**). qPCR was carried out on a CFX96™ (Bio-Rad, Hercules, CA, USA). Each reaction contained SYBR® green I as reporter (0.5×, Sigma, USA), iTaq™ polymerase™ (0.625 U/reaction; BioRad), the primers (250 μnmol/l each, Invitrogen) with a final concentration of 200 μmol/l dNTP (each) and 3 mmol/l $MgCl_2$ in the provided reaction buffer with a final volume of 12 μl. All samples were measured in duplicates. Each plate contained corresponding randomly assigned RT-minus controls (10% of all samples investigated), the no-template-control (NTC), as well as the IS. Data were analyzed using the inbuilt software CFX manager (Version 2.0, Bio-Rad) in the linear regression mode. Expression of target genes was calculated against the IS using a modified comparative ΔΔCq method (Schmittgen and Livak, 2008). First the gene specific Cqs were substracted from the mean Cq of the IS obtained for the same gene giving rise to ΔCq. The values were than substracted from the normalization factor, which was calculated by averaging the ΔCqs of the internal reference genes, of the same sample (ΔΔCq). The obtained ΔΔCq values of the replicates were averaged and expressed as 2ˆ-DDCq in fold changes relative to the IS.

STATISTICAL ANALYSIS

Data are displayed as mean ± SEM. All parameters were tested for normality (Kolmogorov–Smirnov test) prior to analysis. Statistical analysis of data was performed by one way ANOVA followed by LSD *post-hoc* test in normally distributed data and Kruskal–Wallis combined with Mann–Whitney test in groups showing a non-Gaussian distribution. Calculations were performed using SPSS 15 software (SPSS Inc., USA). The number

of independent samples (n) is indicated in figure legends. The significance level was set at 0.05 and is indicated as $^{*}p < 0.05$, $^{**}p < 0.01$; $^{***}p < 0.001$.

RESULTS

THE EFFECT OF HOX/ROX AND IM ON MARKERS OF HEPATOCYTE DAMAGE (ALT AND AST)

Initially the experimental HOX/ROX-PCLS and IM-PCLS models were standardized. Standardization of the models is based on a significant elevation of ALT release as a basic marker of hepatocyte damage. In the IM-PCLS model significantly elevated ALT levels were observed following 4 h of incubation with IM (**Figure 1A**), while AST levels remained unchanged (**Figure 1C**). In the HOX/ROX-PCLS model pronounced and statistically significantly elevated ALT and AST levels were observed after 1 h of hypoxia. No further release of ALT or AST was observed after subsequent ROX (1 h) (**Figures 1B,D**). To analyze whether IM induced inflammatory response in PCLS, we tested the expression of genes associated with inflammation.

CHANGES IN GENE EXPRESSION IN PCLS FOLLOWING HOX/ROX AND INCUBATION WITH IM

IM led to an upregulation of iNOS (**Figure 2A**) and IL-6 (**Figure 2E**) but did not change HO-1 gene expression (**Figure 2C**). In contrast, in the HOX/ROX model we did not observe any increase in iNOS gene expression (**Figure 2B**) but HO-1 (**Figure 2D**) and IL-6 (**Figure 2F**) were significantly upregulated. A shorter HOX-phase (0.5 h) and longer ROX-phase (1.5 h) increased expression of HO-1 (**Figure 2D**) and IL-6 (**Figure 2F**).

THE EFFECT OF HOX/ROX AND IM ON RESPIRATORY FUNCTION OF MITOCHONDRIA IN PCLS

Incubation with IM did not impair mitochondrial respiration (**Figures 3A,C**). Incubation with LPS showed a trend to increasing rate of mitochondrial respiration with glutamate/malate, a complex I substrate (**Figure 3A**). However, HOX/ROX led to a decrease in state 3 respiration, reflecting ATP synthesis, by a factor of 15.4 when mitochondria respired with glutamate/malate (**Figure 3B**) and by a factor of 3.3 when mitochondria respired with succinate (**Figure 3D**), a complex II substrate.

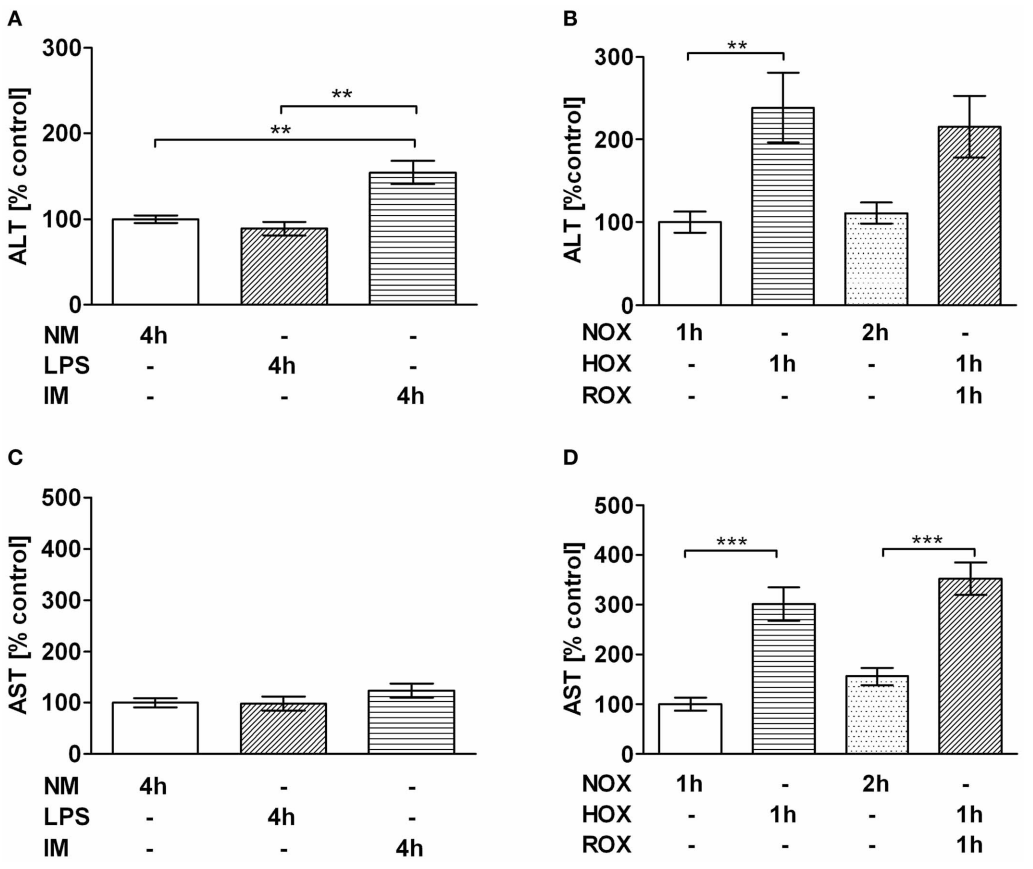

FIGURE 1 | Effect of IM (A,C) and HOX/ROX (B,D) on the release of ALT (A,B) and AST (C,D) from PCLS. (A,C) PCLS were incubated in NM only or NM containing LPS or LPS+IM at 37°C. ALT/AST samples were taken after 4 h incubation. **(B,D)** PCLS were incubated in NM which was either equilibrated with air (NOX, ROX) or nitrogen (HOX). The medium for ALT/AST analysis was taken at the end of the hypoxic phase (1 h) and the end of the subsequent reoxygenation phase (1 h HOX + 1 h ROX). Data are expressed as mean ± SEM of at least $n = 4$ and as a percentage of control. $^{**}p < 0.01$; $^{***}p < 0.001$. Abbreviations used: ALT, alanine aminotransferase; AST, aspartate aminotransferase; NM, normal medium; LPS, lipopolysaccharide; IM, inflammatory mediators; NOX, Normoxia; HOX, Hypoxia; ROX, reoxygenation; PCLS, precision cut liver slices.

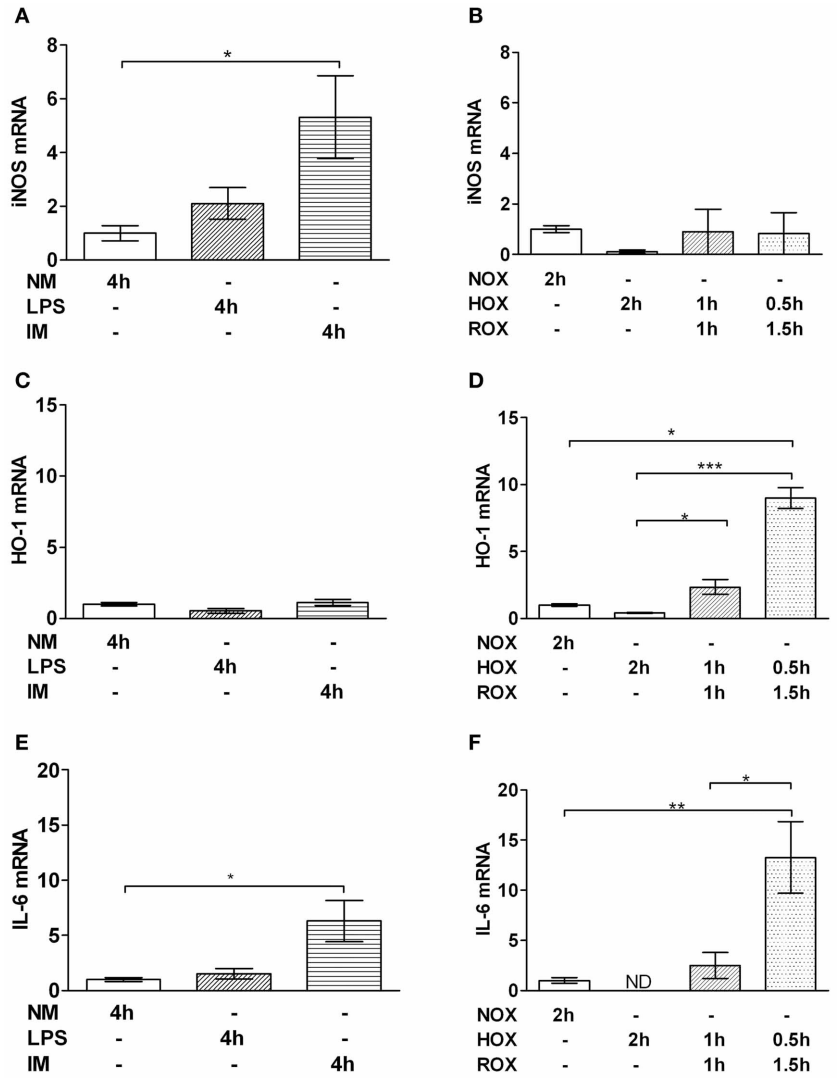

FIGURE 2 | Effect of IM (A,C,E) and HOX/ROX (B,D,F) on gene expression of iNOS (A,B), HO-1 (C,D) and IL-6 (E,F). PCR analysis samples were collected after 4 h of PCLS incubation in NM only or NM containing LPS or LPS + IM at 37°C **(A,C,E)** or after 2 h of PCLS incubation in NM which was either equilibrated with air (NOX, ROX) or nitrogen (HOX) **(B,D,F)**. Data are expressed as mean ± SEM of at least $n = 4$. *$p < 0.05$; **$p < 0.01$, ***$p < 0.001$. mRNA expression is represented as fold increase of the corresponding control. Abbreviations used: iNOS, inducible nitric oxide synthase; HO-1, heme oxygenase 1; NM, normal medium; LPS, lipopolysaccharide; IM, inflammatory mediators; NOX, Normoxia; HOX, Hypoxia; ROX, reoxygenation; PCLS, precision cut liver slices; ND, not detectable.

ACCUMULATION OF FREE IRON UPON HYPOXIA

Since iron is known to induce mitochondrial dysfunction, we determined whether or not free iron levels are increased during 1 h of hypoxia. One hour of hypoxia in liver sections resulted in an increase in intracellular free iron levels by approx. 20 nmol/g tissue (**Figure 4**). In the following experiments we tested the effect of 20 nmol/ml ferrous ion concentration on mitochondrial function.

THE EFFECT OF HOX/ROX AND IRON ON RESPIRATORY FUNCTION OF ISOLATED RAT LIVER MITOCHONDRIA

To better understand the mechanisms of mitochondrial dysfunction under hypoxic conditions and the impact of free iron, we performed experiments with isolated mitochondria. No decrease of respiratory activity of mitochondria was observed following 15 min of hypoxic conditions (**Figure 5**). The presence of iron (Fe) in the hypoxic phase did not influence respiratory activity at this time point. However, after 15 min of ROX mitochondrial function was drastically impaired. The addition of iron chelator desferrioxamine B (Df) abolished the difference in respiration rates between samples with and without iron.

DISCUSSION

The aim of this study was to clarify the impact of two pathophysiologic stressors, IM and HOX/ischemia that typically accompany

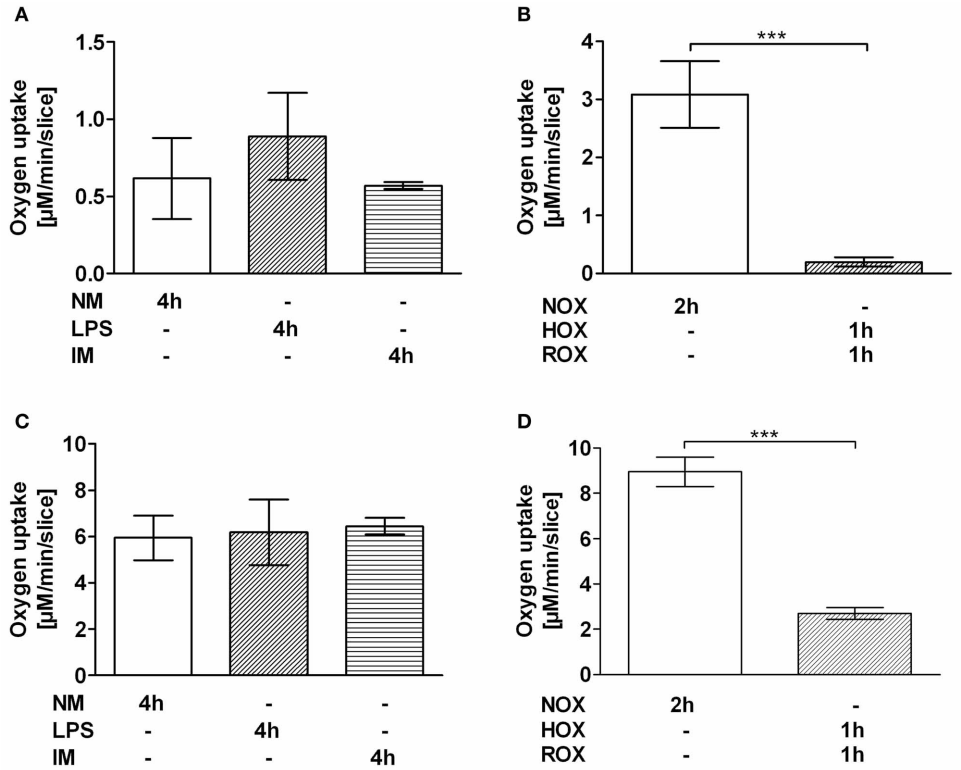

FIGURE 3 | Effect of IM (A,C) and HOX/ROX (B,D) on the mitochondrial state 3 respiration. PCLS mitochondria were stimulated with glutamate + malate **(A,B)** or succinate **(C,D)**. Transition to state 3 respiration was induced by addition of ADP (1 mM). Mitochondrial function was determined after 4 h of PCLS incubation in NM only or NM containing LPS or LPS + IM at 37°C **(A,C)** or after 2 h of PCLS incubation in NM which was either equilibrated with air (NOX, ROX) or nitrogen (HOX) **(B,D)**. Data are expressed as mean ± SEM of at least $n = 4$. $^{***}p < 0.001$. Abbreviations used: NM, normal medium; LPS, lipopolysaccharide; IM, inflammatory mediators; NOX, Normoxia; HOX, hypoxia; ROX, reoxygenation; PCLS, precision cut liver slices.

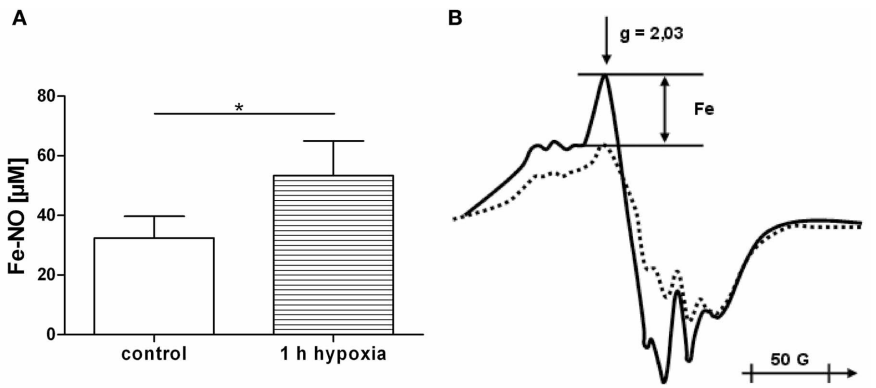

FIGURE 4 | (A,B) Accumulation of free iron in liver sections under hypoxia. The sections were treated with nitrite solution and frozen for EPR analysis either immediately after preparation (control) or after incubation for 1 h at 37°C under nitrogen (1 h hypoxia). The difference in free iron concentration between control and 1 h hypoxia was approx. 20 nmol/g tissue **(A)**. The amplitudes (Fe) of the $g = 2.03$ peak were measured in the EPR spectra **(B)** of control liver sections (dotted line) and after 1 h hypoxia (full line) to determine the concentration of nitrosyl iron complexes. Data are expressed as mean ± SEM of $n = 3$. $^{*}p < 0.05$.

SIRS, and compromise liver function. Since both stressors are strongly linked to and influenced by each other, their effects cannot be dissected *in vivo*. Most *in vitro* models, however, lack the complexity of liver tissue, and the observed responses may therefore not reflect the *in vivo* situation. In this study we have used PCLS in which liver structures are kept intact, including the different liver cell types. This *in vitro* model allowed us to distinguish between the effects of IM and HOX/ROX on liver cells,

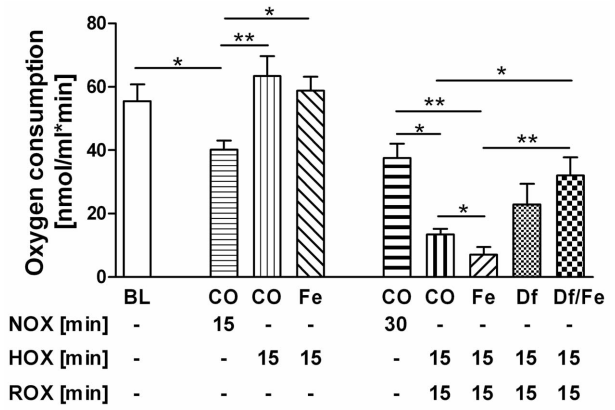

FIGURE 5 | Effect of HOX, ROX, and free iron on state 3 mitochondrial respiration rate. The baseline (BL) represents the respiration of freshly isolated mitochondria. Furthermore, mitochondria were incubated either under air (NOX) or under nitrogen (HOX) with 20 μM $FeSO_4$ (Fe) or without (CO) for 15 min. Subsequently, all samples were incubated under air for further 15 min (ROX). A group of samples received 20 μM desferrioxamine B (Df) immediately after onset of hypoxia. Data are expressed as mean ± SEM of at least $n = 5$. *$p < 0.05$; **$p < 0.01$. Abbreviations used: NOX, Normoxia; HOX, Hypoxia; ROX, reoxygenation; BL, Baseline; CO, control, Fe, $FeSO_4$; Df, desferrioxamine B.

since they can be studied separately. Inflammation affects hepatocytes via IM which are formed by activated immune cells in the blood and by Kupffer cells residing in liver tissue. To simulate the effects of systemic inflammation, we used IM generated *ex vivo* by white blood cells treated with LPS. To simulate effects of IM produced by Kupffer cells, we stimulated PCLS directly with LPS. Both models (HOX/ROX and IM) caused damage to liver cells as seen from increased levels of ALT. Examination of AST levels in both models showed an increase only in the HOX model, suggesting mitochondrial damage. Interestingly, in the HOX model both AST and ALT accumulated during the hypoxic phase, while ROX did not change these values. This suggests that the release of these enzymes is not due to reperfusion induced oxidative damage. Alternatively, the damage to biomembranes under hypoxic conditions may be due to deprivation of ATP and subsequent release of calcium ions. Calcium activates phospholipases, which cause the increase in membrane permeability. It has been shown that the inhibition of phospholipase A2 abolishes the release of ALT in dogs subjected to liver ischemia/reperfusion during reperfusion (Ogata et al., 2001). We did not observe any effects of LPS, although the dose of LPS used in our experiments was reported to induce the release of ALT in *in vivo* (Duvigneau et al., 2008). The fact that only the HOX model induced an increase in AST suggests that HOX predominantly causes mitochondrial dysfunction. This assumption was supported by data relating to the respiratory activity of mitochondria in PCLS. IM did not significantly compromise mitochondrial function, while HOX induced a drastic impairment of respiratory activity. Interestingly, this effect was more pronounced in the presence of glutamate/malate, a substrate of complex I, than in the presence of succinate, a substrate of complex II. This is in line with previous publications carried out in *in vivo* models showing a decrease in mitochondrial function upon ischemia/reperfusion (I/R) due to inhibition of complex I and cytochrome c release (Kuznetsov et al., 2004). Mitochondrial dysfunction might be mediated by changes in iron availability, as both iron deficiency and iron excess impair mitochondrial function (Walter et al., 2002). This is in accordance with reports suggesting the involvement of iron in a transient defect in mitochondrial function observed 8 h after challenge with endotoxin (Duvigneau et al., 2008). Moreover, the release of iron has been suggested to be a key event during oxidative mitochondrial damage and hepatocellular injury (Uchiyama et al., 2008). Free iron concentration in fresh liver sections was about 30 nmol/g tissue which is in line with previously published data (Kozlov et al., 1992). It has also been shown that free iron occurs in the ferrous form. Exposure of liver specimens to warm ischemia for 1 h resulted in an increase of free iron levels of 20 nmol/g tissue compared to controls, which is in accordance with previous publications (Sergent et al., 2005). This concentration was used in this study with isolated mitochondria in order to test whether or not this particular concentration of iron can induce the changes we have observed in experiments with PCLS. To clarify whether iron-mediated mitochondrial damage occurs under HOX or during ROX we used equal short-term HOX and ROX induction (15 min each) with or without adding iron ions. State 3 respiration did not change compared to baseline immediately after HOX phase, but was drastically decreased after 15 min of ROX, suggesting that ferrous iron did not impair mitochondrial function under hypoxic conditions. The decrease in state 3 respiration during ROX was more pronounced in the presence of iron ions. The iron chelator desferrioxamine B increased mitochondrial respiration rates to the levels of NOX controls in samples with or without iron. The latter suggests that endogenous iron ions may contribute to the mitochondrial damage. Interestingly, mitochondria in NOX controls had a lower respiration rate than samples subjected to HOX, suggesting that the mechanisms of mitochondrial damage in this model are strictly oxygen dependent. In the IM model we found a significant upregulation of iNOS after 4 h. Others have reported increased iNOS levels after 3 h of LPS stimulation (Olinga et al., 2001). However, the concentration of LPS used in the cited study was 15 times higher than in our study. Coincidence between upregulation of iNOS and increased release of ALT in our suggests, that damage to hepatocyte membrane occurs in this model in association with the immune response, without affecting mitochondria, since neither the mitochondrial function nor AST levels were affected. These data show that iNOS is a very reliable marker for the inflammatory response. Application of HOX/ROX did not result in an upregulation of iNOS. Thus, our data suggest that the activation of iNOS in HOX models previously reported (Duvigneau et al., 2010) is due to secondary inflammatory response rather than due to hypoxia. HO-1 expression was rapidly upregulated only in the HOX model, but not in the IM model, even though the incubation period was longer in the latter model. We conclude that early upregulation of HO-1 is primarily responsive to changes in the redox balance, presumably via HIF-1α and Nrf2. Previous studies documented an upregulation of HO-1 both during SIRS and hypoxia

in the liver in different *in vivo* models (Bauer et al., 2003; Duvigneau et al., 2010). Here we show that HO-1-upregulation is oxygen rather than IM dependent. Therefore, the increase of HO-1 mRNA seen under conditions of SIRS, have to be attributed primarily to disturbed oxygen delivery to the target cells, due to hypoxia and an inhibition of mitochondrial function. This suggests that activation of HO-1 in SIRS models is mainly due to secondary circulatory failure rather than due to a direct interaction with IM. The predominant pathway of HO-1 regulation is the Nrf2-dependent pathway. It has been shown that Nrf-2 is upregulated during the post-ischemic ROX phase (Leonard et al., 2006). In addition, it has been shown that NF-kB may also be involved in the upregulation of HO-1, although these data are still controversial [reviewed in Paine et al. (2010)].

In contrast to iNOS and HO-1 which were upregulated only in one of the two models, IL-6 responded to both hypoxia and IM. This can be explained by the fact that numerous signaling pathways are known to activate IL-6 mRNA expression, via NF-kB, JNK, C/EBP/(NF)-IL6 and CREB-dependent pathways. It has already been shown that hypoxia induces the (NF)-IL-6 pathway (Yan et al., 1995). In addition, IL-6 may be upregulated by a number of IM via NF-kB-dependent pathway similarly to iNOS (Hur et al., 1999; Li and Verma, 2002). Thus, IL-6 synthesis may be activated by both IM and impaired oxygen delivery. Shortening of the HOX-phase (0.5 h) and extension of the ROX-phase (1.5 h) strongly increased expression of both HO-1 and IL-6, suggesting that either HOX-phase inhibits or ROX-phase activates gene expression most likely through decreased ATP levels.

In summary, in this study we distinguished between the pathological impacts of hypoxia and direct interaction of IM with parenchymal cells in PCLS based models. These *in vitro* models can be used to analyze other parameters accompanying either SIRS or circulatory failure. In addition our data show that accumulation of free iron in hypoxic tissue is critical for mitochondrial function. This is in line with previous reports showing beneficial effects of iron chelators in hypoxia models (Arkadopoulos et al., 2010) and sepsis models (Srinivasan et al., 2012). A clear understanding of whether HOX or IM dependent pathways predominantly cause organ failure in certain pathologic states will contribute to the development of new effective therapy approaches.

The major limitation of this study is that experiments were performed at a defined set of conditions of either hypoxia (e.g., duration of HOX and ROX) or inflammation (e.g., concentration of IM and incubation time). The balance between HOX-dependent and IM-dependent processes may depend on the severity of a disease or an experimental model.

ACKNOWLEDGMENTS

The authors thank Asmita Banerjee, Sidrah Chaudary, and James Ferguson for assistance in the preparation of this manuscript and Christine Kober for excellent technical assistance. Adelheid Weidinger was supported by FFG (Austria) grant 825329.

SUPPLEMENTARY MATERIAL

The Supplementary Material for this article can be found online at: http://www.frontiersin.org/Mitochondrial_Research/10.3389/fphys.2013.00138/abstract

REFERENCES

Arkadopoulos, N., Nastos, C., Kalimeris, K., Economou, E., Theodoraki, K., Kouskouni, E., et al. (2010). Iron chelation for amelioration of liver ischemia-reperfusion injury. *Hemoglobin* 34, 265–277. doi: 10.3109/03630269.2010.484766

Bauer, I., Rensing, H., Florax, A., Ulrich, C., Pistorius, G., Redl, H., et al. (2003). Expression pattern and regulation of heme oxygenase-1/heat shock protein 32 in human liver cells. *Shock* 20, 116–122. doi: 10.1097/01.shk.0000075568.93053.fa

Clarkson, A. N., Sutherland, B. A., and Appleton, I. (2005). The biology and pathology of hypoxia-ischemia: an update. *Arch. Immunol. Ther. Exp.* 53, 213–225.

Dungel, P., Haindl, S., Behling, T., Mayer, B., Redl, H., and Kozlov, A. V. (2011). Neither nitrite nor nitric oxide mediate toxic effects of nitroglycerin on mitochondria. *J. Biochem. Mol. Toxicol.* 25, 297–302. doi: 10.1002/jbt.20389

Duvigneau, J. C., Hartl, R. T., Teinfalt, M., and Gemeiner, M. (2003). Delay in processing porcine whole blood affects cytokine expression. *J. Immunol. Methods* 272, 11–21. doi: 10.1016/S0022-1759(02)00372-1

Duvigneau, J. C., Kozlov, A. V., Zifko, C., Postl, A., Hartl, R. T., Miller, I., et al. (2010). Reperfusion does not induce oxidative stress but sustained endoplasmic reticulum stress in livers of rats subjected to traumatic-hemorrhagic shock. *Shock* 33, 289–298. doi: 10.1097/SHK.0b013e3181aef322

Duvigneau, J. C., Piskernik, C., Haindl, S., Kloesch, B., Hartl, R. T., Hüttemann, M., et al. (2008). A novel endotoxin-induced pathway: upregulation of heme oxygenase 1, accumulation of free iron, and free iron-mediated mitochondrial dysfunction. *Lab. Invest.* 88, 70–77. doi: 10.1038/labinvest.3700691

Hur, G. M., Ryu, Y. S., Yun, H. Y., Jeon, B. H., Kim, Y. M., Seok, J. H., et al. (1999). Hepatic ischemia/reperfusion in rats induces iNOS gene transcription by activation of NF-kappaB. *Biochem. Biophys. Res. Commun.* 261, 917–922. doi: 10.1006/bbrc.1999.1143

Isobe, M., Katsuramaki, T., Hirata, K., Kimura, H., Nagayama, M., and Matsuno, T. (1999). Benefical effects of inducible nitric oxide synthase inhibitor on reperfusion injury in the pig liver. *Transplantation* 68, 803–813.

Izeboud, C. A., Hoebe, K. H. N., Grootendorst, A. F., Nijmeijer, S. M., Van Miert, A. S., Witkamp, R. R., et al. (2004). Endotoxin-induced liver damage in rats is minimized by beta 2-adrenoceptor stimulation. *Inflamm. Res.* 53, 93–99. doi: 10.1007/s00011-003-1228-y

Kielar, M. L., John, R., Bennett, M., Richardson, J. A., Shelton, J. M., Chen, L., et al. (2005). Maladaptive role of IL-6 in ischemic acute renal failure. *J. Am. Soc. Nephrol.* 16, 3315–3325. doi: 10.1681/ASN.2003090757

Kozlov, A. V., Yegorov, D. Y., Vladimirov, Y. A., and Azizova, O. A. (1992). Intracellular free iron in liver tissue and liver homogenate: studies with electron paramagnetic resonance on the formation of paramagnetic complexes with desferal and nitric oxide. *Free Radic. Biol. Med.* 13, 9–16. doi: 10.1016/0891-5849(92)90159-E

Kuznetsov, A. V., Schneeberger, S., Seiler, R., Brandacher, G., Mark, W., Steurer, W., et al. (2004). Mitochondrial defects and heterogeneous cytochrome c release after cardiac cold ischemia and reperfusion. *Am. J. Physiol. Heart Circ. Physiol.* 286, H1633–H1641. doi: 10.1152/ajpheart.00701.2003

Legrand, M., Klijn, E., Payen, D., and Ince, C. (2010). The response of the host microcirculation to bacterial sepsis: does the pathogen matter? *J. Mol. Med.* 88, 127–133. doi: 10.1007/s00109-009-0585-6

Leonard, M. O., Kieran, N. E., Howell, K., Burne, M. J., Varadarajan, R., Dhakshinamoorthy, S., et al. (2006). Reoxygenation-specific activation of the antioxidant transcription factor Nrf2 mediates cytoprotective gene expression in ischemia-reperfusion injury. *FASEB J.* 20, 2624–2626. doi: 10.1096/fj.06-5097fje

Lerche-Langrand, C., and Toutain, H. J. (2000). Precision-cut liver slices: characteristics and use for *in vitro* pharmaco-toxicology. *Toxicology* 153, 221–253. doi: 10.1016/S0300-483X(00)00316-4

Li, Q., and Verma, I. M. (2002). NF-kappaB regulation in the immune system. *Nat. Rev. Immunol.* 2, 725–734. doi: 10.1038/nri910

Lin, T.-T., Wang, B.-M., Li, X.-Y., Pan, Y., Wang, W., Mu, Y., et al. (2009). An insight into the protection of rat liver against ischemia/reperfusion injury by 2-selenium-bridged beta-cyclodextrin. *Hepatol. Res.* 39, 1125–1136. doi: 10.1111/j.1872-034X.2009.00545.x

Murphy, M. P. (2009). How mitochondria produce reactive oxygen species. *Biochem. J.* 417, 1–13. doi: 10.1042/BJ20081386

Ogata, K., Jin, M. B., Taniguchi, M., Suzuki, T., Shimamura, T., Kitagawa, N., et al. (2001). Attenuation of ischemia and reperfusion injury of canine livers by inhibition of type II phospholipase A2 with LY329722. *Transplantation* 71, 1040–1046.

Olinga, P., Merema, M. T., De Jager, M. H., Derks, F., Melgert, B. N., Moshage, H., et al. (2001). Rat liver slices as a tool to study LPS-induced inflammatory response in the liver. *J. Hepatol.* 35, 187–194.

Paine, A., Eiz-Vesper, B., Blasczyk, R., and Immenschuh, S. (2010). Signaling to heme oxygenase-1 and its anti-inflammatory therapeutic potential. *Biochem. Pharmacol.* 80, 1895–1903. doi: 10.1016/j.bcp.2010.07.014

Rouslin, W., Broge, C. W., and Grupp, I. L. (1990). ATP depletion and mitochondrial functional loss during ischemia in slow and fast heart-rate hearts. *Am. J. Physiol.* 259, H1759–H1766.

Schmittgen, T. D., and Livak, K. J. (2008). Analyzing real-time PCR data by the comparative CT method. *Nat. Protoc.* 3, 1101–1108.

Sergent, O., Tomasi, A., Ceccarelli, D., Masini, A., Nohl, H., Cillard, P., et al. (2005). Combination of iron overload plus ethanol and ischemia alone give rise to the same endogenous free iron pool. *Biometals* 18, 567–575. doi: 10.1007/s10534-005-8488-7

Shiva, S., Sack, M. N., Greer, J. J., Duranski, M., Ringwood, L. A., Burwell, L., et al. (2007). Nitrite augments tolerance to ischemia/reperfusion injury via the modulation of mitochondrial electron transfer. *J. Exp. Med.* 204, 2089–2102. doi: 10.1084/jem.20070198

Singer, M., De Santis, V., Vitale, D., and Jeffcoate, W. (2004). Multiorgan failure is an adaptive, endocrine-mediated, metabolic response to overwhelming systemic inflammation. *Lancet* 364, 545–548. doi: 10.1016/S0140-6736(04)16815-3

Skulachev, V. P. (1999). Mitochondrial physiology and pathology; concepts of programmed death of organelles, cells and organisms. *Mol. Aspects Med.* 20, 139–184. doi: 10.1016/S0098-2997(99)00008-4

Srinivasan, G., Aitken, J. D., Zhang, B., Carvalho, F. A., Chassaing, B., Shashidharamurthy, R., et al. (2012). Lipocalin 2 deficiency dysregulates iron homeostasis and exacerbates endotoxin-induced sepsis. *J. Immunol.* 189, 1911–1919. doi: 10.4049/jimmunol.1200892

Tacchini, L., Cairo, G., De Ponti, C., Massip, M., Rosellò-Catafau, J., and Peralta, C. (2006). Up regulation of IL-6 by ischemic preconditioning in normal and fatty rat livers: association with reduction of oxidative stress. *Free Radic. Res.* 40, 1206–1217. doi: 10.1080/10715760600885432

Tenhunen, R., Marver, H. S., and Schmid, R. (1968). The enzymatic conversion of heme to bilirubin by microsomal heme oxygenase. *Proc. Natl. Acad. Sci. U.S.A.* 61, 748–755.

Uchiyama, A., Kim, J.-S., Kon, K., Jaeschke, H., Ikejima, K., Watanabe, S., et al. (2008). Translocation of iron from lysosomes into mitochondria is a key event during oxidative stress-induced hepatocellular injury. *Hepatology* 48, 1644–1654. doi: 10.1002/hep.22498

Walter, P. B., Knutson, M. D., Paler-Martinez, A., Lee, S., Xu, Y., Viteri, F. E., et al. (2002). Iron deficiency and iron excess damage mitochondria and mitochondrial DNA in rats. *Proc. Natl. Acad. Sci. U.S.A.* 99, 2264–2269. doi: 10.1073/pnas.261708798

West, A. P., Brodsky, I. E., Rahner, C., Woo, D. K., Erdjument-Bromage, H., Tempst, P., et al. (2011). TLR signalling augments macrophage bactericidal activity through mitochondrial ROS. *Nature* 472, 476–480. doi: 10.1038/nature09973

Yan, S. F., Tritto, I., Pinsky, D., Liao, H., Huang, J., Fuller, G., et al. (1995). Induction of interleukin 6 (IL-6) by hypoxia in vascular cells. *J. Biol. Chem.* 270, 11463–11471.

Conflict of Interest Statement: The authors declare that the research was conducted in the absence of any commercial or financial relationships that could be construed as a potential conflict of interest.

Received: 22 February 2013; accepted: 22 May 2013; published online: 07 June 2013.

*Citation: Weidinger A, Dungel P, Perlinger M, Singer K, Ghebes C, Duvigneau JC, Müllebner A, Schäfer U, Redl H and Kozlov AV (2013) Experimental data suggesting that inflammation mediated rat liver mitochondrial dysfunction results from secondary hypoxia rather than from direct effects of inflammatory mediators. Front. Physiol. **4**:138. doi: 10.3389/fphys.2013.00138*

This article was submitted to Frontiers in Mitochondrial Research, a specialty of Frontiers in Physiology.

frontiers in PHYSIOLOGY

HYPOTHESIS AND THEORY ARTICLE
published: 20 June 2013
doi: 10.3389/fphys.2013.00147

Mitochondria and FOXO3: breath or die

Judith Hagenbuchner*[1,2] *and Michael J. Ausserlechner*[2,3]

[1] *Department of Pediatrics II, Medical University Innsbruck, Innsbruck, Austria*
[2] *Tyrolean Cancer Research Institute, Innsbruck, Austria*
[3] *Department of Pediatrics I, Medical University Innsbruck, Innsbruck, Austria*

Edited by:
Andrey V. Kuznetsov, Innsbruck Medical University, Austria

Reviewed by:
Uwe Schlattner, University Joseph Fourier, France
Allen Kaasik, Univerisy of Tartu, Estonia

***Correspondence:**
Michael J. Ausserlechner, Department of Pediatrics I, Medical University Innsbruck, Innrain 66, 4th floor, A-6020 Innsbruck, Austria
e-mail: michael.j.ausserlechner@i-med.ac.at

Forkhead box O (FOXO) transcription factors are regulators of cell-type specific apoptosis and cell cycle arrest but also control longevity and reactive oxygen species (ROS). ROS-control by FOXO is mediated by transcriptional activation of detoxifying enzymes such as Superoxide dismutase 2 (SOD2), Catalase or Sestrins or by the repression of mitochondrial respiratory chain proteins resulting in reduced mitochondrial activity. FOXO3 also regulates the adaptation to hypoxia by reducing mitochondrial mass and oxygen consumption during HIF-1α activation. In neuronal tumor cells, FOXO3 triggers ROS-accumulation as a consequence of transient mitochondrial outer membrane permeabilization, which is essential for FOXO3-induced apoptosis in these cells. Cellular ROS levels are affected by the FOXO-targets Bim, BclxL, and Survivin. All three proteins localize to mitochondria and affect mitochondrial membrane potential, respiration and cellular ROS levels. Bim-activation by FOXO3 causes mitochondrial depolarization resulting in a transitory decrease of respiration and ROS production. Survivin, on the other hand, actively changes mitochondrial architecture, respiration-efficacy and energy metabolism. This ability distinguishes Survivin from other anti-apoptotic proteins such as BclxL, which inhibits ROS by inactivating Bim but does not alter mitochondrial function. Importantly, FOXO3 simultaneously also activates ROS-detoxification via induction of SESN3. In this paper we discuss the hypothesis that the delicate balance between ROS-accumulation by Bim-triggered mitochondrial damage, mitochondrial architecture and ROS-detoxifying proteins determines cell fate. We provide evidence for a FOXO self-reactivating loop and for novel functions of FOXO3 in controlling mitochondrial respiration of neuronal cells, which further supports the current view that FOXO transcription factors are information-integrating sentinels of cellular stress and critical modulators of cell homeostasis.

Keywords: forkhead transcription factor, Bcl2-rheostat, BH3-only proteins, mitochondrial respiration, mitochondrial fission

THE FAMILY OF FORKHEAD BOX O TRANSCRIPTION FACTORS

The family of mammalian forkhead box O (FOXO) transcription factors consists of the four members FKHR/FOXO1, FKHRL1/FOXO3, AFX/FOXO4, and FOXO6 which regulate apoptosis and cell cycle, immune response, energy state, stress resistance, and longevity. Although all four mammalian FOXO transcription factors share the same DNA binding motives (Obsil and Obsilova, 2011) and seem to have overlapping functions, knock out animals for single FOXO family members show different defects (Arden, 2008). FOXO1 knockout mice die *in utero* due to defective vasculature (Hosaka et al., 2004), FOXO3 knockout mice suffer from organ inflammation resulting from defective development of regulatory T-cells (Harada et al., 2010; Kerdiles et al., 2010). In contrast FOXO4 and FOXO6 knockout mice present with mild phenotypes (Zhu et al., 2011; Salih et al., 2012). Conditional triple-knock-out in the adult mouse causes a relatively mild neoplastic phenotype, i.e., these mice develop hemangiomas and thymic lymphomas, which suggests that FOXO1, FOXO3, and FOXO4 are involved in the maintenance of the hematopoietic stem cell population and the regulation of endothelial cell homeostasis (Paik et al., 2007; Tothova et al., 2007). In cultured neuroblastoma cells the activation of FOXO3 triggers the intrinsic death pathway and induces programmed cell death via induction of the pro-apoptotic BH3-only proteins Bim and Noxa (Obexer et al., 2007). In addition FOXO3 represses the apoptosis-inhibitor protein Survivin (Guha et al., 2009; Obexer et al., 2009) and determines the sensitivity of neuroblastoma cells to DNA-damaging chemotherapeutic agents. More recently it was shown that beside its function as a tumor-suppressor FOXO3 might also promote cancer cell survival. FOXO3 induces detoxification and stress resistance thereby contributing to tumor stem cell renewal (Naka et al., 2010) and protection of cancer cells from eradication during chemotherapy (Hui et al., 2008) and hypoxia (Bakker et al., 2007).

In this article we will discuss the current knowledge on the involvement of FOXO transcription factors in the regulation of cellular homeostasis with specific emphasis on mitochondrial integrity, morphology and activity. In addition we present our hypothesis that FOXO3 controls a delicate balance between

mitochondrial reactive oxygen species (ROS)-generation and ROS-preventing or detoxifying processes, which is critical for cell death decision in neuronal cells.

GROWTH FACTOR SIGNALING INACTIVATES FOXO TRANSCRIPTION FACTORS

The activity and subcellular localization of FOXO transcription factors (except FOXO6) is regulated by various upstream regulators that modify FOXO proteins via phosphorylation, acetylation, methylation and mono/poly-ubiquitination (Eijkelenboom and Burgering, 2013). Phosphorylation at conserved serine/threonine residues by protein kinase B (PKB) and by serum- and glucocorticoid-induced kinase (SGK) induces the association of FOXO transcription factors with 14-3-3 proteins and their nuclear export and inactivation (Tzivion et al., 2011). This evolutionary conserved FOXO-inactivating pathway directly links FOXO activity to insulin and insulin-like growth factor signaling, suggesting that under normal growth conditions, FOXOs are inactivated and dispensable for the survival of cells. Similar to PKB and SGK, IkB-kinase (IKK) and extracellular-signal regulated kinase (ERK) phosphorylate distinct serines (Ser644 of FOXO3 by IKK and Ser294, Ser344, Ser425 of FOXO3 by ERK) thereby causing FOXO-inactivation (**Figure 1**). Importantly, phosphorylation by PKB, IKK, and ERK also constitutes a signal for poly-ubiquitination and proteasomal degradation of FOXO transcription factors thereby, in addition to functional inactivation, also reducing protein steady state levels (Matsuzaki et al., 2003; Hu et al., 2004; Yang et al., 2008).

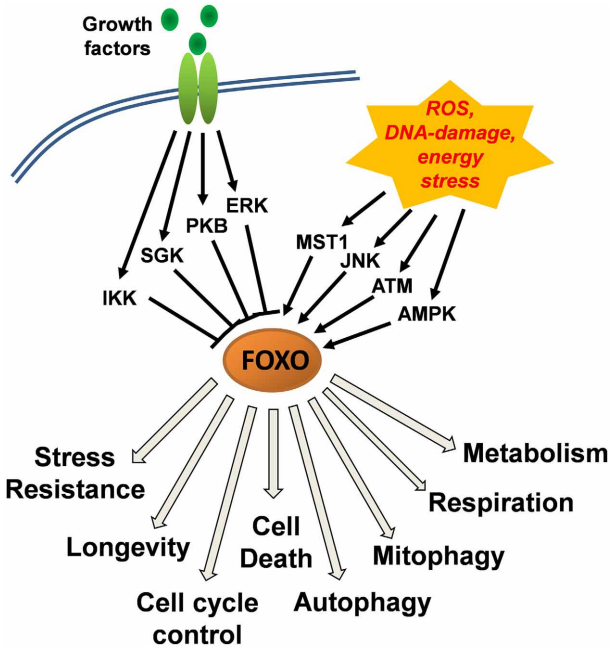

FIGURE 1 | Control of FOXO function downstream of growth-factor and stress-induced kinase signaling cascades. Growth factor signaling via protein kinase B (PKB), serum- and glucocorticoid-induced kinase (SGK), IkB-kinase (IKK), and extracellular-signal regulated kinase (ERK) causes inactivation of FOXO transcription factors and their export from the nucleus. Jun-N-terminal kinase (JNK) and mammalian STE20-like protein kinase 1 (MST1) that are activated upon cellular stress, induce the nuclear accumulation of FOXOs. A main trigger of JNK activation is accumulation of cellular reactive oxygen species (ROS) which together with DNA-damage also activate ataxia telangiectasia mutated (ATM) kinase and induce the interaction between ATM and FOXO and its nuclear accumulation. AMP-activated kinase (AMPK) functions as a cellular energy sensor that increases the activity of nuclear FOXO factors. AMPK thereby acts in concert with either low growth factor availability or high cellular stress and further steers FOXO target recognition.

STRESS KINASE CASCADES THAT ACTIVATE FOXO IN RESPONSE TO ROS AND DNA-DAMAGE

First evidence for the participation of FOXO transcription factors in ROS regulation was found in *C.elegans* studying the FOXO3 homologue DAF-16. There, DAF-16 regulates a stress-resistant-state, where metabolism is shut down and the worm enters so called Dauer-formation to extend lifespan during nutrient deprivation (Braeckman and Vanfleteren, 2007). FOXO3 is also thought to participate in longevity regulation by detoxification of ROS. Several groups found the mitochondrial enzyme superoxide dismutase 2 (SOD2) (Kops et al., 2002), the peroxisome-located Catalase (CAT) (Tan et al., 2008), the antioxidant enzyme peroxiredoxin III (Chiribau et al., 2008) or the redox enzyme sestrin3 (SESN3) (Chen et al., 2010; Hagenbuchner et al., 2012a) induced by FOXO in different tissues. Also the growth arrest and DNA damage repair enzyme GADD45a is activated after stress signaling by FOXO transcription factors and contributes to the survival of damaged cells and stress resistance (Furukawa-Hibi et al., 2002).

Cellular stress induced by accumulation of ROS or DNA-damage overrides the growth factor-induced functional inactivation of FOXO. The response to ROS involves Jun-N-terminal kinase (JNK) and mammalian STE20-like protein kinase 1 (MST1) which phosphorylate FOXO transcription factors directly (Essers et al., 2004; Lehtinen et al., 2006; Sunters et al., 2006) or also target its binding partner 14-3-3 protein (Sunayama et al., 2005). The direct phosphorylation by JNK or MST1 induces the release of FOXO3 from 14-3-3 proteins and causes nuclear accumulation. However, as phosphorylation occurs at a conserved serine in the forkhead domain (Ser209 of FOXO3) it has not been completely clarified, how this phosphorylation affects consensus sequence recognition by FOXO3. According to crystal structures and band shift analyses (Brent et al., 2008), DNA binding by FOXO1 is reduced or event abrogated suggesting that during activation by JNK or MST1, FOXO might at least in part interact with other transcription factors such as p53 (Chung et al., 2012) or c-Myc (Ferber et al., 2012) and thereby regulate target gene expression.

An important sensor of DNA-damage response is the ataxia telangiectasia mutated (ATM), a member of the phosphoinositol-3-kinase-like kinase family. ATM coordinates together with ATM-related kinase (ATR) the cellular response to DNA-damage by activating DNA-repair and signaling pathways. ATM senses DNA double strand breaks and is also activated by ROS in mammalian cells (reviewed in Ditch and Paull, 2012). ATM interacts with FOXO3 and p53 during DNA-damage (Tsai et al., 2008; Chung et al., 2012) and ROS-response (Yalcin et al., 2008) suggesting

that these proteins are tightly interconnected during stress signaling. We recently provided evidence that the FOXO3-ATM complex also overcomes epigenetic silencing of the caspase-8 gene in human neuroblastoma cells by activating the ATM downstream target CREB which in turn triggers methylation-independent activation of the caspase-8 promoter (Geiger et al., 2012).

AMP-activated kinase (AMPK) is a sensor of cellular energy homeostasis and is activated by high AMP to ATP ratios. AMPK phosphorylates FOXO3 on at least six different serine/threonine residues (Thr179, Ser399, Ser413, Ser439, Ser555, Ser588, and Ser626), which does not change subcellular localization of FOXO3 but increases its transcriptional activity and may modulate differential promoter recognition (Greer et al., 2007). AMPK only phosphorylates nuclear FOXO3 thereby acting in concert with growth factor withdrawal or cellular stress signals. The exact mechanism of FOXO3 transcriptional activation by AMPK has not been completely elucidated but phosphorylation by AMPK increases the interaction with CREB-binding protein (CBP) (Wang et al., 2012) and p300 which both affect FOXO3 transcriptional activity and promoter recognition by acetylation. Phosphorylation of FOXO by AMPK has been linked to FOXO-induced autophagy (Chiacchiera and Simone, 2009), neuronal cell death (Davila et al., 2012), and muscle atrophy (Sanchez et al., 2012). Importantly, fission of mitochondria triggers AMPK activation and FOXO3-induced autophagy, which removes mitochondria and contributes to muscle atrophy (Romanello et al., 2010). This suggests an energy-sensing network between AMPK, FOXO3 and mitochondrial architecture.

STEERING FOXO FUNCTION BY ACETYLATION, METHYLATION AND INTERACTION WITH OTHER TRANSCRIPTION FACTORS

Besides kinase cascades FOXO transcription factors are subject to additional post-translational modifications such as acetylation/deacetylation processes, most prominent via acetylation of lysines in the forkhead domain by CBP/p300 (Wang et al., 2012) or deacetylation by the protein deacetylase sirtuin-1 (SIRT1) (Brunet et al., 2004; Kobayashi et al., 2005). Whereas acetylation enhances the expression of pro-apoptotic FOXO-targets, SIRT1 modulates the transcriptional function of FOXO3 in a way which inhibits FOXO3-induced expression of pro-apoptotic genes and increases the expression of genes involved in cell-cycle regulation, DNA-repair and stress resistance. FOXO-deacetylation by SIRT1 may therefore also contribute to longevity and survival of tumor cells, questioning the general view of FOXOs as tumor suppressor proteins (reviewed in (Calnan and Brunet, 2008). Another posttranslational modification is methylation by protein arginine methyltransferases (PRMT) 1 and 6 that add methyl groups to arginine on substrate proteins. In the case of FOXO transcription factors, PRMT1 targets arginine Arg248 and Arg250 (of FOXO1) within the PKB consensus motive, which prevents PKB-mediated phosphorylation of Ser256 (FOXO1). As a consequence nuclear export in presence of active PKB is inhibited and the transcriptional activity of FOXO transcription factors is increased (Yamagata et al., 2008). In contrast SET-domain containing protein 7 (SETD7/SET9), a lysine-methyltransferase was shown to methylate Lys270 in FOXO3, which inhibits DNA-binding, induction of FOXO3 target genes such as Bim and neuronal apoptosis (Xie et al., 2012). Therefore protein methylation significantly steers the activity of FOXO transcription factors and also affects their posttranslational modification by protein kinases.

Furthermore, FOXO proteins have been shown to cooperate with cofactors such as Smad3/4, p53, as well as with nuclear androgen-, glucocorticoid- and retinoic acid receptors (reviewed in, Calnan and Brunet, 2008; van der Vos and Coffer, 2008). Recently it was also shown that FOXO3 interacts with β-catenin and that this interaction converts the transcriptional activity of FOXO3 to promote metastasis instead of apoptosis in colon cancer (Tenbaum et al., 2012).

A recent report suggests that FOXOs may also directly measure the redox status in a cell via reversible oxidation/reduction of cysteine. Oxidation of cysteines in FOXO proteins causes the covalent binding of p300 and CBP via disulfide bonds. These modifications directly affect the transcriptional activity of FOXO transcription factors and thereby allow them to act as sensors of cellular redox status (Dansen et al., 2009). Together with phosphorylation by oxidative stress induced kinases such as JNK or MST1, this mechanism may directly affect target gene regulation by FOXO transcription factors and modulate the cellular response to ROS.

FOXO3 AS A TRIGGER FOR MITOCHONDRIAL ROS

Although FOXO3 has been shown to induce a number of genes that protect against ROS suggesting that they play a critical role in keeping cellular ROS low, we recently demonstrated that in primary neurons and neuroblastoma cells FOXO3 may also increase mitochondrial ROS levels (Hagenbuchner et al., 2012a). The accumulation of ROS was essential for FOXO3-induced cell death in these cell types, since co-treatment with the ROS inhibitor N-Acetyl-L-cystein (NAC) rescued neuroblastoma cells from FOXO3-induced apoptosis. This uncovers an interesting possible feedback regulation between ROS and FOXO3 at mitochondria: on one hand FOXO3 is activated in response to elevated cellular ROS levels and on the other hand FOXO3 itself triggers ROS accumulation by interrupting mitochondrial outer membrane integrity. To investigate such a possible self-amplifying regulation we infected SH-EP/FOXO3 cells that carry a conditional 4OHT-activated FOXO3ERtm fusion protein with a retrovirus coding for a wild-type ECFP-FOXO3 fusion protein. This ECFP-FOXO3 fusion protein can be used to monitor FOXO3 nuclear accumulation by live cell fluorescence microscopy in response to various stimuli (Obexer et al., 2009; Geiger et al., 2012; Hagenbuchner et al., 2012a,b). In SH-EP neuroblastoma cells the PI3K-PKB signaling pathway is highly active, which causes cytoplasmic retention of FOXO3 (Obexer et al., 2007, 2009). In these cells, we studied whether activation of the conditional, PKB-independent FOXO3 allele and FOXO3-induced increase of mitochondrial ROS constitutes a signal to activate cellular FOXO3 protein despite active PKB. A first ROS accumulation was observed already 4 h after FOXO3-activation and at this time point ECFP-FOXO3wt is already equally distributed between nucleus and cytoplasm of the majority of the cells. Interestingly at 6 h, when the first ROS wave already declines,

wild-type ECFP-FOXO3 accumulates in the nucleus of the neuroblastoma cells (**Figure 2**). This supports the hypothesis that some active FOXO3 molecules within a cell may trigger also the nuclear accumulation and thereby hyper-activation of other FOXO3 molecules. The primary, partial activation of FOXO increases the levels of pro-apoptotic Bim, which in turn causes damage to mitochondria, partial release of Cytochrome-*c* and increased ROS production (Hagenbuchner et al., 2012a). The secondary FOXO3 activation might at least in part be regulated by the first ROS accumulation and explain why some FOXO3 targets are immediately activated, such as Bim, whereas others are induced (such as $p27^{Kip1}$, data not shown) or repressed (such as BclxL), (Hagenbuchner et al., 2012a) in delay. Although the relevance of ROS in this FOXO3-induced FOXO3 activation has to be proven, these observations support the hypothesis that oxidative stress activates FOXO3, which enhances further mitochondrial ROS and that this feedback-loop causes an avalanche-like, secondary activation of additional FOXO3 molecules leading to the second wave of ROS accumulation and apoptotic cell death (**Figure 2**).

THE CONNECTION BETWEEN FOXO, PRO-APOPTOTIC Bcl2 PROTEINS, RESPIRATION AND ROS

When analyzing the events that lead to the first accumulation of ROS at the mitochondria, we identified the pro-apoptotic FOXO3-target Bim as a trigger of transitory mitochondrial outer membrane permeabilization. Bim is rapidly induced (within 2–8 h) by FOXO3 (Obexer et al., 2007), leading to translocation

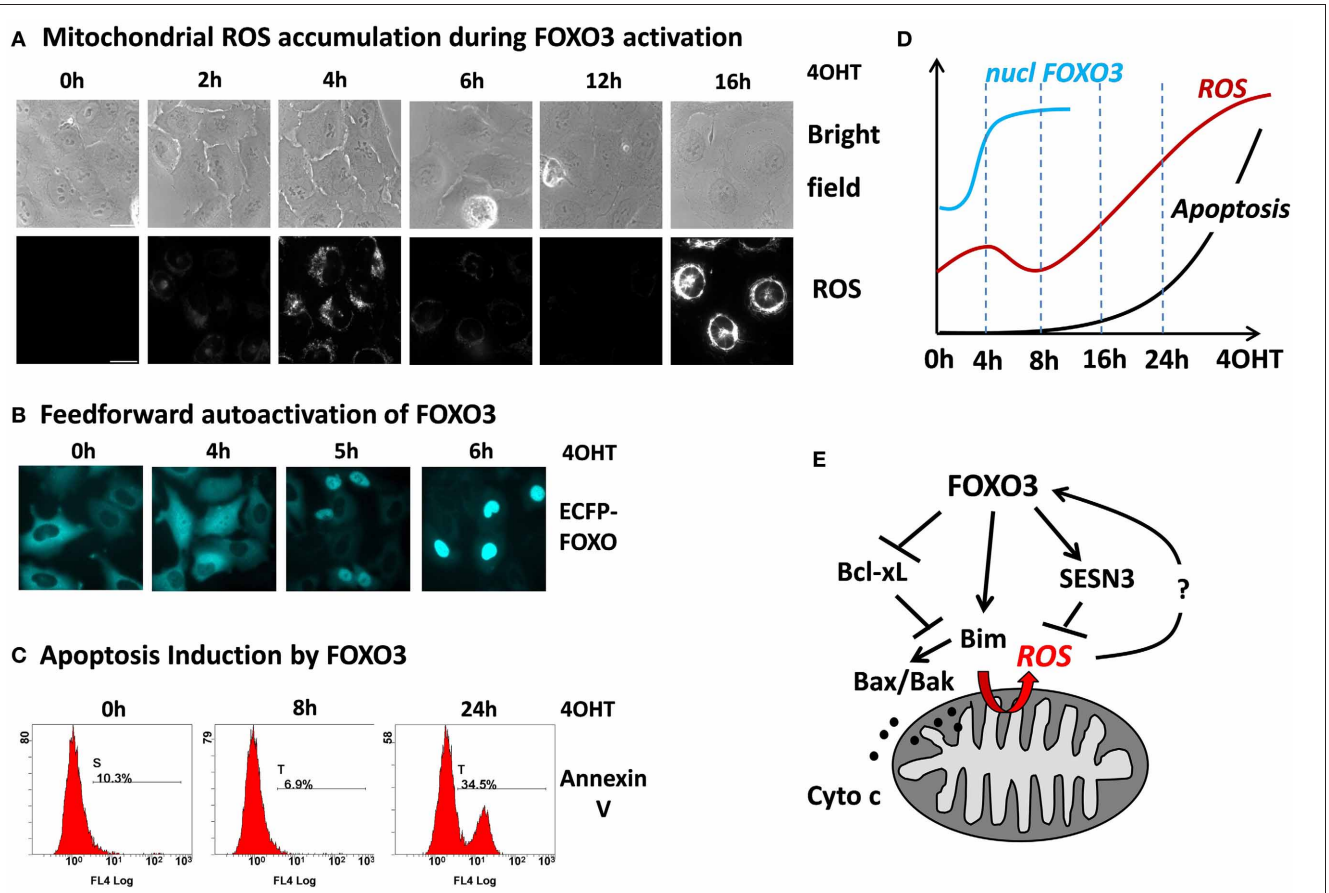

FIGURE 2 | FOXO3 activation causes biphasic ROS accumulation at mitochondria leading to feed forward activation and apoptosis. SH-EP neuroblastoma cells expressing a conditional FOXO3-ERtm protein were treated with 4-OH-tamoxifene (4OHT), which leads to functional activation of this transgene. FOXO3 induces a first ROS accumulation at 4 h with complete SESN3-dependent decay of ROS between 8 and 14 h and strong secondary accumulation of ROS afterwards that finally leads to apoptotic cell death. Accumulation of ROS was detected using MitoTracker Red CMH_2XROS (Invitrogen) by live-cell imaging in an Axiovert200M microscope (Zeiss) **(A)**. Subsequent to the first ROS peak triggered by FOXO3(A3)ERtm nuclear accumulation of ECFP-FOXO3wt is observed suggesting amplifying feed forward activation of additional FOXO3 molecules after primary FOXO3 activation **(B)**. Apoptosis was determined by Annexin-V staining in a FC500 flow cytometer (Beckman-Coulter) **(C)**. The chronology of cellular events in response to FOXO3 activation: after 4 h ECFP-tagged FOXO3 starts to accumulate in the nucleus (blue line, data based on quantification of nuclear FOXO3 by live cell imaging analysis), ROS accumulates first after 4 h, followed by decay to background ROS levels and a second much more intensive ROS accumulation (red line) that also marks the onset of cell death (black line, based on time course experiments using flow cytometric analysis of annexin-V staining). The data was compiled from analyses shown in **(A–C)**, additional unpublished data or data from (Hagenbuchner et al., 2012a) **(D)**. Model of cell death/stress resistance regulation by FOXO3 involving the biphasic accumulation of mitochondrial ROS downstream of Bim, which may constitute a feed forward signal to overcome the ROS-protective capacity of SESN3 **(E)**.

of Bax and to a first minor release of Cytrochrome-*c*, which correlates with the first ROS accumulation (Hagenbuchner et al., 2012a). Knock-down of Bim rescues neuroblastoma cells from ROS-accumulation and FOXO3-induced apoptosis, whereas tetracycline-regulated Bim-expression alone is sufficient to induce ROS. These observations imply that FOXO3 interrupts mitochondrial function by transient outer membrane permeabilization via Bim, which results in Bax/Bak activation and in leaking out of the electron-acceptor Cytochrome-*c* (Hagenbuchner et al., 2012a). As a result of inefficient electron transfer ROS accumulate at mitochondria. The amount of released Cytochrome-*c* seems not sufficient in these neuronal cells to induce immediate apoptosome-mediated caspase-9 activation and cell death, as first signs of apoptosis are evident much later after 18–24 h. Whereas the knock-down of Bim prevents FOXO3-induced ROS accumulation and cell death induction shRNA-mediated elimination of Noxa/PMAIP1, another BH3-only protein that is directly regulated by FOXO3 in neuronal cells, does not influence FOXO3-induced ROS accumulation. This suggests that a weak BH3-only protein such as Noxa, which cannot induce apoptosis by itself but acts as apoptosis-sensitizer is also not potent enough to cause ROS accumulation at mitochondria. The hypothesis that mitochondrial apoptosis is directly connected to transitory permeabilization of the outer mitochondrial membrane leading to mitochondrial ROS accumulation is further supported by the Bim-neutralizing pro-survival protein BclxL: if overexpressed BclxL not only prevents FOXO3-induced cell death but also the biphasic ROS accumulation thereby directly linking FOXO3-induced ROS to the balance of pro- and antiapoptotic Bcl2 proteins at mitochondria (**Figures 2**, **4**). Simultaneously with Bim induction and ROS accumulation, mitochondrial respiration drops to about 70% of untreated controls, but recovers again to 99% after decay of the first ROS wave (Hagenbuchner et al., 2012a). Consistent with the hypothesis that FOXO3-induced mitochondrial ROS results from the detrimental effects of Bim on mitochondrial function, Bim overexpression causes a significant drop of respiration that coincides with high levels of ROS. On the other hand the overexpression of BclxL, which is repressed by FOXO3, also efficiently preserves respiration during FOXO3-activation (Hagenbuchner et al., 2012a). This suggests that FOXO3-activation by e.g., oxidative stress causes an imbalance of FOXO3-regulated Bcl2 proteins in neuronal cells leading to partial membrane permeabilization, transitory decrease in respiration and accumulation of ROS at mitochondria.

In contrast to these "acute FOXO3 effects" on mitochondria in neuronal cells additional mechanisms have been discovered how FOXO3 regulates mitochondrial mass, respiration and ROS production. Two groups recently demonstrated that FOXO3 is activated downstream of hypoxia-inducible factor-1α (HIF-1α) during hypoxia and is involved in the repression of nuclear-encoded mitochondrial genes during hypoxia. In this case, FOXO3 controls the adaptation to low oxygen and slowly shuts down mitochondrial activity by antagonizing c-Myc function. Hypoxia usually increases ROS production from mitochondria, which feeds back into stabilization of HIF-1α. Under hypoxic conditions, FOXO3 prevents hypoxia-induced ROS and HIF-1α stabilization by ROS, which contributes to tumor growth in xenograft models (Jensen et al., 2011; Ferber et al., 2012).

A third mechanism by which FOXO3 modulates mitochondrial activity is by directly regulating mitochondria-encoded genes. In response to glucose restriction in fibroblasts and skeletal muscle cells FOXO3 is phosphorylated by AMPK and subsequently imported into mitochondria where it forms a protein complex containing FOXO3, SIRT3, and mitochondrial RNA polymerase (mtRNAPol). This complex activates the expression of mitochondria-encoded genes, increases mitochondrial respiration and contributes to muscle adaptation during nutrient restriction (Peserico et al., 2013). How this complex affects mitochondrial structure has not been investigated yet.

FOXO3-INDUCED MITOCHONDRIAL ROS—A BALANCE BETWEEN LIFE AND DEATH?

So does FOXO3-induced early ROS accumulation already define the non-reversible activation of programmed cell death? Interestingly, after the first peak around 4 h after FOXO3 activation mitochondrial ROS almost completely goes back to baseline (**Figure 2A** and red line in schematic presentation), which suggests that in parallel to mitochondrial damage also rescue pathways are activated. In a large number of different cell types FOXO-transcription factors play a critical role in the detoxification of ROS and several FOXO3-targets were described for this cell-protective effect, among them SOD2, Catalase (Kops et al., 2002; Hasegawa et al., 2008; Tan et al., 2008) peroxiredoxin III (Chiribau et al., 2008) or the redox enzyme sestrin3 (SESN3) (Chen et al., 2010). SOD2 and Catalase are critically involved in the detoxification of superoxide-radicals and peroxide in various cell types and their activity might explain the decay of ROS and recovery of mitochondrial respiration after the first ROS peak during FOXO3 activation. However, SOD2 and Catalase were not regulated in neuroblastoma cells and therefore do not seem to contribute to the fluctuations of ROS levels during FOXO3-induced apoptosis (Hagenbuchner et al., 2012a). Neuronal cells rely on the thiol-reducing system based on thioredoxin and glutathione, which act as reducers of cellular peroxides (Budanov et al., 2004). In Microarray analyses, however, we identified the antioxidant enzyme SESN3 as a FOXO3 target in neuronal and neuroblastoma cells. SESN3 has two different functions: it acts as an antioxidant factor and is critical for the regeneration of peroxiredoxins. On the other hand SESN3 is also an inhibitor of target of rapamycin complex 1 (TORC1), which may affect FOXO3 activation via the PKB pathway (Budanov and Karin, 2008; Chen et al., 2010). When SESN3 induction is abrogated by short-hairpin technology this also prevents the transitory decline in ROS during FOXO3 activation and accelerates FOXO3-induced apoptosis in neuronal cells. This suggests that FOXO3 activate both, ROS production via Bim-induced mitochondrial damage and in parallel a ROS detoxifying pathway via SESN3. SESN3 induction and ROS detoxification therefore represent a rescue pathway for neuronal cells after FOXO3 activation. The balance between ROS-inducing and ROS-detoxifying molecular players determines whether the cell undergoes FOXO3-induced apoptosis or not.

The second ROS accumulation observed after about 16 h (**Figure 2**) is associated with phosphorylation of p66/SHC, a splice variant of the growth factor SHC, which localizes to mitochondria (Hagenbuchner et al., 2012b). Phosphorylation of p66/SHC correlates with increased H_2O_2 production (Giorgio et al., 2005), suggesting that prolonged FOXO3 activation overcomes the protective effect of SESN3 and continuous oxidative stress leads to phosphorylation of p66. Increased ROS finally causes oxidation of the Cytochrome-*c*-binding protein cardiolipin, which results in elevated levels of free Cytochrome-*c* in the inter-membrane space and finally to effective release of Cytochrome-*c* from mitochondria and apoptosis induction via apoptosome formation and caspase activation (reviewed in, Huttemann et al., 2011).

MITOCHONDRIAL REORGANIZATION AND EFFECTS OF FOXO3

Mitochondrial activity and connectivity regulates oxidative phosphorylation and thereby intracellular ATP production. Electrons from energy rich NADH and FADH2 are transferred through the chain of four large enzyme complexes, leading to a proton flux via the inner mitochondrial membrane. As a side product, mitochondrial respiration leads to production of ROS, mainly through complex I, III and the reduced ubiquinol pool. ROS from complex I are mainly released on the matrix side of mitochondria, whereas complex III releases ROS into the matrix and the inter-membrane space. Within the inter-membrane space free Cytochrome-*c* acts as natural ROS detoxifier by removing unpaired electrons from superoxide leading to O_2 formation and by conversion of hydrogen peroxide. During apoptosis induction, ATP production is reduced and mitochondria undergo reorganization to release Cytochrome-*c* into the cytosol which leads to a sharp increase of ROS from complex I (reviewed in, Sena and Chandel, 2012).

The mitochondrial shape and size are controlled by members of the fusion/fission family which, together with the Bcl2 family, control mitochondrial fragmentation and Cytochrome-*c* release (Karbowski et al., 2006; Sheridan et al., 2008). The main mammalian fission protein is the GTPase dynamin-related protein 1 (DNM1L/Drp1), whose activity is mainly regulated by phosphorylation at Ser616 and Ser637. Ser616 phosphorylation by Cdk1/cyclinB affects GTPase effector domain (GED) function and leads to translocation of Drp1 to the mitochondria during mitosis. De-phosphorylation on Ser637 is thought to be mediated by calcineurin which facilitates the translocation of Drp1 to distinct foci at the outer membrane of mitochondria, where oligomerization of Drp1 induces the fragmentation of mitochondrial networks into single mitochondria (reviewed in, Elgass et al., 2013). Other regulators of mitochondrial fusion, mitofusin 1 and 2 (MFN1 and MFN2) and optic atrophy1 (OPA1) also regulate mitochondrial fusion dynamics. MFN1 and MFN2 are located at the mitochondrial outer membrane and are responsible for connecting separate mitochondria. OPA1 is localized inside the intermembrane space and cooperates with MFN1 and MFN2 to fuse the inner and outer membranes of different mitochondria (reviewed in, Elgass et al., 2013).

Drp1, MFN1, and MFN2 were shown to cooperate with distinct members of the Bcl2 family in the reorganization of mitochondria during apoptosis induction. Active Drp1 facilitates Bax oligomerization during outer membrane permeabilization (Karbowski et al., 2006). BclxL and Bcl2 can bind MFN2, but not MFN1 and BclxL also interacts with Drp1, which interestingly increases its GTPase activity and leads to apoptosis-independent fragmentation of mitochondria in specific cell types (Delivani et al., 2006; Sheridan et al., 2008). Therefore, BclxL can promote either fusion or fission, even in the same cell type.

So how does FOXO3 affect mitochondrial architecture in neuronal cells? We observed de-phosphorylation of Drp1 at Ser637 and its translocation to the mitochondria 8 h after FOXO3 activation, suggesting that Bim-induced ROS may lead to cellular stress-induced de-phosphorylation of Drp1 (Hagenbuchner et al., 2012b). At the same time, Bax is recruited to the mitochondria and small amounts of Cytochrome-*c* are released to the cytoplasm. After 24 h FOXO3 induces MFN1 and MFN2 expression, which correlates with the onset of apoptosis and reorganization of mitochondria. Ectopic expression of BclxL not only blocked Cytochrome-*c* release and apoptosis by sequestering Bim but also prevented the induction of the fusion/fission machinery proteins by FOXO3 (Hagenbuchner et al., 2012b). This implies that induction of Bim and repression of BclxL by FOXO3 significantly affect the mitochondrial fusion/fission machinery via Drp1 recruitment, which, in addition to ROS accumulation and BH3-only-induced Bax-oligomerization may contribute to FOXO3-induced Cytochrome-*c* release and apoptosis (Hagenbuchner et al., 2012b). Beyond Bcl2-family members FOXO3 affects mitochondrial activity and shape also via regulating the FOXO3 target Survivin.

SURVIVIN UNCOUPLES MITOCHONDRIAL FISSION FROM CYTOCHROME-*c* RELEASE AND APOPTOSIS INDUCTION

Survivin belongs to the family of Inhibitors of Apoptosis Proteins (IAPs) and was reported to inhibit apoptosis only when located to the mitochondria (Dohi et al., 2007; Obexer et al., 2009). Survivin contains the characteristic zinc-binding BIR domain but lacks the typical RING domain of other IAP family members. Apoptosis inhibition was ascribed to the ability of Survivin to directly bind and stabilize XIAP, which directly interferes with caspase activation (Dohi et al., 2004). These mechanisms suggest that Survivin prevents apoptosis downstream of mitochondria. However, in neuroblastoma cells we observed a different mode of action of Survivin: Survivin mRNA expression is rapidly repressed by FOXO3 and this leads to rapid loss of cytoplasmic Survivin, whereas mitochondrial Survivin shows significantly higher stability. Ectopically expressed Survivin reduces the number of CMXRos-negative cells during FOXO3-activation, suggesting a role for Survivin at the level of mitochondria (Obexer et al., 2009). In concordance we observed that Survivin prevents Bax accumulation at the mitochondria and the release of Cytochrome-*c* into the cytoplasm after FOXO3-activation. Interestingly, Survivin interferes with FOXO3-induced ROS accumulation. Similar to knock-down of Bim or ectopic expression of BclxL, Survivin inhibits FOXO3-induced ROS, Bax activation and Cytochrome-*c* release (Hagenbuchner et al., 2012b). In contrast

to BclxL, which prevents Drp1 accumulation at mitochondria, Survivin-overexpressing cells showed increased Drp1 levels but reduced Drp1 phosphorylation (unpublished data) and therefore significantly higher amounts of mitochondria-associated Drp1 than control cells (Hagenbuchner et al., 2012b). These increased Drp1 levels resulted in fragmented mitochondria in Survivin-expressing cells (**Figure 3**). The mitochondrial fission phenotype is reversibly either by the use of the Drp1-inhibitor

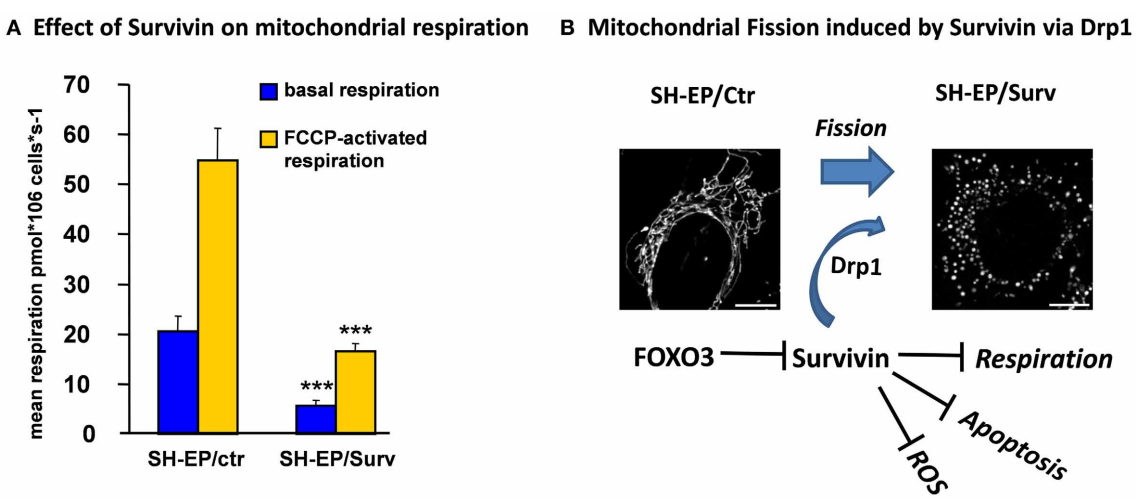

FIGURE 3 | The FOXO3-target Survivin reduces mitochondrial respiration and induces mitochondrial fission in neuronal tumor cells via Drp1 recruitment to mitochondria. Ectopic expression of the anti-apoptotic protein Survivin in neuroblastoma cells reduces basal and FCCP-activated mitochondrial respiration to about one third of control cells. Oxygen consumption of the cells and mitochondrial function were analyzed by high-resolution respirometry (Kuznetsov et al., 2008), using a two-channel Oroboros Oxygraph respirometer. This reduced respiratory activity results from almost absence of respiratory complex I activity (data not shown; $^{***}P < 0.001$, student's *t*-test) **(A)**. Survivin recruits DNM1L/Drp1 to mitochondria and induces mitochondrial fission. Microscopic images were acquired on an Axiovert200M microscope equipped with an Apotome_2 module **(B)**. Mitochondrial fission is associated with apoptosis-protection and significantly reduced capability to accumulate ROS in response to FOXO3 activation or treatment with chemotherapeutic agents (see text) (Hagenbuchner et al., 2012b).

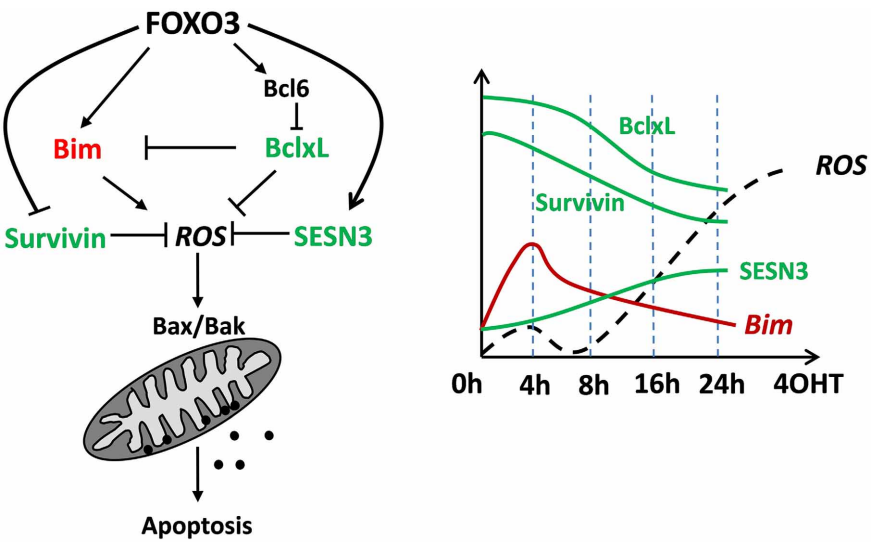

FIGURE 4 | A conceptional view on how FOXO3 regulates mitochondrial ROS and apoptotic cell death in neuronal cells and neuroblastoma tumor cells. Transitory induction of pro-apoptotic Bim by FOXO3 constitutes a first mitochondria-damaging signal that triggers the primary ROS peak at 4 h. In parallel the ROS-detoxifying SESN3 accumulates and critically regulates decay of the ROS after 4–6 h. Bim-neutralizing BclxL and Survivin are both repressed by FOXO3, thereby lowering the ability of the cell to cope with apoptosis-inducing signals. This concerted regulation of pro- and anti-apoptotic ROS-affecting proteins overcomes the protective effect of SESN3 after about 16 h leading to a sharp and continuous increase in ROS, which finally leads to apoptotic cell death. The schematic presentation is based on several time-course immunoblot experiments and data from fluorescence-based mitochondrial ROS measurements not included in this paper.

Mdivi-1 or by knock-down of Drp1 with short-hairpin technology, which both lead to mitochondrial fusion. Also the reduction of Survivin levels reverses the mitochondrial phenotype, suggesting that Survivin actively contributes to mitochondrial fission via Drp1 recruitment. In contrast to the current dogma that Drp1 translocation to mitochondria and mitochondrial fission is associated with apoptosis induction the Survivin-induced fission even protects cells against FOXO3-induced apoptosis and confers resistance to chemotherapeutic agents (Hagenbuchner et al., 2012b). This protective effect is associated with efficient inhibition of FOXO3-induced ROS, which may be ascribed at least in part to significant reduction of mitochondrial respiration by Survivin. In neuronal tumor cells moderate overexpression of Survivin lowers endogenous respiration to about one third of control cells via inactivation of respiratory complex I (**Figure 3**). Survivin-induced changes of mitochondrial shape and mitochondrial respiration reprograms cellular energy metabolism so that the cells become dependent on glycolysis and sensitive to glycolysis inhibitors (Hagenbuchner et al., 2012b). Thereby, by affecting cellular Survivin expression FOXO3 affects mitochondrial shape, respiratory activity and energy metabolism.

FOXO3 was originally described as a tumor-suppressor protein that activates cell death inducers such as TRAIL, Fas ligand, Bim or Noxa or controls detoxification of ROS. In the meantime this view has been challenged as it was shown that FOXO3 may also control mitochondrial respiration during adaptation to hypoxia or is even imported into mitochondria to regulate expression of mitochondrial genes. The fact that FOXOs are inactive under optimal growth conditions suggests that these transcription factors function as homeostasis regulators during stress rather than as typical tumor suppressors. According to our recent studies FOXO3 induces mitochondrial ROS as an essential second messenger during Bcl2-protein controlled apoptotic cell death but also detoxifying proteins that counteract ROS accumulation (**Figure 4**). Importantly, FOXO3 also represses the proto-oncogene Survivin, which we discovered to regulate the mitochondrial fusion/fission machinery and mitochondrial respiration by interfering with complex I activity. By this, the FOXO3-target Survivin reprograms energy metabolism and activates glycolysis to produce energy for survival. So FOXO3 is a transcription factor that directly or indirectly affects mitochondrial respiration, ROS accumulation and even mitochondrial shape, which on one hand affects apoptosis sensitivity of tumor cells, but also may have significant impact on life-span in multicellular organisms.

REFERENCES

Arden, K. C. (2008). FOXO animal models reveal a variety of diverse roles for FOXO transcription factors. *Oncogene* 27, 2345–2350. doi: 10.1038/onc.2008.27

Bakker, W. J., Harris, I. S., and Mak, T. W. (2007). FOXO3a is activated in response to hypoxic stress and inhibits HIF1-induced apoptosis via regulation of CITED2. *Mol. Cell*. 28, 941–953. doi: 10.1016/j.molcel.2007.10.035

Braeckman, B. P., and Vanfleteren, J. R. (2007). Genetic control of longevity in C. elegans. *Exp. Gerontol*. 42, 90–98. doi: 10.1016/j.exger.2006.04.010

Brent, M. M., Anand, R., and Marmorstein, R. (2008). Structural basis for DNA recognition by FoxO1 and its regulation by posttranslational modification. *Structure* 16, 1407–1416. doi: 10.1016/j.str.2008.06.013

Brunet, A., Sweeney, L. B., Sturgill, J. F., Chua, K. F., Greer, P. L., Lin, Y., et al. (2004). Stress-dependent regulation of FOXO transcription factors by the SIRT1 deacetylase. *Science* 303, 2011–2015. doi: 10.1126/science.1094637

Budanov, A. V., and Karin, M. (2008). p53 target genes sestrin1 and sestrin2 connect genotoxic stress and mTOR signaling. *Cell* 134, 451–460. doi: 10.1016/j.cell.2008.06.028

Budanov, A. V., Sablina, A. A., Feinstein, E., Koonin, E. V., and Chumakov, P. M. (2004). Regeneration of peroxiredoxins by p53-regulated sestrins, homologs of bacterial AhpD. *Science* 304, 596–600. doi: 10.1126/science.1095569

Calnan, D. R., and Brunet, A. (2008). The FoxO code. *Oncogene* 27, 2276–2288. doi: 10.1038/onc.2008.21

Chen, C. C., Jeon, S. M., Bhaskar, P. T., Nogueira, V., Sundararajan, D., Tonic, I., et al. (2010). FoxOs inhibit mTORC1 and activate Akt by inducing the expression of Sestrin3 and Rictor. *Dev. Cell*. 18, 592–604. doi: 10.1016/j.devcel.2010.03.008

Chiacchiera, F., and Simone, C. (2009). Inhibition of p38alpha unveils an AMPK-FoxO3A axis linking autophagy to cancer-specific metabolism. *Autophagy* 5, 1030–1033. doi: 10.4161/auto.5.7.9252

Chiribau, C. B., Cheng, L., Cucoranu, I. C., Yu, Y. S., Clempus, R. E., and Sorescu, D. (2008). FOXO3A regulates peroxiredoxin III expression in human cardiac fibroblasts. *J. Biol. Chem*. 283, 8211–8217. doi: 10.1074/jbc.M710610200

Chung, Y. M., Park, S. H., Tsai, W. B., Wang, S. Y., Ikeda, M. A., Berek, J. S., et al. (2012). FOXO3 signalling links ATM to the p53 apoptotic pathway following DNA damage. *Nat. Commun*. 3, 1000. doi: 10.1038/ncomms2008

Dansen, T. B., Smits, L. M., van Triest, M. H., de Keizer, P. L., van Leenen, D., Koerkamp, M. G., et al. (2009). Redox-sensitive cysteines bridge p300/CBP-mediated acetylation and FoxO4 activity. *Nat. Chem. Biol*. 5, 664–672. doi: 10.1038/nchembio.194

Davila, D., Connolly, N. M., Bonner, H., Weisova, P., Dussmann, H., Concannon, C. G., et al. (2012). Two-step activation of FOXO3 by AMPK generates a coherent feed-forward loop determining excitotoxic cell fate. *Cell Death. Differ*. 19, 1677–1688. doi: 10.1038/cdd.2012.49

Delivani, P., Adrain, C., Taylor, R. C., Duriez, P. J., and Martin, S. J. (2006). Role for CED-9 and Egl-1 as regulators of mitochondrial fission and fusion dynamics. *Mol. Cell*. 21, 761–773. doi: 10.1016/j.molcel.2006.01.034

Ditch, S., and Paull, T. T. (2012). The ATM protein kinase and cellular redox signaling: beyond the DNA damage response. *Trends Biochem. Sci*. 37, 15–22. doi: 10.1016/j.tibs.2011.10.002

Dohi, T., Okada, K., Xia, F., Wilford, C. E., Samuel, T., Welsh, K., et al. (2004). An IAP-IAP complex inhibits apoptosis. *J. Biol. Chem*. 279, 34087–34090. doi: 10.1074/jbc.C400236200

Dohi, T., Xia, F., and Altieri, D. C. (2007). Compartmentalized phosphorylation of IAP by protein kinase A regulates cytoprotection. *Mol. Cell*. 27, 17–28. doi: 10.1016/j.molcel.2007.06.004

Eijkelenboom, A., and Burgering, B. M. (2013). FOXOs: signalling integrators for homeostasis maintenance. *Nat. Rev. Mol. Cell Biol*. 14, 83–97. doi: 10.1038/nrm3507

Elgass, K., Pakay, J., Ryan, M. T., and Palmer, C. S. (2013). Recent advances into the understanding of mitochondrial fission. *Biochim. Biophys. Acta*. 1833, 150–161. doi: 10.1016/j.bbamcr.2012.05.002

Essers, M. A., Weijzen, S., Vries-Smits, A. M., Saarloos, I., de Ruiter, N. D., Bos, J. L., et al. (2004). FOXO transcription factor activation by oxidative stress mediated by the small GTPase Ral and JNK. *EMBO J*. 23, 4802–4812. doi: 10.1038/sj.emboj.7600476

Ferber, E. C., Peck, B., Delpuech, O., Bell, G. P., East, P., and Schulze, A. (2012). FOXO3a regulates reactive oxygen metabolism by inhibiting mitochondrial gene expression. *Cell Death. Differ*. 19, 968–979. doi: 10.1038/cdd.2011.179

Furukawa-Hibi, Y., Yoshida-Araki, K., Ohta, T., Ikeda, K., and Motoyama, N. (2002). FOXO forkhead transcription factors induce G(2)-M checkpoint in response to oxidative stress. *J. Biol. Chem*. 277, 26729–26732. doi: 10.1074/jbc.C200256200

Geiger, K., Hagenbuchner, J., Rupp, M., Fiegl, H., Sergi, C., Meister, B.,

et al. (2012). FOXO3/FKHRL1 is activated by 5-aza-2-deoxycytidine and induces silenced caspase-8 in neuroblastoma. *Mol. Biol. Cell*. 23, 2226–2234. doi: 10.1091/mbc.E11-06-0535

Giorgio, M., Migliaccio, E., Orsini, F., Paolucci, D., Moroni, M., Contursi, C., et al. (2005). Electron transfer between cytochrome c and p66Shc generates reactive oxygen species that trigger mitochondrial apoptosis. *Cell* 122, 221–233. doi: 10.1016/j.cell.2005.05.011

Greer, E. L., Oskoui, P. R., Banko, M. R., Maniar, J. M., Gygi, M. P., Gygi, S. P., et al. (2007). The energy sensor AMP-activated protein kinase directly regulates the mammalian FOXO3 transcription factor. *J. Biol. Chem*. 282, 30107–30119. doi: 10.1074/jbc.M705325200

Guha, M., Plescia, J., Leav, I., Li, J., Languino, L. R., and Altieri, D. C. (2009). Endogenous tumor suppression mediated by PTEN involves survivin gene silencing. *Cancer Res*. 69, 4954–4958. doi: 10.1158/0008-5472.CAN-09-0584

Hagenbuchner, J., Kuznetsov, A., Hermann, M., Hausott, B., Obexer, P., and Ausserlechner, M. J. (2012a). FOXO3-induced reactive oxygen species are regulated by BCL2L11 (Bim) and SESN3. *J. Cell Sci*. 125, 1191–1203. doi: 10.1242/jcs.092098

Hagenbuchner, J., Kuznetsov, A. V., Obexer, P., and Ausserlechner, M. J. (2012b). BIRC5/Survivin enhances aerobic glycolysis and drug resistance by altered regulation of the mitochondrial fusion/fission machinery. *Oncogene* 10. doi: 10.1038/onc.2012.500. [Epub ahead of print].

Harada, Y., Harada, Y., Elly, C., Ying, G., Paik, J. H., DePinho, R. A., et al. (2010). Transcription factors Foxo3a and Foxo1 couple the E3 ligase Cbl-b to the induction of Foxp3 expression in induced regulatory T cells. *J. Exp. Med*. 207, 1381–1391. doi: 10.1084/jem.20100004

Hasegawa, K., Wakino, S., Yoshioka, K., Tatematsu, S., Hara, Y., Minakuchi, H., et al. (2008). Sirt1 protects against oxidative stress-induced renal tubular cell apoptosis by the bidirectional regulation of catalase expression. *Biochem. Biophys. Res. Commun*. 372, 51–56. doi: 10.1016/j.bbrc.2008.04.176

Hosaka, T., Biggs, W. H. III, Tieu, D., Boyer, A. D., Varki, N. M., Cavenee, W. K., et al. (2004). Disruption of forkhead transcription factor (FOXO) family members in mice reveals their functional diversification. *Proc. Natl. Acad. Sci. U.S.A*. 101, 2975–2980. doi: 10.1073/pnas.0400093101

Hu, M. C., Lee, D. F., Xia, W., Golfman, L. S., Ou-Yang, F., Yang, J. Y., et al. (2004). IkappaB kinase promotes tumorigenesis through inhibition of forkhead FOXO3a. *Cell* 117, 225–237. doi: 10.1016/S0092-8674(04)00302-2

Hui, R. C., Francis, R. E., Guest, S. K., Costa, J. R., Gomes, A. R., Myatt, S. S., et al. (2008). Doxorubicin activates FOXO3a to induce the expression of multidrug resistance gene ABCB1 (MDR1) in K562 leukemic cells. *Mol. Cancer Ther*. 7, 670–678. doi: 10.1158/1535-7163.MCT-07-0397

Huttemann, M., Pecina, P., Rainbolt, M., Sanderson, T. H., Kagan, V. E., Samavati, L., et al. (2011). The multiple functions of cytochrome c and their regulation in life and death decisions of the mammalian cell: from respiration to apoptosis. *Mitochondrion* 11, 369–381. doi: 10.1016/j.mito.2011.01.010

Jensen, K. S., Binderup, T., Jensen, K. T., Therkelsen, I., Borup, R., Nilsson, E., et al. (2011). FoxO3A promotes metabolic adaptation to hypoxia by antagonizing Myc function. *EMBO J*. 30, 4554–4570. doi: 10.1038/emboj.2011.323

Karbowski, M., Norris, K. L., Cleland, M. M., Jeong, S. Y., and Youle, R. J. (2006). Role of bax and bak in mitochondrial morphogenesis. *Nature* 443, 658–662. doi: 10.1038/nature05111

Kerdiles, Y. M., Stone, E. L., Beisner, D. R., McGargill, M. A., Ch'en, I. L., Stockmann, C., et al. (2010). Foxo transcription factors control regulatory T cell development and function. *Immunity* 33, 890–904. doi: 10.1016/j.immuni.2010.12.002

Kobayashi, Y., Furukawa-Hibi, Y., Chen, C., Horio, Y., Isobe, K., Ikeda, K., et al. (2005). SIRT1 is critical regulator of FOXO-mediated transcription in response to oxidative stress. *Int. J. Mol. Med*. 16, 237–243.

Kops, G. J. P. L., Dansen, T. B., Polderman, P. E., Saarloos, I., Wirtz, K. W. A., Coffer, P. J., et al. (2002). Forkhead transcription factor FOXO3a protects quiescent cells from oxidative stress. *Nature* 419, 316–321. doi: 10.1038/nature01036

Kuznetsov, A. V., Veksler, V., Gellerich, F. N., Saks, V., Margreiter, R., and Kunz, W. S. (2008). Analysis of mitochondrial function *in situ* in permeabilized muscle fibers, tissues and cells. *Nat. Protoc*. 3, 965–976. doi: 10.1038/nprot.2008.61

Lehtinen, M. K., Yuan, Z., Boag, P. R., Yang, Y., Villen, J., Becker, E. B., et al. (2006). A conserved MST-FOXO signaling pathway mediates oxidative-stress responses and extends life span. *Cell* 125, 987–1001. doi: 10.1016/j.cell.2006.03.046

Matsuzaki, H., Daitoku, H., Hatta, M., Tanaka, K., and Fukamizu, A. (2003). Insulin-induced phosphorylation of FKHR (Foxo1) targets to proteasomal degradation. *Proc. Natl. Acad. Sci U.S.A*. 100, 11285–11290. doi: 10.1073/pnas.1934283100

Naka, K., Hoshii, T., Muraguchi, T., Tadokoro, Y., Ooshio, T., Kondo, Y., et al. (2010). TGF-beta-FOXO signalling maintains leukaemia-initiating cells in chronic myeloid leukaemia. *Nature* 463, 676–680. doi: 10.1038/nature08734

Obexer, P., Geiger, K., Ambros, P. F., Meister, B., and Ausserlechner, M. J. (2007). FKHRL1-mediated expression of Noxa and Bim induces apoptosis via the mitochondria in neuroblastoma cells. *Cell Death Differ*. 14, 534–547. doi: 10.1038/sj.cdd.4402017

Obexer, P., Hagenbuchner, J., Unterkircher, T., Sachsenmaier, N., Seifarth, C., Bock, G., et al. (2009). Repression of BIRC5/survivin by FOXO3/FKHRL1 sensitizes human neuroblastoma cells to DNA damage-induced apoptosis. *Mol. Biol. Cell*. 20, 2041–2048. doi: 10.1091/mbc.E08-07-0699

Obsil, T., and Obsilova, V. (2011). Structural basis for DNA recognition by FOXO proteins. *Biochim. Biophys. Acta*. 1813, 1946–1953. doi: 10.1016/j.bbamcr.2010.11.025

Paik, J. H., Kollipara, R., Chu, G., Ji, H., Xiao, Y., Ding, Z., et al. (2007). FoxOs are lineage-restricted redundant tumor suppressors and regulate endothelial cell homeostasis. *Cell* 128, 309–323. doi: 10.1016/j.cell.2006.12.029

Peserico, A., Chiacchiera, F., Grossi, V., Matrone, A., Latorre, D., Simonatto, M., et al. (2013). A novel AMPK-dependent FoxO3A-SIRT3 intramitochondrial complex sensing glucose levels. *Cell Mol. Life Sci.* 11, 2015–2029. doi: 10.1007/s00018-012-1244-6

Romanello, V., Guadagnin, E., Gomes, L., Roder, I., Sandri, C., Petersen, Y., et al. (2010). Mitochondrial fission and remodelling contributes to muscle atrophy. *EMBO J*. 29, 1774–1785. doi: 10.1038/emboj.2010.60

Salih, D. A., Rashid, A. J., Colas, D., Torre-Ubieta, L., Zhu, R. P., Morgan, A. A., et al. (2012). FoxO6 regulates memory consolidation and synaptic function. *Genes Dev*. 26, 2780–2801. doi: 10.1101/gad.208926.112

Sanchez, A. M., Csibi, A., Raibon, A., Cornille, K., Gay, S., Bernardi, H., et al. (2012). AMPK promotes skeletal muscle autophagy through activation of forkhead FoxO3a and interaction with Ulk1. *J. Cell Biochem*. 113, 695–710. doi: 10.1002/jcb.23399

Sena, L. A., and Chandel, N. S. (2012). Physiological roles of mitochondrial reactive oxygen species. *Mol. Cell*. 48, 158–167. doi: 10.1016/j.molcel.2012.09.025

Sheridan, C., Delivani, P., Cullen, S. P., and Martin, S. J. (2008). Bax- or Bak-induced mitochondrial fission can be uncoupled from cytochrome C release. *Mol. Cell*. 31, 570–585. doi: 10.1016/j.molcel.2008.08.002

Sunayama, J., Tsuruta, F., Masuyama, N., and Gotoh, Y. (2005). JNK antagonizes Akt-mediated survival signals by phosphorylating 14-3-3. *J. Cell Biol*. 170, 295–304. doi: 10.1083/jcb.200409117

Sunters, A., Madureira, P. A., Pomeranz, K. M., Aubert, M., Brosens, J. J., Cook, S. J., et al. (2006). Paclitaxel-induced nuclear translocation of FOXO3a in breast cancer cells is mediated by c-Jun NH2-terminal kinase and Akt. *Cancer Res*. 66, 212–220. doi: 10.1158/0008-5472.CAN-05-1997

Tan, W. Q., Wang, K., Lv, D. Y., and Li, P. F. (2008). Foxo3a inhibits cardiomyocyte hypertrophy through transactivating catalase. *J. Biol. Chem*. 283, 29730–29739. doi: 10.1074/jbc.M805514200

Tenbaum, S. P., Ordonez-Moran, P., Puig, I., Chicote, I., Arques, O., Landolfi, S., et al. (2012). beta-catenin confers resistance to PI3K and AKT inhibitors and subverts FOXO3a to promote metastasis in colon cancer. *Nat. Med*. 18, 892–901. doi: 10.1038/nm.2772

Tothova, Z., Kollipara, R., Huntly, B. J., Lee, B. H., Castrillon, D. H., Cullen, D. E., et al. (2007). FoxOs are critical mediators of hematopoietic stem cell resistance to physiologic oxidative stress. *Cell* 128, 325–339. doi: 10.1016/j.cell.2007.01.003

Tsai, W. B., Chung, Y. M., Takahashi, Y., Xu, Z., and Hu, M. C. (2008). Functional interaction between FOXO3a and ATM regulates DNA damage response. *Nat. Cell Biol*. 10, 460–467. doi: 10.1038/ncb1709

Tzivion, G., Dobson, M., and Ramakrishnan, G. (2011). FoxO transcription factors; regulation by

AKT and 14-3-3 proteins. *Biochim. Biophys. Acta*. 1813, 1938–1945. doi: 10.1016/j.bbamcr.2011.06.002

van der Vos, K. E., and Coffer, P. J. (2008). FOXO-binding partners: it takes two to tango. *Oncogene*. 27, 2289–2299. doi: 10.1038/onc.2008.22

Wang, F., Marshall, C. B., Yamamoto, K., Li, G. Y., Gasmi-Seabrook, G. M., Okada, H., et al. (2012). Structures of KIX domain of CBP in complex with two FOXO3a transactivation domains reveal promiscuity and plasticity in coactivator recruitment. *Proc. Natl. Acad. Sci U.S.A*. 109, 6078–6083. doi: 10.1073/pnas.1119073109

Xie, Q., Hao, Y., Tao, L., Peng, S., Rao, C., Chen, H., et al. (2012). Lysine methylation of FOXO3 regulates oxidative stress-induced neuronal cell death. *EMBO Rep*. 13, 371–377. doi: 10.1038/embor.2012.25

Yalcin, S., Zhang, X., Luciano, J. P., Mungamuri, S. K., Marinkovic, D., Vercherat, C., et al. (2008). Foxo3 is essential for the regulation of ataxia telangiectasia mutated and oxidative stress-mediated homeostasis of hematopoietic stem cells. *J. Biol. Chem*. 283, 25692–25705. doi: 10.1074/jbc.M800517200

Yamagata, K., Daitoku, H., Takahashi, Y., Namiki, K., Hisatake, K., Kako, K., et al. (2008). Arginine methylation of FOXO transcription factors inhibits their phosphorylation by Akt. *Mol. Cell* 32, 221–231. doi: 10.1016/j.molcel.2008.09.013

Yang, J. Y., Zong, C. S., Xia, W., Yamaguchi, H., Ding, Q., Xie, X., et al. (2008). ERK promotes tumorigenesis by inhibiting FOXO3a via MDM2-mediated degradation. *Nat. Cell Biol*. 10, 138–148. doi: 10.1038/ncb1676

Zhu, M., Zhang, Q. J., Wang, L., Li, H., and Liu, Z. P. (2011). FoxO4 inhibits atherosclerosis through its function in bone marrow derived cells. *Atherosclerosis* 219, 492–498. doi: 10.1016/j.atherosclerosis.2011.09.038

Conflict of Interest Statement: The authors declare that the research was conducted in the absence of any commercial or financial relationships that could be construed as a potential conflict of interest.

Received: 26 February 2013; accepted: 31 May 2013; published online: 20 June 2013.

*Citation: Hagenbuchner J and Ausserlechner MJ (2013) Mitochondria and FOXO3: breath or die. Front. Physiol. **4**:147. doi: **10.3389/fphys.2013.00147***

This article was submitted to Frontiers in Mitochondrial Research, a specialty of Frontiers in Physiology.

frontiers in
PHYSIOLOGY

REVIEW ARTICLE
published: 28 June 2013
doi: 10.3389/fphys.2013.00152

Mitochondrial NHE1: a newly identified target to prevent heart disease

Bernardo V. Alvarez* and María C. Villa-Abrille*

Centro de Investigaciones Cardiovasculares, Consejo Nacional de Investigaciones Científicas y Técnicas Facultad de Ciencias Médicas, Universidad Nacional de La Plata, La Plata, Argentina

Edited by:
Sabzali Javadov, University of Puerto Rico School of Medicine, Puerto Rico

Reviewed by:
Amadou K. S. Camara, Medical College of Wisconsin, USA
Elena N. Dedkova, Rush University Medical Center, USA

****Correspondence:***
Bernardo V. Alvarez and María C. Villa-Abrille, Centro de Investigaciones Cardiovasculares, Consejo Nacional de Investigaciones Científicas y Técnicas Facultad de Ciencias Médicas, Universidad Nacional de La Plata, Calle 60 y 120, 1900, La Plata, Argentina
e-mail: balvarez@med.unlp.edu.ar; mcvillaabrille@med.unlp.edu.ar

Mitochondrial damage has been associated with early steps of cardiac dysfunction in heart subjected to ischemic stress, oxidative stress and hypertrophy. A common feature for the mitochondrial deterioration is the loss of the mitochondrial membrane potential ($\Delta\Psi$ m) with the concomitant irreversible opening of the mitochondrial permeability transition pore (MPTP) which follows the mitochondrial Ca^{2+} overload, and the subsequent mitochondrial swelling. We have recently characterized the expression of the Na^+/H^+ exchanger 1 (mNHE1) in mitochondrial membranes. This surprising observation provided a unique target for the prevention of the Ca^{2+}-induced MPTP opening, based on the inhibition of the NHE1 m. In this line, inhibition of NHE1 m activity and/or reduction of NHE1 m expression decreased the Ca^{2+}-induced mitochondrial swelling and the release of reactive oxygen species (ROS) in isolated cardiac mitochondria and preserved the $\Delta\Psi$ m in isolated cardiomyocytes. Mitochondrial NHE1 thus represents a novel target to prevent cardiac disease, opening new avenues for future research.

Keywords: ischemia, mitochondrial permeability transition pore, NHE1, mitochondrial swelling, siRNA

SODIUM/PROTON EXCHANGER (NHE)

Sodium/proton exchangers (NHE) are a family of integral membrane proteins present in most organisms. These transporters which catalyze the electroneutral exchange of one intracellular H^+ for one extracellular Na^+ across membrane along their concentrations gradient are crucial for control of intracellular pH (pH_i) and cell volume, and, cell migration and proliferation.

The first NHE isoform to be identified was NHE1, which has a ubiquitous tissue distribution in mammals (Sardet et al., 1989). Since its discovery, nine other human isoforms have been identified (NHE2–NHE10) (Fliegel, 2008; Lee et al., 2008). While NHE1–NHE6 reside in the plasma membrane or recycling endosomes, NHE7–NHE9 are located inside the cell rather than the plasma membrane (Fliegel, 2008). The NHE10 is expressed in the surface of osteoclast (Lee et al., 2008).

NHE1 IN THE HEART

NHE1 is the most studied isoform that accumulates preferentially in microdomains of cells membranes, concentrating along the basolateral membrane of epithelia (Biemesderfer et al., 1992) and the intercalated disks and t-tubules of cardiac myocytes (Petrecca et al., 1999). The sarcolemmal NHE1 is the major Na^+ influx pathway found in the plasma membrane of cardiac cells.

NHE1 is an integral membrane glycoprotein with a predicted molecular mass of 85 kDa. NHE1 can be separated into an N-terminal, membrane-associated domain, and a long C-terminal tail, with both the N-and C-terminal domains being cytoplasmic (Wakabayashi et al., 1997), (Orlowski and Grinstein, 1997). NHE1 is expressed ubiquitously in mammalian cells, where it electroneutrally exchanges one intracellular H^+ for one extracellular Na^+, thus regulating pH_i. The membrane domain composed of 12 transmembrane regions is associated with ionic transport (Wakabayashi et al., 1992), and contains the allosteric H^+ sensor site that determines the exquisite sensitivity of the exchanger to intracellular H^+. The cytoplasmic domain is involved in the regulation of the activity of the exchanger by several mechanisms. Removal of the distal region of the cytosolic tail causes a shift of the pH_i sensitivity to the acidic side and an important inhibition of NHE1 activation by growth factors (Fliegel and Karmazyn, 2004). Cytoplasmic tail contains several phosphorylation sites and a high affinity and a low-affinity calmodulin binding sites (Bertrand et al., 1994). The high-affinity binding site functions as an "autoinhibitory domain" that binds Ca^{2+}-bound calmodulin and allows activation of the exchanger. Deletion of this domain constitutively activates NHE1 and mimics elevated intracellular [Ca^{2+}] (Wakabayashi et al., 1994). In addition, the cytoplasmic tail contains a binding site for the calcineurin B homolog protein CHP1, an essential cofactor for NHE1 (Pang et al., 2001). The exchanger is phosphorylated by different protein kinases in response to hormone and growth factor stimulation, as well as sustained acidosis (Sardet et al., 1990, 1991; Haworth et al., 2003).

Under basal conditions, NHE1 exchanger is relatively quiescent and its activity relies only on the extrusion of the H^+ produced by the metabolic activity of cells as well as the H^+ that enters the cell through acid-loading mechanisms. However, the exchanger has an exquisite sensitivity to the increase in intracellular H^+ levels and enhances its activity once pH_i drops below

a threshold level by allosterically "sensing" pH_i, and by being phosphorylated or by interacting with some associated proteins, thus promoting the rapid extrusion of acid (Leem et al., 1999). NHE1 is constitutively phosphorylated in resting cells, but further phosphorylation is induced by several stimuli acting through G-protein-coupled receptors such as α1-adrenergic receptors, angiotensin II (Ang II), and endothelin-1 (ET-1). Kinases such as the Ca^{2+}-/calmodulin-dependent kinase II (Fliegel et al., 1992), the extracellular signal-regulated kinase (ERK) (Moor and Fliegel, 1999), 90 kDa ribosomal S6 kinase (p90 rsk) (Takahashi et al., 1999), p38 mitogen-activated kinase (p38 MAPK) (Khaled et al., 2001), p160 ROCK (Tominaga et al., 1998), and the Nck-interacting kinase (NIK) (Yan et al., 2001) putatively phosphorylate NHE1 to modulate NHE1 activity. In addition, both protein kinases C and D are thought to influence NHE1 activity in response to growth factor and hormone stimulation without a direct phosphorylation of the exchanger (Fliegel et al., 1992; Haworth et al., 1999). NHE1 is also susceptible to dephosphorylation by protein phosphatases such as PP1 (Misik et al., 2005) and PP2A (Snabaitis et al., 2006). Carbonic anhydrase II (CAII) binds to the regulatory cytosolic domain of NHE1 enhancing its activity. Phosphorylation of the C terminus of NHE1 greatly increased the binding of CAII. This binding was shown to involve a protein–protein interaction, suggesting that both proteins constitute a complex. The inhibition of CAII decreased NHE1 activity significantly (Li et al., 2002).

As previously described, the NHE1, relatively quiescent under basal conditions, however, becomes highly active during ischemia in response to intracellular acidosis, leading to NHE1-mediated Na^+ entry into the cell (Karmazyn, 1999a; Karmazyn et al., 1999). Inhibition of $[Na^+]_i$ accumulation by increasing NHE activity and prevention of Ca^{2+} overload via Na^+/Ca^{2+} exchanger have been proposed as potential mechanisms of cardioprotection by NHE1 blockade (Avkiran, 1999). NHE exchanger inhibitors have proven to protect the heart against ischemia/reperfusion (I/R) injury (Karmazyn, 1999a,b). Moreover, the positive effect that NHE1 inhibition exerts on left ventricular systolic function during revascularization therapy after acute myocardial infarction has been documented (Rupprecht et al., 2000). The protection of the ischemic myocardium by NHE1 inhibition after the onset of reperfusion has been described (Rohmann et al., 1995; Gumina et al., 1998; Hurtado and Pierce, 2000). The decrease in myocardial infarct size, through interference with the action of reactive oxygen species (ROS) generation at the beginning of reperfusion, has also been reported (Koerner et al., 1991; Tanaka et al., 1994; McDonald et al., 1999; Sahna et al., 2002). Fantinelli et al. (2006) described that pharmacological interventions, ROS scavenging and NHE1 inhibition, when applied together and at their maximal effective concentration, did not induce protection further than that obtained separately by each pharmacologic procedure. These findings suggest that both interventions act through a common pathway. The authors proposed that in addition to the effect of preventing intracellular Na+ increase, NHE1 inhibition by cariporide decreases ROS-induced damage.

NHE1 activity is controlled by pH_i and numerous other factors, such as hormones, catecholamines, enzymes, and mechanical stimuli, known to be associated with heart disease (Avkiran and Haworth, 2003; Cingolani et al., 2008; Villa-Abrille et al., 2010; De Giusti et al., 2011). Furthermore, cardiac expression of an activated form of NHE1 that lacks the calmodulin-binding inhibitory domain was sufficient by itself to initiate cardiac hypertrophy and heart failure (Nakamura et al., 2008). Constitutively, active NHE1 leads to pathological changes in activation of the Ca^{2+}-dependent pro-hypertrophic signaling molecules, calcineurin and CaMKII (Nakamura et al., 2008). Similarly, in heart over-expression of activated NHE1 was recently found to elicit specific pathways of gene activation, inducing an increase in cross-sectional area of cardiomyocyte, interstitial fibrosis, and depressed cardiac function, in transgenic mice (Xue et al., 2010).

NHE1 AND MITOCHONDRIA

Emerging evidence supports the fact that mitochondrial dysfunction underlies the causes of numerous cardiac diseases (for review, see Baines, 2010). The mitochondrial death pathway features the sequential loss of mitochondrial membrane potential ($\Delta\Psi$ m), which is accompanied by opening of the mitochondrial permeability transition pore (MPTP), release of ROS and diverse toxic proteins which promote the activation of proteolytic activity of caspases (Teshima et al., 2003). When the MPTP opens, the permeability barrier of the inner membrane becomes disrupted and causes the free movement of protons across it, inducing uncoupling of the oxidative phosphorylation and mitochondria swelling. The MPTP is a large conductance pore thought to be activated by ROS, by increased mitochondrial Ca^{2+} levels and by dissipation of the mitochondrial $\Delta\Psi$ m (Akao et al., 2003; Javadov and Karmazyn, 2007). The MPTP opening can be further increased when Ca^{2+} overload is accompanied by oxidative stress, adenine nucleotide depletion, and elevated phosphate concentrations. Moreover, a decrease in mitochondrial anion superoxide production induced by two known enhancers of ROS production, Ang II and ET-1, upon NHE1 inhibition has been reported (Garciarena et al., 2008). Furthermore, the increase in ROS production induced by the opening of the mitochondrial ATP-dependent K^+ channel was abolished by cariporide (Garciarena et al., 2008).

Studies on the MPTP and its role in reperfusion injury and cardiac hypertrophy have proven fruitful (Piot et al., 2008; Halestrap and Pasdois, 2009). Duchen et al. (1993) and Griffiths and Halestrap (1993) showed that delayed opening of MPTP by the MPTP inhibitor, cyclosporine A (CsA), protects ischemic/reperfusion (I/R) injury in perfused rat hearts. Recently, Piot et al. (2008) reported a decrease in infarct size in patients with acute myocardial infarction by CsA administered at the time of reperfusion. Interestingly, a role of mitochondria in determining cardiac hypertrophy after myocardial infarction has also been proposed (Karmazyn, 1988; Caldiz et al., 2007; Javadov et al., 2008, 2009; Cingolani et al., 2010). NHE1 inhibition was one of the most promising therapeutic strategies for I/R injury based on experimental animal studies. However controversial results were obtained using NHE1 inhibitors in clinical trials: cariporide (GUARDIAN) (Theroux et al., 2000) or EXPEDITION (Mentzer et al., 2008) and Eniporide (ESCAMI) (Zeymer et al., 2001) (for review, see Murphy and Allen, 2009). These trials were unable to

demonstrate a significant reduction in mortality when these compounds were tested in patients after acute myocardial infarction (Theroux et al., 2000; Zeymer et al., 2001) or were suspended early due to undesired effects (Mentzer et al., 2008). In a subgroup of patients who underwent coronary artery bypass graft surgery and were treated with cariporide, a 25% improvement in cardiac performance was detected. Similar beneficial effects were seen in a small trial of 100 patients who received cariporide before percutaneous coronary angioplasty (Rupprecht et al., 2000).

The related myocardial protective effects induced by CsA and NHE1 inhibition prompted us to speculate about the possibility that NHE1 inhibition protects the heart by targeting the mitochondria (Robin et al., 2007). We recently demonstrated that reduction of mNHE1 protein expression (shRNA-NHE1) or specific inhibition of NHE1 (HOE642) at the rat heart mitochondria significantly reduced the Ca^{2+}-induced mitochondrial swelling [**Figures 1**, **2**, modified from Villa-Abrille et al. (2011)]. Interestingly, HOE642 did not provide additional effect on Ca^{2+}-induced mitochondrial swelling, in mitochondria with diminished levels of mNHE1 protein expression, suggesting a direct involvement of mNHE1 on the susceptibility of the MPTP for opening following the Ca^{2+} overload of the mitochondria. Additionally, the immunosuppressive agent, CsA inhibited the MPTP opening and mitochondrial swelling to the same extent as observed in isolated rat heart mitochondria inhibited with HOE642 or isolated mitochondria with reduced NHE1 expression [**Figures 1**, **2**, modified from Villa-Abrille et al. (2011)]. We speculate that a decrease in mitochondrial exchanger function (or reduced expression by siRNA) should increase H^+ concentration on the external side of the MPTP. In this regard, a prevention of MPTP formation by acidosis after an ischemic episode has been reported. Thus, accumulation of H^+ following mNHE1 inhibition or expression reduction should decrease MPTP opening in heart mitochondria subjected to stress conditions. Though numerous studies (Karmazyn, 1988; Kusumoto et al., 2001; Wang et al., 2003; Fantinelli et al., 2006) demonstrated a protective role of NHE1 inhibition I/R injury in the heart, no mitochondrial effect of NHE1 inhibition has been considered. However, a report by Ruiz-Meana et al. (2003) drew attention to this possibility. Furthermore, Aldakkak et al. (2008) demonstrated that the enhanced activation of NHE with alkaline pH_i during ischemic stress leads to an additional increase in mitochondrial Ca^{2+} load, which contributes to greater deterioration of mitochondrial bioenergetics and ROS production on reperfusion. Authors proved that NHE1 blockade at an alkaline pH improved the functional recovery after reperfusion, minimized the increase in mitochondrial $[Ca^{2+}]$, preserved the mitochondrial redox state, and reduced ROS production. These data suggested that both sarcolemmal and mitochondrial NHE1 may be involved in promoting mitochondrial Ca^{2+} loading with I/R injury. In connection with this, Teshima and collaborators (2003) demonstrated that cariporide protects cardiomyocyte against cell death induced by oxidative stress, preserving intracellular Na^+ and Ca^{2+} homeostasis and mitochondrial integrity.

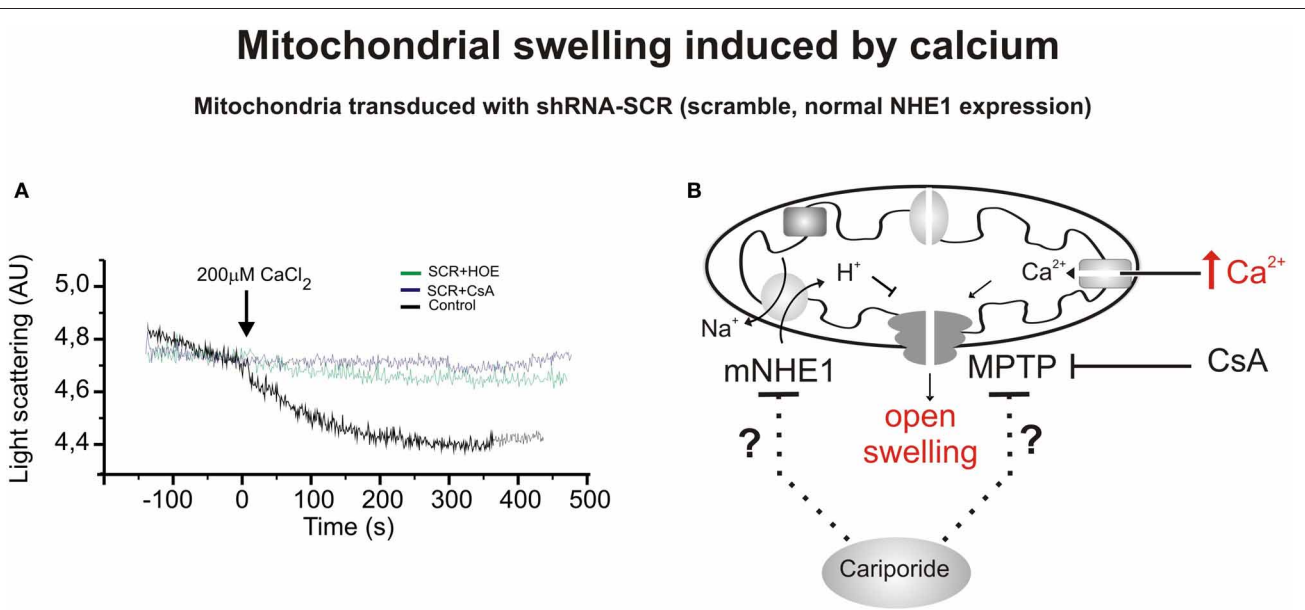

FIGURE 1 | Mitochondrial swelling induced by $CaCl_2$. (A) Typical experiment showing the scattered light absorbance traces of Ca^{2+}-induced swelling in response to addition of $CaCl_2$ to heart mitochondria isolated from rats transduced with shRNA-SCR (SCR, scrambled, control) in the presence or absence of cariporide (HOE642, 10 μM) and Cyclosporine A (CsA, 10 mM). Cariporide and Cyclosporine attenuated Ca^{2+}-induced mitochondrial swelling and the decrease in light scattering in mitochondrial suspensions. Cariporide inhibited the decrease in light scattering in a similar magnitude to CsA. **(B)** Scheme of a mitochondrion showing the $CaCl_2$-induced swelling in mitochondria that expresses scrambled sequence and functional NHE1, and possible mitochondrial site of action of the cariporide. This inhibitor could act on different mitochondrial mechanisms, including NHE. They could act through a decrease in mitochondrial Ca^{2+}, H^+, and $\Delta\Psi m$ affecting the MPTP formation or altering the sensitivity to those factors to induce MPTP formation. Modified from Villa-Abrille et al. (2011).

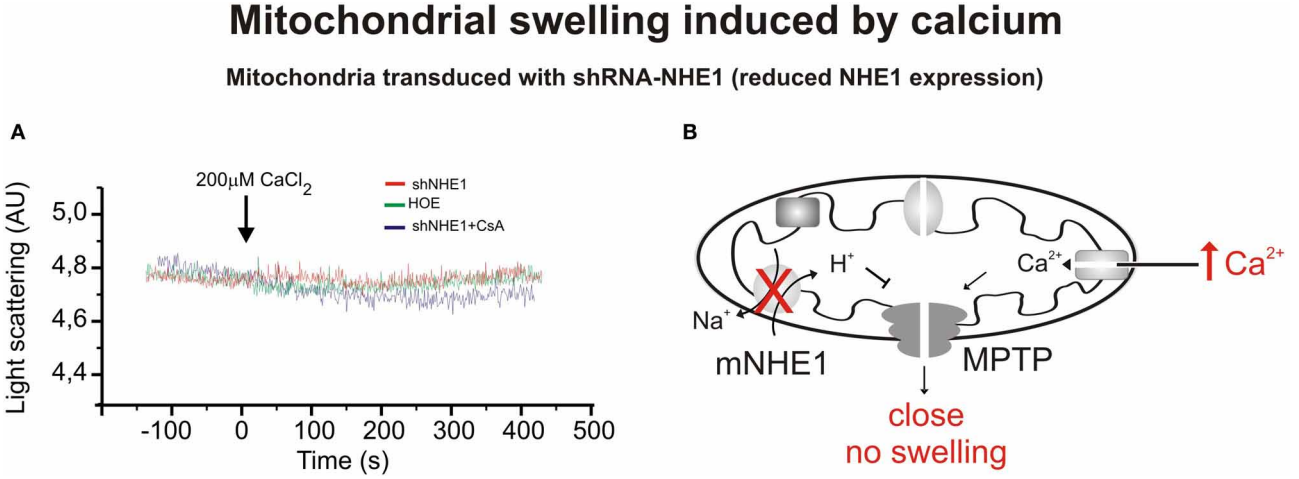

FIGURE 2 | Mitochondrial swelling induced by $CaCl_2$. (A) Typical experiment showing the scattered light absorbance traces of Ca^{2+}-induced swelling in response to addition of $CaCl_2$ for heart mitochondria isolated from rats transduced with shRNA-NHE1 in the presence and absence of cariporide. The shRNA-NHE1 transduction significantly inhibited Ca^{2+}-induced mitochondrial swelling compared with SCR-transduced animals, (as previously shown in **Figure 1**). Cariporide and Cyclosporine attenuated the decrease in light scattering in SCR-transduced rats and did not affect the decrease in light scattering in shRNA-NHE1-transduced rats. These results indicate that the NHE1 participates in the mechanism by which the Ca^{2+} induces MPTP opening and swelling. **(B)** Scheme showing the absence of mitochondrial swelling and MPTP opening induced by Ca^{2+} when NHE1 is silencing. Modified from Villa-Abrille et al. (2011).

The mitochondrial Ca^{2+} overload and the mitochondrial $\Delta\Psi$ m loss induced by oxidative stress were remarkably prevented by cariporide (Teshima et al., 2003). Additionally, Toda et al. (2007) demonstrated that the NHE1 inhibitor, cariporide, diminished the mitochondrial Ca^{2+} overload and MPTP opening induced by Na^+/K^+ ATPase inhibition in isolated cardiomyocytes. Although these effects were proposed to be secondary to prevention of the cytosolic increase in Ca^{2+}, more recently a direct mitochondrial action of NHE1 inhibitors related to the suppression of the myocardial superoxide production has been reported (Garciarena et al., 2008). A "cyclosporine like effect" of NHE1 inhibition was proposed, but the site of action of those compounds was not identified (Garciarena et al., 2008). Garciarena et al. (2008) studied the "anti-ROS effect" of NHE1 inhibitors. The authors analyzed NADPH oxidase-dependent mitochondrial O_2-generation induced by ANG II or ET-1. The NADPH oxidase-dependent mitochondrial release of ROS is the basis of the so-called "ROS-induced ROS release" phenomenon proposed by Zorov et al. (2000) and Kimura et al. (2005). However, there is no clear evidence that sarcolemmal NADPH oxidase-derived ROS interacts with the mitochondria. Accordingly, Zhang et al. (2001) using reconstituted mKATP channels of bovine heart demonstrated that O_2-directly stimulates the opening of these channels. The three NHE1 inhibitors used by Garciarena et al. (2008) blunted the increased mitochondrial ROS production and the redox activation of the kinases, well-known downstream targets of ROS (Sabri et al., 1998; Rothstein et al., 2002). The authors proposed a direct mitochondrial effect rather than a scavenging action of NHE1 inhibitors. Additionally, they showed that cariporide blunted not only the increased O_2-production induced by ANG II/ET-1 but also the production induced by opening the mKATP channel with diazoxide. A mitochondrial action of NHE1 inhibition secondary to changes in cytosol was previously suggested by Javadov et al. (2005). In two previous publications, these authors concluded that the mitochondrial effect of NHE1 inhibitors is indirect and possibly mediated by the prevention of cytosolic Ca^{2+} overload. Thus, inhibition of the sarcolemmal NHE1 alters intracellular Na^+ concentration and promotes Ca^{2+} overload (Javadov et al., 2005, 2008). Accordingly, they did not detect any mitochondria direct effect of the NHE1 inhibitors, and they suggested an action on MPTP function through glycogen synthase kinase 3-β (Javadov et al., 2009). We were unable to determine whether or not under their experimental conditions the effect of NHE1 inhibitors on mitochondrial Ca^{2+} and/or H^+ is prevented.

In 1969, Mitchell and Moyle (1969) proposed the existence of Na^+/H^+ exchange in mitochondria. Later, the existence of two systems capable of catalyze the H^+ transport across the mitochondrial membrane, was described (Garlid et al., 1991). These systems—the unselective K^+/H^+ exchanger (KHE), which catalyzes the transport of virtually all alkali ions in the mitochondrion, and the NHE, which selectively transports Na^+ or Li^+ through mitochondrial membranes—were proposed as the main cation transporters of the mitochondria (Garlid et al., 1991). In addition, Garlid et al. (1991) demonstrated in beef heart mitochondria that solubilized NHE in the organelle can be purified in an active state.

In mitochondria, NHE mediates the exchange of matrix Na^+ for intermembrane H^+ generated by respiration (Garlid, 1988). Thus, H^+ influx in the mitochondrial matrix through the mitochondrial NHE would constitute a form of H^+ leakage not coupled to ATP synthesis, which in turn will dissipate the energy stored as transmitochondrial membrane H^+ gradient.

NHE1 is a typical integral membrane protein with 10–12 predicted spanning segments, a long COOH terminus, and an

NH2-terminal tail that possesses the mitochondrial localization signal. Previous studies using immunofluorescence and three-dimensional confocal microscopy techniques demonstrated the presence of NHE1 in the nuclear membranes isolated from the aortic vascular smooth muscle and liver of human, rabbit, and rat, suggesting a possible role of the nuclear NHE1 in the modulation of intranuclear pH (Bkaily et al., 2004). Our experiments, using isolated cardiomyocytes or mitochondrial lysates demonstrated the expression of the NHE1 protein in mitochondria isolated from rat ventricular myocardium and mitochondria isolated from HEK 293 cells transfected with NHE1-HA cDNA (Villa-Abrille et al., 2011). Besides the expression of NHE1 in the plasma membrane of cardiac cells, we have characterized the expression of NHE1 in mitochondria of cardiac muscle (Villa-Abrille et al., 2011) by several different experimental techniques (immunogold analysis combined with electron microscopy, immunohistochemistry combined with confocal microscopy or immunoblot analysis). Accordingly, Javadov et al. (2011) examined the expression of NHE1 and NHE6 in Percoll-purified rat heart mitochondria by immunoblot analysis and they only observed NHE1 in the mitochondria fraction (Javadov et al., 2011). Retention of NHE1 expression in isolated mitochondria subjected to digitonin allows them to conclude that NHE1 is expressed in the inner mitochondrial membrane (Javadov et al., 2011).

Dual distribution, at both plasma membrane and mitochondria, of others protein like the Na^+/Ca^{+2} exchanger 1-3 (NCX1-3) (Gobbi et al., 2007), and Kv1.3 (Szabo et al., 2005), Kir6.2 (Garg and Hu, 2007), and Ca^{+2}-activated BK potassium channels (Siemen et al., 1999), has been previously reported. In addition, Connexin 43 (Cx43), a constitutive protein that forms cardiac gap junctions contributing to cell-cell coupling, was also localized in mitochondria (Boengler et al., 2005, 2009). Cx43 contains four transmembrane domains as well as amino and carboxy termini located in the cytosol. Cx43 localized in subsarcolemmal mitochondria and its carboxy terminus directed toward the intermembrane space (Boengler et al., 2009).

With the assistance of the RNA interference technique, we evaluated the function and expression of NHE1 in cardiac tissues. With the objective of knocking down the expression of NHE1 in the heart, we injected a lentiviral vector expressing shRNA-NHE1 intramyocardically. The intramyocardial injection of lentivirus carrying a shRNA-NHE1 (silencing of NHE1) not only reduced the expression of NHE1 at the level of mitochondria but also prevented Ca^{2+}-induced swelling of rat heart mitochondria [**Figures 1**, **2**, modified from Villa-Abrille et al. (2011)]. The silencing of NHE also prevents the development of the slow force response (Perez et al., 2011). A decrease in mitochondrial NHE function (or reduced expression by siRNA) should increase H^+ concentration in mitochondrial matrix. In connection with this, the prevention of MPTP formation by acidosis in reperfusion after ischemia has been reported (Cohen et al., 2007; Rodriguez-Sinovas et al., 2009). We reported a delay of MPTP formation in isolated mitochondria by NHE1 inhibition and posttranscriptional NHE1 gene silencing. These findings open a new avenue of research about the mechanism of protection achieved by NHE1 inhibition in reperfusion injury, cardiac hypertrophy, and heart failure. The mechanism by which the opening of the MPTP is prevented at low NHE1 expression is unknown. As previously described under physiological conditions, the mitochondrial NHE introduces cytosolic H^+ into the mitochondrial matrix in exchange for mitochondrial Na^+. Therefore, a decrease in exchanger activity or expression should reduce H^+ and increase Na^+ concentration in the mitochondrial matrix and perhaps increase H^+ concentration on the cytosolic side of the MPTP. The decrease in H^+ matrix concentration would favor and not prevent MPTP formation, but the increase of H^+ on the cytosolic side of the MPTP may inhibit pore formation. In connection with this scenario, the prevention of MPTP formation by acidosis in reperfusion after ischemia has been reported (Cohen et al., 2007). An increase in mitochondrial Na^+ would decrease the inwardly directed Na^+ gradient, affecting the mitochondrial Na^+/Ca^{2+} exchanger, other factors being constant (Murphy and Steenbergen, 2008). A decrease in Ca^{2+} efflux from the mitochondria would increase mitochondrial Ca^{2+} concentration and favor rather than reduce MPTP formation.

The main objective of this review was to emphasize the presence of NHE1 in the mitochondrial membrane and its role in MPTP opening. We are proposing the mitochondrial NHE1 as a novel target to prevent cardiac disease including I/R injury, cardiac hypertrophy, and heart failure. However, we could not rule out the concomitant participation of the sarcolemmal NHE1 in the protective effects achieved by NHE inhibition.

REFERENCES

Akao, M., O'Rourke, B., Kusuoka, H., Teshima, Y., Jones, S. P., and Marban, E. (2003). Differential actions of cardioprotective agents on the mitochondrial death pathway. *Circ. Res.* 92, 195–202. doi: 10.1161/01.RES.0000051862.16691.F9

Aldakkak, M., Stowe, D. F., Heisner, J. S., Spence, M., and Camara, A. K. (2008). Enhanced Na+/H+ exchange during ischemia and reperfusion impairs mitochondrial bioenergetics and myocardial function. *J. Cardiovasc. Pharmacol.* 52, 236–244. doi: 10.1097/FJC.0b013e3181831337

Avkiran, M. (1999). Rational basis for use of sodium-hydrogen exchange inhibitors in myocardial ischemia. *Am. J. Cardiol.* 83, 10G–17G. discussion: 17G–18G. doi: 10.1016/S0002-9149(99)00215-5

Avkiran, M., and Haworth, R. S. (2003). Regulatory effects of G protein-coupled receptors on cardiac sarcolemmal Na+/H+ exchanger activity: signalling and significance. *Cardiovasc. Res.* 57, 942–952. doi: 10.1016/S0008-6363(02)00782-4

Baines, C. P. (2010). The cardiac mitochondrion: nexus of stress. *Annu. Rev. Physiol.* 72, 61–80. doi: 10.1146/annurev-physiol-021909-135929

Bertrand, B., Wakabayashi, S., Ikeda, T., Pouyssegur, J., and Shigekawa, M. (1994). The Na+/H+ exchanger isoform 1 (NHE1) is a novel member of the calmodulin-binding proteins. Identification and characterization of calmodulin-binding sites. *J. Biol. Chem.* 269, 13703–13709.

Biemesderfer, D., Reilly, R. F., Exner, M., Igarashi, P., and Aronson, P. S. (1992). Immunocytochemical characterization of Na(+)-H+ exchanger isoform NHE-1 in rabbit kidney. *Am. J. Physiol.* 263, F833–F840.

Bkaily, G., Nader, M., Avedanian, L., Jacques, D., Perrault, C., Abdel-Samad, D., et al. (2004). Immunofluorescence revealed the presence of NHE-1 in the nuclear membranes of rat cardiomyocytes and isolated nuclei of human, rabbit, and rat aortic and liver tissues. *Can. J. Physiol. Pharmacol.* 82, 805–811. doi: 10.1139/y04-119

Boengler, K., Dodoni, G., Rodriguez-Sinovas, A., Cabestrero, A., Ruiz-Meana, M., Gres, P., et al. (2005). Connexin 43 in cardiomyocyte mitochondria and its increase by ischemic preconditioning. *Cardiovasc. Res.* 67, 234–244. doi: 10.1016/j.cardiores.2005.04.014

Boengler, K., Stahlhofen, S., Van De Sand, A., Gres, P., Ruiz-Meana, M.,

Garcia-Dorado, D., et al. (2009). Presence of connexin 43 in subsarcolemmal, but not in interfibrillar cardiomyocyte mitochondria. *Basic Res. Cardiol.* 104, 141–147. doi: 10.1007/s00395-009-0007-5

Caldiz, C. I., Garciarena, C. D., Dulce, R. A., Novaretto, L. P., Yeves, A. M., Ennis, I. L., et al. (2007). Mitochondrial reactive oxygen species activate the slow force response to stretch in feline myocardium. *J. Physiol.* 584, 895–905. doi: 10.1113/jphysiol.2007.141689

Cingolani, H. E., Perez, N. G., Aiello, E. A., Ennis, I. L., Garciarena, C. D., Villa-Abrille, M. C., et al. (2008). Early signals after stretch leading to cardiac hypertrophy. Key role of NHE-1. *Front. Biosci.* 13, 7096–7114. doi: 10.2741/3213

Cingolani, H. E., Perez, N. G., Caldiz, C. I., Garciarena, C. D., De Giusti, V. C., Correa, M. V., et al. (2010). "Early hypertrophic signals after myocardial stretch. Role of reactive oxygen species and the sodium/hydrogen exchanger," in *Mechanosensitivity in Cells and Tissues: Mechanosensitivy of the Heart,* eds A. Kamkin and I. Kiseleva (Moscow: Springer), 327–371.

Cohen, M. V., Yang, X. M., and Downey, J. M. (2007). The pH hypothesis of postconditioning: staccato reperfusion reintroduces oxygen and perpetuates myocardial acidosis. *Circulation* 115, 1895–1903. doi: 10.1161/CIRCULATIONAHA.106.675710

De Giusti, V. C., Nolly, M. B., Yeves, A. M., Caldiz, C. I., Villa-Abrille, M. C., Chiappe De Cingolani, G. E., et al. (2011). Aldosterone stimulates the cardiac Na(+)/H(+) exchanger via transactivation of the epidermal growth factor receptor. *Hypertension* 58, 912–919. doi: 10.1161/HYPERTENSIONAHA.111.176024

Duchen, M. R., McGuinness, O., Brown, L. A., and Crompton, M. (1993). On the involvement of a cyclosporin A sensitive mitochondrial pore in myocardial reperfusion injury. *Cardiovasc. Res.* 27, 1790–1794. doi: 10.1093/cvr/27.10.1790

Fantinelli, J. C., Cingolani, H. E., and Mosca, S. M. (2006). Na+/H+ exchanger inhibition at the onset of reperfusion decreases myocardial infarct size: role of reactive oxygen species. *Cardiovasc. Pathol.* 15, 179–184. doi: 10.1016/j.carpath.2006.04.005

Fliegel, L. (2008). Molecular biology of the myocardial Na+/H+ exchanger. *J. Mol. Cell. Cardiol.* 44, 228–237. doi: 10.1016/j.yjmcc.2007.11.016

Fliegel, L., and Karmazyn, M. (2004). The cardiac Na-H exchanger: a key downstream mediator for the cellular hypertrophic effects of paracrine, autocrine and hormonal factors. *Biochem. Cell Biol.* 82, 626–635. doi: 10.1139/o04-129

Fliegel, L., Walsh, M. P., Singh, D., Wong, C., and Barr, A. (1992). Phosphorylation of the C-terminal domain of the Na+/H+ exchanger by Ca2+/calmodulin-dependent protein kinase II. *Biochem. J.* 282(Pt 1), 139–145.

Garciarena, C. D., Caldiz, C. I., Correa, M. V., Schinella, G. R., Mosca, S. M., Chiappe De Cingolani, G. E., et al. (2008). Na+/H+ exchanger-1 inhibitors decrease myocardial superoxide production via direct mitochondrial action. *J. Appl. Physiol.* 105, 1706–1713. doi: 10.1152/japplphysiol.90616.2008

Garg, V., and Hu, K. (2007). Protein kinase C isoform-dependent modulation of ATP-sensitive K+ channels in mitochondrial inner membrane. *Am. J. Physiol. Heart Circ. Physiol.* 293, H322–H332. doi: 10.1152/ajpheart.01035.2006

Garlid, K. D. (1988). Sodium/proton antiporters in the mitochondrial inner membrane. *Adv. Exp. Med. Biol.* 232, 37–46. doi: 10.1007/978-1-4757-0007-7_4

Garlid, K. D., Shariat-Madar, Z., Nath, S., and Jezek, P. (1991). Reconstitution and partial purification of the Na(+)-selective Na+/H+ antiporter of beef heart mitochondria. *J. Biol. Chem.* 266, 6518–6523.

Gobbi, P., Castaldo, P., Minelli, A., Salucci, S., Magi, S., Corcione, E., and Amoroso, S. (2007). Mitochondrial localization of Na+/Ca2+ exchangers NCX1-3 in neurons and astrocytes of adult rat brain in situ. *Pharmacol. Res.* 56, 556–565. doi: 10.1016/j.phrs.2007.10.005

Griffiths, E. J., and Halestrap, A. P. (1993). Protection by Cyclosporin A of ischemia/reperfusion-induced damage in isolated rat hearts. *J. Mol. Cell. Cardiol.* 25, 1461–1469. doi: 10.1006/jmcc.1993.1162

Gumina, R. J., Mizumura, T., Beier, N., Schelling, P., Schultz, J. J., and Gross, G. J. (1998). A new sodium/hydrogen exchange inhibitor, EMD 85131, limits infarct size in dogs when administered before or after coronary artery occlusion. *J. Pharmacol. Exp. Ther.* 286, 175–183.

Halestrap, A. P., and Pasdois, P. (2009). The role of the mitochondrial permeability transition pore in heart disease. *Biochim. Biophys. Acta* 1787, 1402–1415. doi: 10.1016/j.bbabio.2008.12.017

Haworth, R. S., McCann, C., Snabaitis, A. K., Roberts, N. A., and Avkiran, M. (2003). Stimulation of the plasma membrane Na+/H+ exchanger NHE1 by sustained intracellular acidosis. Evidence for a novel mechanism mediated by the ERK pathway. *J. Biol. Chem.* 278, 31676–31684. doi: 10.1074/jbc.M304400200

Haworth, R. S., Sinnett-Smith, J., Rozengurt, E., and Avkiran, M. (1999). Protein kinase D inhibits plasma membrane Na(+)/H(+) exchanger activity. *Am. J. Physiol.* 277, C1202–C1209.

Hurtado, C., and Pierce, G. N. (2000). Inhibition of Na(+)/H(+) exchange at the beginning of reperfusion is cardioprotective in isolated, beating adult cardiomyocytes. *J. Mol. Cell. Cardiol.* 32, 1897–1907. doi: 10.1006/jmcc.2000.1222

Javadov, S., Choi, A., Rajapurohitam, V., Zeidan, A., Basnakian, A. G., and Karmazyn, M. (2008). NHE-1 inhibition-induced cardioprotection against ischaemia/reperfusion is associated with attenuation of the mitochondrial permeability transition. *Cardiovasc. Res.* 77, 416–424. doi: 10.1093/cvr/cvm039

Javadov, S., Huang, C., Kirshenbaum, L., and Karmazyn, M. (2005). NHE-1 inhibition improves impaired mitochondrial permeability transition and respiratory function during postinfarction remodelling in the rat. *J. Mol. Cell. Cardiol.* 38, 135–143. doi: 10.1016/j.yjmcc.2004.10.007

Javadov, S., and Karmazyn, M. (2007). Mitochondrial permeability transition pore opening as an endpoint to initiate cell death and as a putative target for cardioprotection. *Cell. Physiol. Biochem.* 20, 1–22. doi: 10.1159/000103747

Javadov, S., Rajapurohitam, V., Kilic, A., Hunter, J. C., Zeidan, A., Said Faruq, N., et al. (2011). Expression of mitochondrial fusion-fission proteins during post-infarction remodeling: the effect of NHE-1 inhibition. *Basic Res. Cardiol.* 106, 99–109. doi: 10.1007/s00395-010-0122-3

Javadov, S., Rajapurohitam, V., Kilic, A., Zeidan, A., Choi, A., and Karmazyn, M. (2009). Anti-hypertrophic effect of NHE-1 inhibition involves GSK-3beta-dependent attenuation of mitochondrial dysfunction. *J. Mol. Cell. Cardiol.* 46, 998–1007. doi: 10.1016/j.yjmcc.2008.12.023

Karmazyn, M. (1988). Amiloride enhances postischemic ventricular recovery: possible role of Na+-H+ exchange. *Am. J. Physiol.* 255, H608–H615.

Karmazyn, M. (1999a). Mechanisms of protection of the ischemic and reperfused myocardium by sodium-hydrogen exchange inhibition. *J. Thromb. Thrombolysis* 8, 33–38.

Karmazyn, M. (1999b). The role of the myocardial sodium-hydrogen exchanger in mediating ischemic and reperfusion injury. *Ann. N.Y. Acad. Sci.* 874, 326–334.

Karmazyn, M., Gan, X. T., Humphreys, R. A., Yoshida, H., and Kusumoto, K. (1999). The myocardial Na(+)-H(+) exchange: structure, regulation, and its role in heart disease. *Circ. Res.* 85, 777–786. doi: 10.1161/01.RES.85.9.777

Khaled, A. R., Moor, A. N., Li, A., Kim, K., Ferris, D. K., Muegge, K., et al. (2001). Trophic factor withdrawal: p38 mitogen-activated protein kinase activates NHE1, which induces intracellular alkalinization. *Mol. Cell. Biol.* 21, 7545–7557. doi: 10.1128/MCB.21.22.7545-7557.2001

Kimura, S., Zhang, G. X., Nishiyama, A., Shokoji, T., Yao, L., Fan, Y. Y., et al. (2005). Mitochondria-derived reactive oxygen species and vascular MAP kinases: comparison of angiotensin II and diazoxide. *Hypertension* 45, 438–444.

Koerner, J. E., Anderson, B. A., and Dage, R. C. (1991). Protection against postischemic myocardial dysfunction in anesthetized rabbits with scavengers of oxygen-derived free radicals: superoxide dismutase plus catalase, N-2-mercaptopropionyl glycine and captopril. *J. Cardiovasc. Pharmacol.* 17, 185–191. doi: 10.1097/00005344-199102000-00002

Kusumoto, K., Haist, J. V., and Karmazyn, M. (2001). Na(+)/H(+) exchange inhibition reduces hypertrophy and heart failure after myocardial infarction in rats. *Am. J. Physiol. Heart Circ. Physiol.* 280, H738–H745.

Lee, S. H., Kim, T., Park, E. S., Yang, S., Jeong, D., Choi, Y., et al. (2008). NHE10, an osteoclast-specific member of the Na+/H+ exchanger family, regulates osteoclast differentiation and survival [corrected]. *Biochem. Biophys. Res. Commun.* 369, 320–326. doi: 10.1016/j.bbrc.2008.01.168

Leem, C. H., Lagadic-Gossmann, D., and Vaughan-Jones, R. D. (1999). Characterization of intracellular pH regulation in the guinea-pig ventricular myocyte. *J. Physiol.* 517(Pt 1), 159–180. doi: 10.1111/j.1469-7793.1999.0159z.x

Li, X., Alvarez, B., Casey, J. R., Reithmeier, R. A., and Fliegel, L. (2002). Carbonic anhydrase II binds to and enhances activity of the Na+/H+ exchanger. *J. Biol. Chem.* 277, 36085–36091. doi: 10.1074/jbc.M111952200

McDonald, M. C., Zacharowski, K., Bowes, J., Cuzzocrea, S., and Thiemermann, C. (1999). Tempol reduces infarct size in rodent models of regional myocardial ischemia and reperfusion. *Free Radic. Biol. Med.* 27, 493–503. doi: 10.1016/S0891-5849(99)00100-8

Mentzer, R. M. Jr., Bartels, C., Bolli, R., Boyce, S., and Buckberg, G. D. (2008). Sodium-hydrogen exchange inhibition by cariporide to reduce the risk of ischemic cardiac events in patients undergoing coronary artery bypass grafting: results of the EXPEDITION study. *Ann. Thorac. Surg.* 85, 1261–1270. doi: 10.1016/j.athoracsur.2007.10.054

Misik, A. J., Perreault, K., Holmes, C. F., and Fliegel, L. (2005). Protein phosphatase regulation of Na+/H+ exchanger isoform I. *Biochemistry* 44, 5842–5852. doi: 10.1021/bi047659s

Mitchell, P., and Moyle, J. (1969). Translocation of some anions cations and acids in rat liver mitochondria. *Eur. J. Biochem.* 9, 149–155. doi: 10.1111/j.1432-1033.1969.tb00588.x

Moor, A. N., and Fliegel, L. (1999). Protein kinase-mediated regulation of the Na(+)/H(+) exchanger in the rat myocardium by mitogen-activated protein kinase-dependent pathways. *J. Biol. Chem.* 274, 22985–22992. doi: 10.1074/jbc.274.33.22985

Murphy, E., and Allen, D. G. (2009). Why did the NHE inhibitor clinical trials fail. *J. Mol. Cell. Cardiol.* 46, 137–141. doi: 10.1016/j.yjmcc.2008.09.715

Murphy, E., and Steenbergen, C. (2008). Mechanisms underlying acute protection from cardiac ischemia-reperfusion injury. *Physiol. Rev.* 88, 581–609. doi: 10.1152/physrev.00024.2007

Nakamura, T. Y., Iwata, Y., Arai, Y., Komamura, K., and Wakabayashi, S. (2008). Activation of Na+/H+ exchanger 1 is sufficient to generate Ca2+ signals that induce cardiac hypertrophy and heart failure. *Circ. Res.* 103, 891–899. doi: 10.1161/CIRCRESAHA.108.175141

Orlowski, J., and Grinstein, S. (1997). Na+/H+ exchangers of mammalian cells. *J. Biol. Chem.* 272, 22373–22376. doi: 10.1074/jbc.272.36.22373

Pang, T., Su, X., Wakabayashi, S., and Shigekawa, M. (2001). Calcineurin homologous protein as an essential cofactor for Na+/H+ exchangers. *J. Biol. Chem.* 276, 17367–17372. doi: 10.1074/jbc.M100296200

Perez, N. G., Nolly, M. B., Roldan, M. C., Villa-Abrille, M. C., Cingolani, E., Portiansky, E. L., et al. (2011). Silencing of NHE-1 blunts the slow force response to myocardial stretch. *J. Appl. Physiol.* 111, 874–880. doi: 10.1152/japplphysiol.01344.2010

Petrecca, K., Atanasiu, R., Grinstein, S., Orlowski, J., and Shrier, A. (1999). Subcellular localization of the Na+/H+ exchanger NHE1 in rat myocardium. *Am. J. Physiol.* 276, H709–H717.

Piot, C., Croisille, P., Staat, P., Thibault, H., Rioufol, G., Mewton, N., et al. (2008). Effect of cyclosporine on reperfusion injury in acute myocardial infarction. *N. Engl. J. Med.* 359, 473–481. doi: 10.1056/NEJMoa071142

Robin, E., Guzy, R. D., Loor, G., Iwase, H., Waypa, G. B., Marks, J. D., et al. (2007). Oxidant stress during simulated ischemia primes cardiomyocytes for cell death during reperfusion. *J. Biol. Chem.* 282, 19133–19143. doi: 10.1074/jbc.M701917200

Rodriguez-Sinovas, A., Cabestrero, A., Garcia Del Blanco, B., Inserte, J., Garcia, A., and Garcia-Dorado, D. (2009). Intracoronary acid infusion as an alternative to ischemic postconditioning in pigs. *Basic Res. Cardiol.* 104, 761–771. doi: 10.1007/s00395-009-0032-4

Rohmann, S., Weygandt, H., and Minck, K. O. (1995). Preischaemic as well as postischaemic application of a Na+/H+ exchange inhibitor reduces infarct size in pigs. *Cardiovasc. Res.* 30, 945–951.

Rothstein, E. C., Byron, K. L., Reed, R. E., Fliegel, L., and Lucchesi, P. A. (2002). H(2)O(2)-induced Ca(2+) overload in NRVM involves ERK1/2 MAP kinases: role for an NHE-1-dependent pathway. *Am. J. Physiol. Heart Circ. Physiol.* 283, H598–H605.

Ruiz-Meana, M., Garcia-Dorado, D., Pina, P., Inserte, J., Agullo, L., and Soler-Soler, J. (2003). Cariporide preserves mitochondrial proton gradient and delays ATP depletion in cardiomyocytes during ischemic conditions. *Am. J. Physiol. Heart Circ. Physiol.* 285, H999–H1006.

Rupprecht, H. J., Vom Dahl, J., Terres, W., Seyfarth, K. M., Richardt, G., Schultheibeta, H. P., et al. (2000). Cardioprotective effects of the Na(+)/H(+) exchange inhibitor cariporide in patients with acute anterior myocardial infarction undergoing direct PTCA. *Circulation* 101, 2902–2908. doi: 10.1161/01.CIR.101.25.2902

Sabri, A., Byron, K. L., Samarel, A. M., Bell, J., and Lucchesi, P. A. (1998). Hydrogen peroxide activates mitogen-activated protein kinases and Na+-H+ exchange in neonatal rat cardiac myocytes. *Circ. Res.* 82, 1053–1062. doi: 10.1161/01.RES.82.10.1053

Sahna, E., Acet, A., Ozer, M. K., and Olmez, E. (2002). Myocardial ischemia-reperfusion in rats: reduction of infarct size by either supplemental physiological or pharmacological doses of melatonin. *J. Pineal Res.* 33, 234–238. doi: 10.1034/j.1600-079X.2002.02924.x

Sardet, C., Counillon, L., Franchi, A., and Pouyssegur, J. (1990). Growth factors induce phosphorylation of the Na+/H+ antiporter, glycoprotein of 110 kD. *Science* 247, 723–726. doi: 10.1126/science.2154036

Sardet, C., Fafournoux, P., and Pouyssegur, J. (1991). Alpha-thrombin, epidermal growth factor, and okadaic acid activate the Na+/H+ exchanger, NHE-1, by phosphorylating a set of common sites. *J. Biol. Chem.* 266, 19166–19171.

Sardet, C., Franchi, A., and Pouyssegur, J. (1989). Molecular cloning, primary structure, and expression of the human growth factor-activatable Na+/H+ antiporter. *Cell* 56, 271–280. doi: 10.1016/0092-8674(89)90901-X

Siemen, D., Loupatatzis, C., Borecky, J., Gulbins, E., and Lang, F. (1999). Ca2+-activated K channel of the BK-type in the inner mitochondrial membrane of a human glioma cell line. *Biochem. Biophys. Res. Commun.* 257, 549–554. doi: 10.1006/bbrc.1999.0496

Snabaitis, A. K., D'Mello, R., Dashnyam, S., and Avkiran, M. (2006). A novel role for protein phosphatase 2A in receptor-mediated regulation of the cardiac sarcolemmal Na+/H+ exchanger NHE1. *J. Biol. Chem.* 281, 20252–20262. doi: 10.1074/jbc.M600268200

Szabo, I., Bock, J., Jekle, A., Soddemann, M., Adams, C., Lang, F., et al. (2005). A novel potassium channel in lymphocyte mitochondria. *J. Biol. Chem.* 280, 12790–12798. doi: 10.1074/jbc.M413548200

Takahashi, E., Abe, J., Gallis, B., Aebersold, R., Spring, D. J., Krebs, E. G., and Berk, B. C. (1999). p90(RSK) is a serum-stimulated Na+/H+ exchanger isoform-1 kinase. Regulatory phosphorylation of serine 703 of Na+/H+ exchanger isoform-1. *J. Biol. Chem.* 274, 20206–20214. doi: 10.1074/jbc.274.29.20206J.

Tanaka, M., Fujiwara, H., Yamasaki, K., and Sasayama, S. (1994). Superoxide dismutase and N-2-mercaptopropionyl glycine attenuate infarct size limitation effect of ischaemic preconditioning in the rabbit. *Cardiovasc. Res.* 28, 980–986. doi: 10.1093/cvr/28.7.980

Teshima, Y., Akao, M., Jones, S. P., and Marban, E. (2003). Cariporide (HOE642), a selective Na+-H+ exchange inhibitor, inhibits the mitochondrial death pathway. *Circulation* 108, 2275–2281. doi: 10.1161/01.CIR.0000093277.20968.C7

Theroux, P., Chaitman, B. R., Danchin, N., Erhardt, L., Meinertz, T., Schroeder, J. S., et al. (2000). Inhibition of the sodium-hydrogen exchanger with cariporide to prevent myocardial infarction in high-risk ischemic situations. Main results of the GUARDIAN trial. Guard during ischemia against necrosis (GUARDIAN) Investigators. *Circulation* 102, 3032–3038. doi: 10.1161/01.CIR.102.25.3032

Toda, T., Kadono, T., Hoshiai, M., Eguchi, Y., Nakazawa, S., Nakazawa, H., et al. (2007). Na+/H+ exchanger inhibitor cariporide attenuates the mitochondrial Ca2+ overload and PTP opening. *Am. J. Physiol. Heart Circ. Physiol.* 293, H3517–H3523. doi: 10.1152/ajpheart.00483.2006

Tominaga, T., Ishizaki, T., Narumiya, S., and Barber, D. L. (1998). p160ROCK mediates RhoA activation of Na-H exchange. *EMBO J.* 17, 4712–4722. doi: 10.1093/emboj/17.16.4712

Villa-Abrille, M. C., Caldiz, C. I., Ennis, I. L., Nolly, M. B., Casarini, M. J., Chiappe De Cingolani, G. E., et al. (2010). The Anrep effect requires transactivation of the epidermal growth factor receptor. *J. Physiol.* 588, 1579–1590. doi: 10.1113/jphysiol.2009.186619

Villa-Abrille, M. C., Cingolani, E., Cingolani, H. E., and Alvarez, B. V. (2011). Silencing of

cardiac mitochondrial NHE1 prevents mitochondrial permeability transition pore opening. *Am. J. Physiol. Heart Circ. Physiol.* 300, H1237–H1251. doi: 10.1152/ajpheart.00840.2010

Wakabayashi, S., Bertrand, B., Ikeda, T., Pouyssegur, J., and Shigekawa, M. (1994). Mutation of calmodulin-binding site renders the Na+/H+ exchanger (NHE1) highly H(+)-sensitive and Ca2+ regulation-defective. *J. Biol. Chem.* 269, 13710–13715.

Wakabayashi, S., Fafournoux, P., Sardet, C., and Pouyssegur, J. (1992). The Na+/H+ antiporter cytoplasmic domain mediates growth factor signals and controls "H(+)-sensing." *Proc. Natl. Acad. Sci. U.S.A.* 89, 2424–2428. doi: 10.1073/pnas.89.6.2424

Wakabayashi, S., Shigekawa, M., and Pouyssegur, J. (1997). Molecular physiology of vertebrate Na+/H+ exchangers. *Physiol. Rev.* 77, 51–74.

Wang, Y., Meyer, J. W., Ashraf, M., and Shull, G. E. (2003). Mice with a null mutation in the NHE1 Na+-H+ exchanger are resistant to cardiac ischemia-reperfusion injury. *Circ. Res.* 93, 776–782. doi: 10.1161/01.RES.0000094746.24774.DC

Xue, J., Mraiche, F., Zhou, D., Karmazyn, M., Oka, T., Fliegel, L., et al. (2010). Elevated myocardial Na+/H+ exchanger isoform 1 activity elicits gene expression that leads to cardiac hypertrophy. *Physiol. Genomics* 42, 374–383. doi: 10.1152/physiolgenomics.00064.2010

Yan, W., Nehrke, K., Choi, J., and Barber, D. L. (2001). The Nck-interacting kinase (NIK) phosphorylates the Na+-H+ exchanger NHE1 and regulates NHE1 activation by platelet-derived growth factor. *J. Biol. Chem.* 276, 31349–31356. doi: 10.1074/jbc.M102679200

Zeymer, U., Suryapranata, H., Monassier, J. P., Opolski, G., Davies, J., Rasmanis, G., et al. (2001). The Na(+)/H(+) exchange inhibitor eniporide as an adjunct to early reperfusion therapy for acute myocardial infarction. Results of the evaluation of the safety and cardioprotective effects of eniporide in acute myocardial infarction (ESCAMI) trial. *J. Am. Coll. Cardiol.* 38, 1644–1650. doi: 10.1016/S0735-1097(01)01608-4

Zhang, D. X., Chen, Y. F., Campbell, W. B., Zou, A. P., Gross, G. J., and Li, P. L. (2001). Characteristics and superoxide-induced activation of reconstituted myocardial mitochondrial ATP-sensitive potassium channels. *Circ. Res.* 89, 1177–1183. doi: 10.1161/hh2401.101752

Zorov, D. B., Filburn, C. R., Klotz, L. O., Zweier, J. L., and Sollott, S. J. (2000). Reactive oxygen species (ROS)-induced ROS release: a new phenomenon accompanying induction of the mitochondrial permeability transition in cardiac myocytes. *J. Exp. Med.* 192, 1001–1014. doi: 10.1084/jem.192.7.1001

Conflict of Interest Statement: The authors declare that the research was conducted in the absence of any commercial or financial relationships that could be construed as a potential conflict of interest.

Received: 01 March 2013; paper pending published: 20 March 2013; accepted: 09 June 2013; published online: 28 June 2013.

Citation: Alvarez BV and Villa-Abrille MC (2013) Mitochondrial NHE1: a newly identified target to prevent heart disease. Front. Physiol. ***4****:152. doi: 10.3389/fphys.2013.00152*

This article was submitted to Frontiers in Mitochondrial Research, a specialty of Frontiers in Physiology.